

7-1-2012

# Historical and topographic drivers of tropical insular diversity: comparative phylogeography of *Eleutherodactylus antillensis* and *E. portoricensis*, two ecologically distinctive frogs of the Puerto Rican Bank

Brittany Barker

Follow this and additional works at: [https://digitalrepository.unm.edu/biol\\_etds](https://digitalrepository.unm.edu/biol_etds)

---

## Recommended Citation

Barker, Brittany. "Historical and topographic drivers of tropical insular diversity: comparative phylogeography of *Eleutherodactylus antillensis* and *E. portoricensis*, two ecologically distinctive frogs of the Puerto Rican Bank." (2012).  
[https://digitalrepository.unm.edu/biol\\_etds/3](https://digitalrepository.unm.edu/biol_etds/3)

This Dissertation is brought to you for free and open access by the Electronic Theses and Dissertations at UNM Digital Repository. It has been accepted for inclusion in Biology ETDs by an authorized administrator of UNM Digital Repository. For more information, please contact [disc@unm.edu](mailto:disc@unm.edu).

**Brittany S. Barker**

*Candidate*

---

**Biology**

*Department*

---

This dissertation is approved, and it is acceptable in quality and form for publication:

*Approved by the Dissertation Committee:*

**Robert B. Waide**, Chairperson

---

**Joseph A. Cook**

---

**Thomas F. Turner**

---

**Javier A. Rodríguez-Robles**

---

---

---

---

---

---

---

---

**HISTORICAL AND TOPOGRAPHIC DRIVERS OF TROPICAL  
INSULAR DIVERSITY: COMPARATIVE PHYLOGEOGRAPHY  
OF *ELEUTHERODACTYLUS ANTILLENIS* AND *E. PORTORICENSIS*,  
TWO ECOLOGICALLY DISTINCTIVE FROGS OF THE PUERTO RICAN  
BANK**

by

**BRITTANY SUZANNE BARKER**

B.S., Zoology,  
Oregon State University, 2003

DISSERTATION

Submitted in Partial Fulfillment of the  
Requirements for the Degree of

**Doctor of Philosophy**

**Biology**

The University of New Mexico  
Albuquerque, New Mexico

**July, 2012**

## ACKNOWLEDGEMENTS

First and foremost, I would like to thank Jed Stoken for his unconditional love and support throughout the entire process of completing this dissertation. I am extremely grateful to my co-advisors, Bob Waide and Joe Cook, for their guidance and financial support through research assistantships, field and laboratory support, to Tom Turner for letting me occasionally use his lab space, and to Javier Rodríguez-Robles for his thoughtful and thorough comments on my manuscripts.

I would like to extend my thanks to the many people who helped me conduct field work in Puerto Rico and the Virgin Islands: Fernando Bird-Picó, Tomas Figueroa, Bill Gould, Wilfredo Falcón-Linero, Jose Fumero, Carolyn Krupp, Skip Lazell, Gad Perry, Clive Petrovic, Renata Platenberg, Alberto Puente-Rolón, Alejandro Ríos-Franceschi, Jessica Snider, Richard Thomas, and Larry Woolbright. I thank Steve Poe, Daniel Medina, and Mason Ryan for helping me collect samples from an introduced population of *E. antillensis* in Panamá City, a side-project which was originally part of this dissertation. Vani Aran, Ashley Montoya, and Mary Farrah helped complete molecular laboratory work for my dissertation.

Several friends and colleagues provided feedback and comments on earlier drafts of my dissertation manuscripts, including Cuervo Lab members and affiliates Kayce Bell, Melissa Fleming, Chris Himes, Andrew Hope, Brooks Kohli, Jason Malaney, Bryan McLean, Jolene Rearick, Yadéeh Sawyer, Fernando Torres-Perez, and Jessica Weber, my OGS dissertation writing group members Carson Metzger and Jen Richter, and my other

colleagues and friends Andrew Crawford, Jennifer Hollis, Jeff Streicher, Matthew Heinicke, Maureen Hickman, Mason Ryan, Daniel Warnock, and Megan Workman.

For advice and help with technical analyses I extend my gratitude to Peter Beerli, Kurt Galbreath, Andrew Hope, Tereza Jezkova, Anson Koehler, Jason Malaney, Fernando Torres-Perez, Peter Smouse, and Elizabeth Walkup.

**HISTORICAL AND TOPOGRAPHIC DRIVERS OF TROPICAL  
INSULAR DIVERSITY: COMPARATIVE PHYLOGEOGRAPHY  
OF *ELEUTHERODACTYLUS ANTILLENSIS* AND *E. PORTORICENSIS*,  
TWO ECOLOGICALLY DISTINCTIVE FROGS OF THE PUERTO RICAN  
BANK**

by

**Brittany Suzanne Barker**

**B.S., ZOOLOGY, OREGON STATE UNIVERSITY, 2003**

**PH.D., BIOLOGY, UNIVERSITY OF NEW MEXICO, 2012**

**Abstract**

Topographically complex islands present opportunities for *in situ* (within-island) allopatric speciation because of increased chances for isolation in separate mountain ranges, as well as greater opportunity for fragmentation by high sea levels and climate-driven changes in habitat distribution. Climatic oscillations of the Quaternary (Pleistocene – Holocene; ~2.5 million years ago to the present) may have influenced the severity of vicariant barriers among and within islands, yet how these events influenced evolution of tropical insular biota is not well understood. This dissertation explores the role of topographic complexity and climate-driven range shifts resulting from sea-level changes and habitat suitability in shaping genetic diversity of two *Eleutherodactylus* frogs (Anura: Eleutherodactylidae) in the Puerto Rican Bank, an archipelago in the eastern Caribbean Sea. Sea level changes significantly altered the size, area, and degree of isolation of terrestrial habitats in the Puerto Rican Bank, and habitat shifts may have occurred in the main island of Puerto Rico. Whereas the Mountain Coquí, *E.*

*portoricensis*, is restricted to cool and moist understory montane forest habitat in Puerto Rico, the Red-eyed Coquí, *E. antillensis*, is a habitat generalist with a broad elevational distribution on most of the larger islands of the Puerto Rican Bank. Hypotheses of population history were formulated using data from paleoenvironmental records and ecological niche models, and tested using a suite of population genetic, phylogenetic, and coalescent analyses of DNA sequence data. I show how basin barriers and Quaternary climatic fluctuations shaped the distribution of genetic diversity in *E. portoricensis* in the Luquillo and Cayey Mountains in eastern Puerto Rico, and how varying degrees of terrestrial connectivity and isolation influenced the persistence and colonization dynamics of *E. antillensis* across the Puerto Rican Bank. To infer whether climate-driven, historical shifts in distributions occurred in *E. portoricensis* and *E. antillensis*, this dissertation also compares patterns of genetic isolation and demography of these species in Puerto Rico, where elevational gradients may have accommodated range shifts during climatic extremes of the Quaternary. The collective findings of this dissertation improve our understanding of topographic and historic factors that promote population divergence and that ultimately produce regional patterns of biodiversity in tropical archipelagos.

## TABLE OF CONENTS

<b>CHAPTER 1 – Introduction</b> .....	1
References.....	7
<b>CHAPTER 2 – Deep intra-island divergence of a montane endemic: phylogeography of the Puerto Rican frog <i>Eleutherodactylus portoricensis</i> (Anura: Eleutherodactylidae)</b> .....	11
Abstract.....	11
Introduction.....	13
Materials and Methods.....	16
Results.....	26
Discussion.....	29
References.....	37
Figures and Tables.....	50
Supporting Information.....	58
<b>CHAPTER 3 – Sea level, topography, and island diversity: phylogeography of the Puerto Rican Red-eyed Coquí, <i>Eleutherodactylus antillensis</i></b> .....	69
Abstract.....	69
Introduction.....	71
Materials and Methods.....	74
Results.....	85



Discussion.....	89
References.....	97
Figures and Tables.....	110
Supporting Information.....	126

**CHAPTER 4 – Habitat stability as a driver of tropical insular diversity:**

**comparative phylogeography of *Eleutherodactylus antillensis* and *E. portoricensis*,**

**two ecologically distinctive Puerto Rican frogs..... 149**

Abstract.....	149
Introduction.....	151
Materials and Methods.....	156
Results.....	172
Discussion.....	179
References.....	189
Figures and Tables.....	207
Supporting Information.....	224

**CHAPTER 5 – Conclusion..... 230**

References.....	237
-----------------	-----

# CHAPTER 1

## Introduction

A major challenge in evolutionary biology is to understand the interplay between historical events, such as changes in climate and geology, and the ecological requirements of organisms, an interaction that determines contemporary patterns of diversity across the landscape. Tropical island systems provide natural laboratories to address this challenge. Species diversity in tropical archipelagoes is partially a result of competition and colonization–extinction dynamics and island characteristics such as size, relative isolation, and age (MacArthur & Wilson, 1967; Losos & Ricklefs, 2009b, a). Topographically complex islands present opportunities for *in situ* allopatric speciation because of increased isolation in separate mountain ranges, as well as greater opportunity for fragmentation by high sea levels and other geological events (Losos & Ricklefs, 2009a). Climatic oscillations of the Quaternary (Pleistocene – Holocene; ~2.5 million years ago to the present) regulated vicariant barriers among islands, and potentially within islands, yet how these events influenced evolution of endemic biota is not well understood. Exploring the historical processes of colonization and persistence in these ecosystems is important for understanding the potential sensitivity of endemic biodiversity to future climate change.

This dissertation explores the role of topographic complexity and climate-driven range shifts resulting from sea-level changes and habitat suitability in shaping genetic diversity of two frog species in the Puerto Rican Bank, an archipelago in the eastern Caribbean Sea. The Puerto Rican Bank is comprised of the main island of Puerto Rico

(8,768 km<sup>2</sup>; maximum elevation 1,338 m) and the “Eastern Islands,” (east of 65.6° W; *ca.* 340 km<sup>2</sup>; maximum elevation 500 m), which includes Vieques, Culebra, the Virgin Islands (St. Thomas, St. John, Tortola, Virgin Gorda, and Anegada), and more than 180 small cays east of Puerto Rico (Fig. 1A-B). The volcanic interior of the Puerto Rican Bank existed since the late Eocene to early Oligocene (van Gestel *et al.*, 1998), and continues to erode through the present-day (Monroe, 1968), providing a mountainous landscape in Puerto Rico. The complex topography of Puerto Rico may facilitate within-island allopatric speciation or climate-driven range shifts along elevational gradients. The Central Mountains, or Cordillera Central, is separated from the Luquillo Mountains in the northeast by the extensive Río Grande de Loíza Basin, which reaches a low point in the Caguas Basin (Fig. 1A).

The dynamic climatic history of the Puerto Rican Bank, coupled with increased opportunities for allopatric speciation in Puerto Rico, provide an excellent opportunity to test hypotheses concerning population persistence, diversification, and extinction. Sea level fluctuations of more than 100 m (Waelbroeck *et al.*, 2002; Siddall *et al.*, 2003; van Daele *et al.*, 2011) produced episodes of isolation or connectivity of populations in this archipelago. Lower sea level during the last glacial period *ca.* 118-12 kya led to varying degrees of connectivity between the Eastern Islands and Puerto Rico (Heatwole & MacKenzie, 1967). In contrast, higher sea level during interglacial periods fragmented the Eastern Islands. Although paleoclimatic data provide strong evidence for cyclical changes in climate in the Caribbean region during the Quaternary (Renken *et al.*, 2002), whether these changes were large enough to significantly influence gene flow and population demography is unclear. Species may have experienced elevational range shifts

in response to Quaternary cooling and warming and changing gradients in precipitation, as inferred for many species in the mainland Neotropics (Bush, 2002; Bush & Flenley, 2007). Alternatively, habitat shifts may have been minimal, and divergence events and past population demographics may be independent of glacial periodicity.

To explore biogeographic processes shaping diversity in the Puerto Rican Bank, I studied genetic diversification in two *Eleutherodactylus* (Anura: Eleutherodactylidae) frogs that are codistributed in Puerto Rico, but that have distinctive ecological requirements. The Mountain Coquí, *Eleutherodactylus portoricensis*, and the Red-eyed Coquí, *E. antillensis*, are small, primarily arboreal species that belong to a group of direct-developing (terraranid) frogs that comprise approximately 27% of the amphibians occurring in the New World tropics (Hedges *et al.*, 2008), and more than 80% of the amphibian diversity in the Caribbean (Hedges, 1999a). Standing water is not required for oviposition or development in either species (Duellman & Trueb, 1994), and therefore dispersal of all life-stages is not expected to be strongly associated with streams. A habitat specialist, *E. portoricensis* is restricted to cool and moist understory montane forest habitat in the Luquillo Mountains, Cayey Mountains, and the Central Mountains of Puerto Rico (Fig. 1A; Schwartz & Henderson, 1991). In contrast, *E. antillensis*, a habitat generalist with a broad elevational distribution (sea level to 1,219 m), occurs in most larger islands of the Puerto Rican Bank (except for Anegada; Henderson & Powell, 1999). The distinctive ecological requirements of these species are expected to influence whether topographic features constitute barriers to gene flow and how these species responded to past climate changes.

Chapter 2 explores how basin barriers and Quaternary climatic fluctuations shaped the distribution of genetic diversity in the montane forest specialist *E. portoricensis*. I tested the hypothesis that basins enhanced allopatric divergence between populations on different mountain ranges, and that disjunct populations in the Luquillo Mountains and the Cayey Mountains became isolated and began diverging during a warm interglacial period. I also tested for climate-driven demographic fluctuations with coalescent analyses and Bayesian skyline plots. My findings highlight the role of topographic complexity in promoting within-island vicariant divergence in Puerto Rico, and provide an example of long-term persistence and lineage diversification despite late Quaternary climatic oscillations.

Chapter 3 explores the role of climate change in shaping evolutionary patterns in archipelagoes by dissecting the role of fluctuating sea levels on intraspecific diversification in *E. antillensis*. I tested two hypotheses encompassing vicariance and dispersal narratives by sequencing one mtDNA locus and four nuDNA introns from populations spanning the entire Puerto Rican Bank. The Sea Vicariance Hypothesis proposes that Eastern Islands populations of *E. antillensis* persisted in a refugium in this region and began diverging from Puerto Rican populations during the penultimate interglacial [190–245 thousands of years ago (kya); Dutton *et al.*, 2009] or the last interglacial (119–130 ka; Siddall *et al.*, 2003; Hearty *et al.*, 2007; van Daele *et al.*, 2011). In contrast, the Eastern Dispersal Hypothesis posits that *E. antillensis* colonized the Eastern Islands region via the land-bridge between these two regions, with divergence from Puerto Rican populations occurring as sea-levels rose during the Holocene interglacial *ca.* 11 ka (Peltier, 2002). This chapter also infers if the *E. antillensis*

population on St. Croix, an island *ca.* 105 km southeast of the Puerto Rican Bank (Fig. 1C) that has never had a direct land connection with this archipelago (Gill *et al.*, 1989), originated from a human-mediated introduction to this island in 1937 (Grant & Beatty, 1944). Because the Sea Vicariance Hypothesis and Eastern Dispersal Hypothesis are concerned with historical processes of gene flow in the PRB, understanding the extent to which human transport has shaped the distribution of *E. antillensis* is critical.

Collectively, the results of this chapter show how varying degrees of connectivity and isolation interact to produce phylogeographic patterns in tropical island systems.

Chapter 4 is a comparative study that builds upon Chapters 2 and 3 to compare spatio-temporal patterns of genetic isolation and persistence in *E. portoricensis* and *E. antillensis*. The study is focused on Puerto Rico, where the mountainous landscape may provide opportunities for climate-driven elevational shifts in species distributions. I estimated ecological niche models under last interglacial *sensu stricto* (LIG; ~130 – 116 ka), last glacial maximum (LGM; ~21 ka), and current climates to visualize population connectivity and quantify changes in suitability over time. Relying on these models, I formulated hypotheses concerning the influence of late Quaternary climate change on gene flow, genetic diversity, and past population demographics. For *E. portoricensis*, the Cayey-Luquillo Refugia Hypothesis predicts deep differentiation between populations in the Cayey and Luquillo Mountains, with divergence dating to the LIG or earlier, due to complete geographic isolation resulting from unstable habitat in the Río Grande de Loíza Basin and surrounding coastal lowlands. For *E. antillensis*, the West-East Refugia Hypothesis predicts shallow differentiation between populations in western and eastern Puerto Rico due to partial geographic isolation resulting from unstable habitat in the Río

Grande de Loíza Basin and surrounding coastal lowlands. Additionally, I tested the hypothesis that population sizes of *E. antillensis* were more affected by late Quaternary climate change than *E. portoricensis* because this habitat generalist occupies a greater elevational range (sea level to 1219 m) and total habitat area than its montane specialist congener, and thus climate-driven habitat changes would have been more extensive. The three hypotheses were tested using population genetic and coalescent analyses of mtDNA and four nuDNA introns. This chapter demonstrates that spatially explicit analyses of historical connectivity and persistence in topographically complex islands can explain observed patterns of genetic endemism and diversity, as shown for tropical rainforest species in the Brazilian Atlantic forest (Carnaval *et al.*, 2009) and the Australian Wet Tropics (Bell *et al.*, 2010).

Chapter 5 provides a summary of the dissertation, highlights conservation implications for tropical insular organisms, and describes topics for further research to better understand the roles of climate change, topography, and anthropogenic land-use in shaping the distribution of diversity in the Puerto Rican Bank and other tropical archipelagos. This dissertation contributes fundamental information for decisions related to the management of dynamic insular systems and provides a foundation for further investigation into the structure of biological diversity in the tropics. In a world of accelerating environmental changes, a historical perspective on the accumulation of diversity can help guide research and conservation in complex tropical ecosystems.

## References

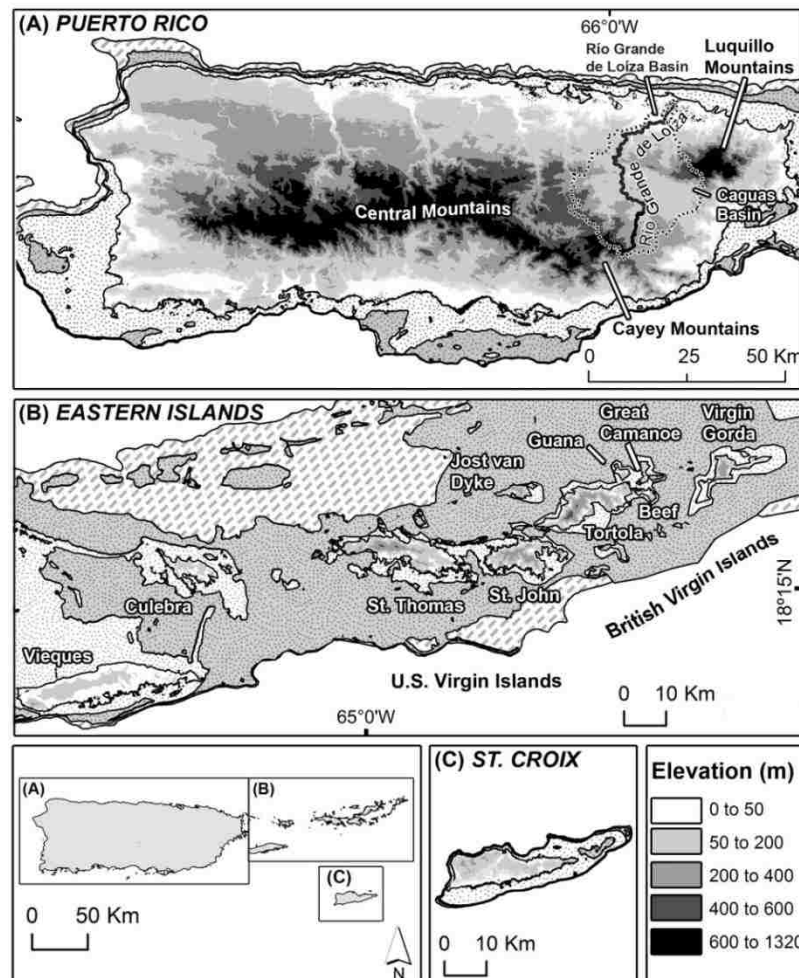
- Bell, R.C., Parra, J.L., Tonione, M., Hoskin, C.J., Mackenzie, J.B., Williams, S.E. & Moritz, C. (2010) Patterns of persistence and diversification indicate resilience to climate change in montane rainforest lizards. *Molecular Ecology*, **19**, 2531-2544.
- Bush, M.B. (2002) Distributional change and conservation on the Andean flank: a palaeoecological perspective. *Global Ecology & Biogeography*, **11**, 463-473.
- Bush, M.B. & Flenley, J.R. (2007) Tropical rainforest responses to climatic change. Springer, Berlin, Germany.
- Carnaval, A.C., Hickerson, M.J., Haddad, C.F.B., Rodrigues, M.T. & Moritz, C. (2009) Stability predicts genetic diversity in the Brazilian Atlantic forest hotspot. *Science*, **323**, 785-789.
- Duellman, W.E. & Trueb, L. (1994) *Biology of Amphibians*, 2nd edn. The John Hopkins University Press, Baltimore, MD.
- Dutton, A., Bard, E., Antonioli, F., Esat, T., Lambeck, K. & McCulloch, M.T. (2009) Phasing and amplitude of sea-level and climate change during the penultimate interglacial. *Nature Geoscience*, **2**, 355-359.
- Gill, I.P., Hubbard, D.K., McLaughlin, P. & Moore, C. (1989) Sedimentological and tectonic evolution of Tertiary St. Croix. In: *12th Caribbean Geological Conference* (ed. D.K. Hubbard), pp. 49-71, Teague Bay, St. Croix, West Indies Laboratory.
- Grant, C. & Beatty, H.A. (1944) Herpetological notes on St. Croix, Virgin Islands. *Herpetologica*, **2**, 110-113.



- Hearty, P.J., Hollin, J.T., Neumann, A.C., O'leary, M.J. & Mcculloch, M. (2007) Global sea-level fluctuations during the Last Interglaciation (MIS 5e). *Quaternary Science Reviews*, **26**, 2090-2112.
- Heatwole, H. & Mackenzie, F. (1967) Herpetogeography of Puerto Rico. IV. Paleogeography, faunal similarity and endemism. *Evolution*, **21**, 429-438.
- Hedges, S.B. (1999) Biogeography of the West Indies: an overview. *Biogeography of the West Indies: patterns and perspectives*, pp. 15-33. CRC Press, Boca Raton.
- Hedges, S.B., Duellman, W.E. & Heinicke, M.P. (2008) New World direct-developing frogs (Anura: Terrarana): molecular phylogeny, classification, biogeography, and conservation. *Zootaxa*, **1737**, 1-182.
- Henderson, R.W. & Powell, R. (1999) West Indian herpetoecology. *Caribbean amphibians and reptiles* (ed. by B.I. Crother), pp. 223-268. Academic Press, San Diego, CA.
- Losos, J.B. & Ricklefs, R. (2009a) Adaptation and diversification on islands. *Nature*, **457**, 830-836.
- Losos, J.B. & Ricklefs, R. (2009b) *The theory of island biogeography revisited*. Princeton University Press, Princeton, NJ.
- MacArthur, R.H. & Wilson, E.O. (1967) *The theory of island biogeography*. Princeton University Press, Princeton, NJ.
- Monroe, W.H. (1968) The age of the Puerto Rico Trench. *Geological Society of America Bulletin*, **79**, 487-494.
- Peltier, W.R. (2002) On eustatic sea level history: Last Glacial Maximum to Holocene. *Quaternary Science Reviews*, **21**, 377-396.

- Renken, R.A., Ward, W.C., Gill, I.P., Gómez-Gómez, F. & Rodríguez-Martínez, J. (2002) Geology and hydrogeology of the Caribbean islands aquifer system of the commonwealth of Puerto Rico and the U.S. Virgin Islands. *U.S. Geological Survey Professional Paper*, **1419**, 1-148.
- Schwartz, A. & Henderson, R.W. (1991) *Amphibians and reptiles of the West Indies*. University of Florida Press, Gainesville, FL.
- Siddall, M., Rohling, E.J., Almogi-Labin, A., Hemleben, C.H., Meischner, D., Schmelzer, I. & Smeed, D.A. (2003) Sea-level fluctuations during the last glacial cycle. *Nature*, **423**, 853-858.
- van Daele, M., van Welden, A., Moernaut, J., Beck, C., Audemard, F., Sanchez, J., Jouanne, F., Carrillo, E., Malavé, G., Lemus, A. & de Batist, M. (2011) Reconstruction of Late-Quaternary sea- and lake-level changes in a tectonically active marginal basin using seismic stratigraphy: the Gulf of Cariaco, NE Venezuela. *Marine Geology*, **279**, 37-51.
- van Gestel, J.-P., Mann, P., Dolan, J.F. & Grindlay, N.R. (1998) Structure and tectonics of the upper Cenozoic Puerto Rico-Virgin Islands carbonate platform as determined from seismic reflection studies. *Journal of Geophysical Research*, **103**, 30,505-30,530.
- Waelbroeck, C., Labeyrie, L., Michel, E., Duplessy, J.C., Mcmanus, J.F., Lambeck, K., Balbon, E. & Labracherie, M. (2002) Sea-level and deep water temperature changes derived from benthic foraminifera isotopic records. *Quaternary Science Reviews*, **21**, 295-305.

**Fig. 1** Map of the Puerto Rican Bank (A and B) and St. Croix (C) illustrating the topography of the islands. The outermost lines in A, B, and C indicate the approximate land configuration at maximum sea level lowering during the Last Glacial Maximum (*ca.* 26.5–19 kya). Diagonal dashes in A and B represent the approximate areas (–200 to 50 m) completely submerged *ca.* 14–10 kya; stippling on medium grey in A, B, and C represents areas (–50 to –25 m) submerged *ca.* 10–8 kya; and stippling on white in A, B, and C represents areas (–25 to 0 m) submerged *ca.* 8–6 kya. The Central Mountains forms the highland “backbone” of Puerto Rico, and are separated from the Luquillo Mountains in the northeast by the Río Grande de Loíza Basin, which reaches a low point in the Caguas Basin.



## CHAPTER 2

### **Deep intra-island divergence of a montane endemic: phylogeography of the Puerto Rican frog *Eleutherodactylus portoricensis* (Anura: Eleutherodactylidae)**

*This chapter was published in substantially similar form as* Brittany S. Barker, Robert B. Waide, and Joseph A. Cook. *Journal of Biogeography*, 38(12):2311-2325.

#### ABSTRACT

**Aim** Hypotheses proposed for lineage diversification of tropical montane species have rarely been tested within oceanic islands. Our goal was to understand how basin barriers and Pleistocene climatic fluctuations shaped the distribution of diversity in *Eleutherodactylus portoricensis* (Eleutherodactylidae), a frog endemic to montane rain forests of Puerto Rico.

**Location** The north-eastern (Luquillo) and south-eastern (Cayey) mountains of Puerto Rico.

**Methods** We generated mitochondrial DNA (mtDNA) control region sequences (*c.* 565 bp) from 144 individual *E. portoricensis* representing 16 localities, and sequenced 646 bp cytochrome *b* and 596 bp nuclear DNA (nDNA) rhodopsin exon and intron 1 from a subset of individuals. We conducted a phylogenetic analysis on the mtDNA sequence data and explored population substructure with maximum parsimony networks, a spatial

analysis of molecular variance, and pairwise  $F_{ST}$  analysis. Coalescent simulations were performed to test alternative models of population divergence in response to late Pleistocene interglacial periods. Historical demography was assessed through coalescent analyses and Bayesian skyline plots.

**Results** We found: (1) two highly divergent groups associated with the disjunct Luquillo and Cayey Mountains, respectively; (2) a shallow mtDNA genetic discontinuity across the La Plata Basin within the Cayey Mountains; (3) phylogeographic congruence between nDNA and mtDNA markers; (4) divergence dates for both mtDNA and nDNA pre-dating the Greenland Interstadial (*c.* 75 ka), and nDNA suggesting divergence prior to the penultimate interglacial (*c.* 245 ka); and (5) historical demographic stability in both lineages.

**Main conclusions** The low-elevation Caguas Basin is a long-term barrier to gene flow between the two montane frog populations. Measures of genetic diversity for mtDNA were similar in both lineages, but lower nDNA diversity in the Luquillo Mountains lineage suggests infrequent dispersal between the two mountain ranges and colonization by a low-diversity founder population. Population divergence began prior to the Greenland Interstadial. Stable population sizes over time indicate a lack of demonstrable demographic response to climatic changes during the last glacial period. This study highlights the importance of topographic complexity in promoting within-island vicariant speciation in the Greater Antilles, and indicates long-term persistence and lineage diversification despite late Pleistocene climatic oscillations.

## **Introduction**

The Greater Antilles, comprising Cuba, Jamaica, Hispaniola and Puerto Rico, form one of three primary island groups and constitute almost 90% of the land mass in the Caribbean Sea. Species diversity in this archipelago is partially a result of competition and colonization–extinction dynamics and island characteristics such as size, relative isolation and age (MacArthur & Wilson, 1967; Ricklefs & Bermingham, 2008; Losos & Ricklefs, 2009). However, topographical complexity may present additional opportunities for allopatric speciation when compared to the smaller islands of the Lesser Antilles (reviewed in Losos & Ricklefs, 2009). Indeed, recent studies have shown that vicariant processes within particular islands may play a larger role in shaping Caribbean diversity than previously thought (e.g. Gifford & Larson, 2008; Jezkova *et al.*, 2009; Rodríguez *et al.*, 2010), with some species exhibiting genetic breaks across arid, low-elevation basins, such as those found in Puerto Rico and Hispaniola (Velo-Antón *et al.*, 2007; Gifford & Larson, 2008).

Climatic oscillations during the Pleistocene have played a role in shaping montane Caribbean diversity by affecting the severity of vicariant processes. Disjunct montane rain forest species may have repeatedly expanded downslope and connected during periods of global cooling and retreated to isolation during warm interglacials, providing potential opportunities for both genetic differentiation and gene flow. Some phylogeographic studies in the mainland Neotropics suggest demographic responses to Pleistocene climate-induced change in forest cover (e.g. Graziotin *et al.*, 2006; Cabanne *et al.*, 2007; Carnaval & Bates, 2007; Streicher *et al.*, 2009). However, palynological data (e.g. Colinvaux *et al.*, 2000), patterns of species distribution (Lomolino *et al.*, 2006),

phylogenetic (Rull, 2008), and coalescent studies (Lessa *et al.*, 2003; Elmer *et al.*, 2007) indicate that past climate change in the Neotropics did not significantly influence patterns of diversification or population demography (reviewed in Antonelli *et al.*, 2010).

There is substantial evidence that climate change occurring since the Last Glacial Maximum (LGM; 21 ka) altered the type and range of habitats in the Caribbean (Schubert, 1988; Orvis *et al.*, 1997; Renken *et al.*, 2002) and led to species extinctions or range shifts (Pregill & Olson, 1981). Within islands of the Greater Antilles, however, large genetic distances have been found between populations in adjacent habitats (e.g. Velo-Antón *et al.*, 2007; Rodríguez-Robles *et al.*, 2008; Rodríguez *et al.*, 2010), indicating long-term persistence and divergence events that occurred independently of Pleistocene glacial periodicity (Ricklefs & Bermingham, 2002; 2008; Cook *et al.*, 2008). The seeming lack of concordance of these data signifies that the role that Pleistocene climatic oscillations had on influencing diversification of Caribbean taxa is still largely an open question.

We studied the historical biogeography and consequences of palaeoenvironmental change on patterns of genetic diversity in the mountain coquí, *Eleutherodactylus portoricensis* Schmidt, 1927, a montane rain forest specialist in Puerto Rico (Fig. 1a–c). This small, terrestrial frog belongs to a group of direct-developing (terraranid) frogs that comprise approximately 27% of the amphibians occurring in the New World tropics (Hedges *et al.*, 2008) and over 80% of the amphibian diversity in the Caribbean (Hedges, 1999). The range of this species spans the Luquillo Mountains, Cayey Mountains and the Cordillera Central of Puerto Rico (Joglar, 1998). *Eleutherodactylus portoricensis* requires cool and moist understory montane forest habitat, cannot survive at temperatures

$\geq 30$  °C, and has a low dehydration tolerance (Beuchat et al., 1984; Stewart, 1995; Woolbright, 1997). In the Luquillo and Cayey Mountains, populations experience mean annual temperatures  $\leq 22$  °C and average annual precipitation  $\geq 2500$  mm per year (Daly et al., 2003). Although recorded at elevations as low as 450 m (Schwartz & Henderson, 1985), *E. portoricensis* has not been found below 600 m since the extirpation of the El Verde population (Luquillo Mountains) in the late 1980s (B.S. Barker, unpublished data; Woolbright, 1997).

First, we test the hypothesis that basins enhanced allopatric divergence between populations on different mountain ranges (the basin barrier hypothesis), specifically predicting that: (1) genetically differentiated populations will occur in the Luquillo and Cayey Mountains on opposite sides of the Caguas Basin, and (2) that the smaller La Plata Basin will promote localized differentiation between populations within the Cayey Mountains (Fig. 1c). The extensive Caguas Basin (0–645 m elevation;  $\geq 30$  km wide; Fig. 1c), has a mean annual temperature of 24–25 °C and average annual precipitation of 1500–2250 mm (Daly et al., 2003). Although higher and narrower than the Caguas Basin, the La Plata Basin (Fig. 1c; 430–645 m;  $\geq 8$  km wide) in the Cayey Mountains has a mean annual temperature of 22–23°C and average annual precipitation  $\leq 2500$  mm, and thus could have acted as a minor barrier to dispersal.

Second, we use coalescent simulations to assess the probability of alternative models of population history, with a specific focus on testing whether disjunct populations of *E. portoricensis* in the Luquillo and Cayey Mountains became isolated and began diverging during a warm interglacial period [i.e. the Holocene interglacial (c. 10 ka) or earlier]. Their narrow dehydration tolerance may have prevented subsequent gene



flow between separate montane populations during the LGM due to increased aridity in the lowlands of Puerto Rico (Renken *et al.*, 2002). If the lowlands were also arid during the Middle Pleniglacial (27–58 ka) and penultimate glacial (125–180 ka), similar to that inferred for particular lowland areas of the South American tropics (van der Hammen, 1974; González *et al.*, 2008; Hessler *et al.*, 2010), then populations that initially diverged during an early interglacial period such as the penultimate interglacial (245 ka) could have continued to persist in isolation.

Lastly, we examine the influence of late Pleistocene climate change on population demography of *E. portoricensis*. Because this species is sensitive to changes in both temperature and moisture, we test the prediction that population expansion in the Luquillo and Cayey Mountains occurred during the Middle Pleniglacial, a time period in which high-resolution pollen data from north-eastern Venezuela indicates that tropical montane forest expanded (González *et al.*, 2008; Hessler *et al.*, 2010), and was followed by population contraction during the arid LGM as montane forests in Puerto Rico shifted upslope (Renken *et al.*, 2002). Awareness of the interplay between past climatic cycles and landscape features will ultimately improve our comprehension of diversification and speciation in the Neotropics.

## **Materials and Methods**

### *Sample collection*

We obtained toe-clip samples from 144 *E. portoricensis* individuals from the Luquillo Mountains (LUQ; 10 localities) and Cayey Mountains (CAY; six localities) during the summer of 2007–2008 (Fig. 1c, Table S1, Supporting Information; an average of nine

individuals per locality, range 2–15). Frogs were hand-captured in the field using clean plastic bags, measured (snout–vent and tibia lengths), and photographed. Due to its sensitive conservation status, we did not collect traditional voucher specimens. Despite extensive search effort at nine historical localities across the Cordillera Central, no additional populations were found (Fig. 1b), suggesting that populations in this region are either extremely reduced or have undergone recent extirpation (B.S. Barker, unpublished data). Toe-clips were stored in 95% ethanol at – 80 °C at the Division of Genomic Resources, Museum of Southwestern Biology, University of New Mexico.

#### *DNA sequence data*

Three different data sets were used in the analyses. First, phylogeographic and historical demographic analyses used the mitochondrial (mtDNA) control region (CR) data set (*c.* 565 bp) for 144 individuals of *E. portoricensis* representing 16 localities across their known range (LUQ, *n* = 73; CAY, *n* = 71; Fig. 1c; Table S1, Supporting Information). Second, a fragment of the mtDNA cytochrome *b* gene (*cyt b*: 646 bp) was sequenced from a subset of 36 individuals (Table S1, Supporting Information), representing three randomly chosen individuals from each locality in order to conduct coalescent simulations and to further resolve phylogenetic relationships. For an independent perspective on population history, we also sequenced a 596 bp fragment of the nuclear DNA (nDNA) rhodopsin (*RHI*) exon (362 bp) and intron 1 (234 bp) from this subset. This locus has shown potential for studies of differentiated lineages of amphibians (e.g. Zheng *et al.*, 2009; Shimada *et al.*, 2011).

DNA was extracted in a total volume of 30  $\mu$ L using a modified CTAB/PVP (cetyl trimethylammonium bromide/polyvinylpyrrolidone) – chloroform/isoamyl alcohol DNA extraction technique (Stewart & Via, 1993; M. Perdue, unpublished data). We amplified the mtDNA CR using primers ControlWrev-L and ControlP-H (Goebel *et al.*, 1999) and the *cyt b* gene using primers MVZ 15 and MVZ 16 (Moritz *et al.*, 1992). *RHI* sequences were obtained using species-specific forward primer Eleu.Rhod-F and reverse primer Rho-4b (see Table S2, Supporting Information, and Zheng *et al.*, 2009 for primers).

Polymerase chain reactions (PCRs) contained approximately 50 ng of template DNA, 10  $\mu$ M of each primer, 10 mM dNTP, 25 mM MgCl<sub>2</sub>, 2  $\mu$ L of 10 $\times$  polymerase reaction buffer and 0.20 unit of AmpliTaq Gold *Taq* polymerase (Applied Biosystems, Foster City, CA, USA) and adjusted to a final volume of 15  $\mu$ L with ddH<sub>2</sub>O. Thermal-cycling profiles for all loci are described in Table S2, Supporting Information. PCR products were electrophoresed on a 0.8% agarose gel stained with ethidium bromide and purified using polyethylene glycol precipitation. Sequencing reactions were conducted using the BigDye Terminator v3.1 Cycle Sequencing Kit (Applied Biosystems) and cleaned with ethanol precipitation. For sequencing the CR, we used species specific primers (Table S2, Supporting Information). Sequences were edited with SEQUENCHER 4.5 (Gene Codes Corporation, Ann Arbor, MI, USA) and aligned using default settings in MUSCLE 3.7 (Edgar, 2004) via the European Bioinformatics Institute web services (<http://www.ebi.ac.uk/Tools/webservices/>). All sequences are deposited in GenBank, under accession numbers listed in Table S2, Supporting Information. The alignments and

Bayesian trees were deposited in TreeBase (<http://www.treebase.org>) with accession number S11623.

Heterozygote sites in *RHI* were identified when two different nucleotides were present at the same position in electropherograms of both strands, with the weakest peak reaching at least 25% of the strongest signal. We used the program PHASE 2.0.2 (Stephens *et al.*, 2001; Stephens & Donnelly, 2003) to infer (phase) the haplotypes of individuals that were polymorphic for more than one segregating site. We ran the algorithm five times, keeping the results of the run that yielded the best goodness-of-fit to an approximate coalescent model. All analyses were run for 1000 iterations with a single thinning interval and 100 burn-in iterations. Independent runs from different starting seeds produced equivalent results, with high probabilities of non-singleton base calls (> 0.90 posterior probability) for all sequences.

A major assumption of phylogeographic analyses is that there has been no selection and no recombination within a locus since the time of coalescence of the gene copies under study. For the coding *cyt b* locus and *RHI* exon, we tested for selection by conducting McDonald–Kreitman (MK) tests (McDonald & Kreitman, 1991), comparing ratios of fixed and polymorphic synonymous and non-synonymous substitutions within and between LUQ and CAY. The MK test did not reject neutrality for the *cyt b* and *RHI* loci. To investigate the possible role of recombination in shaping genetic patterns in *RHI*, we estimated recombination metrics MaxChi (Maynard Smith, 1992) and pairwise homoplasmy index (Bruen *et al.*, 2006) in the program RDP3 (Martin *et al.*, 2010) and SPLITSTREE 4.11.3 (Huson & Bryant, 2006), respectively. We also estimated the minimum number of recombination events (*RM*) through the use of the four-gamete test

(Hudson & Kaplan, 1985) in DNASP 5.10 (Librado & Rozas, 2009). None of these tests detected a signature of recombination.

### *Phylogenetic analyses*

Two data partitions (cyt *b* and CR) were analysed separately and as a concatenated dataset. Phylogenies were first rooted with the sister species, *Eleutherodactylus wightmanae*, and the closely related *Eleutherodactylus coqui* (Heinicke *et al.*, 2007). Because divergent outgroups can confound phylogenetic analysis due to homoplasy (Brandley *et al.*, 2009), we also used mid-point rooting (Hess & De Moraes Russo, 2007). All phylogenies were based on maximum parsimony (MP), maximum likelihood (ML), and Bayesian algorithms. An incongruence length difference (ILD) test (Farris *et al.*, 1995) performed in PAUP\* 4.10b (Swofford, 2003) indicated that the sequences from the CR and cyt *b* markers contained congruent phylogenetic signal (2000 replicates,  $P = 0.758$ ). We used MODELTEST 3.7 (Posada & Crandall, 1998) to select the best-fit model of nucleotide substitution based on Akaike's information criterion (AIC) values for all datasets.

ML analyses were performed with GARLI 0.960 (Zwickl, 2006) using the CIPRES Portal 2.1 (<http://www.phylo.org/portal2>) and employing the model supported by MODELTEST (GTR + I). Two searches were performed to ensure convergence. Using PAUP\*, we performed MP analyses through heuristic searches using 1000 random addition sequence replicates involving tree bisection and reconnection (TBR) branch swapping. Transversions and transitions were treated equally and gaps were treated as a

5<sup>th</sup> state. For both analyses, support was evaluated using 1000 bootstrap replicates (Felsenstein, 1985).

We employed a Bayesian approach to phylogeny reconstruction implemented in MRBAYES 3.1.2 (Huelsenbeck & Ronquist, 2001). The Metropolis-coupled Markov chain Monte Carlo (MCMC) sampling was performed using the model supported by MODELTEST and running four chains for 10,000,000 generations, with default parameters as starting values and sampling every 1000 generations. We discarded 2500 trees as burn-in after checking for stationarity and convergence of the chains with the software TRACER 1.5 (Rambaut & Drummond, 2007). Bayesian posterior probabilities (BPP) were obtained from the 50% majority rule consensus of the remaining trees. Lastly, we generated maximum parsimony networks to portray relationships among haplotypes of CR and *RHI* sequences with NETWORK 4.2 (<http://www.fluxus-technology.com>).

#### *Analysis of genetic structure*

Population genetic summary statistics for each locus, including haplotype ( $h$ ) and nucleotide ( $\pi$ ) diversity and mean pairwise nucleotide differences ( $k$ ), were calculated in ARLEQUIN 3.1 (Excoffier *et al.*, 2005). Population genetic substructure was quantified using only mtDNA CR sequence data. To infer potential barriers across the landscape, we used SAMOVA 1.0 (Dupanloup *et al.*, 2002) to define groups of populations that were geographically homogenous and maximally differentiated from each other. SAMOVAs were performed using pairwise differences  $F$  for a varying number of groups ( $K$ ). Identification of the most probable number of groups was based on the pattern of changes in values of  $F$ -statistic parameters with  $K$ . We used ARLEQUIN to obtain variance

components of the different structures using 10,000 permutations and the fixation index  $F_{ST}$  (Wright, 1951) was computed for pairs of subregions separated by hypothesized barriers (Caguas Basin and La Plata Basin; Fig. 1) with statistical significance tested using 10,000 permutations.

### *Coalescent simulations*

If climate warming during interglacial periods promoted population divergence of the present-day LUQ and CAY lineages, we would predict the distribution of mtDNA and nDNA diversity to reflect relatively recent subdivision from a single glacial-age population. We used coalescent simulations (Kingman, 1982; Hudson, 1992) to test divergence times by setting branch lengths between nodes to be coincident with timing of transitions between recent major glacial–interglacial and glacial interstadial periods: 245 ka (penultimate interglacial; Dutton *et al.*, 2009; Hypothesis 1, or H1), 130 ka (Eemian interglacial; McCulloch *et al.*, 1999; Muhs *et al.*, 2002), 75 ka (Greenland Interstadial 20; González *et al.*, 2008; Hessler *et al.*, 2010; H3), and 10 ka (Holocene interglacial; Renken *et al.*, 2002; H4). We generated four population models that differed in timing of lineage diversification but maintained a two-divergence tree structure (Fig. 2).

Because each branch of the population model requires an estimate of total effective population size ( $N_e$ ), we used both the concatenated mtDNA dataset and the nDNA dataset to estimate  $\theta$  (effective population size scaled by the mutation rate) using a coalescent approach in the program LAMARC 2.1.3 (Kuhner, 2006). Because LAMARC assumes that individuals are drawn from panmictic subpopulations (Kuhner, 2006), and gene flow among LUQ and CAY is non-existent, we estimated  $\theta$  separately for each

lineage and calculated the sum of the effective population sizes for each to avoid obtaining unrealistically high values of  $N_e$ . With the exception of the GTR model available for the LUQ mtDNA dataset, models chosen by MODELTEST were not available in LAMARC; therefore, we chose to employ the F84 model for the remaining datasets. Our search strategy in LAMARC was composed of 10 initial chains and two long final chains, and transition/transversions ratios (calculated in PAUP\*) for the concatenated mtDNA dataset and *RHI* dataset of 9.041 and 1.0 for LUQ, and of 12.754 and 5.073 for CAY, respectively. The initial chains were performed with 500 samples and a sampling interval of 20 (10,000 steps), using a burn-in of 1000 samples for each chain. The two final chains had the same burn-in and interval sampling, but with 10,000 samples (200,000 steps). Point estimates of  $\theta$ , as well as the 95% upper and lower confidence intervals (CI) (100 replicates), were calculated. We assumed  $\mu = 1.91 \times 10^{-8}$ , based on model-corrected terraranid frog mtDNA sequence divergence rates (Crawford, 2003), and calculated  $N_e$  using the equation  $\theta = 2N_e\mu$ . We set the 'Relative mutation rate' option in LAMARC to 1 for mtDNA and 0.0625 for *RHI* based on estimates that rates of divergence in terraranid frog mtDNA is 16 times faster than nDNA (Crawford, 2003). We therefore assume that our study species has comparable DNA divergence rates to those estimated by Crawford (2003). Lastly, we set the relative effective population size to 1 and 4, respectively, so that joint  $\theta$  estimates were reported using the mtDNA scale. Because the mutation rate was calculated relative to mtDNA, we used the mtDNA mutation rate to calculate  $N_e$  from the 'overall  $\theta$ '.

In MESQUITE 2.72 (Maddison & Maddison, 2008) the neutral coalescence of gene sequences was simulated within each of temporal hypotheses (H1, H2, H3, H4; Fig. 2)



using the model of DNA evolution selected via the AIC in MODELTEST. Models were as follows: concatenated mtDNA – GTR + I, base frequencies (A: 0.3053, C: 0.2481, G: 0.1225, T: 0.3241), rate matrix (7.3165, 77.8370, 7.8965, 13.4472, 57.1998, 1.00), proportion of invariant sites (0.8660), scaling factor ( $2.5 \times 10^{-8}$ ); *RHI* – HKY + I, base frequencies (A: 0.2049, C: 0.2269, G: 0.2272, T: 0.3410), proportion of invariant sites (0.9559), transition/transversions (Ti/Tv) ratio (2.541), scaling factor ( $1.5 \times 10^{-8}$ ). To ensure that the characteristics of the simulated data were as realistic as possible, we used various scaling factors for each marker until mean sequence divergences within lineages were approximately equivalent between empirical and simulated data. Because a null hypothesis of population stability could not be rejected (see Results), the effective population size ( $N_e$ ) was held constant through time. Branch widths were adjusted to reflect relative proportions of effective population size in both lineages (LUQ=0.41 and CAY=0.59). Five hundred gene matrices were simulated for each hypothesis at three values of  $N_e$  for the mtDNA (48471, 66340, 94762) and the nDNA (193885, 265361, 379047), corresponding to the 95% lower CI, point estimate, and 95% upper CI of the parameter  $\theta$ , and using a generation length of 2 years. This assumed generation time is based on studies of the closely related *E. coqui* (Stewart & Woolbright, 1996). Differences in  $N_e$  reflect that the number of heritable copies in the population is 1/2N for haploid mtDNA and 2N for autosomal nDNA.

We estimated simulated genealogies in PAUP\* using heuristic parsimony searches with 10 random addition replicates, TBR branch swapping and max-trees set to 100. Each search produced majority-rule consensus trees, from which we calculated  $s$  (Slatkin & Maddison, 1989), a measure of discord between the reconstructed gene tree and the

assignment of individuals into separate lineages. Higher values of  $s$  for a specific locus would indicate that sequences are paraphyletic with respect to their lineage association, a possible indication of either gene flow or incomplete lineage sorting. The distribution of test statistics for the simulated trees were compared (in MESQUITE) with the values of the empirical gene tree and were considered to be significant if found to be less than 5% of the values generated at random.

### *Historical demography*

Evidence of historical changes in population size in all loci was explored with Fu's  $F_S$  (Fu, 1997) and the  $R_2$  statistic (Ramos-Onsins & Rozas, 2002) in DNASP (Librado & Rozas, 2009). Large negative values of  $F_S$  and small positive values of  $R_2$  are indicative of population growth.  $R_2$  has higher power for small samples, in our case *cyt b* and *RHI*, while Fu's  $F_S$  test is better for large samples sizes such as our CR data (Ramos-Onsins & Rozas, 2002). For each test we assessed significance by generating null distributions from 10,000 coalescent simulations of a neutrally evolving, large population of constant size.

To further explore changes in demographic growth over the history of each major lineage, we employed the Bayesian skyline method (Drummond *et al.*, 2005) as implemented in BEAST 1.5.3 (Drummond *et al.*, 2002; Drummond & Rambaut, 2007) using the CR data. This coalescent-based approach estimates the posterior distribution for effective population size at intervals along a phylogeny, thereby allowing inferences of population fluctuations over time. We performed separate analyses for each major lineage, and selected the model of nucleotide substitution using MODELTEST. We used an uncorrelated logarithmic relaxed clock method ( $\mu = 1.91 \times 10^{-8}$ ) and applied five grouped

coalescent intervals ( $m$ ). We ran the analysis multiple times with different numbers of coalescent intervals (2–10) and found that a value of five resulted in an effective sample size (ESS) > 200 for all parameters, indicating good mixing and appropriately small standard deviations. Simulated genealogies and model parameters were sampled every 1000 generations for 50 million generations with 10% of the initial samples discarded as burn-in. TRACER was used to visualize plots, check for appropriately large ESS values, and check for convergence of results and performance of operators.

## Results

### *Phylogenetics*

Concatenation of the two mtDNA gene fragments for 36 individuals resulted in 30 unique haplotypes that were 1211 bp in length, of which 102 characters were variable (four sites in the CR sequence data had indels) and 63 were parsimony informative. The consensus Bayesian tree (harmonic mean  $-\ln L = 2747.73$ ), ML tree ( $-\ln L = -2584.38$ ), and MP trees (tree length = 149, consistency index = 0.636, retention index = 0.910, rescaled consistency index = 0.582) inferred that samples from LUQ are reciprocally monophyletic to a clade containing samples from CAY (MP bootstrap = 100%; ML bootstrap = 100%; BPP = 1.0; Fig. 3). The outgroup-rooted trees (not shown) indicate that samples from LUQ do not form a monophyletic group and that monophyly of the CAY group has lower support than it does in the mid-point rooted phylogeny (MP bootstrap = 75%; ML bootstrap = 69%; BPP = 0.65). These results may be due to very long branches to the highly divergent outgroup species, *E. wightmanae* and *E. coqui*, relative to branches within the ingroup (Rota-Stabelli & Telford, 2008; Brandley *et al.*,

2009). Intralocus diversity was high, as indicated by relatively high haplotype and nucleotide diversity values (Table 1), and no haplotypes were shared between lineages for any of the loci.

### *Genetic structure*

The CR dataset had 89 variable sites and contained a total of 75 unique haplotypes. The MP network of the CR data depicted two main clusters separated by 15 mutational steps (Fig. 4), corresponding to the LUQ and CAY clades inferred by phylogenetic analyses (Fig. 3). The network also defined a minor group (Fig. 4), containing all but one of the Cerro de la Tabla haplotypes, that was separated by 1–6 mutational steps from Carite State Forest haplotypes. This group was almost completely composed of unique haplotypes, although most exhibited shallow differentiation. Average number of nucleotide differences between LUQ and CAY samples in the CR sequence dataset was 23.4, which yields a Tamura–Nei corrected genetic distance (Tamura & Nei, 1993) of 4.4%.

The nDNA *RHI* exhibited substantially less variation (1.8%) than the mtDNA CR (15%) and *cytb* (5.0%). There were 11 variable sites (no indels) and 12 unique haplotypes (Table 1). With no shared haplotypes between LUQ and CAY, there is a clear signature of allelic partitioning into separate montane regions (Fig. 4). Only two haplotypes separated by a single mutational step were recovered from LUQ. In contrast, geographic structure was substantially higher in CAY.

When  $K = 2$ , SAMOVA partitioned LUQ (i.e. sites 7–16) and CAY (i.e. 1–6) groups and the maximum value of  $F_{CT}$  was inferred ( $F_{CT} = 0.69$ ,  $P < 0.001$ ; Table S3,

Supporting Information). The highest degree of genetic variation was explained by differences between groups (68.83%,  $P < 0.001$ ), followed by within populations (26.65%,  $P < 0.001$ ), and lastly by among populations (4.52%,  $P < 0.001$ ). Cerro de la Tabla (sites 1–3) samples were in the same group through all  $K$  values, suggesting strong geographic association of haplotypes from this subregion. Pairwise  $F_{ST}$  estimates for all subregions separated by a hypothesized basin barrier were significantly large at the  $P < 0.001$  level, ranging from 0.23 to 0.75 (Table S4, Supporting Information).

#### *Coalescent simulations*

Empirical estimates of  $s = 1$  and  $s = 2$  were obtained from the mtDNA and nDNA genealogy of *E. portoricensis*, respectively. Both mtDNA and nDNA were consistent with a model of divergence dating to as early as the penultimate interglacial (H1; Table 2). However, a deeper fragmentation event was inferred for nDNA in comparison to mtDNA. While nDNA simulations could reject all models under mean values of  $N_e$ , mtDNA simulations could not reject the model involving divergence during the penultimate interglacial (H1).

#### *Historical demography*

The mtDNA data showed signatures of population expansion for both LUQ and CAY, although these results were not congruent across statistics (Table 1). When applied to the nuclear data, neither Fu's  $F_s$  nor  $R_2$  detected demographic changes in either lineage.

BSPs analyses showed no sudden change in effective population size for LUQ and CAY

lineages (Fig. 5), indicating that the climatic changes during the last glacial period did not influence the demography of *E. portoricensis*.

## **Discussion**

### *Basins as long-term barriers for an island montane endemic*

Large mtDNA genetic distances and reciprocal monophyly between populations of *E. portoricensis* on adjacent mountain ranges, coupled with a lack of recent gene flow at the nDNA locus indicate that the Caguas Basin has acted as a strong barrier to gene flow (Figs 3 & 4) and supports our basin barrier hypothesis. LUQ and CAY populations had significantly high  $F_{ST}$  values, ranging from 0.749 to 0.667 (Table S4, Supporting Information), with the highest amount of genetic variation explained by separation of these montane groups (Table S3, Supporting Information).

Although less extreme in elevation and width in comparison to the Caguas Basin, the La Plata Basin within CAY (Fig. 1c) appears to also have acted as a historical barrier to dispersal. A close association between the subregions of Carite State Forest and Cerro de la Tabla was evident in the form of a single shared mtDNA CR haplotype (Table S3, Supporting Information), and suggests that the La Plata Basin has not completely prevented gene flow or has existed only as a recent barrier (Fig. 4). Lower levels of mtDNA genetic diversity found in the Cerro de la Tabla subregion may reflect increasing isolation of this relatively small mountain peak during the Holocene.

### *Persistent isolation throughout climatic oscillations of the late Pleistocene*

Climatic oscillations during the Pleistocene may have played a role in shaping genetic diversity of *E. portoricensis* by affecting the strength of basin barriers. Throughout at least the latest portion of the Quaternary (2.6 Ma to present day), Caribbean islands experienced episodic warm interglacial periods (Graham, 2003; González *et al.*, 2008) that could have led to isolation and divergence of populations of montane species. The mountains of Puerto Rico may have been elevational refugia; while climate cooling allowed persistence at lower elevations, rising temperatures during interglacials could have restricted distributions to higher elevation fragments of montane rain forest (Streicher *et al.*, 2009). For *E. portoricensis*, currently disjunct LUQ and CAY populations do not appear to have persisted at lower elevations during the LGM.

The distribution of genetic diversity in mtDNA and nDNA loci demonstrates that an extrinsic barrier to gene flow, the Caguas Basin, is probably responsible for phylogeographic structure of *E. portoricensis*, and that levels of genetic diversity within each of the mountain ranges and the relative timing of lineage divergence varied across loci (Tables 1 & 2). Results of the mtDNA coalescent simulations indicate that a penultimate interglacial (H1) origin of the LUQ and CAY lineages best explains the observed variation (Table 2), and results of the nDNA coalescent simulations indicate that divergence occurred prior to the penultimate interglacial. A divergence occurring as early as the penultimate interglacial is plausible: although the following Penultimate Glacial period was cool, it was probably also very dry (Luo *et al.*, 2005). Pollen evidence from the northern Andes in South America suggests a decline in forest environments at the terminal stage of this glaciation (van der Hammen, 1974). *Eleutherodactylus portoricensis* is active at temperatures as low as 15 °C, but its tolerance to desiccation

varies little with temperature (Beuchat *et al.*, 1984), and therefore a paucity of moist forest at low elevations during cool and dry glacial periods may have prevented population persistence. The following warm and humid Eemian interglacial was accompanied by a rapid *c.* 6 °C increase in sea-surface temperatures (McCulloch *et al.*, 1999; Dutton *et al.*, 2009) that were slightly warmer than at present (Muhs *et al.*, 2002) and *E. portoricensis* populations could have continued to diverge. A high-resolution pollen record during the Middle Pleniglacial (28–68 ka) from north-eastern Venezuela suggests that while enhanced orographic precipitation during Greenland Stadials promoted the expansion of tropical montane forests, dry forests and savanna again predominated in the lowlands (González *et al.*, 2008; Hessler *et al.*, 2010). Data from fossils, pollen, eolianite deposits, and geomorphic features indicate that temperatures in the Caribbean during the LGM were about 4.5 °C lower and climate was substantially more arid than in the present day (Schubert, 1988; Orvis *et al.*, 1997; Guilderson *et al.*, 2001), there was greater highland cooling than at sea level (Roy & Lachniet, 2010), and lowland habitats in Puerto Rico were dominated by dry forest that may have extended further upslope (Renken *et al.*, 2002). This climatic evidence, in combination with coalescent simulation results of both mtDNA and nDNA, strongly suggests that the Caguas Basin during the LGM was unsuitable for *E. portoricensis* population persistence. Because the mountains of LUQ were probably connected to CAY by high elevations until the Pliocene, when drainage alterations eroded less resistant rocks (Meyerhoff, 1933), the presently disjunct lineages may have begun diverging earlier than the dates selected for our simulations.



Although mtDNA lineages of *E. portoricensis* are strongly differentiated within both mountain ranges (Figs 3 & 4), differentiation in the nDNA *RHI* dataset within CAY is substantially higher than in LUQ (Fig. 4), a pattern that could not be explained by selection (see the results of the MK test). Therefore, we conclude that the distribution of diversity at the mtDNA and nDNA loci could be a reflection of different demographic histories. A history involving rare contact and infrequent dispersal between LUQ and CAY populations, with the LUQ lineage originating through colonization by a low-diversity founder population followed by population expansion, is reasonable and compatible with the results of phylogeographic analyses. Contrasting signals of gene flow at mtDNA and nDNA loci may in part be explained by the higher mutation rate of mtDNA and four-fold difference in  $N_e$  between the genomes. The faster mutation rate and smaller  $N_e$  of mtDNA would allow rapid lineage sorting, resulting in loss of low frequency haplotypes carried into a population by immigrants. Conversely, the relatively slow mutation rate and larger  $N_e$  of nDNA would permit incoming alleles to persist for longer and potentially increase in frequency before they could be lost via stochastic sorting. While a lack of strong nuclear differentiation within LUQ in combination with strong mitochondrial differentiation may reflect male-biased dispersal (Lampert *et al.*, 2003), this explanation should be rejected due to the deeper divergence date inferred for nDNA relative to mtDNA (Table 2). Moreover, sex-biased dispersal does not occur in adults of the closely related *E. coqui* (Woolbright, 1985); adults of both sexes rarely disperse horizontal distances more than 6 m during a night unless their home range becomes inhospitable (Stewart & Woolbright, 1996). The dispersal capabilities of *E.*

*portoricensis* are undocumented, but populations are patchy (Woolbright, 1997; B.S. Barker, pers. obs.).

For single-island endemics in the Greater Antilles, secondary contact between previously isolated populations has primarily been reported for lowland and/or widespread species (e.g. Velo-Antón *et al.*, 2007; Gifford & Larson, 2008; Rodríguez-Robles *et al.*, 2008) rather than montane species (Rodríguez *et al.*, 2010). In Puerto Rico, deeply differentiated eastern and western lineages of the widespread Puerto Rican *E. coqui* probably persisted in mesic forest refugia throughout the Pleistocene, separated by the arid Rio de Loíza Basin, and only recently attained secondary contact (Velo-Antón *et al.*, 2007). In contrast, there is no evidence that divergent lineages of *Eleutherodactylus auriculatus* in the mountains of Eastern Cuba came into secondary contact during recent glacial periods (Rodríguez *et al.*, 2010), which is more similar to *E. portoricensis*. For mainland terraranid frogs, the formation of divergent lineages has also been attributed to geographic barriers, with limited or no connectivity during late Pleistocene climatic oscillations (Crawford *et al.*, 2007; Elmer *et al.*, 2007; Wang *et al.*, 2008; Streicher *et al.*, 2009). Our study and others (Velo-Antón *et al.*, 2007; Rodríguez *et al.*, 2010) suggest that montane *Eleutherodactylus* lineages effectively persisted in isolation through multiple glacial episodes. Detailed acoustic, ecological and morphological analyses would contribute to the delineation of species boundaries within *E. portoricensis*.

#### *Population demographics*

We did not find genetic signatures of population expansion in *E. portoricensis* in response to climatic oscillations of the late Pleistocene. The non-genealogical statistics

(Fu's  $F_S$  and  $R_2$ ) inferred inconsistent results across loci: signals of expansion were inferred for mtDNA but not for nDNA. Fu's  $F_S$  and  $R_2$  may be non-significant for the *RHI* locus because they become less sensitive with increasing time since the expansion event (Ramos-Onsins & Rozas, 2002), but the BSP analyses of CR data also agreed with a result of no demographic expansion (Fig. 5). Our BSPs differ from those inferred for the co-distributed *E. coqui*, which show a pronounced decline during the LGM followed by a rapid increase during the Holocene (Velo-Antón *et al.*, 2007). Although some investigations of Caribbean fossils attribute range shifts to climatic changes occurring during the late Pleistocene (Pregill & Olson, 1981; Pregill *et al.*, 1994), results for *E. portoricensis* are more in line with molecular studies of Antillean taxa that did not find an association between population demographics and climatic history (Ricklefs & Bermingham, 2001, 2002; Cook *et al.*, 2008).

#### *Conservation implications*

Outstanding levels of biotic perturbation and extinction risk are predicted to occur under future climate change, yet data regarding vertical distributions, dispersal, and adaptive capacities are lacking for many species (La Sorte & Jetz, 2010). *Eleutherodactylus portoricensis* is classified as endangered (IUCN, 2010) and as vulnerable by the Department of Natural and Environmental Resources of Puerto Rico (Departamento de Estado, 2004). Long divergence times and demographic isolation among LUQ and CAY indicate independent evolutionary trajectories between these groups. Numerous populations have become extirpated within the past few decades (Woolbright, 1997; B.S. Barker, unpublished data) and face an uncertain future in light of changing environments.

Recent extirpation and population declines is attributed to the interacting effects of extended drought periods and the infectious disease chytridiomycosis, which has been detected in *E. portoricensis* populations in LUQ and CAY (Burrowes *et al.*, 2008; Longo & Burrowes, 2010). Known populations currently reside within protected areas; however, the small size, isolation, and close proximity to human settlements of the Cerro de la Tabla population may amplify the effects of habitat degradation and stochastic events such as hurricanes and droughts. Projections of future climate change in the northern Caribbean indicate an increase in rain production during the wet seasons, greater annual variability in rainfall and an increase of temperatures between 1 and 4 °C (Angeles *et al.*, 2007; Campbell *et al.*, 2010). Montane habitats are expected to be reduced in size as they shift upward, or disappear completely (UNEP-WCMC, 2009). Increased storms, particularly more intense hurricanes, and predicted increases in the frequency of droughts and/or flooding, are likely to significantly impact Caribbean forest ecosystems (Lewsey *et al.*, 2004). Although *E. portoricensis* populations in LUQ and CAY have apparently remained stable throughout previous glacial cycles, their low thermal tolerance, high sensitivity to desiccation, recent extirpations and declines, and current restriction to a few mountain peaks may make them particularly vulnerable to future climate change.

### **Acknowledgments**

Puerto Rican field collecting conducted by B.S.B was under Departamento de Recursos Naturales y Ambientales (DRNA) permit no. 08-EPE-006 and US Forest Service permit no. CNF-2081-01, obtained with help from A. Puente-Rolón and C. Krupp. W.F. Linero, A.R. Francesc, F. Pico-Bird; J.R. Snider, J. Fumero, and multiple Puerto Rican

undergraduates provided assistance in the field. We thank L.L. Woolbright, A. Puente-Rolón, F. Pico-Bird, W.A. Gould, J.P. Zegarra and R. Thomas for suggestions of localities to search for *E. portoricensis*. We acknowledge technical support from the University of New Mexico (UNM) Department of Biology's Molecular Biology Facility, supported by National Institutes of Health (NIH) Grant Number P20RR18754 from the Institute Development Award (IdeA) Program of the National Center for Research Resources, and University of Alaska Fairbanks Life Science Informatics, a core research resource supported by grant number RR016466 from the National Center for Research Resources (NCRR), a component of the NIH. We thank K. Galbreath, A. Hope, A. Koehler, and F. Torres-Perez for technical advice in phylogeographic analyses and M. Fleming, M. Ryan and the Cook lab group at UNM for reviewing earlier drafts of this manuscript. This manuscript benefited greatly from reviews by A. Crawford and two anonymous referees. For access to field supplies and curatorial support we thank T. Giermakowski in the Museum of Southwestern Biology. This research was supported in part by a grant from the Society for the Study of Amphibians and Reptiles Grants in Herpetology, the UNM Biology Department (Graduate Research Allocation Committee Grant; Grove Summer Research Scholarship), the UNM Office of Graduate Studies (Research Project and Travel Grant), and the UNM Graduate and Professional Student Association (Graduate Research and Development grant). Fieldwork was partially supported by National Science Foundation (NSF) Long Term Ecological Research Grant DEB-0218039 and DEB-0620910.

## References

- Angeles, M.E., Gonzalez, J.E., Erickson, D.J., III & Hernández, J.L. (2007) Predictions of future climate change in the Caribbean region using global general circulation models. *Journal of Climatology*, **27**, 555-569.
- Antonelli, A., Quijada-Mascareñas, A., Crawford, A.J., Bates, J.M., Velazco, P.M. & Wüster, W. (2010) Molecular studies and phylogeography of Amazonian tetrapods and their relation to geological and climatic models. *Amazonia, landscape and species evolution: a look into the past* (ed. by C. Hoorn and F. Wesselingh), pp. 386-404. Wiley-Blackwell, Oxford.
- Beuchat, C.A., Pough, F.H. & Stewart, M.M. (1984) Response to simultaneous dehydration and thermal stress in three species of Puerto Rican frogs. *Journal of Comparative Physiology*, **154**, 579-585.
- Brandley, M.C., Warren, D.L., Leaché, A.D. & McGuire, J.A. (2009) Homoplasy and clade support. *Systematic Biology*, **58**, 184-198.
- Bruen, T.C., Phillipe, H. & Bryant, D. (2006) A simple and robust statistical test for detecting the presence of recombination. *Genetics*, **172**, 2665-2681.
- Burrowes, P.A., Longo, A.V., Joglar, R.L. & Cunningham, A.A. (2008) Geographic distribution of *Batrachochytrium dendrobatidis* in Puerto Rico. *Herpetological Review*, **39**, 321-324.
- Cabanne, G., Santos, F.R. & Miyaki, C.Y. (2007) Phylogeography of *Xiphorhynchus fuscus* (Passeriformes, Dendrocolaptidae): vicariance and recent demographic expansion in southern Atlantic forest. *Biological Journal of the Linnean Society*, **91**, 73-84.

- Campbell, J.D., Taylor, M.A., Stephenson, T.S., Watson, R.A. & Whyte, F.S. (2010) Future climate of the Caribbean from a regional climate model. *International Journal of Climatology*, **31**, doi: 10.1002/joc.2200.
- Carnaval, A.C. & Bates, J.M. (2007) Amphibian DNA shows marked genetic structure and tracks Pleistocene climate change in northeastern Brazil. *Evolution*, **61**, 2942-2957.
- Colinvaux, P.A., De Oliveira, P.E. & Bush, M.B. (2000) Amazonian and neotropical plant communities on glacial time-scales: the failure of the aridity and refuge hypotheses. *Quaternary Science Reviews*, **19**, 141-169.
- Cook, B.D., Pringle, C.M. & Hughes, J.M. (2008) Molecular evidence for sequential colonization and taxon cycling in freshwater decapod shrimps on a Caribbean island. *Molecular Ecology*, **17**, 1066-1075.
- Crawford, A.J. (2003) Relative rates of nucleotide substitution in frogs. *Journal of Molecular Evolution*, **57**, 636-641.
- Crawford, A.J., Bermingham, E. & Polanía, C.S. (2007) The role of tropical dry forest as a long-term barrier to dispersal: a comparative phylogeographical analysis of dry forest tolerant and intolerant frogs. *Molecular Ecology*, **16**, 4789-4807.
- Daly, C., Helmer, E.H. & Quiñones, M. (2003) Mapping the climate of Puerto Rico, Vieques and Culebra. *International Journal of Climatology*, **23**, 1359-1381.
- Departamento de Estado (2004) *Reglamento para regir las especies vulnerables y en peligro de extinción en el estado libre asociado de Puerto Rico*. Reglamento 6766, Departamento de Recursos Naturales y Ambientales, San Juan, Puerto Rico.

Available

at: <http://app.estado.gobierno.pr/ReglamentosOnLine/Reglamentos/6766.pdf>.

Drummond, A.J. & Rambaut, A. (2007) BEAST: Bayesian evolutionary analysis by sampling trees. *BMC Evolutionary Biology*, **7**, 214.

Drummond, A.J., Nicholls, G., Rodrigo, A. & Solomon, W. (2002) Estimating mutation parameters, population history and genealogy simultaneously from temporally spaced sequence data. *Genetics*, **161**, 1307-1320.

Drummond, A.J., Rambaut, A., Shapiro, B. & Pybus, O.G. (2005) Bayesian coalescent inference of past population dynamics from molecular sequences. *Molecular Biology and Evolution*, **22**, 1185-1192.

Dupanloup, I., Schneider, S. & Excoffier, L. (2002) A simulated annealing approach to define the genetic structure of populations. *Molecular Ecology*, **11**, 2571-2581.

Dutton, A., Bard, E., Antonioli, F., Esat, T., Lambeck, K. & McCulloch, M.T. (2009) Phasing and amplitude of sea-level and climate change during the penultimate interglacial. *Nature Geoscience*, **2**, 355-359.

Edgar, R.C. (2004) MUSCLE: multiple sequence alignment method with high accuracy and high throughput. *Nucleic Acids Research*, **32**, 1792-1797.

Elmer, K.R., Dávila, J.A. & Loughheed, S.C. (2007) Cryptic diversity and deep divergence in an upper Amazonian leaf litter frog, *Eleutherodactylus ockendeni*. *BMC Evolutionary Biology*, **7**, 247. doi:10.1186/1471-2148-7-247.

Excoffier, L., Laval, G. & Schneider, S. (2005) Arelquin (version 3.0): an integrated software package for population genetics data analysis. *Evolutionary Bioinformatics Online*, **1**, 47-50.



- Farris, J.S., Källersjö, M., Kluge, A.G. & Bult, C. (1995) Testing significance of incongruence. *Cladistics*, **10**, 315-319.
- Felsenstein, J. (1985) Confidence limits on phylogenies: an approach using the bootstrap. *Evolution*, **39**, 783-791.
- Fu, Y.-X. (1997) Statistical tests of neutrality of mutations against population growth, hitchhiking and background selection. *Genetics*, **147**, 915-925.
- Gifford, M.E. & Larson, A. (2008) *In situ* genetic differentiation in a Hispaniolan lizard (*Ameiva chrysoleama*): a multilocus perspective. *Molecular Phylogenetics and Evolution*, **49**, 277-291.
- Goebel, A.M., Donnelly, J.M. & Atz, M.E. (1999) PCR primers and amplification methods for 12S ribosomal DNA, the control region, cytochrome oxidase I, and cytochrome *b* in bufonids and other frogs, and an overview of PCR primers which have amplified DNA in amphibians successfully. *Molecular Phylogenetics and Evolution*, **11**, 163-199.
- González, C., Dupont, L.M., Behling, H. & Wefer, G. (2008) Neotropical vegetation response to rapid climate changes during the last glacial period: palynological evidence from the Cariaco Basin. *Quaternary Research*, **69**, 217-230.
- Graham, A. (2003) Historical phytogeography of the Greater Antilles. *Brittonia*, **55**, 357-383.
- Grazziotin, F.G., Monzel, M., Echeverrigaray, S. & Bonatto, S.L. (2006) Phylogeography of the *Bothrops jararaca* complex (Serpentes: Viperidae): past fragmentation and island colonization in the Brazilian Atlantic forest. *Molecular Ecology*, **15**, 3969-3982.

- Guilderson, T.P., Fairbanks, R.G. & Rubenstone, J.L. (2001) Tropical Atlantic coral oxygen isotopes: glacial–interglacial sea surface temperatures and climate change. *Marine Geology*, **172**, 75-89.
- van der Hammen, T. (1974) The Pleistocene changes of vegetation and climate in tropical South America. *Journal of Biogeography*, **1**, 3-26.
- Hedges, S.B. (1999) Distribution of patterns of amphibians in the West Indies. *Patterns of distribution of amphibians: a global perspective* (ed. by W.E. Duellman), pp. 211-254. The John Hopkins University Press, Baltimore, MD.
- Hedges, S.B., Duellman, W.E. & Heinicke, M.P. (2008) New World direct-developing frogs (Anura: Terrarana): molecular phylogeny, classification, biogeography, and conservation. *Zootaxa*, **1737**, 1-182.
- Heinicke, M.P., Duellman, W.E. & Hedges, S.B. (2007) Major Caribbean and Central American frog faunas originated by ancient oceanic dispersal. *Proceedings of the National Academy of Sciences USA*, **104**, 10092-10097.
- Hess, P.N. & De Moraes Russo, C.A. (2007) An empirical test of the midpoint rooting method. *Biological Journal of the Linnean Society*, **92**, 669-674.
- Hessler, I., Dupont, L., Bonnefille, R., Behling, H., González, C., Helmens, K.F., Hooghiemstra, H., Lebamba, J., Marie-Pierre, L., Lézine, A.-M., Maley, J., Marret, F. & Vincens, A. (2010) Millennial-scale changes in vegetation records from tropical Africa and South America during the last glacial. *Quaternary Science Reviews*, **29**, 2882-2899.
- Hudson, R.R. (1992) Gene trees, species trees and the segregation of ancestral alleles. *Genetics*, **131**, 509-512.

- Hudson, R.R. & Kaplan, N.L. (1985) Statistical properties of the number of recombination events in the history of a sample of DNA sequences. *Genetics*, **111**, 147-164.
- Huelsenbeck, J.P. & Ronquist, F. (2001) MRBAYES: Bayesian inference of phylogenetic trees. *Bioinformatics*, **17**, 754-755.
- Huson, D.H. & Bryant, D. (2006) Application of phylogenetic networks in evolutionary studies. *Molecular Biology and Evolution*, **23**, 254-267.
- IUCN (2010) *IUCN Red List of Threatened Species*. IUCN Species Survival Commission, Gland, Switzerland.
- Jezkova, T., Leal, M. & Rodríguez-Robles, J.A. (2009) Living together but remaining apart: comparative phylogeography of *Anolis poncensis* and *A. cooki*, two lizards endemic to the aridlands of Puerto Rico. *Biological Journal of the Linnean Society*, **96**, 617-634.
- Joglar, R.L. (1998) *Los coquíes de Puerto Rico: su historia natural y conservación*. Editorial de la Universidad de Puerto Rico, San Juan, Puerto Rico.
- Kingman, J.F.C. (1982) The coalescent. *Stochastic processes and their applications*, **13**, 235-248.
- Kuhner, M.K. (2006) LAMARC 2.0: maximum likelihood and Bayesian estimation of population parameters. *Bioinformatics*, **22**, 768-770.
- La Sorte, F.A. & Jetz, W. (2010) Projected range contractions of montane biodiversity under global warming. *Proceedings of the Royal Society B: Biological Sciences*, **277**, 3401-3410.

- Lampert, K.P., Rand, A.S., Mueller, U.G. & Ryan, M.J. (2003) Fine-scale genetic pattern and evidence for sex-biased dispersal in the túngara frog, *Physalaemus pustulosus*. *Molecular Ecology*, **12**, 3325-3334.
- Lessa, E.P., Cook, J.A. & Patton, J.L. (2003) Genetic footprints of demographic expansion in North America, but not Amazonia, during the Late Quaternary. *Proceedings of the National Academy of Sciences USA*, **100**, 10331-10334.
- Lewsey, C., Cid, G. & Kruse, E. (2004) Assessing climate change impacts on coastal infrastructure in the Eastern Caribbean. *Marine Policy*, **28**, 393-409.
- Librado, P. & Rozas, J. (2009) DnaSP v5: a software for comprehensive analysis of DNA polymorphism data. *Bioinformatics*, **25**, 1451-1452.
- Lomolino, M.V., Riddle, B.R. & Brown, J.H. (2006) *Biogeography*, 3rd edn. Sinauer Associates, Sunderland, MA.
- Longo, A.V. & Burrowes, P.A. (2010) Persistence with chytridiomycosis does not assure survival of direct-developing frogs. *EcoHealth*, **7**, 185-195.
- Losos, J.B. & Ricklefs, R. (2009) Adaptation and diversification on islands. *Nature*, **457**, 830-836.
- Luo, Y., Sun, X. & Jian, Z. (2005) Environmental change during the penultimate glacial cycle: a high-resolution pollen record from ODP Site 1144, South China Sea. *Marine Micropaleontology*, **54**, 107-123.
- MacArthur, R.H. & Wilson, E.O. (1967) *The theory of island biogeography*. Princeton University Press, Princeton, NJ.
- Maddison, W.P. & Maddison, D.R. (2008) *Mesquite: a modular system for evolutionary analysis*, v2.72. Available at: <http://mesquiteproject.org>.

- Martin, D.P., Lemey, P., Lott, M., Moulton, V., Posada, D. & Lefevre, P. (2010) RDP3: a flexible and fast computer program for analyzing recombination. *Bioinformatics*, **26**, 2462-2463.
- Maynard Smith, J. (1992) Analyzing the mosaic structure of genes. *Journal of Molecular Evolution*, **34**, 126-129.
- McCulloch, M.T., Tudhope, A.W., Esat, T., Mortimer, G.E., Chappell, J., Pillans, B., Chivas, A.R. & Omura, A. (1999) Coral record of equatorial sea-surface temperatures during the penultimate deglaciation at Huon Peninsula. *Science*, **283**, 202-204.
- McDonald, J.H. & Kreitman, M. (1991) Adaptive protein evolution at the *Adh* locus in *Drosophila*. *Nature*, **351**, 652-654.
- Meyerhoff, H.A. (1933) Geology of Puerto Rico. *Monographs of the University of Puerto Rico Series B*, No. 1.
- Moritz, C., Schneider, C.J. & Wake, D.B. (1992) Evolutionary relationships within the *Ensatina eschscholtzii* complex confirm the ring species interpretation. *Systematic Biology*, **41**, 273-291.
- Muhs, D.R., Simmons, K.R. & Steinke, B. (2002) Timing and warmth of the Last Interglacial period: new U-series evidence from Hawaii and Bermuda and a new fossil compilation for North America. *Quaternary Science Reviews*, **21**, 1355-1383.
- Orvis, K.H., Clark, G.M., Horn, S.P. & Kennedy, L.M. (1997) Geomorphic traces of Quaternary climates in the Cordillera Central, Dominican Republic. *Mountain Research and Development*, **17**, 323-331.

- Posada, D. & Crandall, K.A. (1998) Modeltest: testing the model of DNA substitution. *Bioinformatics*, **14**, 817-818.
- Pregill, G.K. & Olson, S.L. (1981) Zoogeography of West Indian vertebrates in relation to Pleistocene climatic cycles. *Annual Review of Ecology and Systematics*, **12**, 75-98.
- Pregill, G.K., Steadman, D.W. & Watters, D.R. (1994) Late Quaternary vertebrate faunas of the Lesser Antilles: historical components of Caribbean biogeography. *Bulletin of the Carnegie Museum of Natural History*, **30**, 1-51.
- Rambaut, A. & Drummond, A.J. (2007) *Tracer v1.5*. Available at: <http://beast.bio.ed.ac.uk/Tracer>.
- Ramos-Onsins, R. & Rozas, R. (2002) Statistical properties of new neutrality tests against population growth. *Molecular Biology and Evolution*, **19**, 2092-2100.
- Renken, R.A., Ward, W.C., Gill, I.P., Gómez-Gómez, F. & Rodríguez-Martínez, J. (2002) Geology and hydrogeology of the Caribbean islands aquifer system of the commonwealth of Puerto Rico and the U.S. Virgin Islands. *U.S. Geological Survey Professional Paper*, **1419**, 1-148.
- Ricklefs, R.E. & Bermingham, E. (2001) Nonequilibrium diversity dynamics of the Lesser Antillean avifauna. *Science*, **294**, 1522-1524.
- Ricklefs, R.E. & Bermingham, E. (2002) The concept of the taxon cycle in biogeography. *Global Ecology and Biogeography*, **11**, 353-361.
- Ricklefs, R.E. & Bermingham, E. (2008) The West Indies as a laboratory of biogeography and evolution. *Philosophical Transactions of the Royal Society B: Biological Sciences*, **363**, 2393-2413.

- Rodríguez-Robles, J.A., Jezkova, T. & Leal, M. (2008) Genetic structuring in the threatened "Lagartijo del Bosque Seco" (*Anolis cooki*) from Puerto Rico. *Molecular Phylogenetics and Evolution*, **46**, 503-514.
- Rodríguez, A., Vences, M., Nevado, B., Machordom, A. & Verheyen, E. (2010) Biogeographic origin and radiation of Cuban *Eleutherodactylus* frogs of the *auriculatus* species group, inferred from mitochondrial and nuclear gene sequences. *Molecular Phylogenetics and Evolution*, **54**, 179-186.
- Rota-Stabelli, O. & Telford, M.J. (2008) A multi criterion approach for the selection of optimal outgroups in phylogeny: recovering some support for Mandibulata over Myriochelata using mitogenomics. *Molecular Phylogenetics and Evolution*, **48**, 103-111.
- Roy, A.J. & Lachniet, M.S. (2010) Late Quaternary glaciation and equilibrium-line altitudes of the Mayan Ice Cap, Guatemala, Central America. *Quaternary Research*, **74**, 1-7.
- Rull, V. (2008) Speciation timing and neotropical biodiversity: the Tertiary–Quaternary debate in the light of molecular phylogenetic evidence. *Molecular Ecology*, **17**, 2722-2729.
- Schubert, C. (1988) Climatic changes during the Last Glacial Maximum in northern South America and the Caribbean: a review. *Interciencia*, **13**, 128-137.
- Schwartz, A. & Henderson, R.W. (1985) *A guide to the identification of the amphibians and reptiles of the West Indies exclusive of Hispaniola*. Milwaukee Museum, Inland Press, Milwaukee, WI.

- Shimada, T., Matsui, M., Yambun, P. & Sudin, A. (2011) A taxonomic study of Whitehead's torrent frog, *Meristogenys whiteheadi*, with descriptions of two new species (Amphibia: Ranidae). *Zoological Journal of the Linnean Society*, **161**, 157-183.
- Slatkin, M. & Maddison, W.P. (1989) A cladistic measure of gene flow inferred from the phylogenies of alleles. *Genetics*, **123**, 603-613.
- Stephens, M. & Donnelly, P. (2003) A comparison of Bayesian methods for haplotype reconstruction from population genotype data. *American Journal of Human Genetics*, **73**, 1162-1169.
- Stephens, M., Smith, N.J. & Donnelly, P. (2001) A new statistical method for haplotype reconstruction from population data. *American Journal of Human Genetics*, **68**, 978-989.
- Stewart, M.M. (1995) Climate driven population fluctuations in rain forest frogs. *Journal of Herpetology*, **29**, 437-446.
- Stewart, M.M. & Woolbright, L.L. (1996) Amphibians. *The food web of a tropical rainforest* (ed. by D.P. Reagan and R.B. Waide), pp. 273-320. The University of Chicago Press, Chicago, IL.
- Stewart, N.C., Jr. & Via, L.E. (1993) A rapid CTAB DNA isolation technique useful for RAPD fingerprinting and other PCR amplifications. *BioTechniques*, **14**, 748-750.
- Streicher, J.W., Crawford, A.J. & Edwards, C.W. (2009) Multilocus molecular phylogenetic analysis of the montane *Craugastor podiciferus* species complex (Anura: Craugastoridae) in Isthmian Central America. *Molecular Phylogenetics and Evolution*, **53**, 620-630.



- Swofford, D.L. (2003) *PAUP\*: phylogenetics analysis using parsimony (\*and other methods). Version 4*. Sinauer Associates, Sunderland, MA.
- Tamura, K. & Nei, M. (1993) Estimation of the number of nucleotide substitutions in the control region of mitochondrial DNA in humans and chimpanzees. *Molecular Biology and Evolution*, **10**, 512-526.
- UNEP-WCMC (2009) *Impacts of climate change on biodiversity: a review of the recent scientific literature*. October 2008. Revised March 2009. UNEP-WCMC, Cambridge.
- Velo-Antón, G., Burrowes, P.A., Joglar, R.L., Martínez-Solano, I., Beard, K.H. & Parra-Olea, G. (2007) Phylogenetic study of *Eleutherodactylus coqui* (Anura: Leptodactylidae) reveals deep genetic fragmentation in Puerto Rico and pinpoints origins of Hawaiian populations. *Molecular Phylogenetics and Evolution*, **45**, 716-728.
- Wang, I.J., Crawford, A.J. & Bermingham, E. (2008) Phylogeography of the Pygmy Rain Frog (*Pristimantis ridens*) across the lowland wet forests of Isthmian Central America. *Molecular Phylogenetics and Evolution*, **47**, 992-1004.
- Woolbright, L.L. (1985) Patterns of nocturnal movement and calling by the tropical frog *Eleutherodactylus coqui*. *Herpetologica*, **41**, 1-9.
- Woolbright, L.L. (1997) Local extinctions of anuran amphibians in the Luquillo Experimental Forest of northeastern Puerto Rico. *Journal of Herpetology*, **31**, 572-576.
- Wright, S. (1951) The genetical structure of populations. *Annals of Eugenics*, **15**, 323-354.

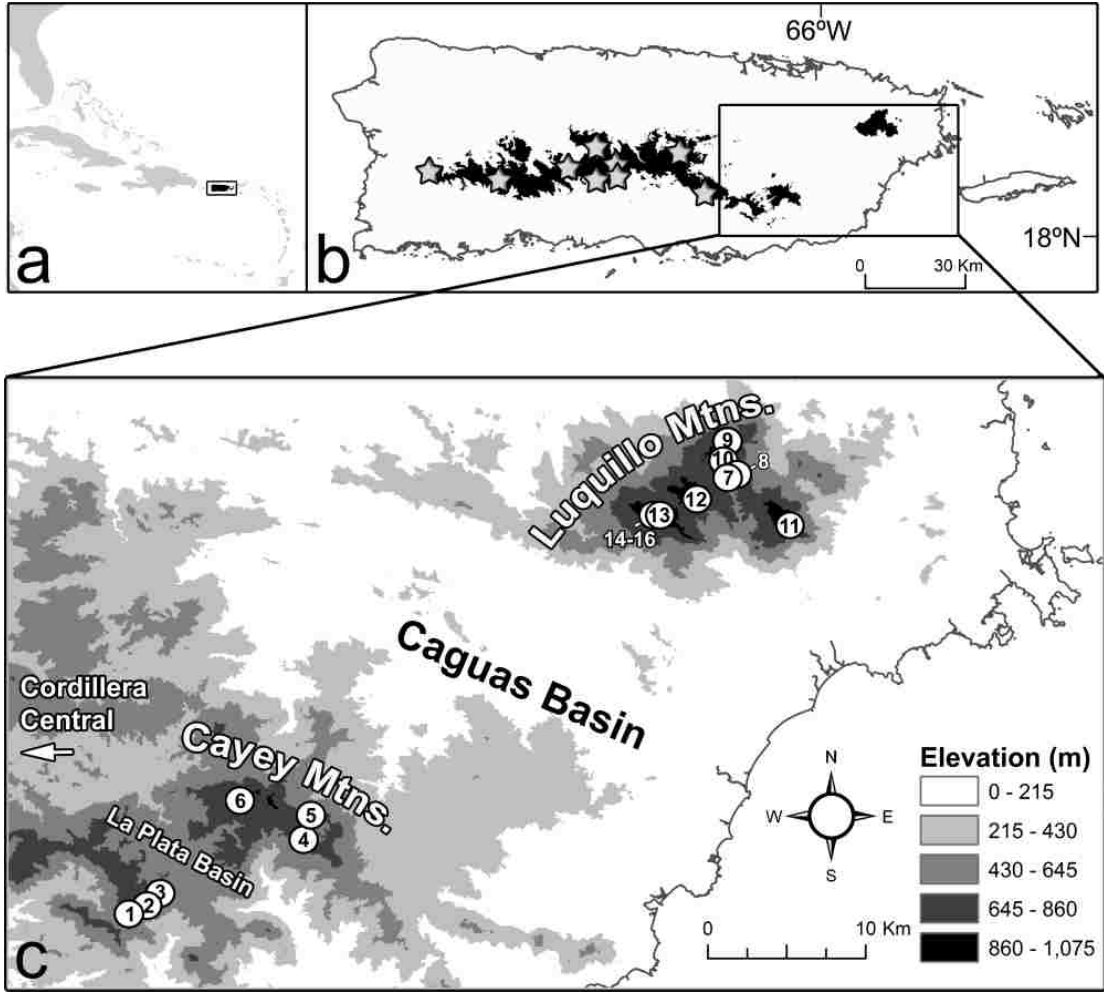
Zheng, Y., Fu, J. & Li, S. (2009) Toward understanding the distribution of Laurasian frogs: a test of Savage's biogeographical hypothesis using the genus *Bombina*. *Molecular Phylogenetics and Evolution*, **52**, 70-83.

Zwickl, D.J. (2006) *Genetic algorithm approaches for the phylogenetic analysis of large biological sequence datasets under the maximum likelihood criterion*. PhD Thesis, The University of Texas at Austin, Austin, TX.

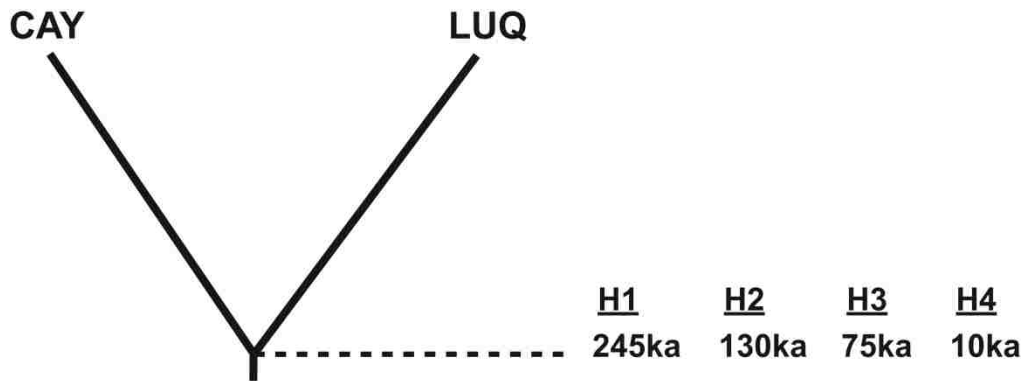
## Figures and Tables

**Fig. 1** (a) A map showing the location of Puerto Rico; (b) all areas with elevations above 600 m in Puerto Rico (in black), illustrating the major mountain ranges and location of the study area (grey stars depict historical localities that were extensively searched for *Eleutherodactylus portoricensis* during the summer of 2007–2008 but no populations were found); (c) a digital elevation map of Puerto Rico depicting sampling locations in the Cayey Mountains (CAY) subregions of Cerro de la Tabla (1–3) and Carite State Forest (4–6), and sampling locations in the Luquillo Mountains subregions of El Yunque (7–10), Pico del Este (11), and El Toro (12–16). The intervening Caguas Basin probably restricted gene flow between populations in the Luquillo and Cayey Mountains as a consequence of warm, dry conditions and the limited elevational distribution of *E. portoricensis*, while the La Plata Basin may have promoted genetic differentiation within the Cayey Mountains. Site numbers correspond to those presented in Table S1, Supporting Information.

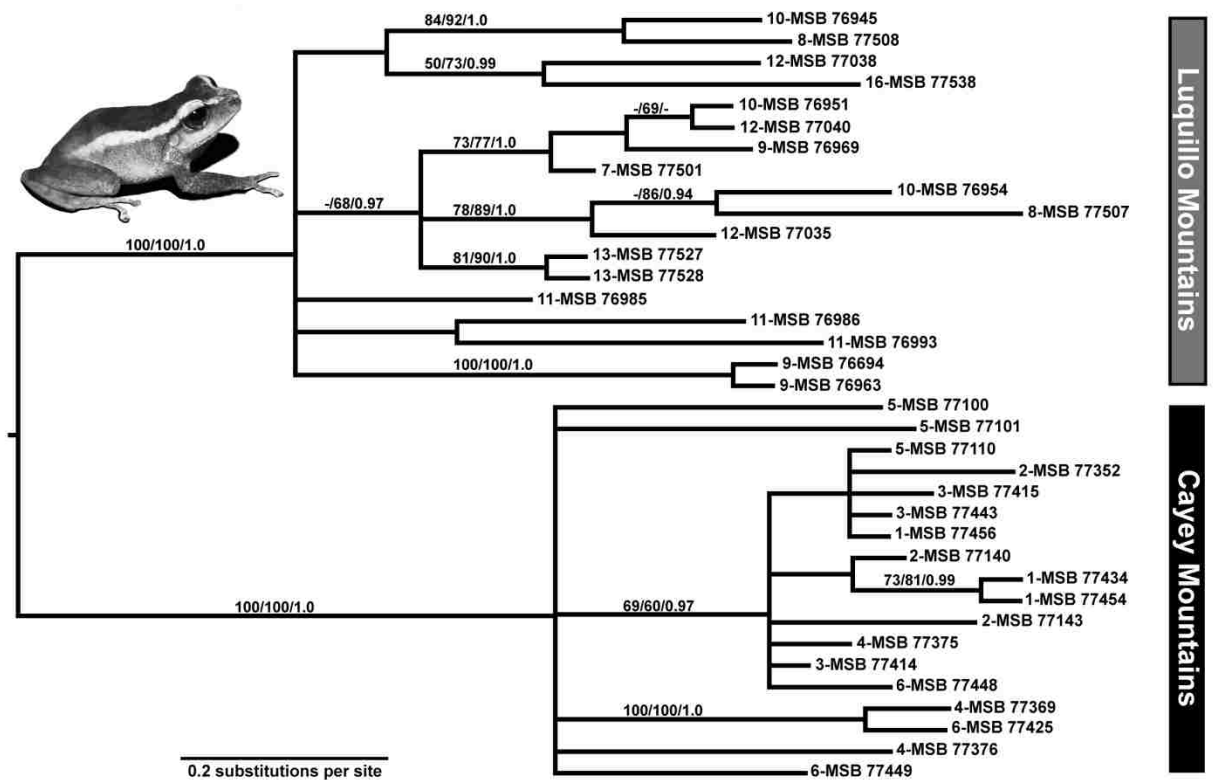
Fig. 1



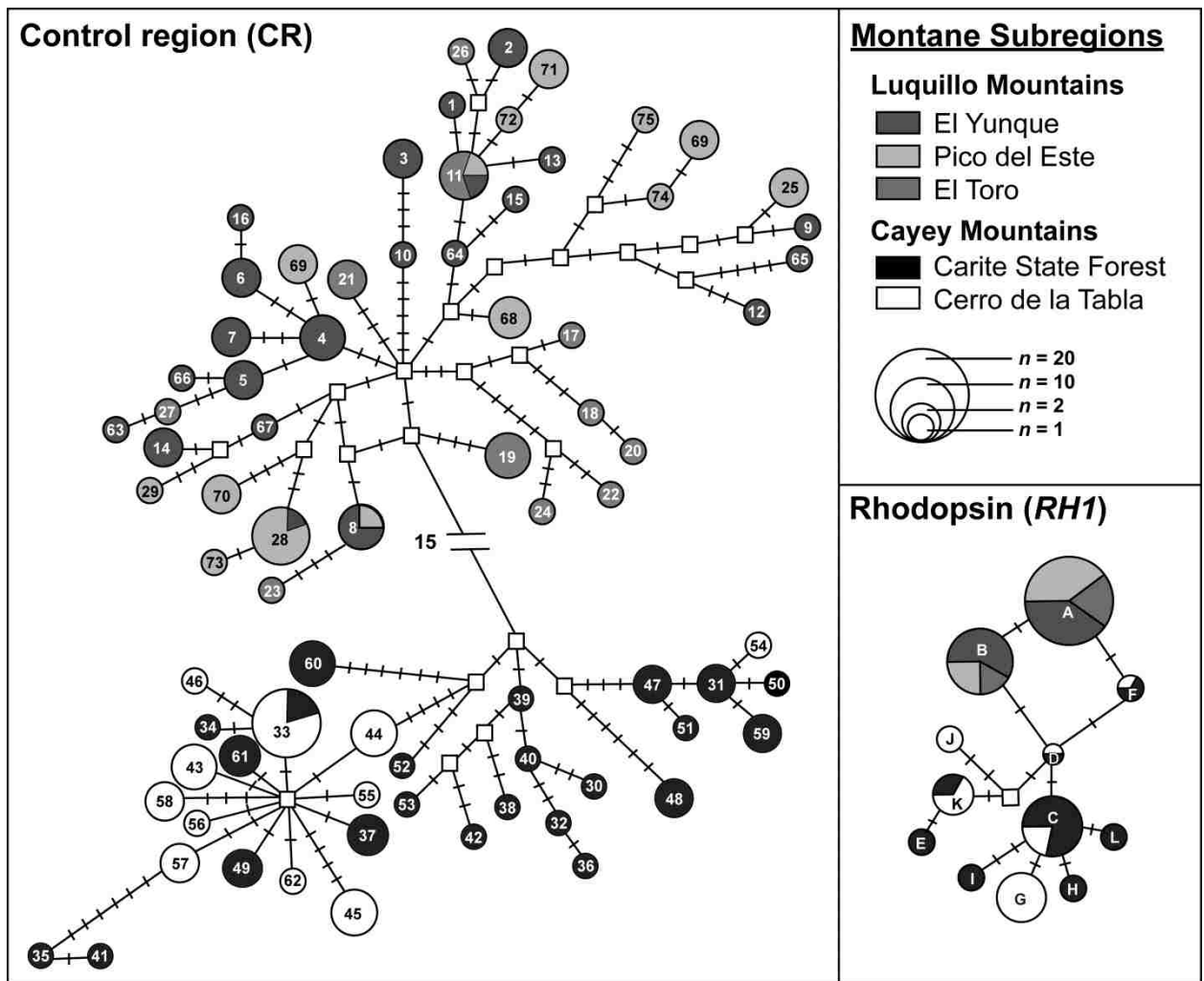
**Fig. 2** Models of population history for coalescent simulations of *Eleutherodactylus portoricensis*. The models are based on a simple test of population divergence in which a single divergence event occurred between the Luquillo Mountains (LUQ) and the Cayey Mountains (CAY) populations in Puerto Rico during a glacial–interglacial or glacial interstadial period, measured in generation time: the penultimate interglacial (H1), the Eemian interglacial (H2), Greenland Interstadial 20 (H3), and the Holocene interglacial (H4). Effective population size ( $N_e$ ) was held constant for all analyses.



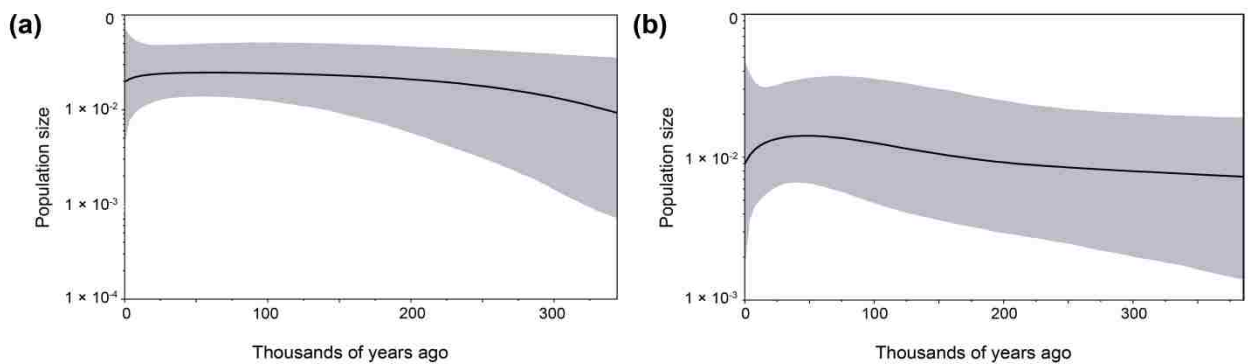
**Fig. 3** Mid-point rooted Bayesian phylogeny for 36 individuals of *Eleutherodactylus portoricensis* (inset image) for 1211 bp of the mitochondrial control region (CR) and cyt *b* gene fragments. Values on nodes refer to maximum parsimony ( $\geq 60\%$ ), maximum likelihood bootstrap values ( $\geq 60\%$ ) and Bayesian posterior probabilities ( $\geq 0.90$ ), respectively. Samples are labeled by site number and photographic voucher number (Table S1, Supporting Information). Samples from the Luquillo and Cayey Mountains in Puerto Rico are indicated.



**Fig. 4** Mitochondrial DNA control region (CR) and nDNA rhodopsin (*RH1*) maximum parsimony network for the Puerto Rican frog *Eleutherodactylus portoricensis*. Circles represent unique haplotypes; hatch marks depict single mutations (15 mutations separate Luquillo and Cayey Mountains populations); empty squares indicate missing (i.e. extant unsampled or extinct ancestral) haplotypes. Circle size is proportional to haplotype frequencies and the fill colour of each circle indicates the subregion (Fig. 1) from which it was sampled, as shown in the legend. Haplotypes are designated numbers (CR) and letters (*RH1*) that correspond to those presented in Table S1, Supporting Information.



**Fig. 5** Bayesian skyline plots for the (a) Luquillo Mountains (LUQ) and (b) Cayey Mountains (CAY) lineages of the Puerto Rican frog *Eleutherodactylus portoricensis* based on mtDNA control region (CR) sequence data, showing effective population size plotted as a function of time [units =  $Ne\mu$ , the product of effective population size and mutation rate (log transformed)]. Note that the time scale begins with the present on the left  $x$  axis: time in thousands of years ago;  $y$  axis: estimated population size. Black lines indicate the median value of effective population size; the shaded grey area represents the 95% highest posterior density.





**Table 1** Summary statistics and results of tests of population expansion for *Eleutherodactylus portoricensis* in the Luquillo (LUQ) and Cayey (CAY) Mountains of Puerto Rico based on mitochondrial (mtDNA) and nuclear (nDNA) sequence data. The number of individuals ( $n$ ), number of segregating sites ( $S$ ), haplotype diversity ( $h$ ), nucleotide diversity ( $\pi$ ), average number of pairwise differences ( $k$ ), Fu's  $F_S$  and Ramos-Onsins & Rozas's  $R_2$  statistic are given.

	mtDNA				nDNA	
	control region (CR)		cyt $b$		rhodopsin ( $RHI$ )	
	LUQ	CAY	LUQ	CAY	LUQ	CAY
Summary statistics						
$n$	73	71	18	18	18	18
$S$	61	40	20	13	1	11
$h$	0.978	0.959	0.948	0.804	0.500	0.798
$\pi$	0.013	0.012	0.006	0.004	0.001	0.003
$k$	7.51	6.972	4.163	2.346	0.500	1.929
Demographic parameters						
Fu's $F_S$	-24.23 $P = 0.000$	-12.260 $P = 0.002$	-5.616 $P = 0.005$	-3.032 $P = 0.032$	1.786 $P = 0.7527$	-2.833 $P =$
0.035						
$R_2$	0.057 $P = 0.271$	0.083 $P = 0.329$	0.139 $P = 0.028$	0.146 $P = 0.010$	0.137 $P = 0.972$	0.120 $P =$
0.176						

**Table 2** Results of coalescent simulations on the Puerto Rican frog *Eleutherodactylus portoricensis* for the concatenated mitochondrial (mtDNA) and rhodopsin (*RHI*) loci. Effective population sizes ( $N_e$ ) were held constant for all analyses. The  $P$ -value represents the probability of observing a value of the test statistic more extreme than those calculated from the empirical data, given simulations on a specific model of population history.

Hypothesis	mtDNA $s$ $P$ -value	<i>RHI</i> $s$ $P$ -value
H1: Divergence event, penultimate interglacial, 245 ka		
Lower 95% $N_e$ confidence limit	0.502	0.004
Mean $N_e$	0.228	< 0.001
Upper 95% $N_e$ confidence limit	0.088	< 0.001
H2: Divergence event, Eemian interglacial, 130 ka		
Lower 95% $N_e$ confidence limit	0.098	< 0.001
Mean $N_e$	0.030	< 0.001
Upper 95% $N_e$ confidence limit	0.004	< 0.001
H3: Divergence event, Greenland interstadial 20, 75 ka		
Lower 95% $N_e$ confidence limit	0.012	< 0.001
Mean $N_e$	0.002	< 0.001
Upper 95% $N_e$ confidence limit	0.002	< 0.001
H4: Divergence event, Holocene interglacial, 10 ka		
Lower 95% $N_e$ confidence limit	< 0.001	< 0.001
Mean $N_e$	< 0.001	< 0.001
Upper 95% $N_e$ confidence limit	< 0.001	< 0.001

## SUPPORTING INFORMATION

**Table S1** Sampling sites (as in Fig. 1), sample names (as in Fig. 3), corresponding haplotype names (as in Fig. 4), and GenBank accession numbers for each individual of *Eleutherodactylus portoricensis* and outgroups *E. wightmanae* and *E. coqui*. Museum catalogue numbers for photographic voucher specimens deposited in the Museum of Southwestern Biology (MSB) at the University of New Mexico are indicated. CR, control region; *cyt b*, cytochrome *b*; *RH1*, rhodopsin exon and intron 1.

Museum catalogue no.	Latitude, Longitude	Elev. (m)	Haplotype no.		GenBank no.		
			CR	<i>RH1</i>	CR	<i>Cyt b</i>	<i>RH1</i>
1. Puerto Rico: Municipality of Guayama, Cerro de la Tabla, km 4.4 on Rd 7741	18.049, -66.129	829					
MSB 77434			44	J, K	HM229923	HM229984	HQ823724, HQ823725
MSB 77454			44	C, G	HM229933	HM229988	HQ823732, HQ823733
MSB 77455			62	—	HM229934	—	—
MSB 77456			33	D, K	HM229935	HM229989	HQ823734, HQ823735
2. Puerto Rico: Municipality of Guayama, Cerro de la Tabla, km 3.1 on Rd 7741	18.052, -66.122	811					
MSB 77139			43	—	HM229880	—	—
MSB 77140			44	F, G	HM229881	HM229975	HQ823706, HQ823707
MSB 77141			45	—	HM229882	—	—
MSB 77142			43	—	HM229883	—	—

MSB 77143	45	G, G	HM229884	HM229976	HQ823708, HQ823709
MSB 77352	46	C, H	HM229885	HM229977	HQ823710, HQ823711
MSB 77353	43	—	HM229886	—	—
MSB 77354	43	—	HM229887	—	—
MSB 77355	45	—	HM229888	—	—
MSB 77357	44	—	HM229889	—	—
MSB 77358	44	—	HM229890	—	—
MSB 77359	45	—	HM229891	—	—
MSB 77360	45	—	HM229892	—	—
MSB 77412	54	—	HM229908	—	—
MSB 77413	55	—	HM229909	—	—
3. Puerto Rico: Municipality of Guayama, Cerro de la Tabla, km 2.1 on Rd 7741 18.057, -66.116 756					
MSB 77414	56	G, G	HM229910	HM229981	HQ823718, HQ823719
MSB 77415	33	C, J	HM229911	HM229982	HQ823720, HQ823721
MSB 77417	33	—	HM229912	—	—
MSB 77418	57	—	HM229913	—	—
MSB 77419	57	—	HM229914	—	—
MSB 77420	58	—	HM229915	—	—
MSB 77421	58	—	HM229916	—	—
MSB 77422	33	—	HM229917	—	—
MSB 77423	33	—	HM229918	—	—
MSB 77441	33	—	HM229924	—	—
MSB 77442	33	—	HM229925	—	—
MSB 77443	33	G, G	HM229926	HM229985	HQ823726, HQ823727
MSB 77444	33	—	HM229927	—	—
4. Puerto Rico: Municipality of San Lorenzo, Carite State Forest, km 6.1 on Rd 7740 18.101, -66.028 725					
MSB 77362	47	—	HM229893	—	—
MSB 77363	48	—	HM229894	—	—

MSB 77364	49	—	HM229895	—	—
MSB 77369	50	C, I	HM229896	HM229978	HQ823712, HQ823713
MSB 77374	49	—	HM229897	—	—
MSB 77375	49	C, F	HM229898	HM229979	HQ823714, HQ823715
MSB 77376	48	C, F	HM229899	HM229980	HQ823716, HQ823717
MSB 77377	51	—	HM229900	—	—
MSB 77378	47	—	HM229901	—	—
MSB 77379	52	—	HM229902	—	—
MSB 77380	53	—	HM229903	—	—
MSB 77381	37	—	HM229904	—	—
MSB 77382	37	—	HM229905	—	—
MSB 77383	49	—	HM229906	—	—
MSB 77385	48	—	HM229907	—	—
5. Puerto Rico: Municipality of San Lorenzo, Carite State Forest, Charco Azul	18.091, -66.032	607			
MSB 77094	30	—	HM229865	—	—
MSB 77095	31	—	HM229866	—	—
MSB 77096	32	—	HM229867	—	—
MSB 77097	33	—	HM229868	—	—
MSB 77099	34	—	HM229869	—	—
MSB 77100	35	C, C	HM229870	HM229972	HQ823700, HQ823701
MSB 77101	36	C, C	HM229871	HM229973	HQ823702, HQ823703
MSB 77103	37	—	HM229872	—	—
MSB 77105	38	—	HM229873	—	—
MSB 77107	39	—	HM229874	—	—
MSB 77109	40	—	HM229875	—	—
MSB 77110	33	D, E	HM229876	HM229974	HQ823704, HQ823705
MSB 77113	41	—	HM229877	—	—
MSB 77115	42	—	HM229878	—	—
MSB 77123	31	—	HM229879	—	—

6. Puerto Rico: Municipality of Patillas, Carite State Forest, near Cerro la Santa, km 20 on Rd 179	18.113, -66.070	762					
MSB 77425			59	C, C	HM229919	HM229983	HQ823722, HQ823723
MSB 77426			59	—	HM229920	—	—
MSB 77427			60	—	HM229921	—	—
MSB 77428			60	—	HM229922	—	—
MSB 77445			60	—	HM229928	—	—
MSB 77446			61	—	HM229929	—	—
MSB 77447			61	—	HM229930	—	—
MSB 77448			61	C, K	HM229931	HM229986	HQ823728, HQ823729
MSB 77449			60	C, L	HM229932	HM229987	HQ823730, HQ823731
7. Puerto Rico: Municipality of Rio Grande, El Yunque National Forest, near Baño de Oro, km 12.6 on Rd 191	18.296, -65.791	752					
MSB 77499			63	—	HM229936	—	—
MSB 77500			28	—	HM229937	—	—
MSB 77501			64	A, B	HM229938	HM229990	HQ823736, HQ823737
8. Puerto Rico: Municipality of Rio Grande, El Yunque National Forest, near Baño de Oro, km 12.3 on Rd 191	18.298, -65.788	700					
MSB 77506			6	—	HM229939	—	—
MSB 77507			65	A, B	HM229940	HM229991	HQ823738, HQ823739
MSB 77508			66	A, A	HM229941	HM229992	HQ823740, HQ823741
MSB 77509			67	—	HM229942	—	—
MSB 77510			8	—	HM229943	—	—
9. Puerto Rico: Municipality of Rio Grande, El Yunque National Forest, El Yunque Rock	18.311, -65.792	1028					
MSB 76692			1	—	HM229815	—	—

MSB 76693			2	—	HM229816	—	—
MSB 76694			3	A, B	HM229817	HM229960	HQ823676, HQ823677
MSB 76695			4	—	HM229818	—	—
MSB 76696			5	—	HM229819	—	—
MSB 76960			13	—	HM229829	—	—
MSB 76961			14	—	HM229830	—	—
MSB 76962			5	—	HM229831	—	—
MSB 76963			3	B, B	HM229832	HM229964	HQ823684, HQ823685
MSB 76964			14	—	HM229833	—	—
MSB 76965			15	—	HM229834	—	—
MSB 76966			16	—	HM229835	—	—
MSB 76967			4	—	HM229836	—	—
MSB 76968			4	—	HM229837	—	—
MSB 76969			2	B, B	HM229838	HM229965	HQ823686, HQ823687
10. Puerto Rico: Municipality of Rio Grande, El Yunque National Forest, before Mt. Britton Spur on Forest Service Rd 10			18.303, -65.795	896			
MSB 76945			6	B, B	HM229820	HM229961	HQ823678, HQ823679
MSB 76946			7	—	HM229821	—	—
MSB 76947			8	—	HM229822	—	—
MSB 76948			9	—	HM229823	—	—
MSB 76949			10	—	HM229824	—	—
MSB 76950			7	—	HM229825	—	—
MSB 76951			11	A, B	HM229826	HM229962	HQ823680, HQ823681
MSB 76953			8	—	HM229827	—	—
MSB 76954			12	A, A	HM229828	HM229963	HQ823682, HQ823683
11. Puerto Rico: Municipality of Rio Grande, El Yunque National Forest, Pico del Este			18.269, -65.758	1021			
MSB 76976			17	—	HM229839	—	—

MSB 76977	11	—	HM229840	—	—
MSB 76979	11	—	HM229841	—	—
MSB 76980	11	—	HM229842	—	—
MSB 76983	18	—	HM229843	—	—
MSB 76984	19	—	HM229844	—	—
MSB 76985	19	A, A	HM229845	HM229966	HQ823688, HQ823689
MSB 76986	20	B, B	HM229846	HM229967	HQ823690, HQ823691
MSB 76987	21	—	HM229847	—	—
MSB 76992	21	—	HM229848	—	—
MSB 76993	22	A, A	HM229849	HM229968	HQ823692, HQ823693
MSB 76994	23	—	HM229850	—	—
MSB 77006	19	—	HM229851	—	—
MSB 77007	24	—	HM229852	—	—
MSB 77009	21	—	HM229853	—	—
12. Puerto Rico: Municipality of Rio Grande, El Yunque National Forest, Tradewinds Trail					
MSB 77031	25	—	HM229854	—	—
MSB 77033	8	—	HM229855	—	—
MSB 77034	26	—	HM229856	—	—
MSB 77035	25	A, A	HM229857	HM229969	HQ823694, HQ823695
MSB 77036	27	—	HM229858	—	—
MSB 77037	28	—	HM229859	—	—
MSB 77038	28	A, A	HM229860	HM229970	HQ823696, HQ823697
MSB 77039	28	—	HM229861	—	—
MSB 77040	11	A, A	HM229862	HM229971	HQ823698, HQ823699
MSB 77041	29	—	HM229863	—	—
MSB 77042	28	—	HM229864	—	—



13. Puerto Rico: Municipality of Rio Grande, El Yunque National Forest, Pico el Toro, 6.92 km from El Toro trailhead on km 10.8 on Rd 186	18.272, -65.829	1051					
MSB 77527			68	B, B	HM229944	HM229993	HQ823742, HQ823743
MSB 77528			68	A, B	HM229945	HM229994	HQ823744, HQ823745
14. Puerto Rico: Municipality of Rio Grande, El Yunque National Forest, El Toro Trail, 6.85 km from El Toro trailhead on km 10.8 on Rd 186	18.272, -65.830	1031					
MSB 77529			69	—	HM229946	—	—
MSB 77530			69	—	HM229947	—	—
MSB 77531			70	—	HM229948	—	—
MSB 77532			68	—	HM229949	—	—
MSB 77533			28	—	HM229950	—	—
15. Puerto Rico: Municipality of Rio Grande, El Yunque National Forest, El Toro Trail, 6.6 km from El Toro trailhead on km 10.8 on Rd 186	18.272, -65.832	1008					
MSB 77534			71	—	HM229951	—	—
MSB 77535			72	—	HM229952	—	—
MSB 77536			73	—	HM229953	—	—
16. Puerto Rico: Municipality of Rio Grande, El Yunque National Forest, El Toro Trail, 6.5 km from El Toro trailhead on km 10.8 on Rd 186	18.272, -65.833	991					
MSB 77537			28	—	HM229954	—	—
MSB 77538			70	A, A	HM229955	HM22995	HQ823746, HQ823747
MSB 77539			74	—	HM229956	—	—
MSB 77540			71	—	HM229957	—	—
MSB 77541			75	—	HM229958	—	—

Outgroups

<i>Eleutherodactylus wightmanae</i>	18.091, -66.032	607						
MSB 77117			—	—	HM229959	HM229996	—	
<i>Eleutherodactylus coqui</i>	18.385, -65.771	88						
MSB 76869			—	—	JF928571	JF928572	—	

**Table S2** Primers used for amplification (amp) and sequencing (seq) of fragments of the mtDNA control region (CR), cytochrome *b* (cyt *b*), and rhodopsin exon and intron 1 (*RHI*) in *Eleutherodactylus portoricensis* and polymerase chain reaction (PCR) conditions used for amplification.

Primer	Use	Source	Sequence (5'–3')	PCR conditions
Control region (CR)				
ControlWRev-L	amp	Goebel <i>et al.</i> (1999)	GACATAYTATGTATAATCGAGCATTCA	94(180),[94(30), 50(30),
ControlP-H	amp	Goebel <i>et al.</i> (1999)	GTCCATAGATTCASTTCCGTCAG	72(45) x 36], 72(300)
ControlELPO-F	seq	this study	ACCATACTATGTTTAATTGAACATTCA	
ControlELPO-R	seq	this study	TGTCGGGATATTTCTGGCTGGCTGG	
Cyt <i>b</i>				
MVZ 15	both	Moritz <i>et al.</i> 1992	GAACTAATGGCCACAC(AT)(AT)TACGNAA	94(180),[94(30), 50(30),
MVZ 16	both	Moritz <i>et al.</i> 1992	AATAGGAARTATCAYTCTGGTTTRAT	72(45) x 36], 72(300)
<i>RHI</i>				
Eleu.Rho-F	both	this study	AAGACTGGGGTGGTACGAAG	95(600),[94(60), 60(45),
Rho4b	both	Zheng <i>et al.</i> (2009)	GAAGTTGCTCATGGGCTTACAGAC	72(60) x 34], 72(300)

## REFERENCES

- Goebel, A.M., Donnelly, J.M. & Atz, M.E. (1999) PCR primers and amplification methods for 12S ribosomal DNA, the control region, cytochrome oxidase 1, and cytochrome *b* in bufonids and other frogs, and an overview of PCR primers which have amplified DNA in amphibians successfully. *Molecular Phylogenetics and Evolution*, **11**, 163-199.
- Moritz, C., Schneider, C.J. & Wake, D.B. (1992) Evolutionary relationships within the *Ensatina eschscholtzii* complex confirm the ring species interpretation. *Systematic Biology*, **41**, 273-291.
- Zheng, Y., Fu, J. & Li, S. (2009) Toward understanding the distribution of Laurasian frogs: a test of Savage's biogeographical hypothesis using the genus *Bombina*. *Molecular Phylogenetics and Evolution*, **52**, 70-83.

**Table S3** Results from a SAMOVA analysis of mtDNA control region (CR) sequences for *Eleutherodactylus portoricensis* from 16 sampling sites in Puerto Rico, across its entire known distribution. Percentages of variation explained by the groupings are indicated. Group composition numbers are populations as given in Fig. 1.  $K$  refers to the number of predefined groups used in the analyses ( $K_{\max} = 8$ ). The most probable structure is indicated in bold, corresponding to the disjunct Luquillo and Cayey Mountains sites represented in Fig. 1. All  $F_{CT}$ ,  $F_{SC}$  and  $F_{ST}$  values have  $P$ -values of  $< 0.001$ .

$K$	Group composition	Among groups ( $F_{CT}$ )	Among populations within groups ( $F_{SC}$ )	Within populations ( $F_{ST}$ )
<b>2</b>	<b>[1-6], [7-16]</b>	<b>68.83 (0.69)</b>	<b>4.52 (0.14)</b>	<b>26.65 (0.73)</b>
3	[1-6], [7-12, 14-16], [13]	67.98 (0.68)	4.64 (0.14)	27.39 (0.73)
4	[1-6], [7-12, 14, 15], [13], [15]	67.08 (0.67)	4.84 (0.15)	28.09 (0.72)
5	[1-6], [7], [8-12, 14], [13], [15]	66.05 (0.66)	5.18 (0.15)	28.77 (0.71)
6	[1-6], [7], [8-12, 14], [13], [15], [16]	65.02 (0.65)	5.42 (0.15)	29.56 (0.65)
7	[1-3], [4-5], [6], [7-12, 14], [13], [15], [16]	64.06 (0.64)	2.75 (0.08)	33.20 (0.67)
8	[1-3], [4-5], [6], [7], [8-12, 14], [13], [15], [16]	63.23 (0.63)	3.04 (0.08)	33.73 (0.66)

**Table S4** *Eleutherodactylus portoricensis* mtDNA control region (CR) pairwise values across high-elevation regions of Puerto Rico separated by the Caguas Valley (Luquillo and Cayey Mountains) and the La Plata Basin (Cayey Mountains subregions of Cerro de la Tabla and Carite State Forest).

	Cerro de la Tabla	Carite State Forest	Luquillo Mtns
Cerro de la Tabla	-	***	***
Carite State Forest	0.22843	-	***
Luquillo Mtns	0.74869	0.66689	-

\*\*\* $P < 0.001$

## CHAPTER 3

### Sea level, topography, and island diversity: phylogeography of the Puerto Rican

#### Red-eyed Coquí, *Eleutherodactylus antillensis*

##### Abstract

Quaternary climatic oscillations caused changes in sea level that altered the size, number, and degree of isolation of islands, particular in land-bridge archipelagoes. Elucidating the demographic effects of these events will increase our understanding of the role of climate change in shaping evolutionary patterns in archipelagoes. The Puerto Rican Bank (Puerto Rico and the Eastern Islands, which comprise Vieques, Culebra, the Virgin Islands, and associated islets) in the eastern Caribbean Sea has a dynamic climatic history, periodically coalescing during glaciations and fragmenting during interglacial periods of the Quaternary. Fragmentation created isolation or even localized extirpation in terrestrial insular faunas. To assess the genetic signature of such phenomena we studied the phylogeography of the frog *Eleutherodactylus antillensis* across the archipelago. We tested hypotheses encompassing vicariance and dispersal narratives by sequencing mtDNA (*ca.* 552 bp) of 285 individuals from 58 localities, and four nuDNA introns (totaling *ca.* 1,633 bp) from 173 of these individuals. We found highest support for models based on a hypothesis of colonization of the Eastern Islands from sources in eastern Puerto Rico during the last glacial period, and lowest support for models based on a hypothesis of divergence of the Eastern Islands populations during the last or penultimate interglacials (*ca.* 120–240 kya). Haplotypes shared between the Puerto Rican

Bank and St. Croix (an island *ca.* 105 km southeast of this archipelago) likely reflect human-mediated introductions. The Río Grande de Loíza Basin in the eastern part of Puerto Rico delineates a phylogeographic break. Our findings illustrate how varying degrees of connectivity and isolation interact to produce phylogeographic patterns in tropical island systems.

## **Introduction**

Ecological and evolutionary studies of island biotas provide fundamental perspectives on speciation, adaptive radiation, community assembly, and biogeography (Losos & Ricklefs, 2009a). Factors such as isolation, topography, island area, and age contribute to biogeographic patterns (MacArthur & Wilson, 1967; Triantis *et al.*, 2008; Whittaker *et al.*, 2008), with historical fluctuations of sea level also hypothesized to play an important role in shaping insular biomes (e.g., Heatwole & MacKenzie, 1967; Carine, 2005).

Quaternary (2.6 mya – present) climatic oscillations changed eustatic sea levels more than 100 m (Waelbroeck *et al.*, 2002; Siddall *et al.*, 2003; van Daele *et al.*, 2011), altering the size, number, and degree of isolation of islands worldwide. During interglacial periods, rising sea levels fragmented and reduced the size of terrestrial habitats, leading to population isolation and smaller population sizes, which facilitated evolutionary divergence or local extirpation (Pregill & Olson, 1981). As sea levels lowered during glacial periods, terrestrial areas expanded, potentially connecting previously isolated populations and allowing colonization of new areas. Although some molecular and biogeographical studies detected high levels of gene flow (e.g. Heaney *et al.*, 2005; Jordan & Snell, 2008) and low levels of endemism (e.g. Heatwole & MacKenzie, 1967; Price & Elliott-Fisk, 2004) in tropical archipelagoes with a history of land-bridge connections, others inferred an absence of gene flow between populations and high endemism despite opportunities to disperse (e.g. Esselstyn & Brown, 2009; Lim *et al.*, 2011). These contrasting results imply that the role of fluctuating sea levels on diversification in tropical insular systems is complex.



We explore the genetic consequences of cyclical sea level fluctuations in the Puerto Rican Bank (hereafter PRB), an archipelago in the eastern Caribbean Sea (Figs 1A-C) comprised of the main island of Puerto Rico (8,768 km<sup>2</sup>; maximum elevation 1,338 m) and the “Eastern Islands,” (east of 65.6° W; *ca.* 340 km<sup>2</sup>; maximum elevation 500 m), which includes Vieques, Culebra, the Virgin Islands (St. Thomas, St. John, Tortola, Virgin Gorda, and Anegada), and more than 180 small cays east of Puerto Rico. Whereas low sea level during glacial periods led to land-bridge connections between the Eastern Islands and Puerto Rico, higher sea level during interglacial periods separated the Eastern Islands from each other and from Puerto Rico (Heatwole & MacKenzie, 1967; Renken *et al.*, 2002). Puerto Rico and the Eastern Islands form distinctive biogeographic clusters (Hedges, 1999b), suggesting limited gene flow between these two regions, despite periodic land-bridge connections.

The distinctive biotas of Puerto Rico and the Eastern Islands suggest disparate evolutionary histories. Previous mtDNA studies in the PRB inferred long-term persistence and diversification in topographically diverse Puerto Rico (e.g. Velo-Antón *et al.*, 2007; Rodríguez-Robles *et al.*, 2008; Jezkova *et al.*, 2009; Rodríguez-Robles *et al.*, 2010; Barker *et al.*, 2011), with sea level fluctuations promoting speciation in the Eastern Islands (Brandley & de Queiroz, 2004; Oneal *et al.*, 2010). However, those studies did not explore population-level responses of species distributed across the archipelago. We use multiple loci to explore demographic phenomena (Edwards & Beerli, 2000; Hudson & Turelli, 2003) and assess the effect of inundations on PRB populations of the Red-eyed Coquí, *Eleutherodactylus antillensis* (Anura: Eleutherodactylidae) Reinhardt and Lütken, 1863. This widespread (sea level to 1,220 m), predominantly arboreal frog occurs in most

larger islands of the PRB (except for Anegada; Henderson & Powell, 1999) and is ideal for testing alternative biogeographic scenarios. Because anurans are intolerant of saltwater (Balinsky, 1981; Duellman & Trueb, 1994), dispersal of *E. antillensis* among islands during high sea-level stands has probably been limited, although there are reported instances of frogs crossing salt-water barriers via rafting (Measey *et al.*, 2007).

We test competing hypotheses to elucidate the relative roles of persistence and dispersal in the genetic structure of a widespread species across a climatically dynamic tropical archipelago. The Sea Vicariance Hypothesis proposes that Eastern Islands populations of *E. antillensis* persisted in a refugium in this region and began diverging from Puerto Rican populations during the penultimate interglacial (190–245 kya; Dutton *et al.*, 2009) or the last interglacial (119–130 kya; Siddall *et al.*, 2003; Hearty *et al.*, 2007; van Daele *et al.*, 2011). This hypothesis predicts a lack of gene flow between populations of *E. antillensis* in Puerto Rico and the Eastern Islands during the last glacial period, when a land-bridge connected these two regions because of low sea levels (ca. 110-12 kya; Waelbroeck *et al.*, 2002; Siddall *et al.*, 2003; van Daele *et al.*, 2011), and thus Eastern Islands populations form a deeply differentiated group endemic to this region. In contrast, the Eastern Dispersal Hypothesis posits that *E. antillensis* colonized the Eastern Islands region via the land-bridge between these two regions, with divergence from Puerto Rican populations occurring as sea-levels rose during the Holocene interglacial ca. 11 kya (Peltier, 2002). This hypothesis predicts (i) shallow differentiation between Eastern Islands and eastern Puerto Rico (the putative source area) populations, and that (ii) genetic signatures of spatial expansion occur in the Eastern Islands due to recent colonization of this region. We focus on how sea-level fluctuations during the past *ca.*

245,000 years shaped genetic diversity in *E. antillensis*, because these events produced dramatic changes in the size, configuration, and isolation of terrestrial habitats in the Puerto Rican Bank, and impacted the connectivity of populations (Heatwole & MacKenzie, 1967).

We also explore the colonization history of a population of *E. antillensis* on St. Croix, an island *ca.* 105 km southeast of the PRB that has never had a direct land connection with this archipelago (Gill *et al.* 1989). Although St. Croix has a high proportion of endemics (Heatwole & MacKenzie, 1967; Brandley & de Queiroz, 2004), several species on this island became established following unintentional human-mediated introductions from sources in the PRB (Platenberg, 2007). We test the hypothesis that the *E. antillensis* population on St. Croix originated from a human-mediated introduction to this island in 1937 (Grant & Beatty, 1944). Because the Sea Vicariance Hypothesis and Eastern Dispersal Hypothesis are concerned with historical processes of gene flow in the PRB, understanding the extent to which human transport has shaped the distribution of *E. antillensis* is critical. An examination of demographic responses to sea-level fluctuations will further elucidate the role of late Quaternary climate change in shaping evolution in tropical archipelagoes.

## **Materials and Methods**

### *Sampling, DNA sequencing, haplotype phasing, and sequence alignment*

We sampled 285 individuals from 58 localities (avg. 4.6 individuals per locality, range 2-5; Figs 1A-C; Table S1, Supporting Information) at elevations of 0–981 m from 12 of the 13 islands where *E. antillensis* occurs (the exception being Great Thatch). A subset of

specimens at each locality (except for Virgin Islands National Park, St. John) was euthanized and deposited at the Museum of Southwestern Biology (MSB), University of New Mexico, Albuquerque and the Museum of Vertebrate Zoology (MVZ), University of California, Berkeley. Tissue samples (liver, thigh muscle, and/or toe-clips) are from the Division of Genomic Resources, MSB, and the Rodríguez-Robles laboratory at the University of Nevada, Las Vegas.

We included 285 *E. antillensis* in analyses of the mitochondrial (mtDNA) control region (CR) (*ca.* 552 bp). Nucleotide sequences from the nuclear DNA (nuDNA) intron-spanning loci  $\beta$ -crystallin (intron 1; CRYBA, *ca.* 192 bp), myosin heavy chain (intron; MYH, 463 bp), rhodopsin (intron 1; RH1, 596 bp), and ribosomal protein L9 (intron 4; RPL9int4, 382 bp) were obtained from 173 specimens representing three randomly chosen individuals from each of the 58 localities (except only two from Great Camanoe). DNA was extracted in a total volume of 30  $\mu$ L using a modified CTAB/PVP (cetyl trimethylammonium bromide/polyvinylpyrrolidone) – chloroform/isoamyl alcohol DNA extraction technique (Stewart & Via, 1993; M. Perdue, unpublished data). Polymerase chain reactions (PCRs) contained approximately 50 ng of template DNA, 10  $\mu$ M of each primer, 10 mM dNTP, 25 mM MgCl<sub>2</sub>, 2  $\mu$ L of 10 $\times$  polymerase reaction buffer and 0.20 unit of AmpliTaq Gold *Taq* polymerase (Applied Biosystems, Foster City, CA, USA) and adjusted to a final volume of 15  $\mu$ L with ddH<sub>2</sub>O. Sequencing reactions were conducted using the BigDye Terminator v3.1 Cycle Sequencing Kit (Applied Biosystems) and cleaned with ethanol precipitation. Primer descriptions and PCR conditions are provided in the Supporting Information (Table S2).

We edited sequences using SEQUENCHER 4.5 (GeneCodes) and deposited them in GenBank (accession numbers JN385299–JN38696; Table S1, Supporting Information). For heterozygote individuals polymorphic at more than one position, the gametic phase was inferred using PHASE 2.1 (Stephens *et al.*, 2001; Stephens & Donnelly, 2003). Multi-base insertion-deletions (indels) were collapsed into single-base polymorphisms for phasing analyses. Five independent runs from different starting seeds were run for 1,000 iterations, with a single thinning interval and 100 burn-in iterations. When PHASE could not reconstruct haplotypes with a posterior probability of  $\geq 0.85$ , PCR fragments were cloned for a minimum of five clones per sample using the pGEM-T-Easy Vector Systems kit (Promega). Finally, we repeated the PHASE analyses using the known haplotypes. We aligned sequences in MAFFT 6 (Kato *et al.*, 2002, <http://mafft.cbrc.jp/alignment/server/>). Alignments and consensus Bayesian trees (see below) were deposited in TreeBase (<http://purl.org/phylo/treebase/phyloids/study/TB2:S11926>).

#### *Neutrality, recombination, and genetic diversity*

We assessed selective neutrality of each locus with the Hudson-Kreitman-Aguade (HKA) test (Hudson *et al.*, 1987), with 10,000 coalescent simulations in HKA (J. Hey, <http://genfaculty.rutgers.edu/hey/software>), and by using Fu's  $F_S$  test (Fu, 1997) with 10,000 coalescent simulations in ARLEQUIN 3.1 (Excoffier *et al.*, 2005). To investigate recombination in the nuDNA markers, we conducted RDP (Martin *et al.*, 2005), Bootscan (Salminen *et al.*, 1995; Martin *et al.*, 2005), Geneconv (Padidam *et al.*, 1999), Chimaera (Posada & Crandall, 2001), MaxChi (Maynard Smith, 1992), and SiScan (Gibbs *et al.*, 2000) tests in RDP 3 (Martin *et al.*, 2010). Recombination was also inferred by calculating

the pairwise homoplasy index [ $\Phi_w$ ] (Bruen *et al.*, 2006) in SPLITSTREE 4.11.3 (Huson & Bryant, 2006). We estimated percentage of fragment length containing segregating sites [S(%)] and nucleotide ( $\pi$ ) diversity for each locus.

### *Phylogenetic and network analyses*

To test predictions of group structure in the Eastern Islands and Puerto Rico, we performed maximum parsimony, neighbor-joining, and Bayesian analyses of CR haplotypes. Phylogenies were first rooted with *Eleutherodactylus brittoni* and *E. cochranæ* (Hedges *et al.*, 2008). Because divergent outgroups can confound phylogenetic analysis due to homoplasy (Brandley *et al.*, 2009), we also used mid-point rooting (Hess & De Moraes Russo, 2007). We constructed parsimony trees and generated bootstrap values using PHYLIP 3.68 (Felsenstein, 1993). Nodal support was evaluated using 2,000 bootstrap replicates, and we used CONSENSE (Felsenstein, 1993) to obtain a 50% majority rule consensus tree. Phylogenetic trees for CR haplotypes were constructed with MEGA 4.1 (Tamura *et al.*, 2007) using the neighbor-joining method based on the Maximum Composite Likelihood model and a gamma parameter of 0.447 (inferred from MODELTEST), with 2,000 bootstrap replicates. We employed a Bayesian approach to phylogenetic reconstruction implemented in MRBAYES 3.1.2 (Huelsenbeck & Ronquist, 2001), using the model of nucleotide substitution for the data set chosen by AIC (GTR +  $\Gamma$ ) in MODELTEST 3.7 (Posada & Crandall, 1998). We ran four chains for 20,000,000 generations each, with default parameters as starting values and sampling every 1,000 generations, and repeated the analysis twice to ensure consistency. We discarded 5000 trees as burn-in and checked for stationarity and convergence of the chains with the

software TRACER 1.5 (Rambaut & Drummond, 2007). Bayesian posterior probabilities (BPP) were obtained from the 50% majority rule consensus of the remaining trees. Indels were treated as a fifth state in the neighbor-joining and maximum parsimony analyses, but not considered in the Bayesian analysis. We generated a maximum parsimony network for CR haplotypes with NETWORK 4.2 (<http://www.fluxus-technology.com>), and created geographic visualizations of nuDNA haplotypes using PHYLOGEOVIZ 2.4.4 (Tsai, 2011). Indels were considered in NETWORK and PHYLOGEOVIZ analyses.

### *Genetic structure*

To explore genetic structure in light of our hypotheses, we estimated the number of populations ( $K$ ), and incorporated sampling locality data in a spatially explicit framework to infer the location of genetic discontinuities between those populations. We first analysed the two marker classes (mtDNA and nuDNA introns) separately to compare patterns of spatial structure in mtDNA, which may exhibit finer population structure due to higher mutation rate and faster coalescence time, to the overall patterns inferred using nuDNA. To define groups for additional hypothesis testing procedures using MIGRATE and DIYABC (see below), we analysed all five loci together. Indels were considered in these analyses. To explore spatial genetic structure in CR, we conducted a spatial analysis of molecular variance (SAMOVA) in SAMOVA 1.0, which defines groups of populations that are geographically homogenous and maximally differentiated from each other (Dupanloup *et al.*, 2002). We inferred groups of *E. antillensis* based on nuDNA and on the five loci with and without a spatially explicit model in GENELAND 3.2.4 (Guillot *et al.*, 2005b; Guillot *et al.*, 2008), and thus four analyses were conducted. GENELAND infers the

number of populations using individual multilocus genotypes and, when provided with coordinates, the spatial location of genetic discontinuities between those populations (Guillot *et al.*, 2005a). For nuDNA, each variable site was encoded as an allele. Including mtDNA in GENELAND analyses violates assumptions of Hardy-Weinberg equilibrium within populations and linkage equilibrium between loci, but encoding each mtDNA sequence as a single haplotype is not statistically problematic (G. Guillot, pers. comm.). For each of the four GENELAND analyses, we examined  $K = 1-10$  distinct groups (five replicates each), with 250,000 MCMC iterations recorded every hundredth step after an initial 10% burn-in, and applied the uncorrelated allele frequency model. We accepted the modal  $K$  value from the posterior distribution as the most probable number of groups (Guillot *et al.*, 2005b). To assess diversity across the range of *E. antillensis*, we used spatial group assignments from GENELAND (see Results; Fig. 2) and estimated the number of haplotypes ( $h$ ), nucleotide diversity ( $\pi$ ), haplotype diversity ( $H_d$ ), and Fu's  $F_S$  (Fu, 1997) with 10,000 coalescent simulations for each group using ARLEQUIN. Indels were considered in these analyses.

To evaluate the Eastern Dispersal Hypothesis, we tested genetic signatures of spatial expansion only with individuals sampled from the 55 localities in the PRB. Repeated colonization events from a small number of founder individuals should result in a gradual decrease in genetic diversity with increasing distance from eastern Puerto Rico. To test for recent spatial expansion from Puerto Rico into the Eastern Islands region (i.e. east of 65.6° W), we regressed haplotype diversity ( $H_d$ ) for each locus (as calculated in ARLEQUIN with indels considered) on longitude using R version 2.12.1 (R Development Core Team, 2010). Because we found evidence for human mediated introductions of *E.*



*antillensis* (see Results), we conducted this analysis and all subsequently reported analyses twice. The first included all samples in the PRB, and the second excluded individuals from localities (28, 30, 34, 35, 41, 47, 49, 51, 52, 54; Figs 1A-B) that shared mtDNA haplotypes (H14, H31, H35; Fig. 3A) with individuals in geographically distant localities in the PRB and/or St. Croix (Table S1, Supporting Information).

#### *Testing alternative models of gene flow*

We constructed gene flow models in accordance with predictions of our *a priori* hypotheses, and assessed the models using Bayesian inference in MIGRATE 3.2.7 (Beerli & Felsenstein, 2001; Beerli, 2006). The model selection procedure inferred parameters using coalescent theory (Kingman, 1982), and then ordered models by their Bayes factors (Beerli & Palczewski, 2010). We evaluated three models that differed in the grouping of PRB populations and their migration rates (Table 1). According to the Sea Vicariance Hypothesis, populations of *E. antillensis* in the Eastern Islands did not exchange migrants with Puerto Rican populations during the last glacial period despite land-bridge connections (Model 1). We tested two gene flow models under the Eastern Dispersal Hypothesis. One model defines a single group comprising eastern Puerto Rico and Eastern Islands populations (Model 2), reflecting that these populations diverged so recently that no differentiation exists, whereas the other model defines two groups, one from eastern Puerto Rico and one from the Eastern Islands, that exchange migrants (Model 3). Models 1 and 3 are similar, except that the latter allows for gene flow between the Eastern Islands and Puerto Rico. In Model 3, we expect that levels of migration are higher from eastern Puerto Rico to the Eastern Islands than in the opposite direction,

assuming that eastern Puerto Rico served as the major source of migrants to the Eastern Islands. The 55 sampling sites from the PRB were pooled into three groups (western Puerto Rico, eastern Puerto Rico, and Eastern Islands) for Models 1 and 3, and into two groups (western Puerto Rico and eastern Puerto Rico/Eastern Islands) for Model 2, based on results of the GENELAND analyses of all loci (see Results; Fig. 2). We allowed for gene flow in either direction between western and eastern Puerto Rico in the three models. Indels were not considered in these analyses.

Settings in MIGRATE were specified to promote convergence and efficiently sample search space. We applied the Felsenstein (1984) model of nucleotide substitution with mutation rates estimated from the data and allowed to vary. To promote convergence, we applied uniform prior distributions for  $\theta$  and  $M$ , and used slice sampling. Prior distributions of  $\theta$  (mean = 0.15 and range 0–0.3) and  $M$  (mean = 500 and range 0–50,000) were selected after conducting preliminary runs with broad prior distributions (P. Beerli, pers. comm.) and then modifying the priors in subsequent runs if posterior distributions were not contained within the bounds of the prior distribution. After a burn-in period of 100,000 generations, we sampled every 100 steps from one long chain (1,000,000 steps each). To calculate Bézier-corrected marginal likelihoods, we applied thermodynamic integration under a static heating scheme (Beerli & Felsenstein, 2001) of four chains (temperatures 1.0, 1.5, 3.0,  $10^3$ ). To efficiently sample the search space when calculating parameters, we applied the randomtree index, set the replicate index to 20, and combined chains from all replicates. This simulation was repeated five times to ensure consistency. In subsequent runs, we changed the random number seed and used Bayesian estimates of  $\theta$  and  $M$  from the previous run as starting values (Beerli

& Felsenstein, 2001). We calculated the natural log Bayes factor by dividing each Bézier-corrected marginal likelihood by the sum of the Bézier-corrected marginal likelihoods of all models (Beerli & Palczewski, 2010).

#### *Testing alternative models of genetic divergence*

Using DIYABC 1.0.4.46 (Cornuet *et al.*, 2010), we performed coalescent simulations (Hudson, 1990) in an approximate Bayesian computation (ABC) framework to explore the history of divergence in populations of *E. antillensis* in the PRB. We generated a divergence model for each hypothesis. Both models of divergence included eastern and western Puerto Rican groups (see GENELAND Results; Fig. 2) and only differed in the timing of divergence of the Eastern Islands group (Fig. 4). Indels were not considered in these analyses.

The priors for all demographic parameters had uniform distributions that were bound by specified minimum and maximum values (Table 2). Each model incorporated an ancestral effective population size ( $N_a$ ) and an effective population size for all three population groups ( $N_1$ ,  $N_2$  and  $N_3$ ). The upper boundaries for the prior distributions of  $N_a$  (1,000,000),  $N_1$  (4,000,000),  $N_2$  (5,000,000), and  $N_3$  (4,000,000) are based on the density of adult male *E. antillensis* per hectare in the PRB (Ovaska, 2005). The divergence time parameter  $t_1$  in the Sea Vicariance model spans the approximate timing of the last interglacial and penultimate interglacial (prior distribution: 120,000 – 240,000 generations),  $t_2$  = divergence time between the Holocene interglacial and the last glacial period (prior distribution: 10 – 120,000 generations), and the divergence time parameter  $t_3$  in the Eastern Dispersal model spans the Holocene interglacial and last glacial period

(prior distribution: 10 – 120,000 generations). Time was number of generations, with a generation length of one year, based on observations that *E. antillensis* may reach reproductive maturity in the subsequent wet season after hatching (Ovaska, 2005), and on studies of the closely related *E. coqui* (Stewart & Woolbright, 1996). We conducted preliminary runs with broad prior distributions, and modified the priors in subsequent runs if posterior distributions were not contained within the bounds of the prior distribution.

Obtaining meaningful estimates of historical demographic parameters (e.g., gene flow, divergence times, changes in population size) depends in part on the accuracy of estimates of mutation rates for individual loci (Hey & Nielson, 2004). The lower bound for the CR mutation rate was set to  $\mu = 0.96 \times 10^{-8}$  nucleotide substitutions per site per year (sub/s/y), based on estimates for nucleotide substitution rates for mtDNA in eleutherodactyline frogs (Crawford, 2003a, b; Crawford *et al.*, 2007). Because this rate was estimate from coding regions of mtDNA, which are may evolve more slowly than CR, we estimated an upper bound for CR by inferring its rate relative to a coding mtDNA locus, cytochrome *b* (*cyt b*), using sequences collected from the Mountain Coquí, *E. portoricensis* in a previous study (Barker *et al.*, 2011) (*cyt b* accession numbers – HM229960-HM229996; CR accession numbers – HM229817, HM229820, HM229826, HM229828, HM229832, HM229838, HM229845, HM229846, HM229849, HM229857, HM229860, HM229862, HM229870, HM229871, HM229876, HM229881, HM229884, HM229885, HM229896, HM229898, HM229899, HM229910, HM229911, HM22919, HM229923, HM229926, HM229931, HM229932, HM229933, HM229935, HM229938, HM229940, HM229941, HM229944, HM229945, HM229955). Mutation rates vary

across species (Nabholz *et al.*, 2009; Lanfear *et al.*, 2010), however, we did not collect *cyt b* sequences for *E. antillensis* because CR had the higher levels of variation needed for assessing geographic structure. We compared the overall mean mtDNA CR and *cyt b* genetic distances (*p*-distances) among individuals of *E. portoricensis* using MEGA 4.1 (Tamura *et al.*, 2007), and determined that the nucleotide substitution rate of mtDNA CR was approximately 4.2 times that of *cyt b*. Based on an estimated coding mtDNA rate  $0.96 \times 10^{-8}$  s/sub/y, we estimated that CR evolves at a rate of  $4.1 \times 10^{-8}$  sub/s/y. This estimate is refined from an earlier study of genetic diversification in *E. portoricensis* (Barker *et al.*, 2011). In two *E. antillensis* individuals for which both CR and *cyt b* sequences were available, CR had approximately three times as much variation as *cyt b*, and therefore we believe that a rate of  $4.1 \times 10^{-8}$  sub/s/y for CR is appropriate for this species. The minimum ( $6.0 \times 10^{-10}$  sub/s/y) and maximum ( $8.2 \times 10^{-9}$  sub/s/y)  $\mu$  values for the nuDNA introns were based on a lower bound estimate of anuran nuDNA (Crawford, 2003a), and a five-fold slower rate than our upper bound for mtDNA (Sheldon *et al.*, 2000; Crawford, 2003b), respectively.

We simulated 1,00,000 data sets for each hypothesis, and used the number of haplotypes, number of segregating sites, average number of pairwise differences, and Tajima's *D* as summary statistics to compare observed and simulated data sets. These summary statistics were chosen based on their success in previous ABC studies (Beaumont, 2008). The 1,000 and 10,000 simulated data sets with summary statistics most similar to the observed data were identified through the direct and logistic regression rejection steps of the ABC algorithm, and used for ABC estimation of parameters.

We evaluated the appropriateness of each model of genetic divergence and its associated parameters, and performed model checking computations as empirical verifications of the performance of the ABC procedure. To check that at least one combination of scenarios and priors produced simulated data sets similar to our observed data, we used the “Pre-evaluate scenario-prior combinations” option in DIYABC that involved a principal component analysis (PCA) of the first 100,000 simulated data sets (Cornuet *et al.*, 2010). As part of the model-checking procedure, we conducted PCA on test quantities obtained with the model posterior combinations from the most strongly supported model, together with 10,000 pseudo-observed data sets (Cornuet *et al.*, 2010). We evaluated the “goodness-of-fit” of each model by using the “Confidence in scenario choice” option in DIYABC, in which 500 data sets per model were simulated with parameter values drawn from the same prior distributions as the models. From these results, we calculated the proportion of times that the most strongly supported model did not have the highest posterior probability when it was the true model (type I error), as well as the proportion of times that the least supported model had the highest posterior probability when it was not the true model (type II error).

## **Results**

### *Neutrality, recombination, and genetic diversity*

Nucleotide variation in the five loci is consistent with neutral expectations according to the HKA test ( $\chi^2 = 6.64$ , d.f. = 4,  $P = 0.16$ ), but significantly negative values of Fu’s  $F_S$  for CR ( $F_S = -25.660$ ,  $P = 0.0002$ ) and RPL9int4 ( $F_S = -23.158$ ,  $P = 0.0002$ ) indicate selection or recent population expansion (Fu, 1997). We did not detect recombination in

the nuDNA data sets. The mtDNA CR data set contained 98 haplotypes with 49 variable positions; seven were single-base pair indels. The four nuDNA loci totaled *ca.* 1,633 bp and exhibited varying levels of polymorphism (Table 3), with CRYBA the least variable (5 variable positions; one a single-base pair indel), and RPL9int4 the most variable (25 variable positions; four single-base pair indels and one five-base pair indel). MYH and RH1 did not contain indels.

#### *Phylogenetic and network analyses*

Phylogenetic analyses of CR revealed a shallow, largely unresolved topology. We present the results of the phylogeny rooted with outgroup taxa (Fig. 5) because it was not appreciably different from the mid-point rooted phylogeny. Only a single clade which contained three haplotypes was well-supported across neighbor-joining, maximum parsimony, and Bayesian analyses, and therefore most CR haplotypes form a basal polytomy. The maximum parsimony network depicts that three CR haplotypes are shared between Puerto Rico and the Eastern Islands (H14, H31, H35; Fig. 3A). Most Eastern Islands populations contain shallowly differentiated private CR haplotypes. Three CR haplotypes from Puerto Rico, St. Thomas, St. John, and Virgin Gorda are shared with St. Croix. Three CRYBA haplotypes, 5 MYH haplotypes, 4 RH1 haplotypes, and 9 RPL9int4 haplotypes occur in the Eastern Islands, but fewer than half of those are endemic to the region. Endemic nuDNA haplotypes are usually restricted to a single island population (e.g. CRYBA, MYH, RH1; Fig. S1, Supporting Information) and occur at low frequencies. There are no unique nuDNA haplotypes in St. Croix.

### *Genetic structure*

Spatial genetic structure across loci (CR, nuDNA loci, all loci combined) identified a distinctive group in western Puerto Rico, but varied with respect to eastern Puerto Rico and the Eastern Islands. SAMOVA analyses of CR did not identify the precise number of populations ( $K$ ) displaying the highest differentiation among groups ( $F_{CT}$ ), because  $F_{CT}$  values increased as  $K$  increased. Some groups contained a single population when  $K \geq 7$ , indicating that group structure was declining, and thus results are presented for  $K = 6$  (c.f. Heuertz *et al.*, 2004; Fig. 3B). GENELAND analyses of nuDNA and all loci conducted with and without a spatially explicit model identified three groups ( $K = 3$ ). The spatial location of genetic discontinuities between populations were identical in analyses of nuDNA and all loci and depicted one group located west of the Río Grande de Loíza in Puerto Rico, a second one comprising all but three sites east of the Río Grande de Loíza, and a third occurring in the Eastern Islands and St. Croix (Fig. 2).

Population genetic statistics for populations in western Puerto Rico, eastern Puerto Rico, and the Eastern Islands varied across loci. For CR, populations from eastern Puerto Rico had fewer private haplotypes than those from western Puerto Rico and the Eastern Islands. Populations from all three groups had significantly negative values of Fu's  $F_S$  for CR (Table 3). For the four nuDNA loci, individuals from the Eastern Islands had fewer haplotypes than those from eastern Puerto Rico (Table 3). Populations in eastern Puerto Rico had significantly negative values of Fu's  $F_S$  for RPL9int4 and populations in western Puerto Rico had significantly negative values of Fu's  $F_S$  for MYH.



Only two loci exhibited a significant trend of declining haplotype diversity with longitude in the Eastern Islands, and therefore the prediction of spatial expansion in the Eastern Islands (Eastern Dispersal Hypothesis) was only partially supported. A significant relationship exists between haplotype diversity and longitude for CRYBA ( $R^2 = 0.26$ ,  $F = 9.26$ , d.f. = 52,  $P < 0.001$ ) and RPL9int4 ( $R^2 = 0.11$ ,  $F = 3.66$ , d.f. = 52,  $P = 0.03$ ), MYH ( $R^2 = 0.10$ ,  $F = 5.56$ , d.f. = 53,  $P = 0.02$ ) but not for CR ( $R^2 = 0.05$ ,  $F = 2.64$ , d.f. = 53,  $P = 0.11$ ) and RH1 ( $R^2 = 0.0$ ,  $F = 0.022$ , d.f. = 53,  $P = 0.88$ ; Fig. S4). Haplotype diversity in CRYBA and RPL9int4 exhibits significant nonlinear relationships with longitude. Specifically, diversity is highest in eastern Puerto Rico, but decreases west of the Río Grande de Loíza, Puerto Rico (*ca.* 66.0° W; Fig. 1A), and in the Eastern Islands (Fig. S4). In contrast, the significant linear trend recovered for MYH shows that diversity increases from west-to-east across the PRB, but this trend was not statistically significant ( $P = 0.085$ ) when potentially introduced samples were excluded from the analysis.

#### *Assessing alternative models of gene flow and genetic divergence*

MIGRATE produced consistent parameter estimates across replicates, and provided stronger support for the Eastern Dispersal Hypothesis than for the Sea Vicariance Hypothesis. Model 3 had the highest support, followed by Model 2, and then Model 1 (Table 1). High levels of gene flow have occurred between Puerto Rico and the Eastern Islands (Model 3), but not to the extent of making populations from these two regions panmictic (Model 2; Table 1). Strong ties between eastern Puerto Rico and the Eastern Islands are supported, but the confidence intervals for migration rates ( $M$ ) were too large

to determine migration directionality. Analyses that excluded potentially introduced samples produced similar results (Tables 1 and 4).

The DIYABC analysis supported the Eastern Dispersal Hypothesis (posterior probability = 0.80; 95% CI: 0.72–0.88), with estimated divergence dates of 67.0 kya (95% CI: 4.5–115.0 kya) between eastern Puerto Rico and Eastern Islands populations, and of 128.0 kya (95% CI: 44.9–222.0 kya) for the split between western and eastern Puerto Rican groups (Table 5). The eastern Puerto Rico group has a larger effective population size than those in the Eastern Islands and western Puerto Rico. The Sea Vicariance Hypothesis had much lower support (posterior probability = 0.20; 95% CI: 0.12–0.28). A pre-evaluation of the models indicated that the observed data set was surrounded by many simulated data sets for each model, indicating that the simulations produced data sets similar to the observed one (Fig. S2, Supporting Information). The observed data set was surrounded by many simulated pseudo-observed data sets of the Eastern Dispersal Hypothesis model (Fig. S3, Supporting Information), indicating a good fit of the model-posterior combination to the pseudo-observed data set (Cornuet *et al.*, 2010). In assessing the goodness-of-fit of the models, we calculated a type I error rate of 0.26 and a type II error rate of 0.22. Analyses that excluded potentially introduced samples produced similar parameter estimates, but provided even stronger support for the Eastern Dispersal Hypothesis (posterior probability = 0.93; 95% CI: 0.90–0.95) than the Sea Vicariance Hypothesis (posterior probability = 0.08; 95% CI: 0.05–0.10).

## **Discussion**

The dynamic history of the Puerto Rican Bank (PRB) left an indelible mark on its biota (Heatwole & MacKenzie, 1967). Sea level changes significantly altered the size, area, and degree of isolation of terrestrial habitats in this archipelago (Heatwole & MacKenzie, 1967; Renken *et al.*, 2002). Brief periods (*ca.* 11-18 kyr) of high sea level stands fragmented the Eastern Islands region to an extent similar to its current configuration (Fig. 1B) at least three times in the past 260,000 years (Dutton *et al.*, 2009; Muhs *et al.*, 2011). Comparatively longer periods of low sea-level stands predominated during the past five glacial periods (Rohling *et al.*, 2009), uniting the Eastern Islands and Puerto Rico into a single landmass. Our multilocus phylogeographic analysis of *E. antillensis* revealed genetic signatures largely consistent with the Eastern Dispersal Hypothesis, suggesting that land connections during glacial periods facilitated colonization from Puerto Rico. These signatures include: 1) Eastern Islands populations sharing most nuDNA haplotypes with Puerto Rican populations (Table 3, Fig. S1, Supporting Information); 2) highest support for a model where gene flow occurs between eastern Puerto Rico and the Eastern Islands (Table 1); and 3) highest support for a model with eastern Puerto Rican and Eastern Islands populations diverging between the last glacial period and the Holocene interglacial (Table 5). The shallow, unresolved CR phylogeny (Fig. 5) suggests that *E. antillensis* populations in the Eastern Islands do not form a deeply differentiated group, and low support for models based on this hypothesis suggest that *E. antillensis* did not persist in a refugium in the Eastern Islands through multiple cycles of sea-level fluctuations.

*Colonization of the Eastern Islands and population structure in E. antillensis*

An estimated divergence date of 50.3 kya between the eastern Puerto Rico and Eastern Islands populations (Table 5) suggests that isolation occurred prior the Holocene interglacial, but the confidence intervals for this split are large (2.7–107.0 kya). A last glacial period divergence may be explained by xeric environments in the lowlands of the PRB during at least some portions of this time period (Renken *et al.*, 2002), which could have promoted isolation of *E. antillensis* following their establishment in the Eastern Islands. Small, arid islands in the PRB do not support populations of *E. antillensis*, and drought is associated with lower population densities of these frogs (Ovaska, 2005). A high-resolution pollen record from north-eastern Venezuela suggests that savanna and xerophytic vegetation expanded 11 times between 28 – 68 ka (González *et al.*, 2008), which could have led to the isolation of mesophilic taxa in the Caribbean Sea. The lowlands of the PRB were particularly arid during the Last Glacial Maximum *ca.* 26.5 – 19 kya (Pregill & Olson, 1981; Renken *et al.*, 2002) and xerophytic vegetation may have inhibited dispersal across terrestrial connections between eastern Puerto Rico and the Eastern Islands. An increase in rainfall following the Last Glacial Maximum was associated with an expansion of mesic forest in the PRB (Renken *et al.*, 2002) and other islands of the Greater Antilles (Higuera-Gundy *et al.*, 1999; Hodell *et al.*, 2008), that may have increased population connectivity, but a concomitant rise in sea-level (Peltier, 2002) would have reduced dispersal opportunities. Whether shared alleles between the two regions are due to incomplete lineage sorting or historical gene flow remains unknown (Eckert & Carstens, 2008). Although migration rates are not significantly higher from eastern Puerto Rico into the Eastern Islands, this result may reflect the low levels of variation in the loci and not necessarily be inconsistent with a history of recent

colonization. Our ability to distinguish between complex population genetic models (e.g., incorporating admixture or changes in population size) may improve with additional independent loci (Beerli & Palczewski, 2010; Cornuet *et al.*, 2010; Robert *et al.*, 2011), especially if they have higher mutation rates than the loci used in this study.

In the GENELAND analysis of all loci, populations of *E. antillensis* in the Eastern Islands form a shallowly differentiated group (Fig. 2), which is consistent with previous work showing that species in this region form a distinctive biogeographic cluster (Hedges, 1999b). However, levels of differentiation between Puerto Rican and Eastern Islands groups of *E. antillensis* are much shallower than those found in the co-distributed lizard *Anolis cristatellus* (Brandley & de Queiroz, 2004) and species of *Amphiacusta* ground crickets (Oneal *et al.*, 2010). This implies that some species persisted in the Eastern Islands despite a reduction in habitat due to a rise in sea level. Endemic species of plants (e.g. *Solanum conocarpum*; Acevedo-Rodríguez, 1996), frogs (*Eleutherodactylus lentus* and *E. schwartzi*; Henderson & Powell, 1999), lizards (e.g. *Anolis ernstwilliamsi*, *A. roosevelti*, *Sphaerodactylus parthenopion*, *Mabuya macleani*; Lazell, 1983; Henderson & Powell, 1999; Mayer & Lazell, 2000), amphisbaenians (e.g. *Amphisbaeana fenestrata*; Henderson & Powell, 1999), and snakes (e.g. *Typhlops richardii*; Henderson & Powell, 1999) survived in the Eastern Islands throughout multiple glacial-interglacial cycles. Despite high endemism in the Eastern Islands region, most islands share faunas, and therefore have low levels of *single-island* endemism (Heatwole & MacKenzie 1967).

A decrease of haplotype diversity across the Eastern Islands in CRYBA and RPL9int4 (Fig. S4, Supporting Information) supports sequential founder events predicted

under the Eastern Dispersal Hypothesis, but this relationship was not observed in other loci. Drift can produce incongruent results across loci, especially in small isolated populations (Excoffier *et al.*, 2009). A lack of detectable spatial expansion may also stem from the establishment of populations from independent source populations (Kolbe *et al.*, 2004). Therefore, inconsistent results across loci regarding spatial expansion can still be consistent with a history of *E. antillensis* colonization of the Eastern Islands during the last glacial period.

#### *Diversification of E. antillensis within Puerto Rico*

Larger patches of suitable habitat, greater topographic and ecological diversity (Ewel & Whitmore, 1973), and less pronounced inundations potentially lowered extinction rates in Puerto Rico relative to the Eastern Islands, and/or promoted diversification in isolated populations (MacArthur & Wilson, 1967; Whittaker *et al.*, 2008). The finding of stronger group structure of populations of *E. antillensis* within Puerto Rico (Figs 2 and 3B) is congruent with studies showing that this island contains the highest species richness (Figueroa Colón, 1996) and the largest proportion of endemics in the PRB (Heatwole & MacKenzie, 1967; Hedges, 1999b). Mountainous regions in Puerto Rico harbor distinctive phylogroups of frogs and lizards (Velo-Antón *et al.*, 2007; Rodríguez-Robles *et al.*, 2010; Barker *et al.*, 2011) and may have shaped genetic diversity in *E. antillensis* by providing mesic refugia during particularly arid glacial periods.

Our analyses of group structure suggest that a historical barrier to dispersal west of the Río Grande de Loíza in Puerto Rico (Figs 2 and 3B) may have shaped genetic diversity in *E. antillensis* in Puerto Rico. Eastern Puerto Rican and western Puerto Rican

groups began diverging an estimated 73.3 kya (Table 5), coinciding with the last glacial period. Similar to the pre-Holocene divergence of the Eastern Islands group scenario, increased aridity of the lowlands of the PRB including the Río Grande de Loíza Basin may have promoted divergence of western and eastern Puerto Rican groups during glacial periods. In combination with strong, cool winds during the last glacial period (Hodell *et al.*, 2008), increased aridity in the highlands connecting the Cayey Mountains (in the southeastern region of Puerto Rico) to the Central Mountains could have inhibited dispersal of *E. antillensis* through higher elevation areas as well. First proposed as a barrier to westward dispersal of the mesophillic Locust Coquí, *E. locustus* (Rivero & Mayorga, 1963), and the Golden Coquí, *E. jasperi* (Drewry & Jones, 1976), the Río Grande de Loíza Basin is the location of genetic discontinuities in *E. coqui* (Velo-Antón *et al.*, 2007) and in the Mountain Garden Lizard, *Anolis krugi* (Rodríguez-Robles *et al.*, 2010). We did not expect a signature of spatial expansion within Puerto Rico, but a significant decrease in haplotype diversity in CRYBA and RPL9int4 in the area west of the Río Grande de Loíza Basin (Fig. S4) suggests that populations of *E. antillensis* may have recently expanded there.

#### *Human-mediated introductions of E. antillensis*

Failure to identify a single unique *E. antillensis* haplotype on St. Croix, an island that has never had a direct land connection with the PRB (Gill *et al.*, 1989), supports anecdotal evidence of a human-mediated introduction to St. Croix in 1937 (Grant & Beatty, 1944). St. Croix populations most likely originated from Eastern Islands sources (Fig. 2). Although our data support the natural occurrence of *E. antillensis* in the Eastern

Islands, three CR haplotypes (H14, H31, H35; Fig. 3A), all occurring in the eastern lowlands of Puerto Rico, are shared with distant Eastern Islands (St. John, Tortola, Guana, Beef, and Virgin Gorda). Incomplete lineage sorting resulting from recent divergence and rapid spatial expansion from eastern Puerto Rico may account for this observation, but these particular shared haplotypes occur within 11 km of a shipping port. A nearly ubiquitous presence of *E. antillensis* in residential gardens and plant nurseries, and frequent transport of horticultural materials in the PRB (Platenberg, 2007) support possible accidental transport of individuals and/or eggs in potted plants between islands. Multiple introductions of the Puerto Rican Coquí, *E. coqui*, and the Cuban Tree Frog, *Osteopilus septentrionalis*, across numerous Virgin Islands (MacLean, 1982; Owen *et al.*, 2005) provide further evidence for trade-mediated human transport of frogs in the PRB.

In conclusion, species that occur in archipelagos with a complex history of connectivity and isolation provide an excellent opportunity to test hypotheses of population persistence, diversification, and extinction. Indeed, *E. antillensis* serves as a model for understanding population responses to Quaternary climatic oscillations and consequent landscape changes in insular systems. Further, phylogeographic studies of taxa broadly distributed in island chains can contribute fundamental information for decisions related to the management of dynamic insular systems.

### **Acknowledgments**

We thank F. Bird-Picó, T. Figueroa, W. Falcón-Linero, J. Fumero, S. Lazell, C.D. Ortiz, G. Perry, C. Petrovic, R. Platenberg, M.J. Quiñones, A. Ríos-Franceschi, Y. Rodríguez,



J.R. Snider, and J.A. Stoken for assistance in the field, M. Farrah and M. Osborne for help in the laboratory, and the Department of Natural and Environmental Resources of Puerto Rico, U.S. Forest Service, the U.S. Virgin Islands Division of Fish and Wildlife, and the National Park Service for granting collecting permits. We acknowledge technical support from the University of New Mexico (UNM) Department of Biology's Molecular Biology Facility, which is supported by National Institutes of Health Grant P20RR18754 from the Institute Development Award Program of the National Center for Research Resources; and from the University of Alaska, Fairbanks Life Science Informatics, a core research resource supported by grant RR016466 from the National Center for Research Resources. T. Giermakowski provided field supplies and curatorial support, and M.P. Heinicke, M.B. Hickman, J. Hollis, C. Metzger, J. Richter, M.J. Ryan, J.W. Streicher, F. Torres-Pérez, T. Turner, D. Warnock, and the Cuervo Lab Group at UNM reviewed earlier drafts of this manuscript. This manuscript benefited greatly from reviews by four anonymous referees. This study was partly funded by grants from the National Science Foundation (DBI-0001975, DEB-0327415) and the American Museum of Natural History to J.A.R.-R., the Undergraduate Opportunities program at the Museum of Southwestern Biology (National Science Foundation DEB-0731350), and awards from the Falconwood Foundation, Society for the Study of Amphibians and Reptiles, the UNM Biology Department, Office of Graduate Studies, and Graduate and Professional Student Association to B.S.B. Fieldwork was partially supported by Long Term Ecological Research Grants (National Science Foundation DEB-0218039 and DEB-0620910).

## References

- Acevedo-Rodríguez, P. (1996) *Flora of St. John, U.S. Virgin Islands*. The New York Botanical Garden Press, Bronx, NY.
- Balinsky, J.B. (1981) Adaptation of nitrogen metabolism to hyperosmotic environment in Amphibia. *Journal of Experimental Zoology*, **215**, 335-350.
- Barker, B.S., Waide, R.B. & Cook, J.A. (2011) Deep intra-island divergence of a montane forest endemic: phylogeography of the Puerto Rican frog *Eleutherodactylus portoricensis* (Anura: Eleutherodactylidae). *Journal of Biogeography*, **38**, 2311-2325.
- Beaumont, A. (2008) Joint determination of topology, divergence time, and immigration in population trees. *Simulations, genetics, and human prehistory* (ed. by S. Matsumura, P. Forster and C. Renfrew), pp. 135-154, Cambridge, MA.
- Beerli, P. (2006) Comparison of Bayesian and maximum-likelihood inference of population genetic parameters. *Bioinformatics*, **22**, 341-345.
- Beerli, P. & Felsenstein, J. (2001) Maximum likelihood estimation of a migration matrix and effective population sizes in  $n$  subpopulations by using a coalescent approach. *Proceedings of the National Academy of Sciences, USA*, **98**, 4563-4568.
- Beerli, P. & Palczewski, M. (2010) Unified framework to evaluate panmixia and migration direction among multiple sampling locations. *Genetics*, **185**, 313-326.
- Brandley, M.C. & de Queiroz, K. (2004) Phylogeny, ecomorphological evolution, and historical biogeography of the *Anolis cristatellus* series. *Herpetological Monographs*, **18**, 90-126.

- Brandley, M.C., Warren, D.L., Leaché, A.D. & McGuire, J.A. (2009) Homoplasy and clade support. *Systematic Biology*, **58**, 184-198.
- Bruen, T.C., Philippe, H. & Bryant, D. (2006) A simple and robust statistical test for detecting the presence of recombination. *Genetics*, **172**, 2665-2681.
- Carine, M. (2005) Spatio-temporal relationships of the Macaronesian endemic flora: a relictual series or window of opportunity? *Taxon*, **54**, 895-903.
- Cornuet, J.-M., Ravigné, V. & Estoup, A. (2010) Inference on population history and model checking using DNA sequence and microsatellite data with the software DIYABC (v. 1.0). *BMC Bioinformatics*, **11**, 401.
- Crawford, A.J. (2003a) Huge populations and old species of Costa Rican and Panamanian dirt frogs inferred from mitochondrial and nuclear gene sequences. *Molecular Ecology*, **12**, 2525-2540.
- Crawford, A.J. (2003b) Relative rates of nucleotide substitution in frogs. *Journal of Molecular Evolution*, **57**, 636-641.
- Crawford, A.J., Bermingham, E. & Polanía, C.S. (2007) The role of tropical dry forest as a long-term barrier to dispersal: a comparative phylogeographical analysis of dry forest tolerant and intolerant frogs. *Molecular Ecology*, **16**, 4789-4807.
- Drewry, G.E. & Jones, K.L. (1976) A new ovoviviparous frog, *Eleutherodactylus jasperi* (Amphibia, Anura, Leptodactylidae). *Journal of Herpetology*, **10**, 161-165.
- Duellman, W.E. & Trueb, L. (1994) *Biology of Amphibians*, 2nd edn. The John Hopkins University Press, Baltimore, MD.
- Dupanloup, I., Schneider, S. & Excoffier, L. (2002) A simulated annealing approach to define the genetic structure of populations. *Molecular Ecology*, **11**, 2571-2581.

- Dutton, A., Bard, E., Antonioli, F., Esat, T., Lambeck, K. & McCulloch, M.T. (2009) Phasing and amplitude of sea-level and climate change during the penultimate interglacial. *Nature Geoscience*, **2**, 355-359.
- Eckert, A. & Carstens, B. (2008) Does gene flow destroy phylogenetic signal? The performance of three methods for estimating species phylogenies in the presence of gene flow. *Molecular Phylogenetics and Evolution*, **49**, 832-842.
- Edwards, S.V. & Beerli, P. (2000) Perspective: gene divergence, population divergence, and the variance in coalescence time in phylogeographic studies. *Evolution*, **54**, 1839-1854.
- Esselstyn, J.A. & Brown, R.M. (2009) The role of repeated sea-level fluctuations in the generation of shrew (Soricidae: *Crocidura*) diversity in the Philippine Archipelago. *Molecular Phylogenetics and Evolution*, **53**, 171-181.
- Ewel, J.J. & Whitmore, J.L. (1973) The ecological life zones of Puerto Rico and the U.S. Virgin Islands. Forest Service Research Paper ITF-18. Río Piedras, PR: United States Department of Agriculture, Forest Service, International Institute of Tropical Forestry. 74 p.
- Excoffier, L., Foll, M. & Petit, R.J. (2009) Genetic consequences of range expansions. *Annual Review of Ecology, Evolution, and Systematics*, **40**, 481-501.
- Excoffier, L., Laval, G. & Schneider, S. (2005) Arlequin (version 3.0): an integrated software package for population genetics data analysis. *Evolutionary Bioinformatics Online*, **1**, 47-50.
- Felsenstein, J. (1984) Distance methods for inferring phylogenies: a justification. *Evolution*, **38**, 16-24.

- Felsenstein, J. (1993) *PHYLIP (Phylogeny Inference Package), Version 3.5c*. In.  
*Distributed by the Author*, Department of Genetics, University of Washington,  
Seattle.
- Figueroa Colón, J.C. (1996) Phytogeographical trends, centers of high species richness  
and endemism, and the question of extinctions in the native flora of Puerto Rico.  
*The scientific survey of Puerto Rico and the Virgin Islands: an eighty-year  
reassessment of the islands' natural history* (ed. by J.C. Figueroa Colón), pp. 89-  
102. Annals of the New York Academy of Sciences, New York, New York.
- Fu, Y.-X. (1997) Statistical tests of neutrality of mutations against population growth,  
hitchhiking and background selection. *Genetics*, **147**, 915-925.
- Gibbs, M.J., Armstrong, J.S. & Gibbs, A.J. (2000) Sister-scanning: a Monte Carlo  
procedure for assessing signals in recombinant sequences. *Bioinformatics*, **16**,  
573-582.
- Gill, I.P., Hubbard, D.K., Mclaughlin, P. & Moore, C. (1989) Sedimentological and  
tectonic evolution of Tertiary St. Croix. In: *12th Caribbean Geological  
Conference* (ed. D.K. Hubbard), pp. 49-71, Teague Bay, St. Croix, West Indies  
Laboratory.
- González, C., Dupont, L.M., Behling, H. & Wefer, G. (2008) Neotropical vegetation  
response to rapid climate changes during the last glacial period: palynological  
evidence from the Cariaco Basin. *Quaternary Research*, **69**, 217-230.
- Grant, C. & Beatty, H.A. (1944) Herpetological notes on St. Croix, Virgin Islands.  
*Herpetologica*, **2**, 110-113.

- Guillot, G., Estoup, A., Mortier, F. & Cosson, J.F. (2005a) A spatial statistical model for landscape genetics. *Genetics*, **170**, 1261-1280.
- Guillot, G., Mortier, F. & Estoup, A. (2005b) GENELAND: a computer package for landscape genetics. *Molecular Ecology Notes*, **5**, 712-715.
- Guillot, G., Santos, F. & Estoup, A. (2008) Analysing georeferenced population genetics data with Geneland: a new algorithm to deal with null alleles and a friendly graphical user interface. *Bioinformatics*, **24**, 1406-1407.
- Heaney, L.R., Walsh, J.S., Jr. & Peterson, A.T. (2005) The roles of geological history and colonization abilities in genetic differentiation between mammalian populations in the Philippine archipelago. *Journal of Biogeography*, **32**, 229-247.
- Hearty, P.J., Hollin, J.T., Neumann, A.C., O'leary, M.J. & Mcculloch, M. (2007) Global sea-level fluctuations during the Last Interglaciation (MIS 5e). *Quaternary Science Reviews*, **26**, 2090-2112.
- Heatwole, H. & Mackenzie, F. (1967) Herpetogeography of Puerto Rico. IV. Paleogeography, faunal similarity and endemism. *Evolution*, **21**, 429-438.
- Hedges, S.B. (1999) Distribution of patterns of amphibians in the West Indies. *Patterns of distribution of amphibians: a global perspective* (ed. by W.E. Duellman), pp. 211-254. The John Hopkins University Press, Baltimore, MD.
- Hedges, S.B., Duellman, W.E. & Heinicke, M.P. (2008) New World direct-developing frogs (Anura: Terrarana): molecular phylogeny, classification, biogeography, and conservation. *Zootaxa*, **1737**, 1-182.

- Henderson, R.W. & Powell, R. (1999) West Indian herpetoecology. *Caribbean amphibians and reptiles* (ed. by B.I. Crother), pp. 223-268. Academic Press, San Diego, CA.
- Hess, P.N. & De Moraes Russo, C.A. (2007) An empirical test of the midpoint rooting method. *Biological Journal of the Linnean Society*, **92**, 669-674.
- Heuertz, M., Fineschi, S., Anzidei, M., Pastorelli, R., Salvini, D., Paule, L., Frascaria-Lacoste, Hardy, O.J., Vekemans, X. & Vendramin, G.G. (2004) Chloroplast DNA variation and postglacial recolonization of common ash (*Fraxinus excelsior* L.) in Europe. *Molecular Ecology*, **13**, 3437-3452.
- Hey, J. & Nielson, R. (2004) Multilocus methods for estimating population sizes, migration rates and divergence time, with applications to the divergence of *Drosophila pseudoobscura* and *D. persimilis*. *Genetics*, **167**, 747-760.
- Higuera-Gundy, A., Brenner, M., Hodell, D.A., Curtis, J.H., Leyden, B.W. & Binford, M.W. (1999) A 10,300 <sup>14</sup>C yr record of climate and vegetation change from Haiti. *Quaternary Research*, **52**, 159-170.
- Hodell, D.A., Anselmetti, F.S., Ariztegui, D., Brenner, M., Curtis, J.H., Gilli, A., Grzesik, D.A., Guilderson, T.P., Müller, A.D., Bush, M.B., Correa-Metrio, A.Y., Escobar, J. & Kutterolf, S. (2008) An 85-ka record of climate change in lowland Central America. *Quaternary Science Reviews*, **27**, 1152-1165.
- Hudson, R.R. (1990) Gene genealogies and the coalescent process. *Oxford Surveys in Evolutionary Biology*, **7**, 1-44.
- Hudson, R.R., Kreitman, M. & Aguadé, M. (1987) A test of neutral molecular evolution based on nucleotide data. *Genetics*, **116**, 153-159.

- Hudson, R.R. & Turelli, M. (2003) Stochasticity overrules the "three-times rule": genetic drift, genetic draft, and coalescence times for nuclear loci versus mitochondrial DNA. *Evolution*, **57**, 182-190.
- Huelsenbeck, J.P. & Ronquist, F. (2001) MRBAYES: Bayesian inference of phylogenetic trees. *Bioinformatics*, **17**, 754-755.
- Huson, D.H. & Bryant, D. (2006) Application of phylogenetic networks in evolutionary studies. *Molecular Biology and Evolution*, **23**, 254-267.
- Jezkova, T., Leal, M. & Rodríguez-Robles, J.A. (2009) Living together but remaining apart: comparative phylogeography of *Anolis poncensis* and *A. cooki*, two lizards endemic to the aridlands of Puerto Rico. *Biological Journal of the Linnean Society*, **96**, 617-634.
- Jordan, M.A. & Snell, H.L. (2008) Historical fragmentation of islands and genetic drift in populations of Galápagos lava lizards (*Microlophus albemarlensis* complex). *Molecular Ecology*, **17**, 1224-1237.
- Katoh, K., Misawa, K., Kuma, K. & Miyata, T. (2002) MAFFT: a novel method for rapid multiple sequence alignment based on fast Fourier transform. *Nucleic Acids Research*, **30**, 3059-3066.
- Kingman, J.F.C. (1982) The coalescent. *Stochastic processes and their applications*, **13**, 235-248.
- Kolbe, J.J., Glor, R.E., Schettino, L.R., Lara, A.C., Larson, A. & Losos, J.B. (2004) Genetic variation increases during biological invasion by a Cuban lizard. *Nature*, **431**, 177-181.



- Lanfear, R., Welch, J. & Bromham, L. (2010) Watching the clock: studying variation in rates of molecular evolution between species. *Trends in Ecology and Evolution*, **25**, 495-503.
- Lazell, J.D., Jr. (1983) Biogeography of the herpetofauna of the British Virgin Islands, with description of a new anole (Sauria: Iguanidae). *Advances in Herpetology and Evolutionary Biology. Essays in Honor of Ernest E. Williams*. (ed. by A.G.J. Rhodin and K. Myata). Museum of Comparative Zoology, Harvard, Cambridge, MA.
- Lim, H.C., Rahman, M.A., Lim, S.L.H., Moyle, R.G. & Sheldon, F.H. (2011) Revisiting Wallace's haunt: coalescent simulations and comparative niche modeling reveal historical mechanisms that promoted avian population divergence in the Malay archipelago. *Evolution*, **65**, 321-334.
- Losos, J.B. & Ricklefs, R. (2009) Adaptation and diversification on islands. *Nature*, **457**, 830-836.
- MacArthur, R.H. & Wilson, E.O. (1967) *The theory of island biogeography*. Princeton University Press, Princeton, NJ.
- Maclean, W. (1982) *Reptiles and amphibians of the Virgin Islands*. Macmillan Caribbean, London, Basingstoke.
- Martin, D.P., Lemey, P., Lott, M., Moulton, V., Posada, D. & Lefevre, P. (2010) RDP3: a flexible and fast computer program for analyzing recombination. *Bioinformatics*, **26**, 2462-2463.
- Martin, D.P., Williamson, C. & Posada, D. (2005) RDP2: recombination detection and analysis from sequence alignments. *Bioinformatics*, **21**, 260-262.

- Mayer, G.C. & Lazell, J. (2000) A new species of *Mabuya* (Sauria: Scincidae) from the British Virgin Islands. *Proceedings of the Biological Society of Washington*, **113**, 871-886.
- Maynard Smith, J. (1992) Analyzing the mosaic structure of genes. *Journal of Molecular Evolution*, **34**, 126-129.
- Measey, G.J., Vences, M., Drewes, R.C., Chiari, Y., Melo, M. & Bourles, B. (2007) Freshwater paths across the ocean: molecular phylogeny of the frog *Ptychocheilichthys newtoni* gives insights into amphibian colonization of oceanic islands. *Journal of Biogeography*, **34**, 7-20.
- Muhs, D.R., Simmons, K.R., Schumann, R.R. & Halley, R.B. (2011) Sea-level history of the past two interglacial periods: new evidence from U-series dating of reef corals from south Florida. *Quaternary Science Reviews*, **30**, 570-590.
- Nabholz, B., Glémin, S. & Galtier, N. (2009) The erratic mitochondrial clock: variations of mutation rate, not population size, affect mtDNA diversity across birds and mammals. *BMC Evolutionary Biology*, **9**, 54.
- Oneal, E., Otte, D. & Knowles, L.L. (2010) Testing for biogeographic mechanisms promoting divergence in Caribbean crickets (genus *Amphispiza*). *Journal of Biogeography*, **37**, 530-540.
- Ovaska, K.E. (2005) The frog (*Eleutherodactylus antillensis*). *Island: fact and theory in nature* (ed. by J.D. Lazell, Jr.), pp. 175-180. University of California Press, Berkeley, CA.
- Owen, J., Perry, G., Lazell, J.D., Jr., Petrovic, C. & Egelhoff, J. (2005) *Osteopilus septentrionalis* (Cuban Tree Frog). *Herpetological Review*, **36**, 76.

- Padidam, M., Sawyer, S. & Fauquet, C.M. (1999) Possible emergence of new geminiviruses by frequent recombination. *Virology*, **265**, 218-225.
- Peltier, W.R. (2002) On eustatic sea level history: Last Glacial Maximum to Holocene. *Quaternary Science Reviews*, **21**, 377-396.
- Platenberg, R.J. (2007) Impacts of introduced species on an island ecosystem: non-native reptiles and amphibians in the U.S. Virgin Islands. In: *Proceedings USDA National Wildlife Research Center Symposia*, pp. 168-174, University of Nebraska, Lincoln.
- Posada, D. & Crandall, K.A. (1998) Modeltest: testing the model of DNA substitution. *Bioinformatics*, **14**, 817-818.
- Posada, D. & Crandall, K.A. (2001) Intraspecific gene genealogies: trees grafting into networks *Trends in Ecology and Evolution*, **16**, 37-45.
- Pregill, G.K. & Olson, S.L. (1981) Zoogeography of West Indian vertebrates in relation to Pleistocene climatic cycles. *Annual Review of Ecology and Systematics*, **12**, 75-98.
- Price, J.P. & Elliott-Fisk, D. (2004) Topographic history of the Maui Nui complex, Hawai'i, and its implications for biogeography. *Pacific Science*, **58**, 27-45.
- R Development Core Team (2010) *R: A language and environment for statistical computing*. R Foundation for Statistical Computing, Vienna, Austria.  
<http://www.r-project.org>.
- Rambaut, A. & Drummond, A.J. (2007) *Tracer*, version 1.5. Available at:  
<http://beast.bio.ed.ac.uk/Tracer>.

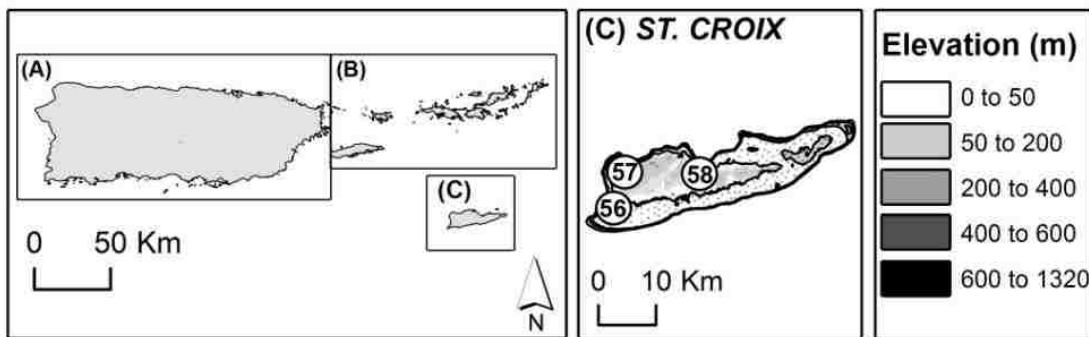
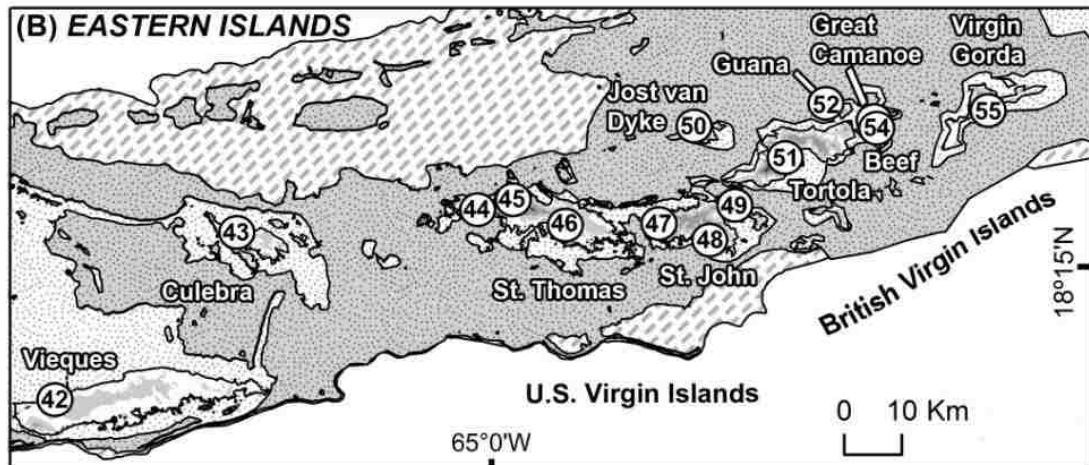
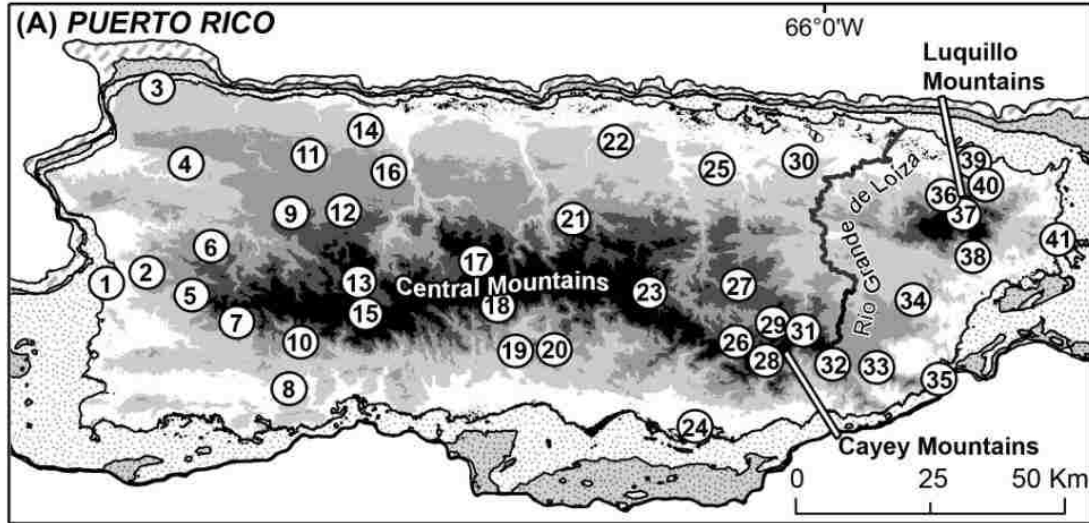
- Renken, R.A., Ward, W.C., Gill, I.P., Gómez-Gómez, F. & Rodríguez-Martínez, J. (2002) Geology and hydrogeology of the Caribbean islands aquifer system of the commonwealth of Puerto Rico and the U.S. Virgin Islands. *U.S. Geological Survey Professional Paper*, **1419**, 1-148.
- Rivero, J.A. & Mayorga, H. (1963) Notes on the distribution of some Puerto Rican frogs with a discussion on the possible origin of *Eleutherodactylus locustus*. *Caribbean Journal of Science*, **3**, 81-85.
- Robert, C.P., Cornuet, J.-M., Marin, J.-M. & Pillai, N.S. (2011) Lack of confidence in approximate Bayesian computation model choice. *Proceedings of the National Academy of Sciences*, **108**, 15112-15117.
- Rodríguez-Robles, J.A., Jezkova, T. & Leal, M. (2008) Genetic structuring in the threatened "Lagartijo del Bosque Seco" (*Anolis cooki*) from Puerto Rico. *Molecular Phylogenetics and Evolution*, **46**, 503-514.
- Rodríguez-Robles, J.A., Jezkova, T. & Leal, M. (2010) Climatic stability and genetic divergence in the tropical insular lizard *Anolis krugi*, the Puerto Rican 'Lagartijo Jardinero de la Montaña'. *Molecular Ecology*, **19**, 1860-1876.
- Rohling, E.J., Grant, K., Bolshaw, M., Roberts, A.P., Siddall, M., Hemleben, C. & Kucera, M. (2009) Antarctic temperature and global sea level closely coupled over the past five glacial cycles. *Nature Geoscience*, **2**, 500-504.
- Salminen, M.O., Carr, J.K., Burke, D.S. & Mccutchan, F.E. (1995) Identification of breakpoints in intergenotypic recombinants of HIV type 1 by bootscanning. *AIDS Research and Human Retroviruses*, **11**, 1423-1425.

- Sheldon, F.H., Jones, C.E. & Mccracken, K.G. (2000) Relative patterns and rates of evolution in heron nuclear and mitochondrial DNA. *Molecular Biology and Evolution*, **17**, 437-450.
- Siddall, M., Rohling, E.J., Almogi-Labin, A., Hemleben, C.H., Meischner, D., Schmelzer, I. & Smeed, D.A. (2003) Sea-level fluctuations during the last glacial cycle. *Nature*, **423**, 853-858.
- Stephens, M. & Donnelly, P. (2003) A comparison of Bayesian methods for haplotype reconstruction from population genotype data. *American Journal of Human Genetics*, **73**, 1162-1169.
- Stephens, M., Smith, N.J. & Donnelly, P. (2001) A new statistical method for haplotype reconstruction from population data. *American Journal of Human Genetics*, **68**, 978-989.
- Stewart, M.M. & Woolbright, L.L. (1996) Amphibians. *The food web of a tropical rainforest* (ed. by D.P. Reagan and R.B. Waide), pp. 273-320. The University of Chicago Press, Chicago, IL.
- Stewart, N.C., Jr. & Via, L.E. (1993) A rapid CTAB DNA isolation technique useful for RAPD fingerprinting and other PCR amplifications. *BioTechniques*, **14**, 748-750.
- Tamura, K., Dudley, J., Nei, M. & Kumar, S. (2007) MEGA4: Molecular Evolutionary Genetics Analysis (MEGA) software version 4.0. *Molecular Biology and Evolution*, **24**, 1596-1599.
- Triantis, K.A., Mylonas, M. & Whittaker, R.J. (2008) Evolutionary species-area curves as revealed by single-island endemics: insights for the inter-provincial species-area relationship. *Ecography*, **31**, 401-407.

- Tsai, Y.-H.E. (2011) PHYLOGEOVIZ: a web-based program that visualizes genetic data on maps. *Molecular Ecology Resources*, **11**, 557-561.
- van Daele, M., van Welden, A., Moernaut, J., Beck, C., Audemard, F., Sanchez, J., Jouanne, F., Carrillo, E., Malavé, G., Lemus, A. & de Batist, M. (2011) Reconstruction of Late-Quaternary sea- and lake-level changes in a tectonically active marginal basin using seismic stratigraphy: the Gulf of Cariaco, NE Venezuela. *Marine Geology*, **279**, 37-51.
- Velo-Antón, G., Burrowes, P.A., Joglar, R.L., Martínez-Solano, I., Beard, K.H. & Parra-Olea, G. (2007) Phylogenetic study of *Eleutherodactylus coqui* (Anura: Leptodactylidae) reveals deep genetic fragmentation in Puerto Rico and pinpoints origins of Hawaiian populations. *Molecular Phylogenetics and Evolution*, **45**, 716-728.
- Waelbroeck, C., Labeyrie, L., Michel, E., Duplessy, J.C., Mcmanus, J.F., Lambeck, K., Balbon, E. & Labracherie, M. (2002) Sea-level and deep water temperature changes derived from benthic foraminifera isotopic records. *Quaternary Science Reviews*, **21**, 295-305.
- Whittaker, R.J., Triantis, K.A. & Ladle, R.J. (2008) A general dynamic theory of oceanic island biogeography. *Journal of Biogeography*, **35**, 977-994.

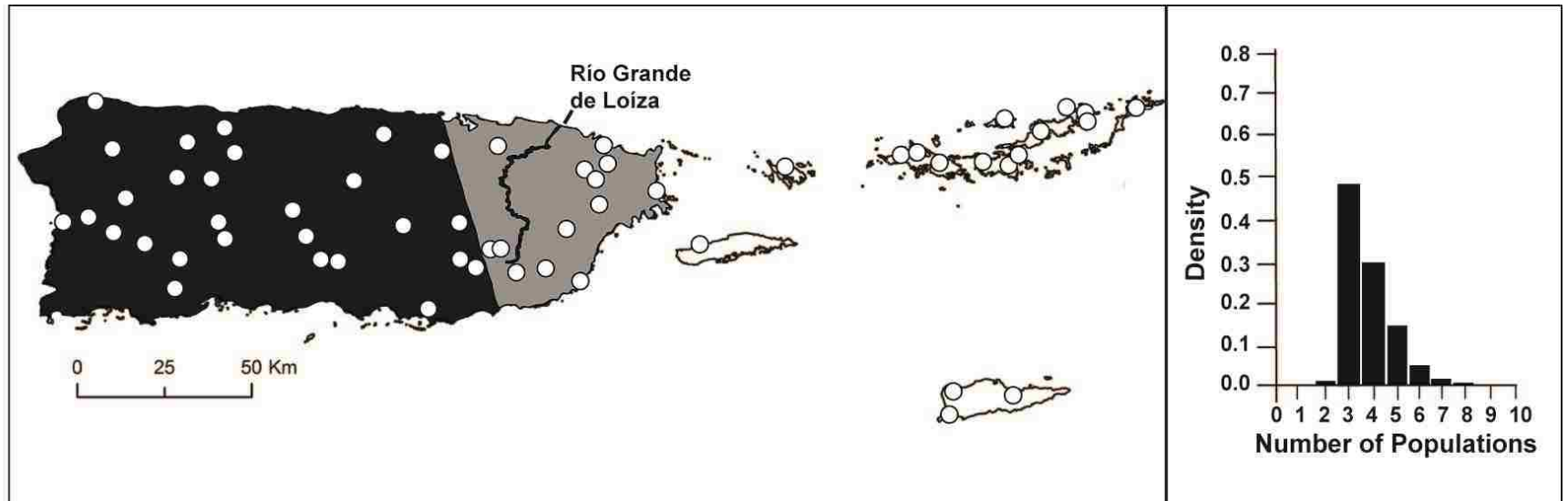
## Figures and Tables

**Fig. 1** Map of the Puerto Rican Bank (A and B) and St. Croix I illustrating the topography of the islands and the geographic location of the sampling localities of *Eleutherodactylus antillensis* (see Table S1, Supporting Information, for specific locality data). The outermost lines in A, B, and C indicate the approximate land configuration at maximum sea level lowering during the Last Glacial Maximum (*ca.* 26.5–19 kya). Diagonal dashes in A and B represent the approximate areas (–200 to 50 m) completely submerged *ca.* 14–10 kya; stippling on medium grey in A, B, and C represents areas (–50 to –25 m) submerged *ca.* 10–8 kya; and stippling on white in A, B, and C represents areas (–25 to 0 m) submerged *ca.* 8–6 kya.



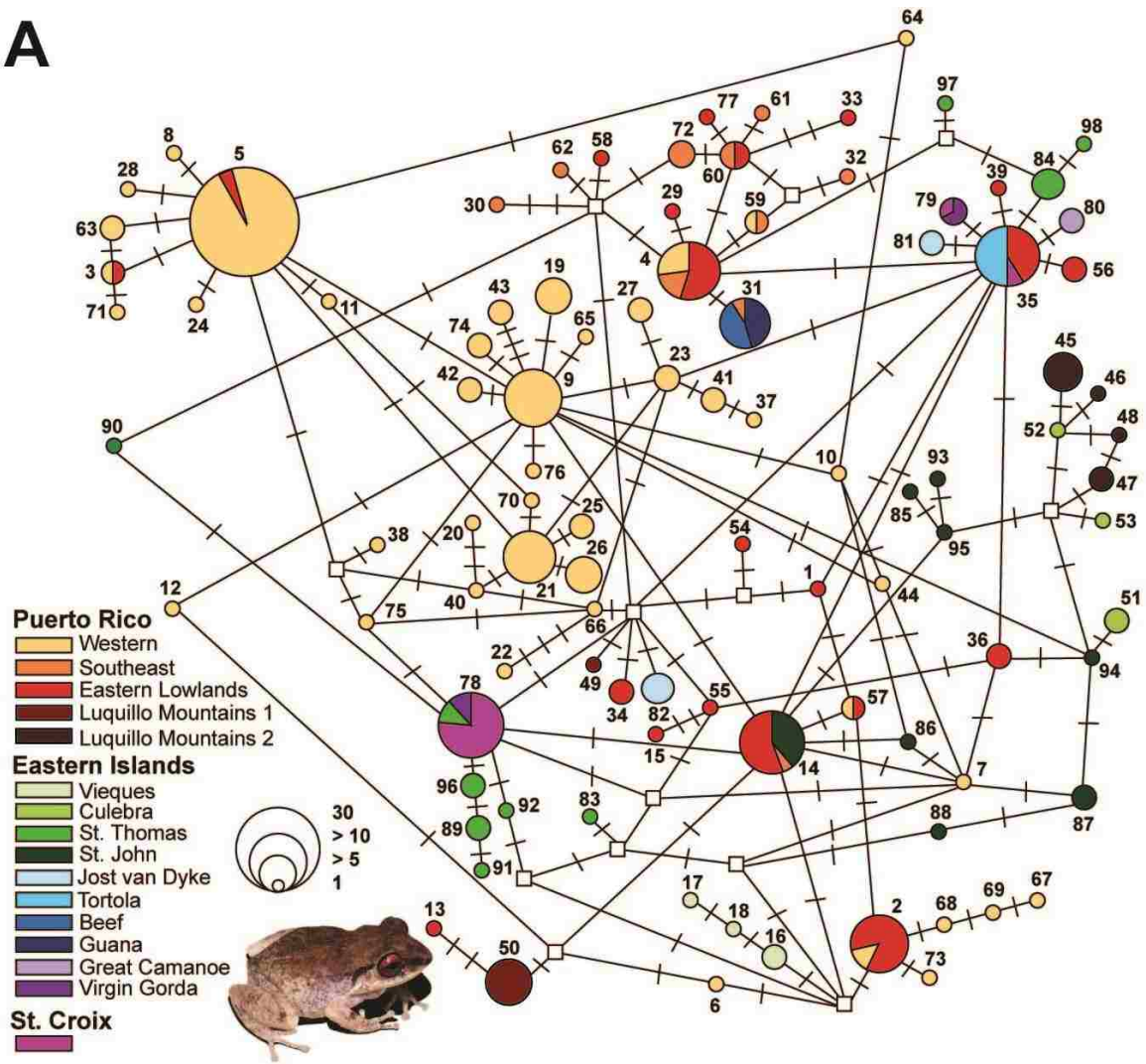


**Fig. 2** Results of the GENELAND analysis based on all loci (the mtDNA control region and four nuDNA introns) for *Eleutherodactylus antillensis*. A map of estimated group membership, indicated by different shades of grey (left panel), and a histogram of posterior probability values for each value of  $K$  (number of populations; right panel) are presented. Groups correspond to those presented in Table 3 and Fig. 4, as follows: western Puerto Rico (black), eastern Puerto Rico (grey), and Eastern Islands (white). The location of the Río Grande De Loíza in Eastern Puerto Rico is indicated.

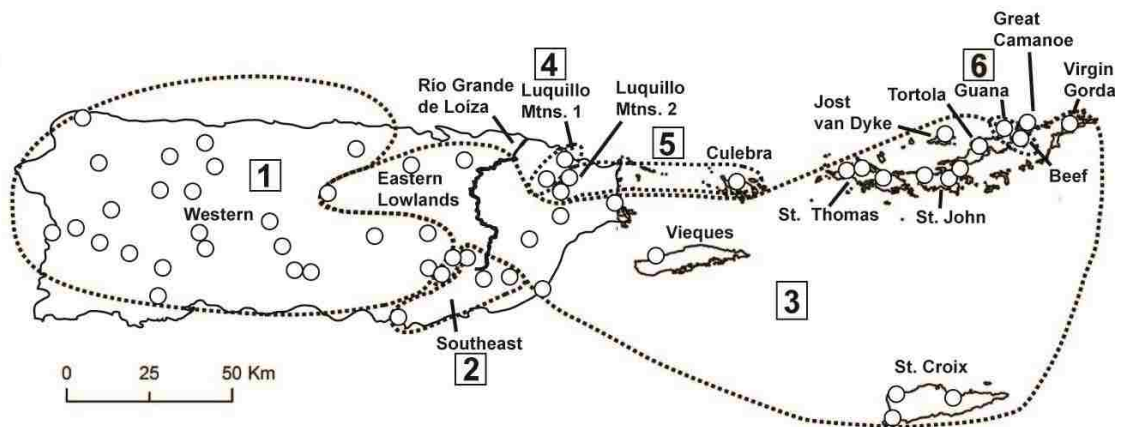


**Fig. 3** (A) Maximum parsimony network representing the relationships among haplotypes of the mtDNA control region of 285 individuals of *Eleutherodactylus antillensis* (inset image). Indels were considered in this analysis. Circles represent unique haplotypes; hatch marks depict single mutations; empty squares indicate missing (i.e. extant unsampled or extinct ancestral) haplotypes. Circle size is proportional to haplotype frequency, and the colour of each circle indicates the individual island from which the haplotype was sampled, except for in Puerto Rico, where circles are coloured by SAMOVA results. Numbers designating haplotypes correspond to those presented in Table S1 and Fig. 5. Photo by Dave Dennis. (B) Genetic partitions of populations of *E. antillensis* identified by the SAMOVA analysis of the mtDNA control-region for  $K = 6$ , where  $K$  is the number of predefined groups. Groups are depicted with dashed lines. When  $K = 6$ , the first group includes all but four localities west of the Río Grande de Loíza in Puerto Rico (Western); the second includes four localities in southeastern Puerto Rico (Southeast); the third includes five eastern Puerto Rico localities (Eastern Lowlands), St. Croix and all Eastern Islands except for Culebra, Beef, and Guana; the fourth includes two localities in the Luquillo Mountains region (Luquillo Mountains 1); the fifth includes two localities in the Luquillo Mountains (Luquillo Mountains 2) and Culebra; and the sixth includes Beef and Guana.

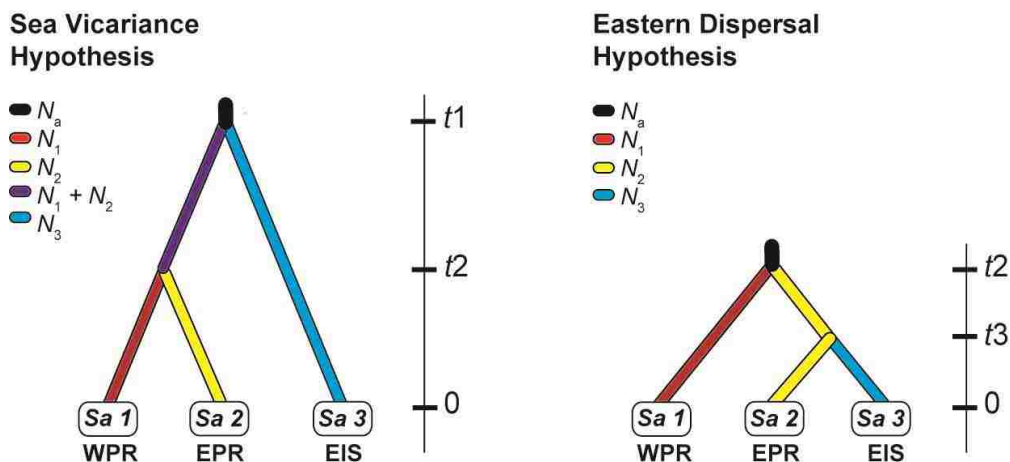
**A**



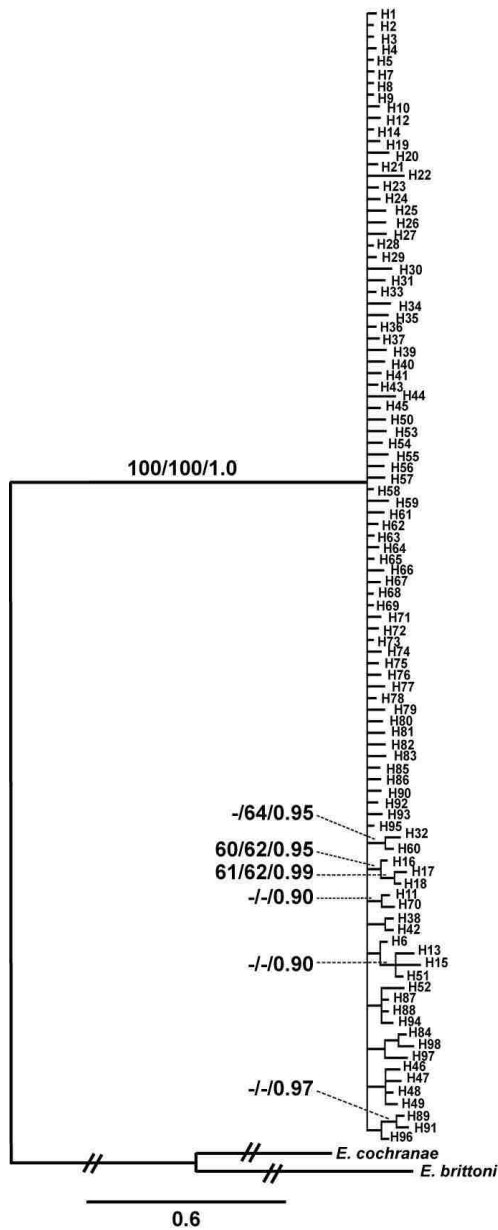
**B**




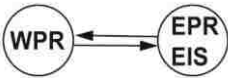

**Fig. 4** The two hypotheses of population history for *Eleutherodactylus antillensis* tested in DIYABC 1.0.4.46, which differ in their estimated divergence time for the Eastern Islands group. The Sea Vicariance Hypothesis depicts the Eastern Islands group diverging from an ancestral population between the last and the penultimate interglacials ( $t_1$ ) and persisting in an isolated refugium since this divergence event despite land-bridge connections across the Puerto Rican Bank during the last glacial period. The Eastern Dispersal Hypothesis model depicts a shallow history for the Eastern Islands group due to recent colonization from eastern Puerto Rican sources during the last glacial period, and the Eastern Islands groups diverging from the eastern Puerto Rican group during the Holocene interglacial ( $t_3$ ) due to rising sea-levels. In both models, the eastern and western Puerto Rican groups began diverging between the Holocene interglacial and the last glacial period ( $t_2$ ). *Sa 1* includes samples from western Puerto Rico (WPR); *Sa 2* includes samples from eastern Puerto Rico (EPR); and *Sa 3* includes samples from the Eastern Islands (EIS). The ancestral effective population size ( $N_a$ ) and effective population size for WPR ( $N_1$ ), EPR ( $N_2$ ), and EIS ( $N_3$ ) groups are indicated.



**Fig. 5** Bayesian tree for 98 unique mitochondrial control region haplotypes of *Eleutherodactylus antillensis*. *Eleutherodactylus brittoni* and *E. cochranae* were used as outgroup taxa. Values on nodes refer to maximum parsimony ( $\geq 60\%$ ), neighbor-joining ( $\geq 60\%$ ), and Bayesian posterior probabilities ( $\geq 0.90$ ), respectively. Haplotype numbers correspond to those in Table S1. Branches to outgroup taxa are truncated for display purposes.



**Table 1** Models of gene flow used for testing the Sea Vicariance Hypothesis and the Eastern Dispersal Hypothesis in MIGRATE 3.2.7. The Bézier log marginal likelihood, log Bayes factor, and rank of each model are indicated. WPR = western Puerto Rico, EPR = eastern Puerto Rico, EIS = Eastern Islands.

	Sea Vicariance Hypothesis	Eastern Dispersal Hypothesis	Eastern Dispersal Hypothesis
	<b>Model 1</b>	<b>Model 2</b>	<b>Model 3</b>
			
<b>All samples</b>			
Bézier log marginal likelihood	-5181	-5046	-4746
Log Bayes factor	-436	-300	0
Rank of model	3	2	1
<b>Excluding potentially introduced samples</b>			
Bézier log marginal likelihood	-4930	-4792	-4745
Log Bayes factor	-184	-46	0
Rank of model	3	2	1

**Table 2** Prior distributions used for the coalescent simulations (performed in DIYABC 1.0.4.46) of population history of *Eleutherodactylus antillensis* groups in western Puerto Rico (WPR), eastern Puerto Rico (EPR), and the Eastern Islands (EIS). Prior distributions for the following demographic parameters were uniform distributions: ancestral effective population size ( $N_a$ ); effective population size for WPR ( $N_1$ ), EPR ( $N_2$ ), and EIS ( $N_3$ ) groups;  $t_1$  = divergence time (in thousands of generations) between the last interglacial and the penultimate interglacial;  $t_2$  = divergence time (in thousands of generations) between the Holocene interglacial and the last glacial period; and  $t_3$  = divergence time (in thousands of generations) between the Holocene interglacial and the last glacial period. The divergence time parameter  $t_2$  has a prior distribution that overlaps with  $t_3$  and therefore we used the “set condition” option to impose the rule that  $t_2 > t_3$  for the following two reasons: first, DIYABC does not allow two divergence time parameters to have overlapping prior distributions unless the “set condition” option is applied, and second, according to the Eastern Dispersal Hypothesis, the EIS group has a very recent history of divergence (Holocene interglacial). Prior distributions for the mutation rate ( $\mu$ ) were drawn from a uniform distribution across loci, and individual locus mutation rates were then drawn from a gamma distribution to allow for rate heterogeneity across sites. Models of nucleotide substitution are provided.

Symbol	Description	Prior distribution
$N_a$	Ancestral effective population size	Uniform ( $10, 1 \times 10^6$ )
$N_1$	Effective population size of WPR group	Uniform ( $10, 4 \times 10^6$ )
$N_2$	Effective population size of EPR group	Uniform ( $10, 5 \times 10^6$ )
$N_3$	Effective population size of EIS group	Uniform ( $10, 4 \times 10^6$ )
$t_1$	Divergence time between the last interglacial and the penultimate interglacial	Uniform (120.0, 240.0)
$t_2$	Divergence time between the Holocene interglacial and the last glacial period	Uniform (0.001, 120.0)
$t_3$	Divergence time between the Holocene interglacial and the last glacial period	Uniform (0.001, 120.0)
Mutation rate parameters		
$\mu$ , mitochondrial DNA	Mean mutation rate (per site per generation)	Uniform ( $0.96 \times 10^{-8}, 4.1 \times 10^{-8}$ )
	Individual locus mutation rate (per site per generation) Model	Gamma ( $0.96 \times 10^{-8}, 4.1 \times 10^{-8}$ ) Hasegawa, Kishino and Yano (HKY) model, % invariant sites = 83, shape of gamma = 0.73
$\mu$ , autosomal diploid DNA	Mean mutation rate (per site per generation)	Uniform ( $6.0 \times 10^{-10}, 8.2 \times 10^{-9}$ )
	Individual locus mutation rate (per site per generation) Model	Gamma ( $6.0 \times 10^{-10}, 8.2 \times 10^{-9}$ ) Hasegawa, Kishino and Yano (HKY) model, % invariant sites = 0, shape of gamma = 2



**Table 3** Descriptive statistics for the five loci used in this study. Sequence length (L, including alignment gaps; bp, base pairs), number of segregating sites (S) with percentage of sequence length in parentheses; and nucleotide diversity ( $\pi$ ), are shown. The following statistics are reported for western Puerto Rican, eastern Puerto Rican, and Eastern Islands populations of *Eleutherodactylus antillensis*: sample size ( $N$ ), number of haplotypes ( $h$ ), with number of private haplotypes in parentheses; haplotype diversity ( $H_d$ ); nucleotide diversity ( $\pi$ ); and Fu's  $F_S$ . Significant  $F_S$  values at  $P < 0.02$  are indicated with an asterisk.

Locus	L (bp)	S (%)	$\pi$	western Puerto Rico				eastern Puerto Rico						
				<i>N</i>	<i>h</i> (# priv)	$H_d$	$\pi$	Fu's $F_S$	<i>N</i>	<i>h</i> (# priv)	$H_d$	$\pi$	Fu's $F_S$	<i>N</i>
<b>mtDNA</b>														
CR	552	49 (8.8)	0.0065	140	51 (45)	0.933	0.0055	-26.379*	63	27 (19)	0.939	0.0063	-16.183*	67
<b>nuDNA</b>														
CRYBA	192	5 (2.6)	0.0019	84	4 (1)	0.146	0.0020	-0.774	39	4 (1)	0.376	0.0031	-0.145	41
MYH	463	9 (1.9)	0.0017	84	5 (2)	0.115	0.0004	-4.033*	39	6 (2)	0.594	0.0018	-1.711	41
RHI	596	8 (1.3)	0.0018	84	4 (1)	0.623	0.0021	2.684	39	6 (3)	0.503	0.0013	-1.490	41
RPL9int4	382	25 (6.5)	0.0070	84	13 (7)	0.499	0.0038	-3.743	39	29 (20)	0.944	0.0110	-13.884*	41

---

**Eastern Islands**

---

$h$ (# priv)	$H_d$	$\pi$	Fu's $F_S$
30 (27)	0.953	0.0060	-21.721*
3 (1)	0.180	0.0010	-1.318
5 (2)	0.653	0.0023	0.522
4 (1)	0.534	0.0010	-0.090
9 (3)	0.498	0.0042	-1.309

---

**Table 4** Scaled effective population sizes ( $\theta$ ) and scaled migration rates ( $M$ ) estimated from the Bayesian MIGRATE 3.2.7 analysis for all loci of western Puerto Rican (WPR), eastern Puerto Rican (EPR), and Eastern Islands (EIS) populations of *E. antillensis*. Values are presented as the average of 20 replicate MIGRATE runs per data set, with the 95% confidence intervals in parentheses.  $\Theta = N_e\mu$  for mtDNA and  $4N_e\mu$  for nuDNA, where  $N_e$  = effective population size, and  $\mu$  = mutation rate per site per generation.  $M = m/\mu$ , where  $m$  = immigration rate.

	$\Theta$			$M$			
	WPR	EPR	EIS	EPR to WPR	WPR to EPR	EIS to EPR	EPR to EIS
<b>All samples</b>	0.0086 (0 – 0.0224)	0.0021 (0 – 0.0107)	0.0003 (0 – 0.0107)	572 (0 – 2267)	1237 (0 – 3200)	747 (0 – 2467)	683 (0 – 2400)
<b>Excludes potentially introduced samples</b>	0.0090 (0 – 0.0230)	0.0003 (0 – 0.0107)	0.0003 (0 – 0.0107)	498 (0 – 2267)	1334 (0 – 3200)	731 (0 – 2467)	692 (0 – 2400)

**Table 5** Posterior probabilities ( $PP$  [(95 % CI)]) and parameter estimates of models of population history of *Eleutherodactylus antillensis* in Puerto Rico and the Eastern Islands tested in DIYABC 1.0.4.46. Median parameter estimates (95% CI) for the following demographic parameters are given below each model: ancestral effective population size ( $N_a$ ); effective population size for western Puerto Rico ( $N_1$ ), eastern Puerto Rico ( $N_2$ ), and Eastern Islands ( $N_3$ ) groups;  $t_1$  = divergence time (in thousands of generations) between the last interglacial and the penultimate interglacial;  $t_2$  = divergence time (in thousands of generations) between the Holocene interglacial and the last glacial period.; and  $t_3$  = divergence time (in thousands of generations) between the Holocene interglacial and the last glacial period. Median parameter estimates for mutation rate ( $\mu$ ) parameters are also provided.

Hypothesis	<i>PP</i>	Demographic parameters							Mutation parameters	
		<i>N<sub>a</sub></i>	<i>N<sub>1</sub></i>	<i>N<sub>2</sub></i>	<i>N<sub>3</sub></i>	<i>t<sub>1</sub></i>	<i>t<sub>2</sub></i>	<i>t<sub>3</sub></i>	Mitochondrial DNA $\mu$	Autosomal diploid DNA $\mu$
<b>Sea Vicariance</b>										
All data	0.20	$3.0 \times 10^5$	$2.5 \times 10^6$	$3.1 \times 10^6$	$2.3 \times 10^6$	–	76.9	140.0	$1.6 \times 10^{-8}$	$9.0 \times 10^{-10}$
		$(8.6 \times 10^4 - 7.8 \times 10^5)$	$(1.1 \times 10^6 - 3.9 \times 10^6)$	$(1.3 \times 10^6 - 4.8 \times 10^6)$	$(9.0 \times 10^5 - 3.8 \times 10^6)$		$(5.5 - 118.0)$	$(121.0 - 222.0)$	$(9.6 \times 10^{-9} - 3.1 \times 10^{-8})$	$(6.0 \times 10^{-10} - 3.5 \times 10^{-9})$
Excludes potentially introduced samples	0.08	$3.1 \times 10^5$	$2.9 \times 10^6$	$3.2 \times 10^6$	$2.2 \times 10^6$	–	82.4	136.0	$1.6 \times 10^{-8}$	$1.1 \times 10^{-9}$
		$(8.6 \times 10^4 - 8.2 \times 10^5)$	$(1.4 \times 10^6 - 3.9 \times 10^6)$	$(1.3 \times 10^6 - 4.8 \times 10^6)$	$(8.5 \times 10^5 - 3.6 \times 10^6)$		$(6.4 - 119.0)$	$(120.0 - 218.0)$	$(9.6 \times 10^{-9} - 3.1 \times 10^{-8})$	$(6.0 \times 10^{-10} - 4.8 \times 10^{-9})$
<b>Eastern Dispersal</b>										
All data	0.80	$2.7 \times 10^5$	$1.8 \times 10^6$	$3.0 \times 10^6$	$1.8 \times 10^6$	50.3	73.3	–	$2.5 \times 10^{-8}$	$2.5 \times 10^{-9}$
		$(7.3 \times 10^4 - 7.0 \times 10^5)$	$(4.6 \times 10^5 - 3.8 \times 10^6)$	$(1.1 \times 10^6 - 4.9 \times 10^6)$	$(6.0 \times 10^5 - 3.8 \times 10^6)$	$(2.7 - 107.0)$	$(24.7 - 117.0)$		$(1.3 \times 10^{-8} - 4.0 \times 10^{-8})$	$(6.9 \times 10^{-10} - 7.6 \times 10^{-9})$
Excludes potentially introduced samples	0.93	$1.9 \times 10^5$	$2.4 \times 10^6$	$2.9 \times 10^6$	$1.8 \times 10^6$	38.4	59.8	–	$2.8 \times 10^{-8}$	$2.0 \times 10^{-9}$
		$(5.8 \times 10^4 - 6.5 \times 10^5)$	$(6.2 \times 10^5 - 3.9 \times 10^6)$	$(1.0 \times 10^6 - 4.9 \times 10^6)$	$(7.0 \times 10^5 - 3.7 \times 10^6)$	$(1.8 - 102.0)$	$(16.8 - 116.0)$		$(1.4 \times 10^{-8} - 4.0 \times 10^{-8})$	$(6.7 \times 10^{-10} - 7.3 \times 10^{-9})$

## Supporting Information

**Fig. S1** Georeferenced pie diagrams for each sampling locality of *Eleutherodactylus antillensis*. Each circle depicts relative haplotype frequencies for the nuclear intron-spanning loci (A)  $\beta$ -crystallin; (B) myosin heavy chain; (C) rhodopsin, and (D) ribosomal protein L9. For each locus, each unique haplotype was assigned a random colour.

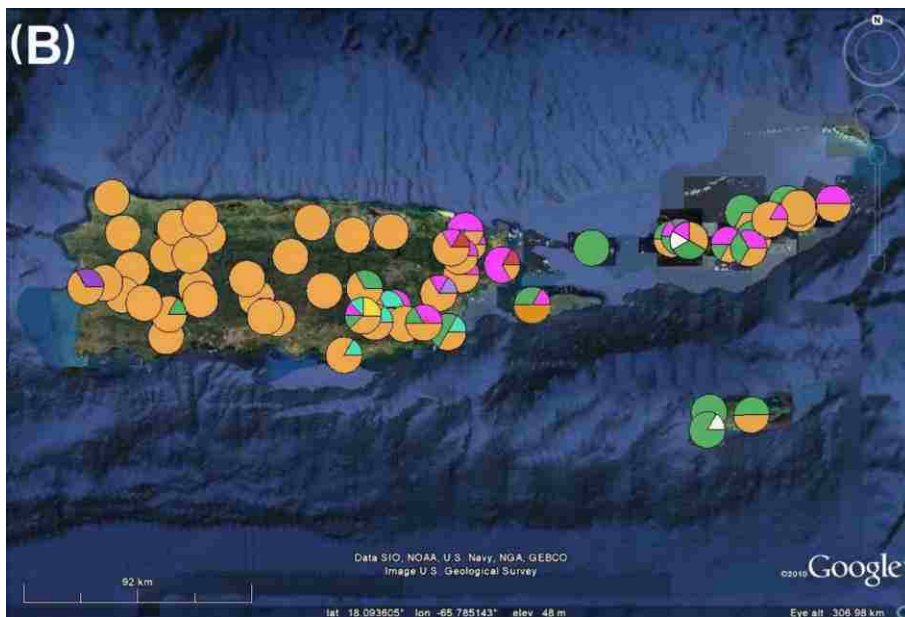
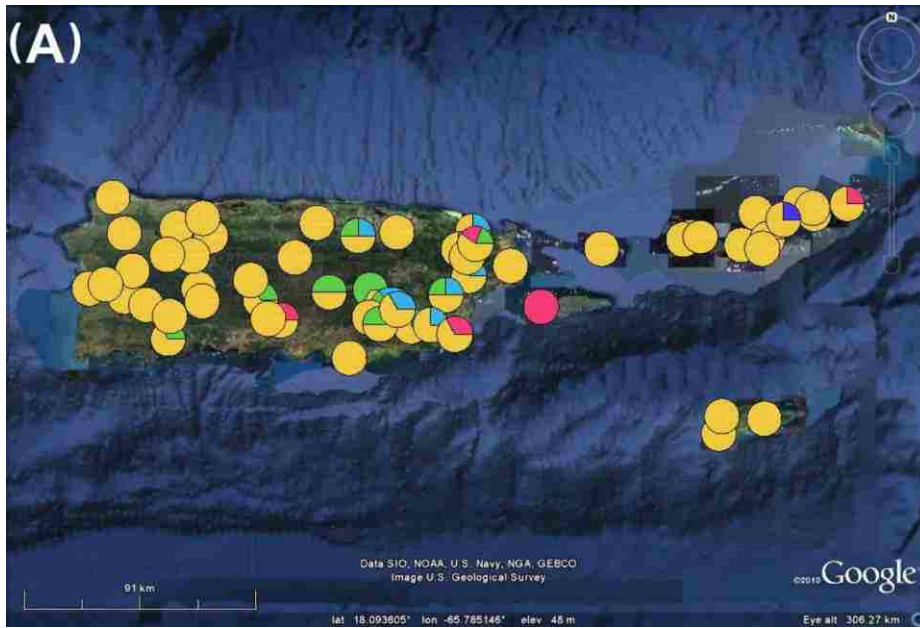
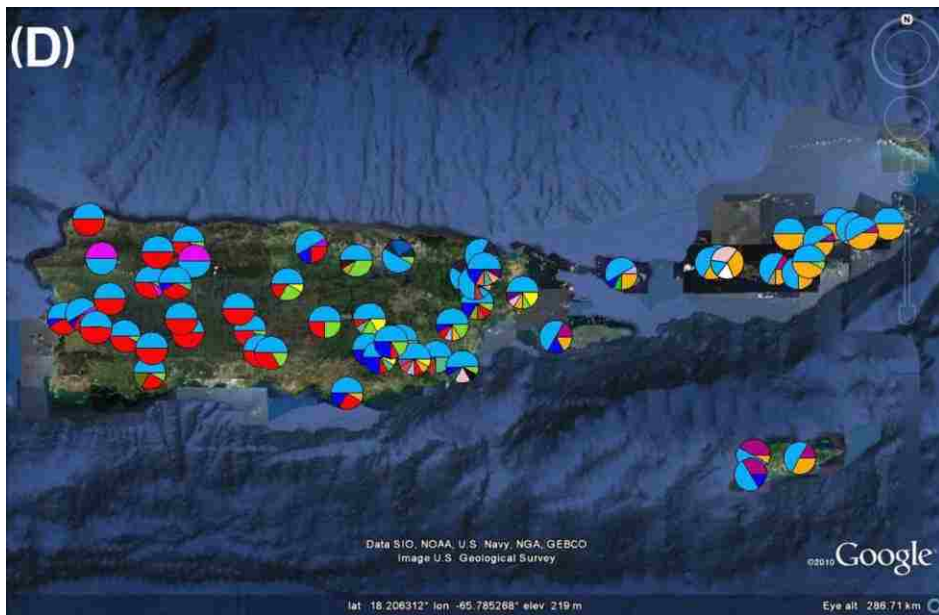
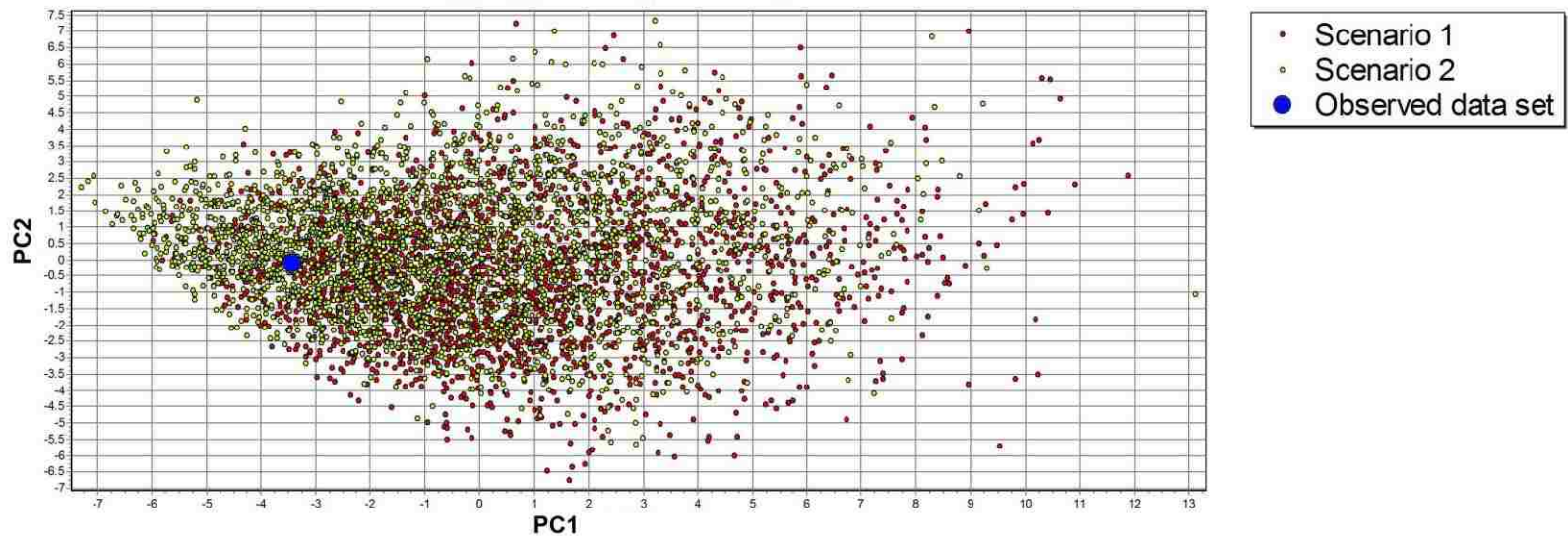


Fig. S1 cont.

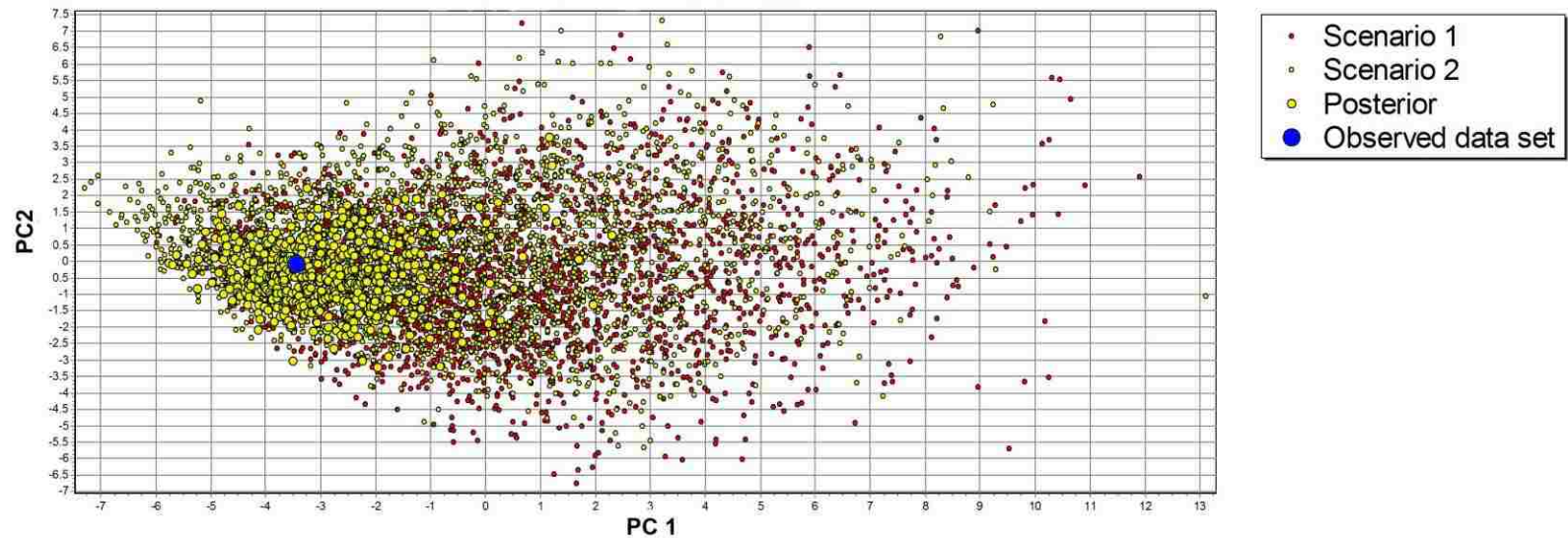




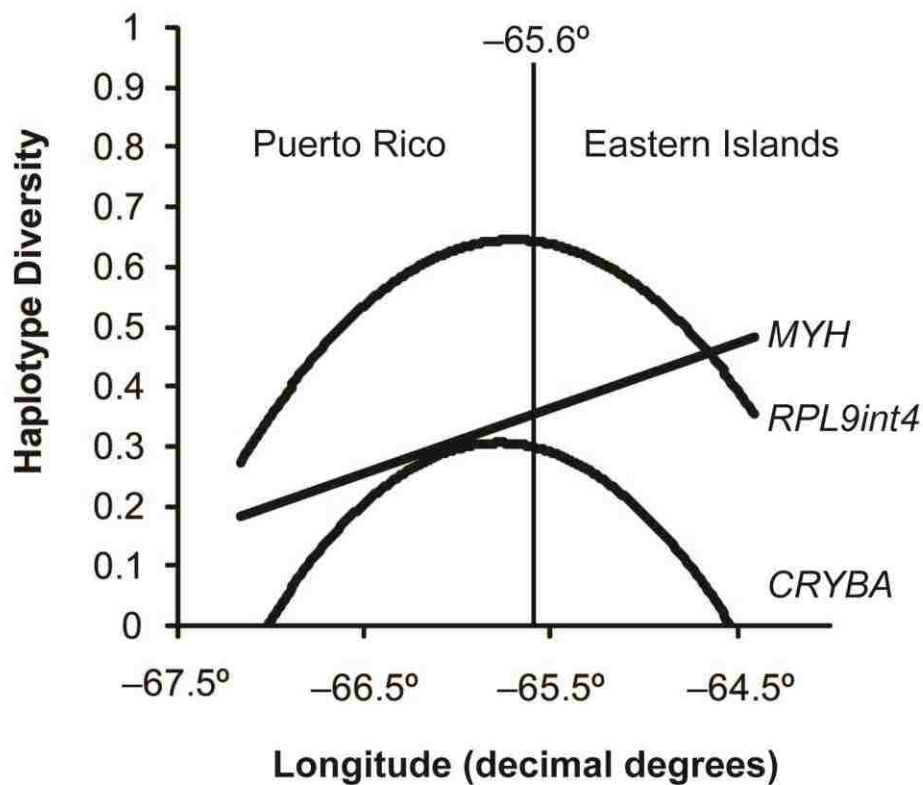
**Fig. S2** Results of a principal component analysis (PCA), performed in DIYABC 1.0.4.46, of the first 100,000 simulated data sets of two divergence models for *Eleutherodactylus antillensis*. The observed data set falls within the simulated data sets, indicating that each model produced data sets similar to the observed one. Results based on all data are depicted (see text for details). Scenario 1 = Sea Vicariance Hypothesis; Scenario 2 = Eastern Dispersal Hypothesis.



**Fig S3** Results of a principal component analysis (PCA), performed in DIYABC 1.0.4.46, of the test quantities obtained with the Eastern Dispersal Hypothesis model posterior combinations together with 10,000 pseudo-observed data sets. The observed data set falls within the simulated data sets, indicating a good fit of the model-posterior combination to the pseudo-observed data set. Results based on all data are depicted (see text for details). Scenario 1 = Sea Vicariance Hypothesis, Scenario 2 = Eastern Dispersal Hypothesis.



**Fig. S4** Longitudinal genetic diversity gradients along the Puerto Rican Bank, plotted by sampling localities from west (left) to east (right). Statistically significant linear (MYH) and nonlinear (CRYBA, RPL9int4) relationships are shown, but note that the trend for MYH is not significant when potentially human-introduced samples are excluded from the analysis (see text for details). A decrease in haplotype diversity occurring at approximately  $-66.0^\circ$  is spatially congruent with the Río Grande de Loíza Basin in eastern Puerto Rico (Fig. 1A). Haplotype diversity for the mitochondrial DNA CR and nuDNA RH1 showed no significant relationship with longitude, and are not shown.



**Table S1** Catalogue numbers for traditional and photographic voucher specimens deposited in the Museum of Southwestern Biology (MSB) at the University of New Mexico, Albuquerque, and the Museum of Vertebrate Zoology (MVZ) at the University of California, Berkeley. Collection locality numbers (as in Figs 1A-C), locality descriptions, control region (CR) haplotype (hap.) numbers (as in Figs 3 and 4), and GenBank accession numbers for the two outgroup taxa (*Eleutherodactylus cochranae* and *E. brittoni*) and individuals of *Eleutherodactylus antillensis* included in this study are provided. BVI = British Virgin Islands; PR = Puerto Rico; USVI = United States Virgin Islands. CR = mtDNA control region; CRYBA =  $\beta$ -crystallin; MYH = myosin heavy chain; RH1 = rhodopsin; RPL9int4 = ribosomal protein L9.

Taxon and institutional voucher	CR hap. no.	Collection locality no.	Collection locality description	GenBank No.						
				Lat	Long	CR	CRYBA	MYH	RH1	RPL9int4
<i>Eleutherodactylus</i>										
<i>brittoni</i>										
MSB 77784	-	-	PR: Muni. Of Orocovis; Bosque Estatal de Toro Negro, Km. 26 on Rd. 143, near Lago el Guineo	18.159	-66.521	JN385585	—	—	—	—
<i>Eleutherodactylus</i>										
<i>cochranae</i>										
MSB 77836	-	-	PR: Muni. Of Arecibo; Intersection of Rd. 635 and Rd. 651	18.456	66.737	JN385584	—	—	—	—
<i>Eleutherodactylus</i>										
<i>antillensis</i>										
MVZ 235025	1	21	PR: Municipality of Morovis; Barrio Río Grande, north of Río Grande de Morovis, 965 m W Km. 42.5 (interior) on Rd. 155	18.2947	-66.41432	JN385299	—	—	—	—
MSB 77068	2	25	PR: Municipality of Bayamón; ca. 100 m northwest of intersection of Calle 1 and Comerío Ave. (=Rd. 167), along Calle 2	18.3697	-66.18621	JN385433	—	—	—	—
MSB 77085	2	25	PR: Municipality of Bayamón; ca. 100 m northwest of intersection of Calle 1 and Comerío Ave. (=Rd. 167), along Calle 2	18.3697	-66.18621	JN385434	JN385748, JN385749	JN386094, JN386095	JN386440, JN386441	JN386786, JN386787
MSB 77086	2	25	PR: Municipality of Bayamón; ca. 100 m northwest of intersection of Calle 1 and Comerío Ave. (=Rd. 167), along Calle 2	18.3697	-66.18621	JN385435	JN385750, JN385751	JN386096, JN386097	JN386442, JN386443	JN386788, JN386789
MSB 77087	2	25	PR: Municipality of Bayamón; ca. 100 m northwest of intersection of Calle 1 and Comerío Ave. (=Rd. 167), along Calle 2	18.3697	-66.18621	JN385436	JN385752, JN385753	JN386098, JN386099	JN386444, JN386445	JN386790, JN386791
MSB 77130	2	28	PR: Municipality of Guayama; end of Rd. 742, area surrounding Lago Carite	18.0668	-66.10204	JN385438	—	—	—	—
MSB 77137	2	28	PR: Municipality of Guayama; end of Rd. 742, area surrounding Lago Carite	18.0668	-66.10204	JN385441	JN385758, JN385759	JN386104, JN386105	JN386450, JN386451	JN386796, JN386797
MSB 77430	2	29	PR: Municipality of Cayey; Bosque Estatal de Carite, Km. 23.6 on Rd. 184	18.1144	-66.06364	JN385494	—	—	—	—
MSB 77433	2	29	PR: Municipality of Cayey; Bosque Estatal de Carite, Km. 23.6 on Rd. 184	18.1144	-66.06364	JN385497	JN385824, JN385825	JN386170, JN386171	JN386516, JN386517	JN386862, JN386863
MSB 77459	2	26	PR: Municipality of Cayey; Barrio Culebras Bajo, Km. 8 on Rd. 738	18.0886	-66.14309	JN385500	JN385828, JN385829	JN386174, JN386175	JN386520, JN386521	JN386866, JN386867
MSB 77461	2	26	PR: Municipality of Cayey; Barrio Culebras Bajo, Km. 8 on Rd. 738	18.0886	-66.14309	JN385502	JN385830, JN385831	JN386176, JN386177	JN386522, JN386523	JN386868, JN386869
MVZ 235026	2	21	PR: Municipality of Morovis; Barrio Río Grande, north of Río Grande de Morovis, 965 m W Km. 42.5 (interior) on Rd. 155	18.2947	-66.41432	JN385300	—	—	—	—

MVZ 235029	2	21	PR: Municipality of Morovis; Barrio Río Grande, north of Río Grande de Morovis, 965 m W Km. 42.5 (interior) on Rd. 155	18.2947	-66.41432	JN385303	JN385590, JN385591	JN385936, JN385937	JN386282, JN386283	JN386628, JN386629
MVZ 251429	2	27	PR: Municipality of Cidra; Barrio Bayamón, Sector Certeneja, Km. 11.2 on Rd. 172, area surrounding Lago de Cidra	18.1841	-66.14052	JN385354	JN385654, JN385655	JN386000, JN386001	JN386346, JN386347	JN386692, JN386693
MVZ 251432	2	27	PR: Municipality of Cidra; Barrio Bayamón, Sector Certeneja, Km. 11.2 on Rd. 172, area surrounding Lago de Cidra	18.1841	-66.14052	JN385357	JN385656, JN385657	JN386002, JN386003	JN386348, JN386349	JN386694, JN386695
MVZ 235027	3	21	PR: Municipality of Morovis; Barrio Río Grande, north of Río Grande de Morovis, 965 m W Km. 42.5 (interior) on Rd. 155	18.2947	-66.41432	JN385301	JN385586, JN385587	JN385932, JN385933	JN386278, JN386279	JN386624, JN386625
MVZ 235031	3	22	PR: Municipality of Vega Alta, Bosque Estatal de Vega, Km. 0.45 on Rd. 676	18.4143	-66.33575	JN385305	—	—	—	—
MSB 77251	4	23	PR: Municipality of Barranquitas; San Cristóbal Canyon, trailhead ca. 1 km southeast of Km. 17.7 on Rd. 156, along trail to canyon floor	18.1756	-66.2898	JN385464	JN385786, JN385787	JN386132, JN386133	JN386478, JN386479	JN386824, JN386825
MSB 77431	4	29	PR: Municipality of Cayey; Bosque Estatal de Carite, Km. 23.6 on Rd. 184	18.1144	-66.06364	JN385495	JN385822, JN385823	JN386168, JN386169	JN386514, JN386515	JN386860, JN386861
MSB 77432	4	29	PR: Municipality of Cayey; Bosque Estatal de Carite, Km. 23.6 on Rd. 184	18.1144	-66.06364	JN385496	—	—	—	—
MSB 77457	4	26	PR: Municipality of Cayey; Barrio Culebras Bajo, Km. 8 on Rd. 738	18.0886	-66.14309	JN385498	JN385826, JN385827	JN386172, JN386173	JN386518, JN386519	JN386864, JN386865
MSB 77458	4	26	PR: Municipality of Cayey; Barrio Culebras Bajo, Km. 8 on Rd. 738	18.0886	-66.14309	JN385499	—	—	—	—
MSB 77460	4	26	PR: Municipality of Cayey; Barrio Culebras Bajo, Km. 8 on Rd. 738	18.0886	-66.14309	JN385501	—	—	—	—
MVZ 235028	4	21	PR: Municipality of Morovis; Barrio Río Grande, north of Río Grande de Morovis, 965 m W Km. 42.5 (interior) on Rd. 155	18.2947	-66.41432	JN385302	JN385588, JN385589	JN385934, JN385935	JN386280, JN386281	JN386626, JN386627
MVZ 251430	4	27	PR: Municipality of Cidra; Barrio Bayamón, Sector Certeneja, Km. 11.2 on Rd. 172, area surrounding Lago de Cidra	18.1841	-66.14052	JN385355	—	—	—	—
MVZ 251431	4	27	PR: Municipality of Cidra; Barrio Bayamón, Sector Certeneja, Km. 11.2 on Rd. 172, area surrounding Lago de Cidra	18.1841	-66.14052	JN385356	—	—	—	—
MVZ 264478	4	24	PR: Municipality of Salinas, Comunidad Aguirre, Rd. 705, ca. 1 km east of Central Aguirre	17.9599	-66.2237	JN385360	JN385658, JN385659	JN386004, JN386005	JN386350, JN386351	JN386696, JN386697
MVZ 264481	4	24	PR: Municipality of Salinas, Comunidad Aguirre, Rd. 705, ca. 1 km east of Central Aguirre	17.9599	-66.2237	JN385362	JN385662, JN385663	JN386008, JN386009	JN386354, JN386355	JN386700, JN386701
MSB 77216	5	15	PR: Municipality of Adjuntas; Barrio Guilarte, intersection of Rd. 518 and Reyes Rivera Rd., along Rd. 518	18.1428	-66.74703	JN385457	JN385776, JN385777	JN386122, JN386123	JN386468, JN386469	JN386814, JN386815
MSB 77226	5	15	PR: Municipality of Adjuntas; Barrio Guilarte, intersection of Rd. 518 and Reyes Rivera Rd., along Rd. 518	18.1428	-66.74703	JN385459	JN385778, JN385779	JN386124, JN386125	JN386470, JN386471	JN386816, JN386817
MSB 77227	5	15	PR: Municipality of Adjuntas; Barrio Guilarte, intersection of Rd. 518 and Reyes Rivera Rd., along Rd. 518	18.1428	-66.74703	JN385460	JN385780, JN385781	JN386126, JN386127	JN386472, JN386473	JN386818, JN386819
MSB 77228	5	15	PR: Municipality of Adjuntas; Barrio Guilarte, intersection of Rd. 518 and Reyes Rivera Rd., along Rd. 518	18.1428	-66.74703	JN385461	—	—	—	—
MSB 77270	5	7	PR: Municipality of Sabana Grande; Maricao State Forest, Km. 8.3 on Rd. 120	18.1295	-66.95499	JN385468	JN385790, JN385791	JN386136, JN386137	JN386482, JN386483	JN386828, JN386829

MSB 77272	5	7	PR: Municipality of Sabana Grande; Maricao State Forest, Km. 8.3 on Rd. 120	18.1295	-66.95499	JN385470	—	—	—	—
MSB 77276	5	8	PR: Municipality of Guánica; Palomas, Km. 8.3 on Rd. 116	18.0130	-66.87622	JN385473	—	—	—	—
MSB 77293	5	8	PR: Municipality of Guánica; Palomas, Km. 8.3 on Rd. 116	18.0130	-66.87622	JN385474	—	—	—	—
MSB 77294	5	8	PR: Municipality of Guánica; Palomas, Km. 8.3 on Rd. 116	18.0130	-66.87622	JN385475	JN385796, JN385797	JN386142, JN386143	JN386488, JN386489	JN386834, JN386835
MSB 77315	5	5	PR: Municipality of San Germán; Maricao State Forest, Km. 9.9 to 10.3 on Rd. 119	18.1576	-67.03645	JN385478	—	—	—	—
MSB 77319	5	5	PR: Municipality of San Germán; Maricao State Forest, Km. 9.9 to 10.3 on Rd. 119	18.1576	-67.03645	JN385479	JN385802, JN385803	JN386148, JN386149	JN386494, JN386495	JN386840, JN386841
MSB 77322	5	5	PR: Municipality of San Germán; Maricao State Forest, Km. 9.9 to 10.3 on Rd. 119	18.1576	-67.03645	JN385482	JN385806, JN385807	JN386152, JN386153	JN386498, JN386499	JN386844, JN386845
MSB 77346	5	1	PR: Municipality of Mayagüez; Barrio Mayagüez, intersection of Rd. 102 and Eliseo F Y Guillot Rd., along Rd. 102	18.1845	-67.16688	JN385483	JN385808, JN385809	JN386154, JN386155	JN386500, JN386501	JN386846, JN386847
MSB 77347	5	1	PR: Municipality of Mayagüez; Barrio Mayagüez, intersection of Rd. 102 and Eliseo F Y Guillot Rd., along Rd. 102	18.1845	-67.16688	JN385484	—	—	—	—
MSB 77348	5	1	PR: Municipality of Mayagüez; Barrio Mayagüez, intersection of Rd. 102 and Eliseo F Y Guillot Rd., along Rd. 102	18.1845	-67.16688	JN385485	—	—	—	—
MSB 77349	5	1	PR: Municipality of Mayagüez; Barrio Mayagüez, intersection of Rd. 102 and Eliseo F Y Guillot Rd., along Rd. 102	18.1845	-67.16688	JN385486	JN385810, JN385811	JN386156, JN386157	JN386502, JN386503	JN386848, JN386849
MSB 77350	5	1	PR: Municipality of Mayagüez; Barrio Mayagüez, intersection of Rd. 102 and Eliseo F Y Guillot Rd., along Rd. 102	18.1845	-67.16688	JN385487	JN385812, JN385813	JN386158, JN386159	JN386504, JN386505	JN386850, JN386851
MSB 77512	5	33	PR: Municipality of Yabucoa; Barrio Calabazas, ca. 0.5 km northwest of intersection of Rd. 182 and Rd. 7, along Rd. 182	18.0640	-65.92127	JN385508	—	—	—	—
MSB 77790	5	14	PR: Municipality of Arecibo; Barrio Dominguito, ca. 1.5 km south of intersection of Cam Denton St. and Rd. 651, pasture west of Rd. 651	18.4283	-66.74782	JN385384	JN385690, JN385691	JN386036, JN386037	JN386382, JN386383	JN386728, JN386729
MSB 77879	5	11	PR: Municipality of Camuy; Abra Honda Barrio, Comunidad Matojillo, ca. 0.5 km northeast of intersection of Carro de Jesús Rd. and Rd. 486	18.3953	-66.84489	JN385402	—	—	—	—
MVZ 235030	5	22	PR: Municipality of Vega Alta, Bosque Estatal de Vega, Km. 0.45 on Rd. 676	18.4143	-66.33575	JN385304	JN385592, JN385593	JN385938, JN385939	JN386284, JN386285	JN386630, JN386631
MVZ 235043	5	2	PR: Municipality of Mayagüez; Barrio Juan Alonso, Km. 4.9 on Rd. 105	18.1989	-67.09987	JN385312	JN385602, JN385603	JN385948, JN385949	JN386294, JN386295	JN386640, JN386641
MVZ 250852	5	13	PR: Municipality of Adjuntas; Barrio Yayales, Km. 77.6 on Rd. 135 (a few meters from intersection of Rd. 131 and Rd. 135)	18.1856	-66.76475	JN385346	JN385642, JN385643	JN385988, JN385989	JN386334, JN386335	JN386680, JN386681
MVZ 250853	5	13	PR: Municipality of Adjuntas; Barrio Yayales, Km. 77.6 on Rd. 135 (a few meters from intersection of Rd. 131 and Rd. 135)	18.1856	-66.76475	JN385347	JN385644, JN385645	JN385990, JN385991	JN386336, JN386337	JN386682, JN386683
MVZ 250867	5	6	PR: Municipality of Las Marías; Barrio Furnias, Sector Santa Rosa, Km. 22.6 on Rd. 119	18.2473	-67.00492	JN385333	JN385628, JN385629	JN385974, JN385975	JN386320, JN386321	JN386666, JN386667
MVZ 250878	5	10	PR: Municipality of Yauco; Km. 10.4 on Rd. 128, area surrounding Embalse (=Lake) Lucchetti	18.0914	-66.86353	JN385348	JN385646, JN385647	JN385992, JN385993	JN386338, JN386339	JN386684, JN386685
MVZ 250879	5	10	PR: Municipality of Yauco; Km. 10.4 on Rd. 128, area surrounding Embalse (=Lake) Lucchetti	18.0914	-66.86353	JN385349	—	—	—	—

MVZ 250881	5	10	PR: Municipality of Yauco; Km. 10.4 on Rd. 128, area surrounding Embalse (=Lake) Lucchetti	18.0914	-66.86353	JN385351	JN385648, JN385649	JN385994, JN385995	JN386340, JN386341	JN386686, JN386687
MVZ 250882	5	10	PR: Municipality of Yauco; Km. 10.4 on Rd. 128, area surrounding Embalse (=Lake) Lucchetti	18.0914	-66.86353	JN385352	JN385650, JN385651	JN385996, JN385997	JN386342, JN386343	JN386688, JN386689
MVZ 235032	6	22	PR: Municipality of Vega Alta, Bosque Estatal de Vega, Km. 0.45 on Rd. 676	18.4143	-66.33575	JN385306	JN385594, JN385595	JN385940, JN385941	JN386286, JN386287	JN386632, JN386633
MVZ 235033	7	22	PR: Municipality of Vega Alta, Bosque Estatal de Vega, Km. 0.45 on Rd. 676	18.4143	-66.33575	JN385307	—	—	—	—
MVZ 235034	8	22	PR: Municipality of Vega Alta, Bosque Estatal de Vega, Km. 0.45 on Rd. 676	18.4143	-66.33575	JN385308	JN385596, JN385597	JN385942, JN385943	JN386288, JN386289	JN386634, JN386635
MSB 77271	9	7	PR: Municipality of Sabana Grande; Maricao State Forest, Km. 8.3 on Rd. 120	18.1295	-66.95499	JN385469	JN385792, JN385793	JN386138, JN386139	JN386484, JN386485	JN386830, JN386831
MSB 77275	9	7	PR: Municipality of Sabana Grande; Maricao State Forest, Km. 8.3 on Rd. 120	18.1295	-66.95499	JN385472	—	—	—	—
MSB 77320	9	5	PR: Municipality of San Germán; Maricao State Forest, Km. 9.9 to 10.3 on Rd. 119	18.1576	-67.03645	JN385480	JN385804, JN385805	JN386150, JN386151	JN386496, JN386497	JN386842, JN386843
MSB 77321	9	5	PR: Municipality of San Germán; Maricao State Forest, Km. 9.9 to 10.3 on Rd. 119	18.1576	-67.03645	JN385481	—	—	—	—
MSB 77791	9	14	PR: Municipality of Arecibo; Barrio Dominguito, ca. 1.5 km south of intersection of Cam Denton St. and Rd. 651, pasture west of Rd. 651	18.4283	-66.74782	JN385385	—	—	—	—
MSB 77792	9	14	PR: Municipality of Arecibo; Barrio Dominguito, ca. 1.5 km south of intersection of Cam Denton St. and Rd. 651, pasture west of Rd. 651	18.4283	-66.74782	JN385386	JN385692, JN385693	JN386038, JN386039	JN386384, JN386385	JN386730, JN386731
MSB 77793	9	14	PR: Municipality of Arecibo; Barrio Dominguito, ca. 1.5 km south of intersection of Cam Denton St. and Rd. 651, pasture west of Rd. 651	18.4283	-66.74782	JN385387	—	—	—	—
MSB 77830	9	16	PR: Municipality of Arecibo; Barrio Esperanza, ca. 5 km southwest of intersection between Hwy. 10 and Rd. 626, end of Rd. 626	18.3668	-66.72152	JN385391	—	—	—	—
MSB 77856	9	12	PR: Municipality of Utuado; Caguana Barrio, Rd. 111, bridge over Tanamá River, ca. 1.8 km west of Parque Ceremonial Indígena Caguana	18.2985	-66.78244	JN385396	—	—	—	—
MSB 78583	9	17	PR: Municipality of Jayuya; Barrio Coabey, La Piedra Escrita recreation area, between Km. 7.7 and Km. 8 on Rd. 144	18.2164	-66.57351	JN385504	JN385832, JN385833	JN386178, JN386179	JN386524, JN386525	JN386870, JN386871
MVZ 235040	9	2	PR: Municipality of Mayagüez; Barrio Juan Alonso, Km. 4.9 on Rd. 105	18.1989	-67.09987	JN385309	JN385598, JN385599	JN385944, JN385945	JN386290, JN386291	JN386636, JN386637
MVZ 238947	9	20	PR: Municipality of Juana Díaz; Barrio Guayabal, Sector Cuevas, Km. 5.6 on Rd. 552	18.0788	-66.46144	JN385326	JN385618, JN385619	JN385964, JN385965	JN386310, JN386311	JN386656, JN386657
MVZ 238948	9	20	PR: Municipality of Juana Díaz; Barrio Guayabal, Sector Cuevas, Km. 5.6 on Rd. 552	18.0788	-66.46144	JN385327	JN385620, JN385621	JN385966, JN385967	JN386312, JN386313	JN386658, JN386659
MVZ 238949	9	20	PR: Municipality of Juana Díaz; Barrio Guayabal, Sector Cuevas, Km. 5.6 on Rd. 552	18.0788	-66.46144	JN385328	—	—	—	—
MVZ 235041	10	2	PR: Municipality of Mayagüez; Barrio Juan Alonso, Km. 4.9 on Rd. 105	18.1989	-67.09987	JN385310	—	—	—	—
MVZ 235042	11	2	PR: Municipality of Mayagüez; Barrio Juan Alonso, Km. 4.9 on Rd. 105	18.1989	-67.09987	JN385311	JN385600, JN385601	JN385946, JN385947	JN386292, JN386293	JN386638, JN386639



MVZ 235044	12	2	PR: Municipality of Mayagüez; Barrio Juan Alonso, Km. 4.9 on Rd. 105	18.1989	-67.09987	JN385313	—	—	—	—
MVZ 235048	13	30	PR: Municipality of San Juan, Bosque Urbano del Nuevo Milenio, ca. 2.4 km S intersection btwn. Guaracanal St. (=Rd. 847) and Luis Muñoz Rivera Ave. (=Hwy. 1), along Guaracanal St.	18.3822	-66.04502	JN385314	JN385604, JN385605	JN385950, JN385951	JN386296, JN386297	JN386642, JN386643
MSB 77409	14	31	PR: Municipality of San Lorenzo; Barrio Espino, ca. 550 m from intersection of Rd. 745 and Los Rosarios Rd., end of Los Rosarios Rd.	18.1168	-66.03617	JN385492	—	—	—	—
MSB 77664	14	49	USVI: St. John; East End Rd. (=Rte. 10), Brown Bay trailhead	18.3559	-64.7009	JN385543	JN385884, JN385885	JN386230, JN386231	JN386576, JN386577	JN386922, JN386923
MSB 77665	14	49	USVI: St. John; East End Rd. (=Rte. 10), Brown Bay trailhead	18.3559	-64.7009	JN385544	JN385886, JN385887	JN386232, JN386233	JN386578, JN386579	JN386924, JN386925
MSB 77670	14	49	USVI: St. John; East End Rd. (=Rte. 10), Brown Bay trailhead	18.3559	-64.7009	JN385546	—	—	—	—
MSB 77671	14	49	USVI: St. John; East End Rd. (=Rte. 10), Brown Bay trailhead	18.3559	-64.7009	JN385547	JN385888, JN385889	JN386234, JN386235	JN386580, JN386581	JN386926, JN386927
MSB 77681	14	48	USVI: St. John; Virgin Islands Environmental Resource Station	18.3222	-64.72313	JN385550	—	—	—	—
MSB 77685	14	47	USVI: St. John; North Shore Road (=Rte. 20), Caneel Hill trailhead across from Lind Point Rd.	18.3365	-64.79282	JN385552	—	—	—	—
MSB 77716	14	47	USVI: St. John; North Shore Road (=Rte. 20), Caneel Hill trailhead across from Lind Point Rd.	18.3365	-64.79282	JN385559	JN385902, JN385903	JN386248, JN386249	JN386594, JN386595	JN386940, JN386941
MVZ 235049	14	30	PR: Municipality of San Juan, Bosque Urbano del Nuevo Milenio, ca. 2.4 km S intersection btwn. Guaracanal St. (=Rd. 847) and Luis Muñoz Rivera Ave. (=Hwy. 1), along Guaracanal St.	18.3822	-66.04502	JN385315	—	—	—	—
MVZ 235051	14	30	PR: Municipality of San Juan, Bosque Urbano del Nuevo Milenio, ca. 2.4 km S intersection btwn. Guaracanal St. (=Rd. 847) and Luis Muñoz Rivera Ave. (=Hwy. 1), along Guaracanal St.	18.3822	-66.04502	JN385317	—	—	—	—
MVZ 235052	14	30	PR: Municipality of San Juan, Bosque Urbano del Nuevo Milenio, ca. 2.4 km S intersection btwn. Guaracanal St. (=Rd. 847) and Luis Muñoz Rivera Ave. (=Hwy. 1), along Guaracanal St.	18.3822	-66.04502	JN385318	JN385608, JN385609	JN385954, JN385955	JN386300, JN386301	JN386646, JN386647
MVZ 264446	14	41	PR: Municipality of Ceiba; ca. 0.5 km west of intersection between Hwy. 3 (ca. Km. 52) and Colonia (=Street) Santa María, along Colonia Santa María	18.2668	-65.633527	JN385378	JN385682, JN385683	JN386028, JN386029	JN386374, JN386375	JN386720, JN386721
MVZ 264453	14	41	PR: Municipality of Ceiba; ca. 0.5 km west of intersection between Hwy. 3 (ca. Km. 52) and Colonia (=Street) Santa María, along Colonia Santa María	18.2668	-65.633527	JN385381	—	—	—	—
MVZ 264472	14	34	PR: Municipality of Las Piedras; Industrial Zone, Félix López Figueroa Street, across the street from fire station	18.1668	-65.866781	JN385371	JN385674, JN385675	JN386020, JN386021	JN386366, JN386367	JN386712, JN386713
MVZ 264482	14	35	PR: Municipality of Yabucoa; Barrio Camino Nuevo, ca. 1.9 km east of intersection of Hwy. 53 and Rd. 9914, along Rd. 9914; ca. 0.4 km west of Playa Lucía	18.0336	-65.833351	JN385363	JN385664, JN385665	JN386010, JN386011	JN386356, JN386357	JN386702, JN386703
MVZ 264483	14	35	PR: Municipality of Yabucoa; Barrio Camino Nuevo, ca. 1.9	18.0336	-65.833351	JN385364	—	—	—	—

MVZ 264484	14	35	km east of intersection of Hwy. 53 and Rd. 9914, along Rd. 9914; ca. 0.4 km west of Playa Lucía PR: Municipality of Yabucoa; Barrio Camino Nuevo, ca. 1.9 km east of intersection of Hwy. 53 and Rd. 9914, along Rd. 9914; ca. 0.4 km west of Playa Lucía	18.0336	-65.833351	JN385365	JN385666, JN385667	JN386012, JN386013	JN386358, JN386359	JN386704, JN386705
MVZ 264485	14	35	PR: Municipality of Yabucoa; Barrio Camino Nuevo, ca. 1.9 km east of intersection of Hwy. 53 and Rd. 9914, along Rd. 9914; ca. 0.4 km west of Playa Lucía	18.0336	-65.833351	JN385366	—	—	—	—
MVZ 235050	15	30	PR: Municipality of San Juan, Bosque Urbano del Nuevo Milenio, ca. 2.4 km S intersection btwn. Guaracanal St. (=Rd. 847) and Luis Muñoz Rivera Ave. (=Hwy. 1), along Guaracanal St.	18.3822	-66.04502	JN385316	JN385606, JN385607	JN385952, JN385953	JN386298, JN386299	JN386644, JN386645
MVZ 238951	16	42	PR: Municipality of Vieques; Mosquito, Km. 9.9 on Rd. 200	18.1267	-65.52278	JN385319	—	—	—	—
MVZ 238956	16	42	PR: Municipality of Vieques; Mosquito, Km. 9.9 on Rd. 200	18.1267	-65.52278	JN385322	—	—	—	—
MVZ 238958	16	42	PR: Municipality of Vieques; Mosquito, Km. 9.9 on Rd. 200	18.1267	-65.52278	JN385323	JN385614, JN385615	JN385960, JN385961	JN386306, JN386307	JN386652, JN386653
MVZ 238952	17	42	PR: Municipality of Vieques; Mosquito, Km. 9.9 on Rd. 200	18.1267	-65.52278	JN385320	JN385610, JN385611	JN385956, JN385957	JN386302, JN386303	JN386648, JN386649
MVZ 238953	18	42	PR: Municipality of Vieques; Mosquito, Km. 9.9 on Rd. 200	18.1267	-65.52278	JN385321	JN385612, JN385613	JN385958, JN385959	JN386304, JN386305	JN386650, JN386651
MSB 77186	19	18	PR: Municipality of Orocovis; Bosque Estatal de Toro Negro, intersection of Rd. 143 and road to Cerro Maravillas radio tower, along Rd. 143	18.1484	-66.53928	JN385449	JN385766, JN385767	JN386112, JN386113	JN386458, JN386459	JN386804, JN386805
MSB 77188	19	18	PR: Municipality of Orocovis; Bosque Estatal de Toro Negro, intersection of Rd. 143 and road to Cerro Maravillas radio tower, along Rd. 143	18.1484	-66.53928	JN385450	—	—	—	—
MSB 77201	19	19	PR: Municipality of Villalba; Barrio Villalba Abajo, Km. 61.2 on Rd. 149 and north to intersection of Rd. 149 and Rd. 5550, along Rd. 149	18.0838	-66.50444	JN385452	—	—	—	—
MSB 77202	19	19	PR: Municipality of Villalba; Barrio Villalba Abajo, Km. 61.2 on Rd. 149 and north to intersection of Rd. 149 and Rd. 5550, along Rd. 149	18.0838	-66.50444	JN385453	JN385770, JN385771	JN386116, JN386117	JN386462, JN386463	JN386808, JN386809
MSB 77203	19	19	PR: Municipality of Villalba; Barrio Villalba Abajo, Km. 61.2 on Rd. 149 and north to intersection of Rd. 149 and Rd. 5550, along Rd. 149	18.0838	-66.50444	JN385454	—	—	—	—
MSB 77204	19	19	PR: Municipality of Villalba; Barrio Villalba Abajo, Km. 61.2 on Rd. 149 and north to intersection of Rd. 149 and Rd. 5550, along Rd. 149	18.0838	-66.50444	JN385455	JN385772, JN385773	JN386118, JN386119	JN386464, JN386465	JN386810, JN386811
MVZ 238945	19	20	PR: Municipality of Juana Díaz; Barrio Guayabal, Sector Cuevas, Km. 5.6 on Rd. 552	18.0788	-66.46144	JN385324	JN385616, JN385617	JN385962, JN385963	JN386308, JN386309	JN386654, JN386655
MVZ 238946	19	20	PR: Municipality of Juana Díaz; Barrio Guayabal, Sector Cuevas, Km. 5.6 on Rd. 552	18.0788	-66.46144	JN385325	—	—	—	—
MVZ 250874	20	4	PR: Municipality of Moca; Barrio Capá, Km. 16.5 on Rd. 112	18.3760	-67.03922	JN385329	JN385622, JN385623	JN385968, JN385969	JN386314, JN386315	JN386660, JN386661
MVZ 250851	21	13	PR: Municipality of Adjuntas; Barrio Yayales, Km. 77.6 on Rd. 135 (a few meters from intersection of Rd. 131 and Rd. 135)	18.1856	-66.76475	JN385345	JN385640, JN385641	JN385986, JN385987	JN386332, JN386333	JN386678, JN386679

MVZ 250859	21	9	PR: Municipality of Lares; Km. 27.0 on Rd. 129	18.3010	-66.87178	JN385338	—	—	—	—
MVZ 250862	21	9	PR: Municipality of Lares; Km. 27.0 on Rd. 129	18.3010	-66.87178	JN385341	JN385638, JN385639	JN385984, JN385985	JN386330, JN386331	JN386676, JN386677
MVZ 250868	21	6	PR: Municipality of Las Marías; Barrio Furnias, Sector Santa Rosa, Km. 22.6 on Rd. 119	18.2473	-67.00492	JN385334	JN385630, JN385631	JN385976, JN385977	JN386322, JN386323	JN386668, JN386669
MVZ 250870	21	6	PR: Municipality of Las Marías; Barrio Furnias, Sector Santa Rosa, Km. 22.6 on Rd. 119	18.2473	-67.00492	JN385335	JN385632, JN385633	JN385978, JN385979	JN386324, JN386325	JN386670, JN386671
MVZ 250872	21	6	PR: Municipality of Las Marías; Barrio Furnias, Sector Santa Rosa, Km. 22.6 on Rd. 119	18.2473	-67.00492	JN385337	—	—	—	—
MVZ 250875	21	4	PR: Municipality of Moca; Barrio Capá, Km. 16.5 on Rd. 112	18.3760	-67.03922	JN385330	JN385624, JN385625	JN385970, JN385971	JN386316, JN386317	JN386662, JN386663
MVZ 264457	21	3	PR:Municipality of Isabela; Barrio Bajura, ca. 1.3 km east of intersection between Road 110 and Road 4466, along Road 4466	18.5002	-67.083536	JN385373	JN385676, JN385677	JN386022, JN386023	JN386368, JN386369	JN386714, JN386715
MVZ 264458	21	3	PR:Municipality of Isabela; Barrio Bajura, ca. 1.3 km east of intersection between Road 110 and Road 4466, along Road 4466	18.5002	-67.083536	JN385374	JN385678, JN385679	JN386024, JN386025	JN386370, JN386371	JN386716, JN386717
MVZ 264463	21	3	PR:Municipality of Isabela; Barrio Bajura, ca. 1.3 km east of intersection between Road 110 and Road 4466, along Road 4466	18.5002	-67.083536	JN385377	—	—	—	—
MVZ 250876	22	4	PR: Municipality of Moca; Barrio Capá, Km. 16.5 on Rd. 112	18.3760	-67.03922	JN385331	JN385626, JN385627	JN385972, JN385973	JN386318, JN386319	JN386664, JN386665
MSB 77819	23	16	PR: Municipality of Arecibo; Barrio Esperanza, ca. 5 km southwest of intersection between Hwy. 10 and Rd. 626, end of Rd. 626	18.3668	-66.72152	JN385388	JN385694, JN385695	JN386040, JN386041	JN386JN386, JN386387	JN386732, JN386733
MSB 77828	23	16	PR: Municipality of Arecibo; Barrio Esperanza, ca. 5 km southwest of intersection between Hwy. 10 and Rd. 626, end of Rd. 626	18.3668	-66.72152	JN385390	JN385696, JN385697	JN386042, JN386043	JN386388, JN386389	JN386734, JN386735
MVZ 250877	23	4	PR: Municipality of Moca; Barrio Capá, Km. 16.5 on Rd. 112	18.3760	-67.03922	JN385332	—	—	—	—
MVZ 250871	24	6	PR: Municipality of Las Marías; Barrio Furnias, Sector Santa Rosa, Km. 22.6 on Rd. 119	18.2473	-67.00492	JN385336	—	—	—	—
MVZ 250860	25	9	PR: Municipality of Lares; Km. 27.0 on Rd. 129	18.3010	-66.87178	JN385339	JN385634, JN385635	JN385980, JN385981	JN386326, JN386327	JN386672, JN386673
MVZ 250861	25	9	PR: Municipality of Lares; Km. 27.0 on Rd. 129	18.3010	-66.87178	JN385340	JN385636, JN385637	JN385982, JN385983	JN386328, JN386329	JN386674, JN386675
MSB 77873	26	11	PR: Municipality of Camuy; Abra Honda Barrio, Comunidad Matojillo, ca. 0.5 km northeast of intersection of Carro de Jesús Rd. and Rd. 486	18.3953	-66.84489	JN385398	JN385706, JN385707	JN386052, JN386053	JN386398, JN386399	JN386744, JN386745
MSB 77874	26	11	PR: Municipality of Camuy; Abra Honda Barrio, Comunidad Matojillo, ca. 0.5 km northeast of intersection of Carro de Jesús Rd. and Rd. 486	18.3953	-66.84489	JN385399	—	—	—	—
MSB 77877	26	11	PR: Municipality of Camuy; Abra Honda Barrio, Comunidad Matojillo, ca. 0.5 km northeast of intersection of Carro de Jesús Rd. and Rd. 486	18.3953	-66.84489	JN385401	JN385710, JN385711	JN386056, JN386057	JN386402, JN386403	JN386748, JN386749
MVZ 250863	26	9	PR: Municipality of Lares; Km. 27.0 on Rd. 129	18.3010	-66.87178	JN385342	—	—	—	—
MVZ 250849	27	13	PR: Municipality of Adjuntas; Barrio Yayales, Km. 77.6 on	18.1856	-66.76475	JN385343	—	—	—	—

MVZ 250850	27	13	Rd. 135 (a few meters from intersection of Rd. 131 and Rd. 135) PR: Municipality of Adjuntas; Barrio Yayales, Km. 77.6 on Rd. 135 (a few meters from intersection of Rd. 131 and Rd. 135)	18.1856	-66.76475	JN385344	—	—	—	—
MVZ 250880	28	10	PR: Municipality of Yauco; Km. 10.4 on Rd. 128, area surrounding Embalse (=Lake) Lucchetti	18.0914	-66.86353	JN385350	—	—	—	—
MVZ 251428	29	27	PR: Municipality of Cidra; Barrio Bayamón, Sector Certeneja, Km. 11.2 on Rd. 172, area surrounding Lago de Cidra	18.1841	-66.14052	JN385353	JN385652, JN385653	JN385998, JN385999	JN386344, JN386345	JN386690, JN386691
MVZ 264475	30	24	PR: Municipality of Salinas; Barrio Plena, Road 712, Km. 1.2 to Km. 2.1	18.0169	-66.216773	JN385358	—	—	—	—
MSB 77543	31	52	BVI: Guana Island; along Longman's Point trail near Guana Island Hotel	18.4786	-64.578	JN385512	—	—	—	—
MSB 77546	31	52	BVI: Guana Island; Guana Island Hotel	18.4786	-64.578	JN385513	JN385844, JN385845	JN386190, JN386191	JN386536, JN386537	JN386882, JN386883
MSB 77549	31	52	BVI: Guana Island; Guana Island Hotel	18.4786	-64.578	JN385514	JN385846, JN385847	JN386192, JN386193	JN386538, JN386539	JN386884, JN386885
MSB 77567	31	52	BVI: Guana Island; Guana Island Hotel	18.4786	-64.578	JN385520	JN385854, JN385855	JN386200, JN386201	JN386546, JN386547	JN386892, JN386893
MSB 77626	31	54	BVI: Beef; ca. 1.5 km east of Terrance B. Lettsome International Airport, along Beef Island Rd. (=Waterfront Dr.)	18.4432	-64.52629	JN385533	JN385872, JN385873	JN386218, JN386219	JN386564, JN386565	JN386910, JN386911
MSB 77627	31	54	BVI: Beef; ca. 1.5 km east of Terrance B. Lettsome International Airport, along Beef Island Rd. (=Waterfront Dr.)	18.4432	-64.52629	JN385534	JN385874, JN385875	JN386220, JN386221	JN386566, JN386567	JN386912, JN386913
MSB 77628	31	54	BVI: Beef; ca. 1.5 km east of Terrance B. Lettsome International Airport, along Beef Island Rd. (=Waterfront Dr.)	18.4432	-64.52629	JN385535	JN385876, JN385877	JN386222, JN386223	JN386568, JN386569	JN386914, JN386915
MSB 77629	31	54	BVI: Beef; ca. 1.5 km east of Terrance B. Lettsome International Airport, along Beef Island Rd. (=Waterfront Dr.)	18.4432	-64.52629	JN385536	—	—	—	—
MSB 77630	31	54	BVI: Beef; ca. 1.5 km east of Terrance B. Lettsome International Airport, along Beef Island Rd. (=Waterfront Dr.)	18.4432	-64.52629	JN385537	—	—	—	—
MSB 77730	31	52	BVI: Guana Island; Guana Island Hotel	18.4786	-64.578	JN385563	—	—	—	—
MVZ 264477	31	24	PR: Municipality of Salinas, Comunidad Aguirre, Rd. 705, ca. 1 km east of Central Aguirre	17.9599	-66.2237	JN385359	—	—	—	—
MVZ 264480	32	24	PR: Municipality of Salinas, Comunidad Aguirre, Rd. 705, ca. 1 km east of Central Aguirre	17.9599	-66.2237	JN385361	JN385660, JN385661	JN386006, JN386007	JN386352, JN386353	JN386698, JN386699
MVZ 264486	33	35	PR: Municipality of Yabucoa; Barrio Camino Nuevo, ca. 1.9 km east of intersection of Hwy. 53 and Rd. 9914, along Rd. 9914; ca. 0.4 km west of Playa Lucía	18.0336	-65.833351	JN385367	JN385668, JN385669	JN386014, JN386015	JN386360, JN386361	JN386706, JN386707
MVZ 264467	34	34	PR: Municipality of Las Piedras; Industrial Zone, Félix López Figueroa Street, across the street from fire station	18.1668	-65.866781	JN385368	JN385670, JN385671	JN386016, JN386017	JN386362, JN386363	JN386708, JN386709
MVZ 264474	34	34	PR: Municipality of Las Piedras; Industrial Zone, Félix López Figueroa Street, across the street from fire station	18.1668	-65.866781	JN385372	—	—	—	—

MSB 77136	35	28	PR: Municipality of Guayama; end of Rd. 742, area surrounding Lago Carite	18.0668	-66.10204	JN385440	JN385756, JN385757	JN386102, JN386103	JN386448, JN386449	JN386794, JN386795
MSB 77138	35	28	PR: Municipality of Guayama; end of Rd. 742, area surrounding Lago Carite	18.0668	-66.10204	JN385442	—	—	—	—
MSB 77555	35	55	BVI: Virgin Gorda, Gorda Peak National Park, main trailhead west of North Sound Rd.	18.4774	-64.40352	JN385519	JN385852, JN385853	JN386198, JN386199	JN386544, JN386545	JN386890, JN386891
MSB 77568	35	51	BVI: Tortola; Ridge Rd., ca. 2.9 km northeast of Sage Mountain National Park, along Ridge Rd.	18.4225	-64.64452	JN385521	JN385856, JN385857	JN386202, JN386203	JN386548, JN386549	JN386894, JN386895
MSB 77569	35	51	BVI: Tortola; Ridge Rd., ca. 2.9 km northeast of Sage Mountain National Park, along Ridge Rd.	18.4225	-64.64452	JN385522	JN385858, JN385859	JN386204, JN386205	JN386550, JN386551	JN386896, JN386897
MSB 77570	35	51	BVI: Tortola; Ridge Rd., ca. 2.9 km northeast of Sage Mountain National Park, along Ridge Rd.	18.4225	-64.64452	JN385523	—	—	—	—
MSB 77571	35	51	BVI: Tortola; Ridge Rd., ca. 2.9 km northeast of Sage Mountain National Park, along Ridge Rd.	18.4225	-64.64452	JN385524	JN385860, JN385861	JN386206, JN386207	JN386552, JN386553	JN386898, JN386899
MSB 77573	35	51	BVI: Tortola; Ridge Rd., ca. 2.9 km northeast of Sage Mountain National Park, along Ridge Rd.	18.4225	-64.64452	JN385525	—	—	—	—
MSB 77745	35	56	USVI: St. Croix; entrance to Sandy Point National Wildlife Refuge, along Tranberg Rd.	17.6870	-64.8793	JN385568	JN385914, JN385915	JN386260, JN386261	JN386606, JN386607	JN386952, JN386953
MVZ 264451	35	41	PR: Municipality of Ceiba; ca. 0.5 km west of intersection between Hwy. 3 (ca. Km. 52) and Colonia (=Street) Santa María, along Colonia Santa María	18.2668	-65.633527	JN385380	—	—	—	—
MVZ 264455	35	41	PR: Municipality of Ceiba; ca. 0.5 km west of intersection between Hwy. 3 (ca. Km. 52) and Colonia (=Street) Santa María, along Colonia Santa María	18.2668	-65.633527	JN385382	JN385686, JN385687	JN386032, JN386033	JN386378, JN386379	JN386724, JN386725
MVZ 264468	35	34	PR: Municipality of Las Piedras; Industrial Zone, Félix López Figueroa Street, across the street from fire station	18.1668	-65.866781	JN385369	—	—	—	—
MSB 77044	36	38	PR: Municipality of Naguabo; Barrio Río Blanco, 600 m south of intersection of Rd. 191 and Rd. 969, along Rd. 191	18.2330	-65.78362	JN385428	JN385742, JN385743	JN386088, JN386089	JN386434, JN386435	JN386780, JN386781
MVZ 264471	36	34	PR: Municipality of Las Piedras; Industrial Zone, Félix López Figueroa Street, across the street from fire station	18.1668	-65.866781	JN385370	JN385672, JN385673	JN386018, JN386019	JN386364, JN386365	JN386710, JN386711
MVZ 264459	37	3	PR: Municipality of Isabela; Barrio Bajura, ca. 1.3 km east of intersection between Road 110 and Road 4466, along Road 4466	18.5002	-67.083536	JN385375	JN385680, JN385681	JN386026, JN386027	JN386372, JN386373	JN386718, JN386719
MVZ 264462	38	3	PR: Municipality of Isabela; Barrio Bajura, ca. 1.3 km east of intersection between Road 110 and Road 4466, along Road 4466	18.5002	-67.083536	JN385376	—	—	—	—
MVZ 264447	39	41	PR: Municipality of Ceiba; ca. 0.5 km west of intersection between Hwy. 3 (ca. Km. 52) and Colonia (=Street) Santa María, along Colonia Santa María	18.2668	-65.633527	JN385379	JN385684, JN385685	JN386030, JN386031	JN386376, JN386377	JN386722, JN386723
MSB 77789	40	14	PR: Municipality of Arecibo; Barrio Dominguito, ca. 1.5 km south of intersection of Cam Denton St. and Rd. 651, pasture west of Rd. 651	18.4283	-66.74782	JN385383	JN385688, JN385689	JN386034, JN386035	JN386380, JN386381	JN386726, JN386727
MSB 77825	41	16	PR: Municipality of Arecibo; Barrio Esperanza, ca. 5 km southwest of intersection between Hwy. 10 and Rd. 626, end of Rd. 626	18.3668	-66.72152	JN385389	—	—	—	—
MSB 77832	41	16	PR: Municipality of Arecibo; Barrio Esperanza, ca. 5 km southwest of intersection between Hwy. 10 and Rd. 626, end	18.3668	-66.72152	JN385392	JN385698, JN385699	JN386044, JN386045	JN386390, JN386391	JN386736, JN386737

			of Rd. 626								
MSB 77846	42	12	PR: Municipality of Utuado; Caguana Barrio, Rd. 111, bridge over Tanamá River, ca. 1.8 km west of Parque Ceremonial Indígena Caguana	18.2985	-66.78244	JN385393	—	—	—	—	—
MSB 77847	42	12	PR: Municipality of Utuado; Caguana Barrio, Rd. 111, bridge over Tanamá River, ca. 1.8 km west of Parque Ceremonial Indígena Caguana	18.2985	-66.78244	JN385394	JN385700, JN385701	JN386046, JN386047	JN386392, JN386393	JN386738, JN386739	
MSB 77855	43	12	PR: Municipality of Utuado; Caguana Barrio, Rd. 111, bridge over Tanamá River, ca. 1.8 km west of Parque Ceremonial Indígena Caguana	18.2985	-66.78244	JN385395	JN385702, JN385703	JN386048, JN386049	JN386394, JN386395	JN386740, JN386741	
MSB 77858	43	12	PR: Municipality of Utuado; Caguana Barrio, Rd. 111, bridge over Tanamá River, ca. 1.8 km west of Parque Ceremonial Indígena Caguana	18.2985	-66.78244	JN385397	JN385704, JN385705	JN386050, JN386051	JN386396, JN386397	JN386742, JN386743	
MSB 77875	44	11	PR: Municipality of Camuy; Abra Honda Barrio, Comunidad Matojillo, ca. 0.5 km northeast of intersection of Carro de Jesús Rd. and Rd. 486	18.3953	-66.84489	JN385400	JN385708, JN385709	JN386054, JN386055	JN386400, JN386401	JN386746, JN386747	
MSB 76710	45	37	PR: Municipality of Río Grande; El Yunque National Forest, intersection of Rd. 191 and Rd. 9938, along Rd. 9938	18.2958	-65.790727	JN385403	—	—	—	—	
MSB 76712	45	37	PR: Municipality of Río Grande; El Yunque National Forest, intersection of Rd. 191 and Rd. 9938, along Rd. 9938	18.2958	-65.790727	JN385404	JN385712, JN385713	JN386058, JN386059	JN386404, JN386405	JN386750, JN386751	
MSB 76737	45	37	PR: Municipality of Río Grande; El Yunque National Forest, intersection of Rd. 191 and Rd. 9938, along Rd. 9938	18.2958	-65.790727	JN385405	JN385714, JN385715	JN386060, JN386061	JN386406, JN386407	JN386752, JN386753	
MSB 76744	45	37	PR: Municipality of Río Grande; El Yunque National Forest, intersection of Rd. 191 and Rd. 9938, along Rd. 9938	18.2958	-65.790727	JN385406	—	—	—	—	
MSB 76800	45	37	PR: Municipality of Río Grande; El Yunque National Forest, intersection of Rd. 191 and Rd. 9938, along Rd. 9938	18.2958	-65.790727	JN385412	JN385722, JN385723	JN386068, JN386069	JN386414, JN386415	JN386760, JN386761	
MSB 76839	45	39	PR: Municipality of Río Grande; Barrio Mameyes, 2.1 km north of intersection of Hwy. 3 and Rd. 968, Costa Real Condominiums	18.3854	-65.77005	JN385413	—	—	—	—	
MSB 76745	46	40	PR: Municipality of Río Grande; El Yunque National Forest, 0.5 km south of intersection between Rd. 191 and Rd. 988, along Rd. 988	18.3375	-65.76043	JN385407	—	—	—	—	
MSB 76761	47	40	PR: Municipality of Río Grande; El Yunque National Forest, 0.5 km south of intersection between Rd. 191 and Rd. 988, along Rd. 988	18.3375	-65.76043	JN385408	—	—	—	—	
MSB 76771	47	40	PR: Municipality of Río Grande; El Yunque National Forest, 0.5 km south of intersection between Rd. 191 and Rd. 988, along Rd. 988	18.3375	-65.76043	JN385409	JN385716, JN385717	JN386062, JN386063	JN386408, JN386409	JN386754, JN386755	
MSB 76778	47	40	PR: Municipality of Río Grande; El Yunque National Forest, 0.5 km south of intersection between Rd. 191 and Rd. 988, along Rd. 988	18.3375	-65.76043	JN385411	JN385720, JN385721	JN386066, JN386067	JN386412, JN386413	JN386758, JN386759	
MSB 76776	48	40	PR: Municipality of Río Grande; El Yunque National Forest, 0.5 km south of intersection between Rd. 191 and Rd. 988, along Rd. 988	18.3375	-65.76043	JN385410	JN385718, JN385719	JN386064, JN386065	JN386410, JN386411	JN386756, JN386757	
MSB 76841	49	39	PR: Municipality of Río Grande; Barrio Mameyes, 2.1 km north of intersection of Hwy. 3 and Rd. 968, Costa Real Condominiums	18.3854	-65.77005	JN385414	JN385724, JN385725	JN386072, JN386073	JN386418, JN386419	JN386764, JN386765	

MSB 76852	50	39	PR: Municipality of Río Grande; Barrio Mameyes, 2.1 km north of intersection of Hwy. 3 and Rd. 968, Costa Real Condominiums	18.3854	-65.77005	JN385415	JN385726, JN385727	JN386073, JN386074	JN386419, JN386420	JN386765, JN386766
MSB 76885	50	39	PR: Municipality of Río Grande; Barrio Mameyes, 2.1 km north of intersection of Hwy. 3 and Rd. 968, Costa Real Condominiums	18.3854	-65.77005	JN385416	—	—	—	—
MSB 76890	50	39	PR: Municipality of Río Grande; Barrio Mameyes, 2.1 km north of intersection of Hwy. 3 and Rd. 968, Costa Real Condominiums	18.3854	-65.77005	JN385417	JN385728, JN385729	JN386074, JN386075	JN386420, JN386421	JN386766, JN386767
MSB 76900	50	36	PR: Municipality of Río Grande; El Yunque National Forest, Km. 19.5 on Rd. 186 near entrance to El Verde Field Station	18.3219	-65.82071	JN385418	JN385732, JN385733	JN386078, JN386079	JN386424, JN386425	JN386770, JN386771
MSB 76904	50	43	PR: Municipality of Culebra; Culebra National Wildlife Refuge, 0.25 - 1.0 km past gate entrance to refuge	18.3253	-65.30328	JN385419	—	—	—	—
MSB 76927	50	36	PR: Municipality of Río Grande; El Yunque National Forest, Km. 19.5 on Rd. 186 near entrance to El Verde Field Station	18.3219	-65.82071	JN385421	—	—	—	—
MSB 76937	50	36	PR: Municipality of Río Grande; El Yunque National Forest, Km. 19.5 on Rd. 186 near entrance to El Verde Field Station	18.3219	-65.82071	JN385424	JN385740, JN385741	JN386086, JN386087	JN386432, JN386433	JN386778, JN386779
MSB 76940	50	36	PR: Municipality of Río Grande; El Yunque National Forest, Km. 19.5 on Rd. 186 near entrance to El Verde Field Station	18.3219	-65.82071	JN385425	JN385730, JN385731	JN386076, JN386077	JN386422, JN386423	JN386768, JN386769
MSB 76943	50	36	PR: Municipality of Río Grande; El Yunque National Forest, Km. 19.5 on Rd. 186 near entrance to El Verde Field Station	18.3219	-65.82071	JN385427	—	—	—	—
MSB 76922	51	43	PR: Municipality of Culebra; Culebra National Wildlife Refuge, 0.25 - 1.0 km past gate entrance to refuge	18.3253	-65.30328	JN385420	JN385736, JN385737	JN386082, JN386083	JN386428, JN386429	JN386774, JN386775
MSB 76934	51	43	PR: Municipality of Culebra; Culebra National Wildlife Refuge, 0.25 - 1.0 km past gate entrance to refuge	18.3253	-65.30328	JN385423	—	—	—	—
MSB 76929	52	43	PR: Municipality of Culebra; Culebra National Wildlife Refuge, 0.25 - 1.0 km past gate entrance to refuge	18.3253	-65.30328	JN385422	JN385738, JN385739	JN386084, JN386085	JN386430, JN386431	JN386776, JN386777
MSB 76942	53	43	PR: Municipality of Culebra; Culebra National Wildlife Refuge, 0.25 - 1.0 km past gate entrance to refuge	18.3253	-65.30328	JN385426	JN385734, JN385735	JN386080, JN386081	JN386426, JN386427	JN386772, JN386773
MSB 77045	54	38	PR: Municipality of Naguabo; Barrio Río Blanco, 600 m south of intersection of Rd. 191 and Rd. 969, along Rd. 191	18.2330	-65.78362	JN385429	—	—	—	—
MSB 77048	55	38	PR: Municipality of Naguabo; Barrio Río Blanco, 600 m south of intersection of Rd. 191 and Rd. 969, along Rd. 191	18.2330	-65.78362	JN385430	—	—	—	—
MSB 77053	56	38	PR: Municipality of Naguabo; Barrio Río Blanco, 600 m south of intersection of Rd. 191 and Rd. 969, along Rd. 191	18.2330	-65.78362	JN385431	JN385744, JN385745	JN386090, JN386091	JN386436, JN386437	JN386782, JN386783
MSB 77065	56	38	PR: Municipality of Naguabo; Barrio Río Blanco, 600 m south of intersection of Rd. 191 and Rd. 969, along Rd. 191	18.2330	-65.78362	JN385432	JN385746, JN385747	JN386092, JN386093	JN386438, JN386439	JN386784, JN386785
MSB 77088	57	25	PR: Municipality of Bayamón; ca. 100 m northwest of intersection of Calle 1 and Comerío Ave. (=Rd. 167), along Calle 2	18.3697	-66.18621	JN385437	—	—	—	—
MSB 77252	57	23	PR: Municipality of Barranquitas; San Cristóbal Canyon, trailhead ca. 1 km southeast of Km. 17.7 on Rd. 156, along trail to canyon floor	18.1756	-66.2898	JN385465	JN385788, JN385789	JN386134, JN386135	JN386480, JN386481	JN386826, JN386827
MSB 77135	58	28	PR: Municipality of Guayama; end of Rd. 742, area surrounding Lago Carite	18.0668	-66.10204	JN385439	JN385754, JN385755	JN386100, JN386101	JN386446, JN386447	JN386792, JN386793
MSB 77150	59	32	PR: Municipality of Patillas; Barrio Egozcue, 300 m from intersection of Rd. 181 and Rd. 759	18.0593	-65.99223	JN385443	JN385760, JN385761	JN386106, JN386107	JN386452, JN386453	JN386798, JN386799

MSB 77297	59	8	PR: Municipality of Guánica; Palomas, Km. 8.3 on Rd. 116	18.0130	-66.87622	JN385477	JN385800, JN385801	JN386146, JN386147	JN386492, JN386493	JN386838, JN386839
MSB 77169	60	32	PR: Municipality of Patillas; Barrio Egozcue, 300 m from intersection of Rd. 181 and Rd. 759	18.0593	-65.99223	JN385444	—	—	—	—
MSB 77175	60	32	PR: Municipality of Patillas; Barrio Egozcue, 300 m from intersection of Rd. 181 and Rd. 759	18.0593	-65.99223	JN385447	JN385764, JN385765	JN386110, JN386111	JN386456, JN386457	JN386802, JN386803
MSB 77513	60	33	PR: Municipality of Yabucoa; Barrio Calabazas, ca. 0.5 km northwest of intersection of Rd. 182 and Rd. 7, along Rd. 182	18.0640	-65.92127	JN385509	JN385838, JN385839	JN386184, JN386185	JN386530, JN386531	JN386876, JN386877
MSB 77515	60	33	PR: Municipality of Yabucoa; Barrio Calabazas, ca. 0.5 km northwest of intersection of Rd. 182 and Rd. 7, along Rd. 182	18.0640	-65.92127	JN385511	JN385842, JN385843	JN386188, JN386189	JN386534, JN386535	JN386880, JN386881
MSB 77170	61	32	PR: Municipality of Patillas; Barrio Egozcue, 300 m from intersection of Rd. 181 and Rd. 759	18.0593	-65.99223	JN385445	—	—	—	—
MSB 77174	62	32	PR: Municipality of Patillas; Barrio Egozcue, 300 m from intersection of Rd. 181 and Rd. 759	18.0593	-65.99223	JN385446	JN385762, JN385763	JN386108, JN386109	JN386454, JN386455	JN386800, JN386801
MSB 77184	63	18	PR: Municipality of Orocovich; Bosque Estatal de Toro Negro, intersection of Rd. 143 and road to Cerro Maravillas radio tower, along Rd. 143	18.1484	-66.53928	JN385448	—	—	—	—
MSB 77189	63	18	PR: Municipality of Orocovich; Bosque Estatal de Toro Negro, intersection of Rd. 143 and road to Cerro Maravillas radio tower, along Rd. 143	18.1484	-66.53928	JN385451	JN385768, JN385769	JN386114, JN386115	JN386460, JN386461	JN386806, JN386807
MSB 77214	64	18	PR: Municipality of Orocovich; Bosque Estatal de Toro Negro, intersection of Rd. 143 and road to Cerro Maravillas radio tower, along Rd. 143	18.1484	-66.53928	JN385456	JN385774, JN385775	JN386120, JN386121	JN386466, JN386467	JN386812, JN386813
MSB 77220	65	15	PR: Municipality of Adjuntas; Barrio Guilarte, intersection of Rd. 518 and Reyes Rivera Rd., along Rd. 518	18.1428	-66.74703	JN385458	—	—	—	—
MSB 77243	66	19	PR: Municipality of Villalba; Barrio Villalba Abajo, Km. 61.2 on Rd. 149 and north to intersection of Rd. 149 and Rd. 5550, along Rd. 149	18.0838	-66.50444	JN385462	JN385782, JN385783	JN386128, JN386129	JN386474, JN386475	JN386820, JN386821
MSB 77250	67	23	PR: Municipality of Barranquitas; San Cristóbal Canyon, trailhead ca. 1 km southeast of Km. 17.7 on Rd. 156, along trail to canyon floor	18.1756	-66.2898	JN385463	JN385784, JN385785	JN386130, JN386131	JN386476, JN386477	JN386822, JN386823
MSB 77253	68	23	PR: Municipality of Barranquitas; San Cristóbal Canyon, trailhead ca. 1 km southeast of Km. 17.7 on Rd. 156, along trail to canyon floor	18.1756	-66.2898	JN385466	—	—	—	—
MSB 77254	69	23	PR: Municipality of Barranquitas; San Cristóbal Canyon, trailhead ca. 1 km southeast of Km. 17.7 on Rd. 156, along trail to canyon floor	18.1756	-66.2898	JN385467	—	—	—	—
MSB 77274	70	7	PR: Municipality of Sabana Grande; Maricao State Forest, Km. 8.3 on Rd. 120	18.1295	-66.95499	JN385471	JN385794, JN385795	JN386140, JN386141	JN386486, JN386487	JN386832, JN386833
MSB 77295	71	8	PR: Municipality of Guánica; Palomas, Km. 8.3 on Rd. 116	18.0130	-66.87622	JN385476	JN385798, JN385799	JN386144, JN386145	JN386490, JN386491	JN386836, JN386837
MSB 77388	72	31	PR: Municipality of San Lorenzo; Barrio Espino, ca. 550 m from intersection of Rd. 745 and Los Rosarios Rd., end of Los Rosarios Rd.	18.1168	-66.03617	JN385488	JN385814, JN385815	JN386160, JN386161	JN386506, JN386507	JN386852, JN386853
MSB 77394	72	31	PR: Municipality of San Lorenzo; Barrio Espino, ca. 550 m from intersection of Rd. 745 and Los Rosarios Rd., end of Los Rosarios Rd.	18.1168	-66.03617	JN385489	JN385816, JN385817	JN386162, JN386163	JN386508, JN386509	JN386854, JN386855



MSB 77405	72	31	PR: Municipality of San Lorenzo; Barrio Espino, ca. 550 m from intersection of Rd. 745 and Los Rosarios Rd., end of Los Rosarios Rd.	18.1168	-66.03617	JN385490	JN385818, JN385819	JN386164, JN386165	JN386510, JN386511	JN386856, JN386857
MSB 77408	72	31	PR: Municipality of San Lorenzo; Barrio Espino, ca. 550 m from intersection of Rd. 745 and Los Rosarios Rd., end of Los Rosarios Rd.	18.1168	-66.03617	JN385491	—	—	—	—
MSB 77429	73	29	PR: Municipality of Cayey; Bosque Estatal de Carite, Km. 23.6 on Rd. 184	18.1144	-66.06364	JN385493	JN385820, JN385821	JN386166, JN386167	JN386512, JN386513	JN386858, JN386859
MSB 77464	74	17	PR: Municipality of Jayuya; Barrio Coabey, La Piedra Escrita recreation area, between Km. 7.7 and Km. 8 on Rd. 144	18.2164	-66.57351	JN385503	—	—	—	—
MSB 78584	74	17	PR: Municipality of Jayuya; Barrio Coabey, La Piedra Escrita recreation area, between Km. 7.7 and Km. 8 on Rd. 144	18.2164	-66.57351	JN385505	JN385834, JN385835	JN386180, JN386181	JN386526, JN386527	JN386872, JN386873
MSB 77466	75	17	PR: Municipality of Jayuya; Barrio Coabey, La Piedra Escrita recreation area, between Km. 7.7 and Km. 8 on Rd. 144	18.2164	-66.57351	JN385506	JN385836, JN385837	JN386182, JN386183	JN386528, JN386529	JN386874, JN386875
MSB 77467	76	17	PR: Municipality of Jayuya; Barrio Coabey, La Piedra Escrita recreation area, between Km. 7.7 and Km. 8 on Rd. 144	18.2164	-66.57351	JN385507	—	—	—	—
MSB 77514	77	33	PR: Municipality of Yabucoa; Barrio Calabazas, ca. 0.5 km northwest of intersection of Rd. 182 and Rd. 7, along Rd. 182	18.0640	-65.92127	JN385510	JN385840, JN385841	JN386186, JN386187	JN386532, JN386533	JN386878, JN386879
MSB 77551	78	55	BVI: Virgin Gorda, Gorda Peak National Park, main trailhead west of North Sound Rd.	18.4774	-64.40352	JN385515	—	—	—	—
MSB 77552	78	55	BVI: Virgin Gorda, Gorda Peak National Park, main trailhead west of North Sound Rd.	18.4774	-64.40352	JN385516	JN385848, JN385849	JN386194, JN386195	JN386540, JN386541	JN386886, JN386887
MSB 77656	78	45	USVI: St. Thomas; ca. 300 m south of St. Peter Mountian Rd. (=Rte. 40), Upper Estate St. Peter	18.3592	-64.94996	JN385540	—	—	—	—
MSB 77659	78	45	USVI: St. Thomas; ca. 300 m south of St. Peter Mountian Rd. (=Rte. 40), Upper Estate St. Peter	18.3592	-64.94996	JN385542	JN385882, JN385883	JN386228, JN386229	JN386574, JN386575	JN386920, JN386921
MSB 77734	78	58	USVI: St. Croix; ca. 500 m east of intersection of Estate Hermon Hill Rd. with Contentment Rd. (=Rte. 70), along Estate Hermon Hill Rd.	17.7382	-64.71516	JN385564	JN385908, JN385909	JN386254, JN386255	JN386600, JN386601	JN386946, JN386947
MSB 77735	78	58	USVI: St. Croix; ca. 500 m east of intersection of Estate Hermon Hill Rd. with Contentment Rd. (=Rte. 70), along Estate Hermon Hill Rd.	17.7382	-64.71516	JN385565	JN385910, JN385911	JN386256, JN386257	JN386602, JN386603	JN386948, JN386949
MSB 77736	78	58	USVI: St. Croix; ca. 500 m east of intersection of Estate Hermon Hill Rd. with Contentment Rd. (=Rte. 70), along Estate Hermon Hill Rd.	17.7382	-64.71516	JN385566	—	—	—	—
MSB 77739	78	58	USVI: St. Croix; ca. 500 m east of intersection of Estate Hermon Hill Rd. with Contentment Rd. (=Rte. 70), along Estate Hermon Hill Rd.	17.7382	-64.71516	JN385567	JN385912, JN385913	JN386258, JN386259	JN386604, JN386605	JN386950, JN386951
MSB 77746	78	56	USVI: St. Croix; entrance to Sandy Point National Wildlife Refuge, along Tranberg Rd.	17.6870	-64.8793	JN385569	—	—	—	—
MSB 77747	78	56	USVI: St. Croix; entrance to Sandy Point National Wildlife Refuge, along Tranberg Rd.	17.6870	-64.8793	JN385570	JN385916, JN385917	JN386262, JN386263	JN386608, JN386609	JN386954, JN386955
MSB 77748	78	56	USVI: St. Croix; entrance to Sandy Point National Wildlife Refuge, along Tranberg Rd.	17.6870	-64.8793	JN385571	JN385918, JN385919	JN386264, JN386265	JN386610, JN386611	JN386956, JN386957
MSB 77749	78	56	USVI: St. Croix; entrance to Sandy Point National Wildlife Refuge, along Tranberg Rd.	17.6870	-64.8793	JN385572	—	—	—	—
MSB 77752	78	57	USVI: St. Croix; Creque Dam Rd., Mt. Victory Camp	17.7475	-64.86926	JN385573	—	—	—	—

MSB 77756	78	57	USVI: St. Croix; Creque Dam Rd., Mt. Victory Camp	17.7475	-64.86926	JN385575	JN385922, JN385923	JN386268, JN386269	JN386614, JN386615	JN386960, JN386961
MSB 77760	78	58	USVI: St. Croix; ca. 500 m east of intersection of Estate Hermon Hill Rd. with Contentment Rd. (=Rte. 70), along Estate Hermon Hill Rd.	17.7382	-64.71516	JN385576	—	—	—	—
MSB 77769	78	57	USVI: St. Croix, Brooks Hill, Mahogany Rd. (=Rte. 76), entrance to St. Croix Leap, along Mahogany Rd.	17.7286	-64.85865	JN385577	JN385924, JN385925	JN386270, JN386271	JN386616, JN386617	JN386962, JN386963
MSB 77771	78	57	USVI: St. Croix, Brooks Hill, Mahogany Rd. (=Rte. 76), entrance to St. Croix Leap, along Mahogany Rd.	17.7286	-64.85865	JN385578	—	—	—	—
MSB 77553	79	55	BVI: Virgin Gorda, Gorda Peak National Park, main trailhead west of North Sound Rd.	18.4774	-64.40352	JN385517	—	—	—	—
MSB 77554	79	55	BVI: Virgin Gorda, Gorda Peak National Park, main trailhead west of North Sound Rd.	18.4774	-64.40352	JN385518	JN385850, JN385851	JN386196, JN386197	JN386542, JN386543	JN386888, JN386889
MSB 77754	79	57	USVI: St. Croix; Creque Dam Rd., Mt. Victory Camp	17.7475	-64.86926	JN385574	JN385920, JN385921	JN386266, JN386267	JN386612, JN386613	JN386958, JN386959
MSB 77592	80	53	BVI: Great Camanoe; around Low Bay boat dock	18.4629	-64.53426	JN385526	JN385862, JN385863	JN386208, JN386209	JN386554, JN386555	JN386900, JN386901
MSB 77593	80	53	BVI: Great Camanoe; around Low Bay boat dock	18.4629	-64.53426	JN385527	JN385864, JN385865	JN386210, JN386211	JN386556, JN386557	JN386902, JN386903
MSB 77602	81	50	BVI: Jost van Dyke; Roach Hill, ca. 1.4 km from intersection of Mountain Trail Rd. and East End Rd., along Mountain Trail Rd.	18.4477	-64.74007	JN385528	JN385866, JN385867	JN386212, JN386213	JN386558, JN386559	JN386904, JN386905
MSB 77604	81	50	BVI: Jost van Dyke; Roach Hill, ca. 1.4 km from intersection of Mountain Trail Rd. and East End Rd., along Mountain Trail Rd.	18.4477	-64.74007	JN385530	—	—	—	—
MSB 77603	82	50	BVI: Jost van Dyke; Roach Hill, ca. 1.4 km from intersection of Mountain Trail Rd. and East End Rd., along Mountain Trail Rd.	18.4477	-64.74007	JN385529	JN385868, JN385869	JN386214, JN386215	JN386560, JN386561	JN386906, JN386907
MSB 77605	82	50	BVI: Jost van Dyke; Roach Hill, ca. 1.4 km from intersection of Mountain Trail Rd. and East End Rd., along Mountain Trail Rd.	18.4477	-64.74007	JN385531	JN385870, JN385871	JN386216, JN386217	JN386562, JN386563	JN386908, JN386909
MSB 77607	82	50	BVI: Jost van Dyke; Roach Hill, ca. 1.4 km from intersection of Mountain Trail Rd. and East End Rd., along Mountain Trail Rd.	18.4477	-64.74007	JN385532	—	—	—	—
MSB 77649	83	45	USVI: St. Thomas; Caret Bay, 220 m northwest of Crown Mountain Rd. (=Rte. 33), West Caret Bay ghut	18.3643	-64.97834	JN385538	JN385878, JN385879	JN386224, JN386225	JN386570, JN386571	JN386916, JN386917
MSB 77650	84	45	USVI: St. Thomas; Caret Bay, 220 m northwest of Crown Mountain Rd. (=Rte. 33), West Caret Bay ghut	18.3643	-64.97834	JN385539	JN385880, JN385881	JN386226, JN386227	JN386572, JN386573	JN386918, JN386919
MSB 77657	84	45	USVI: St. Thomas; ca. 300 m south of St. Peter Mountain Rd. (=Rte. 40), Upper Estate St. Peter	18.3592	-64.94996	JN385541	—	—	—	—
MSB 77777	84	44	USVI: St. Thomas; Fortuna Hill, ca. 820 m southwest of intersection of Bordeaux Rd. and Edward D. Newton/Fortuna Rd., along private road to Fortuna Ranch	18.3559	-65.00633	JN385582	JN385928, JN385929	JN386274, JN386275	JN386620, JN386621	JN386966, JN386967
MSB 77669	85	49	USVI: St. John; East End Rd. (=Rte. 10), Brown Bay trailhead	18.3559	-64.7009	JN385545	—	—	—	—
MSB 77673	86	48	USVI: St. John; Virgin Islands Environmental Resource Station	18.3222	-64.72313	JN385548	JN385890, JN385891	JN386236, JN386237	JN386582, JN386583	JN386928, JN386929

MSB 77680	87	48	USVI: St. John; Virgin Islands Environmental Resource Station	18.3222	-64.72313	JN385549	JN385892, JN385893	JN386238, JN386239	JN386584, JN386585	JN386930, JN386931
MSB 77717	87	47	USVI: St. John; North Shore Road (=Rte. 20), Caneel Hill trailhead across from Lind Point Rd.	18.3365	-64.79282	JN385560	JN385904, JN385905	JN386250, JN386251	JN386596, JN386597	JN386942, JN386943
MSB 77684	88	47	USVI: St. John; North Shore Road (=Rte. 20), Caneel Hill trailhead across from Lind Point Rd.	18.3365	-64.79282	JN385551	JN385894, JN385895	JN386240, JN386241	JN386586, JN386587	JN386932, JN386933
MSB 77692	89	46	USVI: St. Thomas; ca. 230 m northwest of intersection of Frenchman Bay Rd. (=Rte. 30) and Beverly Hills E Rd., Williamsson's Ghut	18.3229	-64.91082	JN385553	JN385896, JN385897	JN386242, JN386243	JN386588, JN386589	JN386934, JN386935
MSB 77700	89	46	USVI: St. Thomas; Wintberg Peak, near intersection of Rte. 39 and Lemon Tree Rd., along Lemon Tree Rd.	18.3481	-64.90594	JN385555	JN385898, JN385899	JN386244, JN386245	JN386590, JN386591	JN386936, JN386937
MSB 77694	90	46	USVI: St. Thomas; ca. 230 m northwest of intersection of Frenchman Bay Rd. (=Rte. 30) and Beverly Hills E Rd., Williamsson's Ghut	18.3229	-64.91082	JN385554	—	—	—	—
MSB 77701	91	46	USVI: St. Thomas; Wintberg Peak, near intersection of Rte. 39 and Lemon Tree Rd., along Lemon Tree Rd.	18.3481	-64.90594	JN385556	—	—	—	—
MSB 77702	92	46	USVI: St. Thomas; Wintberg Peak, near intersection of Rte. 39 and Lemon Tree Rd., along Lemon Tree Rd.	18.3481	-64.90594	JN385557	JN385900, JN385901	JN386246, JN386247	JN386592, JN386593	JN386938, JN386939
MSB 77706	93	47	USVI: St. John; North Shore Road (=Rte. 20), Caneel Hill trailhead across from Lind Point Rd.	18.3365	-64.79282	JN385558	—	—	—	—
MSB 77721	94	48	USVI: St. John; intersection of Bordeaux Mountain Rd (=Rte. 108) and Bay Forest Rd, along Bordeaux Mountain Rd.	18.3354	-64.72759	JN385561	JN385906, JN385907	JN386252, JN386253	JN386598, JN386599	JN386944, JN386945
MSB 77723	95	48	USVI: St. John; intersection of Bordeaux Mountain Rd (=Rte. 108) and Bay Forest Rd, along Bordeaux Mountain Rd.	18.3354	-64.72759	JN385562	—	—	—	—
MSB 77773	96	44	USVI: St. Thomas; Fortuna Hill, ca. 820 m southwest of intersection of Bordeaux Rd. and Edward D. Newton/Fortuna Rd., along private road to Fortuna Ranch	18.3559	-65.00633	JN385579	—	—	—	—
MSB 77775	96	44	USVI: St. Thomas; Fortuna Hill, ca. 820 m southwest of intersection of Bordeaux Rd. and Edward D. Newton/Fortuna Rd., along private road to Fortuna Ranch	18.3559	-65.00633	JN385580	—	—	—	—
MSB 77776	97	44	USVI: St. Thomas; Fortuna Hill, ca. 820 m southwest of intersection of Bordeaux Rd. and Edward D. Newton/Fortuna Rd., along private road to Fortuna Ranch	18.3559	-65.00633	JN385581	JN385926, JN385927	JN386272, JN386273	JN386618, JN386619	JN386964, JN386965
MSB 77778	98	44	USVI: St. Thomas; Fortuna Hill, ca. 820 m southwest of intersection of Bordeaux Rd. and Edward D. Newton/Fortuna Rd., along private road to Fortuna Ranch	18.3559	-65.00633	JN385583	JN385930, JN385931	JN386276, JN386277	JN386622, JN386623	JN386968, JN386969

**Table S2** Primers used for amplification (amp) and sequencing (seq) of fragments of the mtDNA control region (CR), nuclear intron-spanning loci  $\beta$ -crystallin (CRYBA), myosin heavy chain (MYH), rhodopsin (RH1), and ribosomal protein L9 (RPL9int4) in *Eleutherodactylus antillensis*, and 147mplicon size (bp, base pairs). PCR conditions used for amplification of loci are depicted as follows: initial denaturation temperature(sec), [(denaturation temperature(sec), annealing temperature(sec), extension temperature(sec) x number of cycles)], final extension temperature(sec). Sources for primers are indicated.

Primer	Use	Sequence (5'-3')	Amplicon size (bp)	PCR conditions	Reference
<b>CR</b>					
controlELAN-F	amp	ATCATTCTATGTTTAATTGAACATTCA	552	94(180), [94(30), 60(30), 72(45) × 36], 72(360)	This study
controlANT-F	seq	TTGCCGAACCCAATTTCAA			This study
controlANT-R	amp	CATGAATGGGTAATATTCGATGGTAR			This study
<b>CRYBA</b>					
CRYB1Ls	amp, seq	CGCCTGATGTCTTTCCGCC	192	95(600), [94(60), 50(45), 72(60) × 34], 72(300)	Dolman and Phillips (2004)
CRYB2Ls	both	CCAATGAAGTTCTCTTTCTCAA			Dolman and Phillips (2004)
<b>MYH</b>					
Eleu.MYH2-F	amp, seq	GCTGCAGATCCTTCACTGACT	463	95(600), [94(60), 60(45), 72(60) × 34], 72(300)	This study
Eleu.MYH2-R	amp, seq	GAGAGATTTTCGTAAGATTGC			This study

**Table S2** Continued**RH1**

Eleu.Rho-F	amp, seq	AAGACTGGGGTGGTACGAAG	596	95(600), [94(60),	This study
Rho4b	amp, seq	GAAGTTGCTCATGGGCTTACAGAC		60(45), 72(60) × 34],	Zheng et al. (2009)
				72(300)	

**RPL9int4**

RPL94F	amp, seq	CGTGTKGACAAATGGTGGGGTAA	382	95(600), [94(60),	Pinho et al. (2009)
RPL95R	amp, seq	ATGGGAAAGTGAGCRTACACAGA		60(45), 72(60) × 34],	Pinho et al. (2009)
				72(300)	

## CHAPTER 4

### **Habitat stability as a driver of tropical insular diversity: comparative phylogeography of *Eleutherodactylus antillensis* and *E. portoricensis*, two ecologically distinctive Puerto Rican frogs**

#### **Abstract**

To assess effects of historical climate change on tropical insular species, we explored how late Quaternary climate change may have influenced gene flow and diversification in two *Eleutherodactylus* frogs from Puerto Rico. The Mountain Coquí, *Eleutherodactylus portoricensis*, is restricted to montane rainforest in Puerto Rico, whereas the Red-eyed Coquí, *E. antillensis*, is a habitat generalist distributed across the entire island. We estimated ecological niche models (ENMs) under last interglacial, last glacial maximum, and current climatic conditions, and combined these models across the three time periods to estimate a habitat stability surface and infer location of refugia for each species. Using population genetic data and coalescent analyses of two mitochondrial (mtDNA) genes and four nuclear (nuDNA) loci, we explored if refugia promoted population persistence and the accumulation of genetic endemism. Collectively, our results suggest that *E. portoricensis* persisted in isolated refugia corresponding to the Cayey and Luquillo Mountains of eastern Puerto Rico since before the last interglacial, and that *E. antillensis* has persisted in partially isolated refugia in western and eastern Puerto Rico, with divergence beginning after the last glacial maximum. For both species, habitat suitability values were lower in the Río Grande de Loíza and coastal lowlands than at higher

elevations across the three time periods, but these unsuitable areas have been a stronger barrier to gene flow to *E. portoricensis* than *E. antillensis*, probably due to its narrower physiological tolerances. We did not find evidence for climate-driven changes in population size for *E. portoricensis*, and a lack of migration between mountain ranges following their split suggests that elevational range shifts were not extensive enough to bring isolated populations into secondary contact. A recent and rapid increase in the population size of *E. antillensis* in western Puerto Rico, combined with a significant positive correlation between nuDNA genetic diversity and habitat stability surfaces, suggests that climate changes more strongly affected past population demographics of this species. The reciprocal monophyly and deep divergence of *E. portoricensis* populations in the Luquillo and Cayey Mountains suggest the presence of two species, and these lineages should be managed as distinct population segments. Habitat stability fostered population persistence of these species, demonstrating the importance of the continuous presence of habitat in generating endemic diversity in Puerto Rico.

## **Introduction**

Contemporary climatic change is affecting species' distributions, with important consequences for the long-term persistence and evolutionary potential of these lineages (Parmesan, 2006; 2011). Tropical island species are predicted to undergo elevational shifts in distribution in response to changing climate, potentially leading to reductions in population size (e.g. Chen *et al.*, 2009; Corlett, 2011; Feeley *et al.*, 2011). The isolation and relatively small area of many tropical islands (Gillespie *et al.*, 2008) may place island endemics at particularly high risk for impacts from environmental change (Frankham, 1998). Exploring the historical processes of persistence of island biotas is therefore essential for understanding the potential responses of endemic biodiversity to habitat alteration.

Elevational gradients on topographically complex tropical islands likely accommodated range shifts during climatic extremes of the Quaternary (the last 2.6 million years [Ma]; Gibbard *et al.*, 2010), but these putative shifts have not been adequately investigated. Elevational changes in distribution are demonstrated by vegetation records from mainland tropical areas that show plant species repeatedly expanding and contracting along elevational gradients in response to changes in temperature and precipitation during the Quaternary (González *et al.*, 2008; Hessler *et al.*, 2010). The dispersal capabilities and present-day elevational distribution of insular species may also provide clues into how Quaternary climate change affected demography. Compared to montane specialists, habitat generalists with wide elevational distributions probably used a broader habitat mosaic during periods of past climatic change, and therefore may have been more likely to colonize changing environments



during climatic extremes of the Quaternary (Williams *et al.*, 2009). In contrast, populations of montane specialists associated with tropical forests likely contracted upslope during periods of interglacial warming, and expanded down-slope during periods of glacial cooling. However, there is increasing evidence that tropical montane species persisted in isolated pockets of stable habitats, or refugia, through multiple glacial cycles (Hugall *et al.*, 2002; Bell *et al.*, 2010), suggesting that downward elevational shifts may not have been large enough to promote gene flow among previously isolated populations.

Multilocus phylogeographic studies that incorporate spatially explicit models of population history provide useful insights into how populations responded to past climate change, but this type of study has rarely been conducted on species from tropical islands. Analysis of multilocus DNA, together with ecological niche models (ENMs), can elucidate how habitat specificity of tropical species influences their response to climate change. Distinctive sensitivities of habitat generalists and specialists to past climatic change may produce distinctive patterns of population genetic structure, genetic diversity, and changes in population size (e.g. Carnaval *et al.*, 2009; Bell *et al.*, 2010). With appropriate climatological datasets, ENMs can be projected onto historical climatic scenarios and used to formulate and/or test hypotheses concerning population-level responses to past climate change (Knowles & Alvarado-Serrano, 2010; Galbreath *et al.*, 2011). Herein, we use multiple DNA loci in combination with ENMs to explore and compare population-level responses in a montane forest specialist and a habitat generalist *Eleutherodactylus* frog species (Anura: Eleutherodactylidae) from Puerto Rico, the smallest and most easterly of the Greater Antilles, in the Caribbean Sea.

Puerto Rico's topographic complexity and dynamic climatic history has motivated investigations of how Quaternary climate change shaped species distributions and evolutionary dynamics. The Central Mountains, or Cordillera Central, forms the highland "backbone" of Puerto Rico. This range is separated from the Luquillo Mountains in the northeast by the extensive Río Grande de Loíza Basin, which reaches a low point of nearly 0 m in the Caguas Basin (Fig. 1). Paleoclimatic data from Puerto Rico provide strong evidence for fluctuations between dry, glacial and wetter, interglacial climate that were associated with changes in vegetative cover (reviewed in Renken *et al.*, 2002), but it is not clear whether these changes were large enough to detectably influence demographic patterns. Phylogeographic studies of Puerto Rican species reveal genetic signatures of varied population histories, ranging from asynchronous expansion of species pairs (Cook *et al.*, 2010) to long-term demographic stability (Barker *et al.*, 2011), which is in line with the view that past climate change did not significantly alter species distributions in the Greater Antilles (Ricklefs & Bermingham, 2008). Indeed, the high local endemism in montane rainforests of Puerto Rico suggests population persistence of montane species during periods of rapid climatic change (Figueroa Colón, 1996). Phylogeographic studies also indicate that geographic barriers such as low-elevation valleys promoted genetic isolation among populations of Puerto Rican fauna (Velo-Antón *et al.*, 2007; Barker *et al.*, 2011), with divergence occurring independently of glacial periodicity. However, most phylogeographic studies of Puerto Rican taxa are based on a single mitochondrial (mtDNA) locus, or did not incorporate historical climate data to infer past species distributions. Single-locus perspectives are susceptible to errors caused by stochastic lineage sorting (Maddison & Knowles, 2006) or selection (Ballard &

Whitlock, 2004), and may have low precision for estimating population genetic parameters such as genetic diversity, divergence times, migration rates, growth rates, and effective population size (Knowles & Carstens, 2006; Brito & Edwards, 2008).

We explore the role of late Quaternary climate change in shaping population structure and historical demographics of a montane forest frog, *Eleutherodactylus portoricensis* and a more broadly distributed congener, *E. antillensis*. *Eleutherodactylus portoricensis*, the Mountain Coquí, is restricted to mountainous regions above 273 m in Puerto Rico (Drewry & Rand, 1983), whereas *E. antillensis*, the Red-eyed Coquí, has one of the broadest elevational (sea level to 1,219 m) and geographic ranges of any species in the Puerto Rican Bank (Henderson & Powell, 1999). Although codistributed in mountainous regions of Puerto Rico, *E. antillensis* is distributed along forest edge habitats and not within the dense, closed-canopy forest where *E. portoricensis* is found (Thomas, 1966; Stewart & Woolbright, 1996; Joglar, 1998). The narrowly distributed *E. portoricensis* dies at temperatures  $\geq 30^{\circ}\text{C}$ , but can tolerate more dehydration at cooler temperatures than *E. antillensis*, demonstrating its physiological specialization to montane environments (Beuchat *et al.*, 1984). The widespread *E. antillensis* can survive at higher temperatures, and its tolerance to dehydration increases with increasing temperature, allowing it thrive in many warm and dry low elevation habitats in the Puerto Rican Bank (van Berkum *et al.*, 1982; Beuchat *et al.*, 1984). The possibility for long-term persistence in isolated montane refugia despite late Quaternary climatic oscillations was inferred for *E. portoricensis* (Barker *et al.*, 2011), with low-elevation habitat in the Caguas Basin (Fig. 1) forming a significant barrier to gene flow between populations in the Luquillo Mountains and the Cayey Mountains, a southeastern extension of the

Cordillera Central (Fig. 1). A recent study of *E. antillensis* indicated shallow levels of population differentiation across the species' range in Puerto Rico, but it was not clear whether past climate change had a role in shaping geographic structure (Barker et al., in revision).

We developed two hypotheses concerning the role of past climatic change in shaping gene flow among conspecific populations of *E. portoricensis* and *E. antillensis* by projecting ENMs for each species last interglacial *sensu stricto* (LIG; ~130 – 116 thousand years ago [kya]), last glacial maximum (LGM; ~21 kya), and current climates. We measured constancy of ENMs to identify areas that maintained suitable habitats across these three time periods to investigate the role of habitat refugia in promoting population persistence and the evolution of endemic biodiversity (Noonan & Wray, 2006; Araújo *et al.*, 2008; Carnaval & Moritz, 2008; Moussalli *et al.*, 2009) in Puerto Rico. For *E. portoricensis*, the Cayey-Luquillo Refugia Hypothesis predicts deep differentiation between populations in the Cayey and Luquillo Mountains, with divergence dating to the LIG or earlier, due to complete geographic isolation resulting from unstable habitat in the Río Grande de Loíza Basin and surrounding coastal lowlands. For *E. antillensis*, the West-East Refugia Hypothesis predicts shallow differentiation between populations in western and eastern Puerto Rico due to partial geographic isolation resulting from unstable habitat in the Río Grande de Loíza Basin and surrounding coastal lowlands.

Using estimates of habitat stability since the LIG, we also explored the extent to which climate change may have influenced past demography. In addition to occupying mountainous regions of Puerto Rico, the habitat generalist *E. antillensis* is distributed across the relatively flat and wide lowlands of this island. Unsuitable temperature and

precipitation regimes may displace more populations in the wide lowlands of Puerto Rico compared to those along mountain slopes, which may only need to slightly shift in elevational distribution. We therefore test the hypothesis that *E. antillensis* experienced greater climate-driven fluctuations in population size than *E. portoricensis* because this habitat generalist occupies a greater elevational range (sea level to 1219 m) and total habitat area than its montane specialist congener, and thus climate-driven habitat changes would be more extensive. Specifically, we test the prediction that (1) detectable climate-driven changes in effective population size ( $N_e$ ) have occurred in *E. antillensis*, but not in *E. portoricensis*, and (2) a positive correlation exists between genetic diversity and habitat stability in *E. antillensis*. This new perspective into the genetic consequences of late Quaternary climate change in Puerto Rico provides insight into demographic responses to climate change in the Caribbean biodiversity hotspot and improves our understanding of the processes that regulate regional patterns of biodiversity in tropical insular systems.

## **Materials and Methods**

### *Ecological niche modeling*

We created ecological niche models for *E. portoricensis* and *E. antillensis* using georeferenced records from field surveys and online databases. Precise occurrence records (< 15 m uncertainty) were collected and recorded with a hand-held GPS unit for each population of the two study species that we detected in Puerto Rico between 2001 and 2008 (Fig. 1). Because *E. portoricensis* was synonymous with *E. coqui* prior to 1966 (Thomas, 1966) and precise georeferenced records were often unavailable for museum

specimens, we used recent (2001-2008) records from the PRGAP project (Gould *et al.*, 2008), and long-term amphibian monitoring surveys from the El Verde and the Bisley watersheds in the Luquillo Mountains of northeastern Puerto Rico (Woolbright, 1997). We note that records used to construct ENMs for *E. portoricensis* corresponded to the general area that specimens were collected subsequent to 1966, and thus believe that the data adequately encompass the range of the species. Records for *E. antillensis* were also compiled from the GBIF Data Portal (<http://www.gbif.org>, 26 July 2011). To account for the clustering of occurrence records (e.g. potentially due to denser sampling near field stations or towns), we removed all sites < 5 km apart, resulting in 62 records for *E. antillensis*. Due to clustering of occurrence records for the spatially-restricted *E. portoricensis*, we removed all sites < 1 km apart, resulting in 19 records.

Ecological niche modelling has become a standard approach for addressing questions of biological responses to environmental change at local, regional, and continental scales (Zimmerman *et al.*, 2010; Svenning *et al.*, 2011). Several assumptions are made in the inference of ENMs, including that (i) species distribution is mainly determined by the environment, and not influenced by biotic interactions; (ii) suitable habitat for a species is fully occupied, and (iii) niche requirements of a species remain constant over space and time (Elith & Leathwick, 2009; Nogués-Bravo, 2009). None of these assumptions can be robustly tested with available data for *E. portoricensis* and *E. antillensis*, but factors other than the bioclimatic variables used to estimate our ENMs may affect that distribution of *E. antillensis* at small spatial scales. Relative abundances of *E. antillensis* decrease with forest successional stage in montane forests of Puerto Rico (Herrera-Montes & Brokaw, 2010). Whether non-climatic factors, such as competition, or

microclimate variables such as the minimum temperatures in dense montane forests (Herrera-Montes & Brokaw, 2010), explain the absence of this species from this habitat is unknown. Nevertheless, the WorldClim data incorporate annual trends (e.g., mean annual temperature, annual precipitation), aspects of seasonality (e.g., annual range in temperature and precipitation) and extreme or potentially limiting environmental factors (e.g., temperature of the coldest and warmest months, precipitation of the wettest and driest months) that are known to be important in shaping Puerto Rican frog distributions. Temperature affects elevational limits (Beuchat *et al.*, 1984); the amount of precipitation is critical to foraging success and movements of larger frogs (van Berkum *et al.*, 1982; Pough *et al.*, 1983; Stewart, 1985; Townsend, 1985; Woolbright, 1985; Woolbright & Stewart, 1987); extensive droughts lead to decreased calling, breeding activity (Drewry, 1970; Beuchat *et al.*, 1984; Ovaska & Caldbeck, 1997), and survival (Stewart, 1995); and both temperature and precipitation affect plant distributions (Ewel & Whitmore, 1973), which can indirectly influence frog densities (Stewart & Woolbright, 1996).

To construct ENMs for each species, we acquired current and past bioclimatic data from the WorldClim database (<http://worldclim.org/>) at a spatial resolution of 2.5 min (4 x 4 km), and applied a mask that encompassed the Puerto Rican Bank and St. Croix (an island *ca.* 105 km southeast of Puerto Rico). Climate data for the LGM were derived from simulation runs using the Community Climate System Model version 3 (CCSM) (Collins *et al.*, 2006) and the Model for Interdisciplinary Research on Climate version 3.2 (MIROC) (Hasumi & Emori, 2004), originally available from the Paleoclimate Modeling Intercomparison Project Phase 2 (<http://pmip2.lsce.ipsl.fr/>) and

downscaled to 2.5 min (Waltari *et al.*, 2007). LIG climatic data were derived from simulations under the CCSM general circulation model (Otto-Bliesner *et al.*, 2006).

The ENMs for *E. portoricensis* and *E. antillensis* under current (1950-2000) climatic conditions were constructed in MAXENT 3.3.3 (Phillips *et al.*, 2004; Phillips *et al.*, 2006) and projected onto simulated climate for the LIG and LGM. We used the default parameters of MAXENT (i.e. convergence threshold of 0.00001, 10,000 background points, regularization multiplier of 1, convergence threshold of  $10^{-5}$ ) with the following user-selected features: maximum number of iterations (1,000) values, 75% of occurrence records for training and 25% for model testing, application of a random seed, duplicate presence records removal, ten replicate runs, and logistic probabilities used for the output (Phillips & Dudík, 2008). Sampling for both species covered their entire known range so pseudo-absence records were not included in the construction of ENMs (Phillips *et al.*, 2009). The program selected both suitable regularization values and functions of environmental variables based on consideration of sample size. To test for model over-fitting (Beaumont *et al.*, 2005), we constructed the ENM using the two highest-contributing parameters for each species and this ENM was not qualitatively different from the null model (Fig. S1, Supporting Information). Because MAXENT is relatively robust to autocorrelation, we included all 19 environmental parameters obtained from the WorldClim database. Following Pearson *et al.* (2007), we used the 10<sup>th</sup> percentile training presence as a suitability threshold, that is, we assumed that a cell is suitable when its suitability score is greater than the 10<sup>th</sup> percentile of training presence points.



### *Estimating habitat stability and refugia from ENMs*

For each species, we predicted that areas with low suitability scores across current, LIG, and LGM climatic periods inhibit gene flow and decrease the likelihood of population persistence. In contrast, areas with consistently high suitability scores across the three time periods promote population persistence and gene flow. We summed the ENMs across the three climatic periods in ARCGIS 9.3 (ESRI 2007) to estimate a habitat stability surface. As a result, each pixel had a value that ranged from 0 (never predicted to be suitable) to 3 (perfectly predicted across all time periods; c.f. Graham *et al.*, 2006). We generated two stability surfaces for each species to accommodate different scenarios of LGM climate (CCSM and MIROC).

To formulate hypotheses from stability surfaces, we inferred the number and location of putative habitat refugia, which represent regions with particularly high levels of suitability across three time periods. We explored the number and location of putative refugia by reclassifying each stability surface to show the highest 20%, 25%, and 30% of values (c.f. Chan *et al.*, 2011). For each three of these three analyses, we calculated a composite result showing areas where estimates using CCSM and MIROC scenarios for LGM climate were concordant. We categorized a region as a habitat refugium if contained at least one sampling locality and was geographically contiguous.

For testing hypotheses of genetic isolation (i.e. the Cayey-Luquillo Refugia and East-West Refugia Hypothesis), we assigned individuals to one of two groups according to where they were sampled with respect to the inferred refugia (see Results). Assigning individuals to groups was straightforward for *E. portoricensis* because refugia were isolated under all three reclassifications, and all sampling localities fell within a

refugium. We opted to group *E. antillensis* individuals by refugia inferred from the highest 25% of stability surface values because this reclassification depicted the areas of highest stability which were also geographically isolated, whereas the highest 30% values stability surface values depicted a narrow area of connectivity in the vicinity of the Cayey and Central Mountains. Individuals from sampling localities located outside of inferred habitat refugia were assigned to the most geographically proximate habitat refugium.

### *Sequence data*

We expanded the nucleotide sequence dataset of Barker et al. (2011) by adding sequences from the intron-spanning loci  $\beta$ -crystallin (intron 1; CRYBA, *ca.* 191 bp), myosin heavy chain (intron; MYH, 338 bp), and ribosomal protein L9 (intron 4; RPL9int4, *ca.* 371 bp) from 36 specimens of *E. portoricensis* that represented three randomly chosen individuals from each sampling locality (Fig. 1). For *E. antillensis*, we used mtDNA control region (CR) sequences of 203 individuals from 41 localities across the species' range in mainland Puerto Rico, and four nuDNA introns [CRYBA, MYH, RH1 (rhodopsin intron 1), and RPL9int4] from 123 of these individuals (Barker et al., in revision). DNA extraction, PCR, and cycle sequencing procedures follow Barker *et al.* (2011); primers and PCR conditions are described in Barker *et al.* (in revision). Tissue samples (liver, thigh muscle, and/or toe-clips) are from the Division of Genomic Resources, MSB and the Rodríguez-Robles laboratory at the University of Nevada, Las Vegas. Voucher specimens are archived at the Museum of Southwestern Biology (MSB), University of New Mexico, Albuquerque, or the Museum of Vertebrate Zoology (MVZ), University of

California, Berkeley. Due to the sensitive conservation status of *E. portoricensis*, we did not collect voucher specimens.

We used two different combinations of data sets in the analyses. Population genetic analyses used the full mtDNA CR and nuDNA data sets for each species. To reduce computations times in isolation with migration (IM) analyses and reconstruction of population size through time using extended Bayesian skyline plots (EBSPs), we only used CR sequences from individuals for which nuDNA sequences were also available ( $N = 36$  for *E. portoricensis* and  $N = 123$  for *E. antillensis*). In some instances, we used an even smaller subset of the *E. antillensis* CR and nuDNA data sets due to issues with convergence (see below). The *cyt b* data set for *E. portoricensis* was also included in IM and EBSP analyses, as well as in Bayesian inference of species trees.

We edited sequences using SEQUENCHER 4.5 (GeneCodes) and deposited sequences in GenBank (Table S1, Supporting Information). For heterozygote individuals polymorphic at multiple positions, we inferred the gametic phase using PHASE 2.1 (Stephens *et al.*, 2001; Stephens & Donnelly, 2003). Multi-base insertion-deletions (indels) were collapsed into single-base polymorphisms for phasing analyses. We ran five independent runs from different starting seeds for 1,000 iterations, with a single thinning interval and 100 burn-in iterations. When PHASE could not reconstruct haplotypes with a posterior probability of  $\geq 0.85$  (Garrick *et al.*, 2010), we cloned PCR fragments for a minimum of five clones per sample using the pGEM-T-Easy Vector Systems kit (Promega). Finally, we repeated the PHASE analyses using information from known haplotypes. Sequence alignments were conducted in MAFFT 6 (Kato *et al.*, 2002, <http://mafft.cbrc.jp/alignment/server/>), except for mtDNA (CR and *cyt b*) and RH1

sequences for *E. portoricensis*, which were aligned in MUSCLE 3.7 (Edgar, 2004) in a previous study (Barker *et al.*, 2011).

#### *Recombination, neutrality, and genetic diversity*

Population genetic, coalescent, and phylogenetic analyses used in this study assume that there is no recombination within each locus and that loci are not under selection. To test for recombination in the three nuDNA loci sequenced from *E. portoricensis* (CRYBA, MYH, and RPL9int4), we conducted RDP (Martin *et al.*, 2005), Bootscan (Salminen *et al.*, 1995; Martin *et al.*, 2005), Geneconv (Padidam *et al.*, 1999), Chimaera (Posada & Crandall, 2001), MaxChi (Maynard Smith, 1992), and SiScan (Gibbs *et al.*, 2000) tests in RDP 3 (Martin *et al.*, 2010). For each species, we assessed selective neutrality of each locus with the Hudson-Kreitman-Aguade (HKA) test (Hudson *et al.*, 1987), with 10,000 coalescent simulations in HKA (J. Hey, <http://genfaculty.rutgers.edu/hey/software>). We used ARLEQUIN 3.1 (Excoffier *et al.*, 2005) to calculate haplotype diversity ( $H_d$ ) and nucleotide diversity ( $\pi$ ) for *E. portoricensis* and *E. antillensis* datasets clustered by inferred refugia and tested for departures from neutrality by comparing Tajima's  $D$  (Tajima, 1989) and Fu's  $F_S$  (Fu, 1997) statistics to 10,000 coalescent simulations of a large, neutrally evolving population of constant size.

#### *Genetic structure*

To quantify and visualize population genetic structure in light of the Cayey-Luquillo Refugia Hypothesis and East-West Refugia Hypothesis, we generated maximum parsimony networks of mtDNA CR and inferred the number of population clusters ( $K$ )

from nuDNA for each species. We generated a maximum parsimony network in NETWORK 4.2 (<http://www.fluxus-technology.com>) and estimated population structure using STRUCTURE 2.3.3 (Pritchard *et al.*, 2000). We ran STRUCTURE with and without prior population information and applied both correlated (Falush *et al.*, 2003) and uncorrelated frequency models, for a total of four analyses for each species. Incorporating population information priors does not bias analyses towards inferring population differences when none exist (Hubisz *et al.*, 2009). For each analysis, we employed the admixture model of ancestry and ran separate analyses for all values of  $K$  between 1 and 8 using a MCMC length of 100,000 generations following a burn-in of the same length. We visualized bar plots showing coefficients of cluster membership estimated for each individual using DISTRUCT 1.1 (Rosenberg, 2004).

#### *Testing models of genetic isolation*

To test the prediction that unstable habitats within Puerto Rico inhibit gene flow (Cayey-Luquillo Refugia Hypothesis and West-East Refugia Hypothesis), we tested for correlations between genetic distance and these putative barriers. We assigned a pairwise value of 1 to sampling localities belonging to different refugia, to indicate that intervening unstable habitats promote genetic isolation. In contrast, sampling locations belonging to the same habitat refugium were assigned a pairwise value of 0, signifying that stable habitats promote gene flow.

We calculated genetic distances separately for the mtDNA CR and nuDNA data to account for potentially different genetic structure resulting from the distinctive mode of inheritance of these genetic markers. We treated indels as a fifth state (Giribet &

Wheeler, 1999; Simmons & Ochoterena, 2000), coding each as a single mutational event (Simmons & Ochoterena, 2000). In ARLEQUIN, the net number of nucleotide differences between sampling localities ( $D_A$ ) (Nei, 1972) was calculated for the mtDNA CR dataset using the Tamura and Nei model of evolution and applying 10,000 permutations. We calculated  $D_A$  between sampling localities for each nuDNA locus separately, and then calculated a multi-locus mean for each sampling site in ARLEQUIN. As a second measure of historical population connectivity, we calculated Rousset's genetic distance for mtDNA CR [ $\phi_{ST} / (1 - \phi_{ST})$ ] and  $F_{ST}$  for nuDNA [ $(F_{ST} / 1 - F_{ST})$ ] (Rousset, 1997) with 10,000 permutations in IBDWS (Jensen *et al.*, 2005). The  $\phi$  statistic incorporates measures of evolutionary distance between alleles with the frequency-based analysis of  $F$ -statistics (Excoffier *et al.*, 2005; Holsinger & Weir, 2009), and  $F_{ST}$  may be more informative in situations where there is little sequence divergence among haplotypes.

For each species, we evaluated support for genetic isolation due to unstable habitat barriers (isolation by barrier) relative to a null model of isolation by geographic distance (Wright, 1943). We measured Euclidean distance between sampling localities in ArcGIS 9.3, and used a Mantel test (Mantel, 1967) to measure the correlation between genetic distance and geographic distance and the correlation between genetic distance and the presence of unstable habitat barriers. If unstable habitat barriers strongly contribute to genetic isolation, then a significant positive correlation with genetic distance should remain after partialling out the effects of isolation by geographic distance (Shirk *et al.*, 2010). Pearson correlation coefficients and associated bootstrapped 95% confidence intervals were calculated and assessed for statistical significance with 10,000 permutations in the R package Ecodist (Goslee & Urban, 2007) in R version 2.12.1 (R

Development Core Team, 2010). Negative genetic distances were set to zero prior to this analysis.

### *Mutation rates*

Obtaining meaningful estimates of demographic parameters (e.g., gene flow, divergence times, changes in population size) depends in part on the accuracy of estimates of mutation rates for individual loci (Hey & Nielson, 2004). We used a mutation rate ( $\mu$ ) of  $4.1 \times 10^{-8}$  substitutions per site per year (sub/s/y) per lineage for the non-coding mtDNA CR (Barker et al., in revision) and  $\mu = 0.96 \times 10^{-8}$  sub/s/y per lineage for *cyt b* (Crawford et al., 2007). We relied on divergence time estimates of major clades of eleutherodactyline frogs (Heinicke *et al.*, 2007) and RH1 sequences from several representative species of these clades (Heinicke *et al.*, 2009) to estimate a mutation rate for RH1 in eleutherodactyline frogs. We downloaded RH1 sequences from *Euhyas planirostris* (DQ283821), *Haddadus binotatus* (DQ283807), *Pristimantis pluvicanorus* (AY844559), and *Ischnocnema* sp. 521 (DQ283788) from GenBank, aligned the sequences in MAFFT 6, and identified a 271 bp fragment which aligned across the five taxa, corresponding to the exon portion of the RH1 locus. We estimated the mean rate of substitution in the 271 bp RH1 fragment in BEAST 1.62 by employing a Yule speciation model, applying the substitution model selected in ModelTest (HKY + I), and a strict molecular clock (based on the results of likelihood ratio tests of clock-like evolution). The most recent common ancestor (mrca) of taxon sets containing two or more different species was assigned a normal prior mean and standard deviation that corresponded to estimates of divergence times for eleutherodactyline frogs. Specifically, the mrca of

species within the Caribbean Clade of eleutherodactyline frogs (*E. antillensis* and *E. planirostris*) was set to 29.09 million years (MY) (SD = 5.05 MY); the mrca of species in the Caribbean Clade with other eleutherodactyline frogs was set to 47.28 MY (SD = 7.9 MY); the mrca of species within the Middle American Clade (*H. binotatus*) and South American Clade (*P. pluvicanorus*) of eleutherodactyline frogs was set to 45.25 MY (SD = 7.62 MY); and the mrca of the Southeast Brazil Clade (*Ischnocnema* sp. 521) with other eleutherodactyline frogs was set to 49.79 MY (SD = 8.3 MY) (Heinicke *et al.*, 2007). Assuming a generation time of 1 year, as shown for *E. antillensis* (Ovaska, 2005) and the closely related *E. coqui* (Stewart & Woolbright, 1996), the inferred average  $\mu$  of RH1 is  $1.11 \times 10^{-9}$  sub/s/yr per lineage for RH1 in these frogs. This estimate is on par with nucleotide substitution rates of other amphibian nuDNA genes (Crawford, 2003b).

#### *Coalescent estimates of gene flow, divergence, and population size changes*

We used the program IMA2 (Hey, 2010) to estimate migration rates between population groups in inferred refugia, time since population divergence of these groups, and changes in population size since divergence from a common ancestor. An important assumption of the IM model is that the two analyzed populations are more closely related to each other than they are to other populations (Hey, 2006). We cannot address this assumption for *E. portoricensis* due to a lack of samples from the Central Mountains, but a previous study of *E. antillensis* across its range in the Puerto Rican Bank indicated close ties between populations in eastern Puerto Rico and those in the “Eastern Islands,” which includes Vieques, Culebra, and the Virgin Islands (Barker *et al.*, in revision). Because the divergence times of these groups have overlapping confidence intervals, there is no



strong evidence from this study to suggest that eastern Puerto Rican populations are more closely related to those in the Eastern Islands than they are to those in western Puerto Rico. Therefore, we have no reason to believe that this assumption is being violated.

Priors, heating parameters, the number of chains, and an appropriate burn-in length were optimized through several preliminary Markov Chain Monte Carlo (MCMC) runs. Due to issues with convergence with analyzing the full data set for *E. antillensis*, we randomly selected a single individual from each of the 41 localities to represent populations in western and eastern Puerto Rico. We applied the Hasegawa-Kishino-Yano model for each data set (Hasegawa *et al.*, 1985). The upper limit of the prior for divergence time was set to 10.0 for *E. portoricensis* and 3.4 for *E. antillensis*. Because the estimate of divergence time for *E. portoricensis* showed a bimodal distribution, we also carried out separate IM analyses with an upper *t* prior of 1.5, which effectively excluded the older divergence time. The upper limit of the prior for migration was set to 0.85 for *E. portoricensis* and 1.2 for *E. antillensis*, and the upper limit of the prior for effective population size was set to 17.0 for *E. portoricensis* and 12.0 for *E. antillensis*. Final runs for both species included 150 chains, had a 96 hour burn-in (approximately  $1.7 \times 10^8$  steps), and were continued for  $3.0 \times 10^7$  steps. Examination of convergence diagnostics (e.g. low autocorrelations between variables, high swap rates, high ESS values, trend plots, high acceptance ratios) indicated stationarity. IMA2 calculated mutation rate scalars for CRYBA, MYH, and RPL9int4 and used a geometric mean of all mutation rates to convert divergence times to demographic scales. We conducted two runs, began with different seeds, to ensure that parameters estimates were consistent.

To further explore changes in demographic growth, we employed the Extended Bayesian Skyline Plot (Heled & Drummond, 2008), as implemented in BEAST 1.6.2, using the mtDNA (CR and *cyt b* for *E. portoricensis*; only CR for *E. antillensis*) data and nuDNA datasets. Separate analyses were conducted for differentiated groups of *E. portoricensis* (Cayey and Luquillo Mountains) and *E. antillensis* (western and eastern Puerto Rico). We estimated mutation rates for CRYBA, MYH, and RPLint4 from the CR ( $\mu = 4.1 \times 10^{-8}$ ), *cyt b* ( $\mu = 0.96 \times 10^{-8}$ ), and RH1 ( $\mu = 1.11 \times 10^{-9}$ ) data sets using a uniform prior. The minimum and maximum  $\mu$  values for CRYBA, MYH and RPL9int4 were based on a sixteen-fold (Crawford, 2003b) slower rate ( $\mu = 6.7 \times 10^{-10}$ ) than our lower bound for mtDNA and a five-fold slower rate ( $\mu = 8.2 \times 10^{-9}$ ) than our upper bound for mtDNA (Sheldon *et al.*, 2000; Crawford, 2003b), respectively. A strict molecular clock for each locus was calibrated based on the likelihood ratio tests of clock-like evolution (Felsenstein, 1988) performed using PAUP\* version 4b10 (Swofford, 2000). The model of nucleotide substitution that encompassed the model chosen by AIC in MODELTEST was set for each partition (Table 1). Due to issues with convergence with analyzing the full data set for western Puerto Rico populations of *E. antillensis* (N = 93), we randomly selected a single individual from each of the 31 localities to represent populations in this region. Simulated genealogies and model parameters were sampled every 5,000 generations for 500,000,000 generations for each Cayey and Luquillo populations of *E. portoricensis*, and every 5,000 generations for 700,000,000 and 1,000,000,000 for eastern and western populations of *E. antillensis*, respectively. We discarded 10% of the initial samples as burn-in, and assessed convergence by comparing the two analyses to ensure that each replicate produced the same demographic patterns.

We used TRACER 1.5 to combine the two independent runs, check for appropriately large effective sample size (ESS) values (all > 200), and check for convergence of results and performance of operators (Rambaut & Drummond, 2007).

### *Spatial analyses of genetic diversity in E. antillensis*

Genetic diversity is a function of  $N_e$ , which in turn can be influenced by climate driven changes in habitat suitability. To test for statistical associations between genetic diversity and habitat stability in *E. antillensis*, we estimated a genetic diversity surface and tested for correlations with numeric values from each of the two stability surfaces. We did not conduct these analyses for *E. portoricensis* due to its limited range and the coarse resolution of the bioclimatic data, particularly those for the LGM. We estimated genetic diversity in *E. antillensis* populations at each sampling locality using Watterson's estimate of the population mutation rate  $\theta$  ( $\hat{\theta}_w$ ), where  $\theta = 4N_e\mu$  (Watterson, 1975) in ARLEQUIN 3.1. We also estimated genetic diversity for each locality using average number of pairwise differences ( $\hat{\pi}_n$ ) (Tajima, 1983). For each locus, a genetic diversity surface was estimated using the Genetic Landscapes GIS Toolbox (Vandergast *et al.*, 2011) in ARCGIS 9.3 (ESRI 2007). We averaged genetic landscapes for each nuDNA locus into a single multi-locus genetic landscape, and calculated the coverage of the sample variance, which represents the dispersion of genetic landscape values for individual loci from the average multi-locus genetic landscape (Vandergast *et al.*, 2011). We used the threshold for presence under current climate to mask the resulting genetic diversity surface, so that areas of species absence were not included in the analyses. To evaluate the statistical association between the genetic diversity and habitat stability surfaces, we calculated

Pearson's correlation coefficients and their corresponding *P*-values in the program SAM (Rangel *et al.*, 2006). We also report a corrected *P*-value to account for spatial autocorrelation using Dutilleul's (1993) method.

#### *Multilocus phylogenetic analysis of E. portoricensis*

We estimated a species tree using Bayesian Evolutionary Analysis Sampling Trees (\*BEAST; Heled & Drummond, 2008) in BEAST 1.62 (Drummond & Rambaut, 2007) to examine species relationships from multilocus data for *E. portoricensis* as well as to obtain a second estimate of the time since divergence of the Cayey and Luquillo Mountains populations. The model of nucleotide substitution that encompassed the model chosen by AIC in MODELTEST (Posada & Crandall, 1998) was set for each partition as follows: mtDNA CR = GTR + I +  $\Gamma$ , *cyt b* = HKY +  $\Gamma$ , CRYBA = GTR + I +  $\Gamma$ , MYH = HKY + I, RH1 = HKY + I, and RPL9int4 = HKY + I. Model parameters were estimated with the tree topologies in the analysis. We linked the *cyt b* and CR trees because these loci do not evolve independently, applied a Yule tree prior, and fixed the molecular clock for each locus based on the results of likelihood ratio tests of clock-like evolution. We set mutation rates and mutation rate priors as described for the EBSP analyses. Two independent runs of 300,000,000 generations were performed, sampling once every 1,000 trees, with 10% of the initial samples discarded as burn-in. We used TRACER to check for appropriately large ESS values and check for convergence of results and performance of operators. A consensus tree with divergence times was obtained from the 30,000 trees after discarding the first 10% as burn-in.

## Results

### *Ecological niche modeling*

ENMs for each species had good predictive power for contemporary species occurrences. The mean area under the receiving operating characteristic curve (AUC) for the test data from the 10 cross-validated runs was 0.99 for *E. portoricensis* and 0.91 for *E. antillensis*, indicating that both ENMs performed better than a random model (maximum value of AUC = 1; value of AUC for a random model = 0.5). All models produced predictions that were significantly better than random ( $P < 0.001$  for all alternative threshold values) based on a binomial test of omission. A small standard deviation for *E. portoricensis* (SD = 0.001) and *E. antillensis* (SD = 0.034) for the AUC showed that model performance was robust to variation in the selection of datasets for training. Precipitation seasonality (coefficient of variation) was the highest contributing variable to the ENM for both species (Table 2). The ENMs of both species under current climate conditions were largely concordant with distribution models inferred in previous studies (Gould *et al.*, 2008), with one exception. Although *E. antillensis* is distributed in high elevation areas of Puerto Rico, populations are only distributed in edge habitat, and not within dense, closed-canopy forest (Stewart & Woolbright, 1996; Joglar, 1998). Therefore, *E. antillensis*' presence in montane regions may have been slightly overestimated.

For *E. portoricensis*, habitat suitability across all three times periods is extremely low (0 – 0.05) in the Río Grande de Loíza Basin and surrounding coastal lowlands, suggesting that populations in the Cayey and Luquillo Mountains have remained isolated since at least the LIG. The ENM under LIG climate indicates a severely restricted distribution in the Cayey Mountains (Fig. 2A), suggesting elevational contractions in this

mountain range. There were remarkable differences between ENMs estimated using CCSM and MIROC scenarios of LGM climatic conditions. Whereas the projection of ENM under the CCSM scenario indicated that *E. portoricensis* was absent from the Luquillo Mountains, the one inferred with MIROC indicated that suitability in the Luquillo Mountains is high (Fig. 2A). Reclassifications of the highest 20%, 25%, and 30% stability surface values depicted two isolated refugia corresponding to the Cayey and Luquillo Mountains (Fig. 3A). Isolation in these two refugia separated by unstable habitat provides the basis for the Cayey-Luquillo Refugia Hypothesis.

For *E. antillensis*, habitat suitability across all three times periods is lowest in the Río Grande de Loíza Basin and coastal lowlands of western Puerto Rico. The ENM for *E. antillensis* under LIG climate indicates lower suitability in the Río Grande de Loíza Basin and coastal lowlands than the ENM under current climate, suggesting island-wide elevational shifts in distribution (Fig. 4A). The ENMs under LGM climate also depicts lower suitability in lowland habitats than those at higher-elevation regions, but the LGM projection under the MIROC scenario depicts higher suitability throughout the Cordillera Central, Cayey Mountains, and eastern Puerto Rico than the projection under the CCSM scenario. Habitat stability is highest in eastern Puerto Rico and the Central Mountains, and lowest in the lowlands of western Puerto Rico and the Río Grande de Loíza Basin (Fig. 4B). Reclassifications of the highest 20%, 25%, and 30% stability surface values depicted a refugium in eastern Puerto Rico and another in western Puerto Rico, but varied with respect to their isolation. Reclassifications of the highest 20% and 25% show isolation of these refugia, but the highest 30% values stability surface values depict a narrow area of connectivity in the vicinity of the Cayey and Central Mountains (Fig. 5A).

Partial isolation in two refugia, separated by unstable habitat in the vicinity of the Río Grande de Loíza Basin, provides the basis for the East-West Refugia Hypothesis.

#### *Recombination, neutrality, and genetic diversity*

We did not detect recombination in the three nuDNA loci sequenced from *E. portoricensis* (CRYBA, MYH, and RPL9int4). Nucleotide variation in all loci is consistent with neutral expectations according to the HKA test in *E. portoricensis* ( $\chi^2 = 3.296$ , d.f. = 4,  $P = 0.51$ ) and *E. antillensis* ( $\chi^2 = 6.64$ , d.f. = 4,  $P = 0.16$ ). Tajima's  $D$  was not significant for any loci in either species. Significantly negative values of Fu's  $F_S$  indicate selection or recent population expansion (Fu, 1997) and were inferred for CR in *E. portoricensis* and *E. antillensis* populations in both refugia, for *cyt b* in Luquillo Mountains populations of *E. portoricensis*, for MYH in the Cayey Mountains populations of *E. portoricensis* and western populations of *E. antillensis*, and for RPL9int4 in eastern populations of *E. antillensis* (Table 1). Single-base pair indels were contained in CRYBA and RPL9int4, and multi-base pair indels in RPL9int4 ranged in size from 3 to 46 base pairs. MYH and RH1 did not contain indels. With the exception of RH1,  $H_d$  and  $\pi$  for *E. portoricensis* were higher in Luquillo Mountains populations than in Cayey Mountains, but there were no apparent trends in these statistics for western and eastern populations of *E. antillensis* (Table 1).

#### *Genetic structure*

Genetic structure of both mtDNA CR and nuDNA in *E. portoricensis* provided strong support for the Cayey-Luquillo Refugia Hypothesis. The maximum parsimony network

of the mtDNA CR data for *E. portoricensis* depicts two clusters, Cayey Mountains (35 haplotypes) and Luquillo Mountains (40 haplotypes) separated by 15 mutational steps (Fig. 3B). STRUCTURE analysis of nuDNA both with and without prior population, and under the correlated and uncorrelated allele frequencies model, information inferred two clusters and supported the prediction of genetic isolation between individuals in the inferred Cayey and Luquillo Mountains refugia. Because the results of these analyses were similar, we only present the analysis with prior population information (Fig. 3C). In all analyses, individuals in each mountain range have membership coefficients  $\geq 0.90$  to their assigned cluster, indicating very limited admixture between geographically isolated groups.

Genetic structure in *E. antillensis* supported the prediction of partial genetic isolation between individuals in the inferred western and eastern refugia (West-East Refugia Hypothesis). The mtDNA CR maximum parsimony network depicts 71 shallowly differentiated haplotypes, of which three are shared between western and eastern refugia in Puerto Rico (Fig. 5B). STRUCTURE analyses of nuDNA with and without prior population information, and under the correlated and uncorrelated allele frequencies model, inferred two clusters and indicated some level of genetic isolation between individuals in the inferred western and eastern refugia. Because the results of these four analyses were similar, we only present the correlated frequencies analysis with prior population information (Fig. 5C). Mixed membership of many individuals indicates admixture between these refugia. Nevertheless, sixty four of the 90 individuals (64%) in the western habitat refugium and 25 of the 33 individuals (76%) in the eastern habitat refugium have membership coefficients  $\geq 0.90$  of belonging to their assigned cluster.



### *Testing models of genetic isolation*

For *E. portoricensis*, unstable habitat in the Río Grande de Loíza Basin and surrounding lowlands has acted as a very strong barrier to gene flow. This barrier exhibited very high correlations with Nei's genetic distance in both mtDNA CR ( $r = 0.989$ ,  $P = 0.0026$ ) and nuDNA ( $r = 0.883$ ,  $P = 0.0022$ ; Table 3), and partialling out the effects of isolation by barrier resulted in weak (CR) or nonsignificant (nuDNA) correlations. While the absolute value of the correlations differed, the analysis based on Rousset's genetic distances using mtDNA and nuDNA markers provided similar levels of support.

According to analyses of genetic isolation for *E. antillensis*, unstable habitat in the Río Grande de Loíza Basin and surrounding lowlands has acted as a weak barrier to gene flow. For mtDNA CR, Nei's genetic distance exhibits a higher correlation with geographic distance ( $r = 0.497$ ,  $P = 0.0001$ ) than with a barrier ( $r = 0.269$ ,  $P = 0.0016$ ; Table 4), and the relationship remained significant ( $r = 0.446$ ,  $P = 0.0001$ ) after partialling out the effects of isolation by barrier (Table 4). Partialling out the effects of isolation by distance resulted in a weak and nonsignificant correlation ( $r = 0.115$ ,  $P = 0.0764$ ), indicating that a model of isolation by geographic distance best explains CR genetic isolation for *E. antillensis*. In contrast, a model of genetic isolation by barrier had the strongest support for nuDNA ( $r = 0.200$ ,  $P = 0.0026$ ) and the relationship remained significant after partialling out the effects of geographic distance ( $r = 0.179$ ,  $P = 0.0050$ ). Analyses based on Rousset's genetic distance produced very low and/or nonsignificant results for all models. These results may reflect the low levels of differentiation present in these loci, particularly for nuDNA.

### *Coalescent estimates of gene flow, divergence, and population size changes*

In all IM analyses, the current population sizes and migration parameters had posterior probability distributions with single narrow peaks and bounds that fell within the prior distributions, and ESS values were all  $> 200$ . In *E. portoricensis*, the estimate of divergence time showed a bimodal distribution, which could represent two alternative demographic histories that are similarly probable. We carried out separate IM analyses with an upper  $t$  prior limit ( $t = 1.5$ ) that excluded the older divergence time [1.5 million years ago (mya)]. According to the analysis with an upper  $t$  prior limit of 1.5, the Cayey and Luquillo Mountains populations split an estimated 172.9 kya [95% highest posterior density interval (HPD): 106.6 – 256.8 kya] (Table 5). In both analyses, the Luquillo Mountains population is approximately twice the size of the Cayey Mountains population. The migration parameters were not significant in the analysis which had a lower  $t$  prior limit, indicating that migration did not occur after population divergence. In contrast, results of the analysis with a higher  $t$  prior limit showed that significant levels of bidirectional migration occurred between Cayey and Luquillo Mountains populations after they split (Table 5). Western and eastern populations of *E. antillensis* split at 4.7 kya (95% HPD: 0.05 – 15.5 kya), and have similar effective population sizes (Table 5). Significant unidirectional migration is indicated from eastern into western populations, indicating that gene flow occurred after population divergence.

The Extended Bayesian Skyline Plot (EBSP) analyses revealed that effective population sizes have increased since the population divergence events of both species. The EBSP for *E. portoricensis* populations in the Cayey Mountains and Luquillo

Mountains depict a gradual increase in size over the past 500,000 years, with the increase being more pronounced in the Luquillo Mountains population (Fig. 6). The EBSPs for *E. antillensis* depicts that the eastern population has gradually increased in size over the past 300,000 years and that the western populations began rapidly increasing *ca.* 20 kya, which corresponds to the transition between the last glacial period and the Holocene interglacial (18-12 kya).

#### *Spatial analyses of genetic diversity in E. antillensis*

The prediction that genetic diversity increases with habitat stability for *E. antillensis* was only partially supported. MtDNA CR  $\hat{\theta}_w$  was negatively correlated with habitat stability, but this relationship was not significant when correcting for spatial autocorrelation (Table 6). Average nuDNA  $\hat{\theta}_w$  was positively correlated with habitat stability, a relationship that was marginally significant when accounting for spatial autocorrelation. Neither mtDNA CR  $\hat{\pi}_n$  nor average nuDNA  $\hat{\pi}_n$  were significantly associated with habitat stability.

Illustrations of the genetic landscapes for *E. antillensis* showed that mtDNA CR  $\hat{\pi}_n$ , as well as average nuDNA  $\hat{\theta}_w$  and  $\hat{\pi}_n$ , were generally highest in eastern Puerto Rico (Figs. S2B-D, Supporting Information). In contrast, we did not detect any particular trend in the mtDNA CR  $\hat{\theta}_w$  genetic landscape (Fig. S2A, Supporting Information). Sampling variances were low (i.e. < 0.10), except in some coastal lowland areas.

#### *Multilocus phylogenetic analysis of E. portoricensis*

The \*BEAST analysis inferred that *E. portoricensis* samples from the Cayey Mountains are reciprocally monophyletic to a clade containing samples from the Luquillo Mountains

(BPP = 1.0; Fig. 7). A mean divergence time of 365.3 kya (95% HPD = 247.4 – 500.1 kya) indicates that the Cayey and Luquillo Mountains populations became isolated prior to the LIG, supporting the Cayey-Luquillo Refugia Hypothesis. This estimated mean divergence time is more in line with the IM analysis carried out with a lower divergence time prior.

## **Discussion**

This comparative assessment of spatio-temporal patterns of persistence and isolation highlights the differential responses of a montane endemic, *E. portoricensis* and a widespread habitat generalist, *E. antillensis*. By combining analyses of multi-locus diversity with spatial modeling of ecological niche models (ENMs) under current and past climatic conditions, we aim to shed light on the role of past climate change in shaping regional patterns of biodiversity in tropical archipelagos. We formulated hypotheses concerning genetic isolation in each species by measuring constancy of suitable habitat during three time periods, as estimated by ENMs, with the aim of inferring if stable habitats promote population persistence and the accumulation of endemic genetic diversity. We also tested the hypothesis that *E. antillensis* experienced greater climate-driven fluctuations in population size than *E. portoricensis* because the former is a habitat generalist that occupies a greater elevational range and total habitat area, and thus climate-driven habitat changes would be more extensive.

*Topography, late Quaternary climate change, and genetic isolation in Puerto Rico*

The number and location of inferred refugia for *E. portoricensis* and *E. antillensis* was corroborated by genetic analyses, which suggests that the continuous presence of suitable habitats plays an important role in shaping the distribution of genetic endemism in these species. The Cayey-Luquillo Refugia Hypothesis for *E. portoricensis* is strongly supported, as shown by (i) individuals from the Cayey and Luquillo Mountains have a strong ( $\geq 0.90$ ) probability of belonging to different clusters (Fig. 3C), (ii) a high correlation between mtDNA CR and nuDNA genetic distances and the presence of a wide band (i.e.  $\geq 30$  km) of unstable habitat around the two refugia after removing the effects of geographic distance (Table 3), and (iii) divergence of the Cayey Mountains and Luquillo Mountains populations began prior to the LIG (Fig. 7, Table 5). Partial isolation predicted by the West-East Refugia Hypothesis for *E. antillensis* is also supported because (i) most individuals from western and eastern refugia have a strong probability ( $\geq 0.90$ ) of belonging to a separate cluster (Fig. 5C), and (ii) divergence of western and eastern populations occurred after the LGM, followed by significant levels of east-to-west migration (Table 5).

Habitat stability appears to play an important role in generating genetic endemism in *E. portoricensis* and *E. antillensis*, and these results are in agreement with paleontological studies in the Greater Antilles. Although there is strong evidence for fluctuating temperature and precipitation regimes in the Greater Antilles at multiple times in the late Quaternary (Orvis *et al.*, 1997; Guilderson *et al.*, 2001; Renken *et al.*, 2002), recent paleontological studies from this region showed that these changing climatic regimes did not lead to large range shifts and extinctions, at least during the transition

between the last glacial period and the Holocene interglacial (18-12 kya) (MacPhee, 2009). A paleontological study of land snail fauna at a 450 m site in Jamaica inferred that species diversity remained remarkably similar over the past 45,000 years (Goodfriend & Mitterer, 1993), suggesting that forest habitat was continuously present. Similarly, deep divergence of Cayey and Luquillo Mountains populations of *E. portoricensis* provide strong evidence for persistent forest habitat over several late Quaternary climatic fluctuations. Cayey and Luquillo Mountains populations of *E. portoricensis* began diverging prior to the LIG, which suggests that montane forest habitat has been continuously present since this splitting event, and thus this species was resilient to warm temperatures during that time period, which were as high or higher than the present interglacial (Kukla *et al.*, 2002; Muhs *et al.*, 2002).

Genetic discontinuities in both *E. portoricensis* and *E. antillensis* occur in the vicinity of the Río Grande de Loíza Basin, an area where habitat for both species was unstable. The Río Grande de Loíza Basin has existed since the Miocene (*ca.* 23.0 to 5.3 mya), and continues to lose elevation due to intense alluvial erosion (Renken *et al.*, 2002), resulting in a relatively warm and dry landscape which separates much of eastern and western Puerto Rico, as well as the Cayey Mountains from the Luquillo Mountains. First proposed as a barrier to westward dispersal of the mesophillic Locust Coquí, *E. locustus* (Rivero & Mayorga, 1963), and the Golden Coquí, *E. jasperi* (Drewry & Jones, 1976), this basin also coincides with genetic discontinuities in *E. coqui* (Velo-Antón *et al.*, 2007) and in the Mountain Garden Lizard, *Anolis krugi* (Rodríguez-Robles *et al.*, 2010). Precipitation seasonality (i.e., the coefficient of variation of monthly precipitation) is higher in the Río Grande de Loíza Basin than in montane regions of Puerto Rico (Daly

*et al.*, 2003), and the finding that this bioclimatic variable contributes most strongly to the ENM of both *E. portoricensis* and *E. antillensis* (Table 2) may explain why this landscape feature is associated with genetic discontinuities in both species.

Marked differences in the depth of genetic isolation within *E. portoricensis* and *E. antillensis* associated with the Río Grande de Loíza Basin likely track species-specific physiological tolerances to climatic conditions in this region. *Eleutherodactylus portoricensis* is intolerant to warm, desiccating conditions (Beuchat *et al.*, 1984; Woolbright, 1997). Significant correlations of genetic distance with the presence of unstable habitat barriers, even after partitioning out the effects of geographic distance (Table 3), suggest that this basin has been a strong barrier to gene flow in *E. portoricensis*. Vicariance resulting from the gradual erosion of mountains which once connected the Luquillo and Cayey Mountains at the eastern edge of the Río Grande de Loíza Basin (Meyerhoff, 1933) probably initiated allopatric divergence, with populations became increasingly isolated as the basin lowered and became warmer and dryer. According to the IM analysis with the lower  $t$  prior, migration did not occur between populations in the Cayey and Luquillo Mountains following this splitting event, which suggests that climate-driven elevational range shifts were not extensive enough to increase habitat suitability in the Río Grande de Loíza Basin to the point where isolated populations could make secondary contact. The estimated divergence time inferred from IMA2 when using the lower  $t$  prior (172.9 kya) is similar to the one inferred by the \*BEAST analysis (365.3 kya), and therefore a history of pre-LIG divergence and absence of subsequent migration is probably a more likely demographic history than the alternative demographic history inferred by IMA2, which involved an ancient (1.5 mya)

divergence time followed by gene flow. Our findings corroborate the deep divergence within *E. portoricensis* inferred in a previous study (Barker *et al.*, 2011), but provide a more robust assessment of history due to the inclusion of additional loci and more refined mutation rates.

Wider physiological tolerances in *E. antillensis* probably explain shallower levels of divergence between populations on opposite sides of the Río Grande de Loíza Basin, but habitat surrounding this region has still acted as barrier to gene flow. This species has a higher critical thermal maximum than *E. portoricensis* (Beuchat *et al.*, 1984) and can rehydrate quickly at warm temperatures (van Berkum *et al.*, 1982). Nevertheless, *E. antillensis* is absent from small, arid islands and most xeric habitats in the Puerto Rican Bank (Ovaska *et al.*, 2000) and populations have lower densities following long periods of drought (Ovaska, 2005), suggesting that very xeric conditions inhibit persistence or gene flow. An estimated split between western and eastern populations at 4.7 kya (95% HPD: 15.5 – 0.4 kya) suggests that divergence occurred between the end of the LGM and the early Holocene. Although there does not appear to be a significant increase in connectivity between suitable habitats in western and eastern Puerto Rico occurring between the LGM and the present-day (Fig. 4A), there is good evidence that the lowlands of the PRB were cooler and dryer during the LGM than the present-day, which may have promoted divergence of western and eastern Puerto Rican populations. The onset of increasing mesic climate in Puerto Rico (Renken *et al.*, 2002) and the expansion of lowland mesic forests throughout the Greater Antilles (Higuera-Gundy *et al.*, 1999; Hodell *et al.*, 2008) may have increased connectivity and gene flow between these regions. After accounting for differences in area, eastern Puerto Rico has a higher



percentage of stable habitats than western Puerto Rico (Fig. 4B), which may explain why populations from this region acted as sources to western populations. Although unstable habitat explains only a small portion of genetic isolation in mtDNA and nuDNA (Table 4), these results may be explained by the recent divergence time of western and eastern populations and the lack of resolution in the DNA sequence datasets needed for these Mantel tests. Collectively, the results provide support for the hypothesis that unstable habitat in the Río Grande de Loíza Basin and surrounding coastal lowlands partially isolated western and eastern populations of *E. antillensis*.

#### *Population demography and past climate change*

Populations of *E. portoricensis* in the Cayey and Luquillo Mountains did not appear to experience climate-driven changes in size during the late Quaternary. Although the effective population size ( $N_e$ ) of *E. portoricensis* in the Cayey Mountains is smaller than the Luquillo Mountains (Table 5), there were no sudden changes in  $N_e$  associated with a range contraction inferred for the Cayey Mountains during the LIG (Figs 2A and 6).

Elevational shifts of *E. portoricensis* may simply not have been large enough to detectably influence  $N_e$ . A paucity of fossils from Puerto Rico, or other Caribbean islands, makes it difficult to ascertain how extensive elevational shifts of montane forest were during the late Quaternary. Isolated pockets of 600 year old Palo Colorado trees, *Cyrilla racemiflora* L., at elevations < 400 m in Puerto Rico provide evidence for late Holocene elevational range shifts because this species currently dominant at elevations > 600 m (Scatena, 1998). *Eleutherodactylus portoricensis* has undergone upslope contractions of *ca.* 300 m in the Luquillo Mountains over the past 30 years (Woolbright,

1997; Longo & Burrowes, 2010), providing evidence that elevational range shifts do occur to some extent. Populations may remain sufficiently high and uniform in core suitable areas so that extirpation of peripheral populations at lower elevation does not demonstrably affect overall  $N_e$ . Indeed, montane specialist herpetofauna in the Australian Wet Tropics seem to maintain high and uniform local abundances within their narrow ranges (Williams *et al.*, 2009).

Our hypothesis that climate-driven demographic changes occurred in *E. antillensis* was largely supported. Western Puerto Rican populations began a large and rapid increase in size *ca.* 20 kya (Fig. 6), which coincides with the onset of increasing mesic climate in Puerto Rico and the expansion of lowland mesic forests throughout the Greater Antilles. Coastal lowland habitat in western Puerto Rico probably became increasingly suitable throughout the Holocene, allowing western populations to rapidly grow. Average nuDNA  $\hat{\theta}_w$  in *E. antillensis* was positively correlated with habitat stability, a relationship that remained marginally significant after accounting for spatial autocorrelation, providing further support that this species has expanded into historically unsuitable areas.

#### *Multilocus phylogenetic analysis of E. portoricensis*

Independently evolving metapopulations (de Queiroz, 2007) of *E. portoricensis* occur within the Luquillo and Cayey Mountains, and the results of Bayesian species delimitation (Fig. 7) provide strong support that these lineages are comprised of two species. Reciprocal monophyly of the Luquillo and Cayey Mountains lineages (Donoghue, 1985) and exclusive coalescence of alleles of populations within each lineage

(Baum & Shaw, 1995) support the delineation of *E. portoricensis* into two species according to a phylogenetic species concept. Including fossil calibration points in the \*BEAST analysis would probably improve the accuracy of divergence time estimates (McCormack *et al.*, 2010), but fossils are lacking. A robust description of these lineages should be conducted by integrating multi-locus data with other sources of information, such as morphological, behavioral, and ecological traits. Moreover, the inclusion of samples from populations in the Cordillera Central would provide a more comprehensive evaluation of the diversity present in *E. portoricensis*. However, this may be complicated because extensive searches at nine historical localities across the Cordillera Central during the summer of 2007-2008 found no individuals, suggesting that populations were either extremely reduced or extirpated (unpublished data).

As currently recognized, *E. portoricensis* is classified as endangered (IUCN, 2011) and as vulnerable by the Department of Natural and Environmental Resources of Puerto Rico (Departamento de Estado, 2004). In addition to apparent declines or extirpations in the Cordillera Central, populations at two sites in the El Verde and the Bisley watersheds (*ca.* 350 m) were extirpated by 1989 and 1993, respectively (Woolbright, 1997). A population in the Palo Colorado forest (661 m) is almost extirpated (Longo & Burrowes, 2010). The discovery of two putative species within the nominal *E. portoricensis* has obvious conservation implications, because each occupies a more restricted distribution comprised of fewer populations. Accordingly, each might require different conservation and management strategies. We suggest that the Luquillo and Cayey Mountains lineages of *E. portoricensis* should each, at a minimum, be classified as a “distinct population segment” under criteria used to identify such units

(U.S. Federal Register, 1996), namely that the reciprocal monophyly and deep temporal divergence of *E. portoricensis* populations on these mountain range provide strong evidence for independent evolutionary trajectories. Although *E. portoricensis* has apparently persisted in narrow ranges through past warming events, additional threats to this species and other Puerto Rican montane specialists, including disease, deforestation, and invasive species (Joglar *et al.*, 2007; Hedges & Díaz, 2011), highlight the need to protect these highly endemic ecosystems. Understanding the relative roles of landscape features, dispersal capabilities, and habitat characteristics that enable population persistence will improve predictions of future climate change impacts on biotas from Puerto Rico and other tropical insular systems.

### **Acknowledgments**

We thank F. Bird-Picó, T. Figueroa, W. Falcón-Linero, J. Fumero, S. Lazell, C.D. Ortiz, G. Perry, C. Petrovic, R. Platenberg, M.J. Quiñones, A. Ríos-Franceschí, Y. Rodríguez, J.R. Snider, and L. Woolbright for assistance in the field, M. Farrah, A. Montoya, and M. Osborne for help in the laboratory, and the Department of Natural and Environmental Resources of Puerto Rico and U.S. Forest Service for granting collecting permits. We acknowledge technical support from the University of New Mexico (UNM) Department of Biology's Molecular Biology Facility, which is supported by National Institutes of Health Grant P20RR18754 from the Institute Development Award Program of the National Center for Research Resources; and from the University of Alaska, Fairbanks Life Science Informatics, a core research resource supported by grant RR016466 from the National Center for Research Resources. T. Giermakowski provided field supplies

and curatorial support, and T.F. Turner, C. Metzger, and J. Richter reviewed earlier drafts of this manuscript. This study was partly funded by grants from the National Science Foundation (DBI-0001975, DEB-0327415) and the American Museum of Natural History to J.A.R.-R., the Undergraduate Opportunities program at the Museum of Southwestern Biology (National Science Foundation DEB-0731350), and awards from the Society for the Study of Amphibians and Reptiles, the UNM Biology Department, Office of Graduate Studies, and Graduate and Professional Student Association to B.S.B. Fieldwork was partially supported by Long Term Ecological Research Grants (National Science Foundation DEB-0218039 and DEB-0620910).

## References

- Araújo, M., Nogués-Bravo, D., Diniz-Filho, J., Haywood, A., Valdes, P. & Rahbek, C. (2008) Quaternary climate changes explain diversity among reptiles and amphibians. *Ecography*, **31**, 8-15.
- Ballard, J.W.O. & Whitlock, M.C. (2004) The incomplete natural history of mitochondria. *Molecular Ecology*, **13**, 729-744.
- Barker, B.S., Waide, R.B. & Cook, J.A. (2011) Deep intra-island divergence of a montane forest endemic: phylogeography of the Puerto Rican frog *Eleutherodactylus portoricensis* (Anura: Eleutherodactylidae). *Journal of Biogeography*, **38**, 2311-2325.
- Baum, D. & Shaw, K. (1995) Genealogical perspectives on the species problem. *Experimental and molecular approaches to plant biosystematics* (ed. by P. Hoch and A. Stephenson), pp. 289-303, Missouri Botanical Garden, St. Louis.
- Beaumont, L., Hughes, L. & Poulsen, M. (2005) Predicting species distributions: use of climatic parameters in BIOCLIM and its impact on predictions of species' current and future distributions. *Ecological Modelling*, **186**, 250-269.
- Bell, R.C., Parra, J.L., Tonione, M., Hoskin, C.J., Mackenzie, J.B., Williams, S.E. & Moritz, C. (2010) Patterns of persistence and diversification indicate resilience to climate change in montane rainforest lizards. *Molecular Ecology*, **19**, 2531-2544.
- Beuchat, C.A., Pough, F.H. & Stewart, M.M. (1984) Response to simultaneous dehydration and thermal stress in three species of Puerto Rican frogs. *Journal of Comparative Physiology B*, **154**, 579-585.

- Brito, P.H. & Edwards, S.V. (2008) Multilocus phylogeography and phylogenetics using sequence-based markers. *Genetica*, **135**, 439-455.
- Carnaval, A. & Moritz, C. (2008) Historical climate modelling predicts patterns of current biodiversity in the Brazilian Atlantic forest. *Journal of Biogeography*, **35**, 1187-1201.
- Carnaval, A.C., Hickerson, M.J., Haddad, C.F.B., Rodrigues, M.T. & Moritz, C. (2009) Stability predicts genetic diversity in the Brazilian Atlantic forest hotspot. *Science*, **323**, 785-789.
- Chan, L., Brown, J. & Yoder, A. (2011) Integrating statistical genetic and geospatial methods brings new power to phylogeography. *Molecular Phylogenetics and Evolution*, **59**, 523-537.
- Chen, I.-C., Shiu, H.-J., Benedick, S., Holloway, J.D., Khen Chey, V., Barlow, H.S., Hill, J.K. & Thomas, C.D. (2009) Elevation increases in moth assemblages over 42 years on a tropical mountain. *Proceedings of the National Academy of Sciences, USA*, **106**, 1479-1483.
- Collins, W.D., Bitz, C.M., Blackmon, M.L., Bonan, G.B., Bretherton, C.S., Carton, J.A., Chang, P., Doney, S.C., Hack, J.J., Henderson, T.B., Kiehl, J.T., Large, W.G., Mckenna, D.S., Santer, B.D. & Smith, R.D. (2006) The community climate system model version 3 (CCSM3). *Journal of Climate*, **19**, 2122-2143.
- Cook, B.D., Pringle, C.M. & Hughes, J. (2010) Immigration history of amphidromous species on a Greater Antillean island. *Journal of Biogeography*, **37**, 270-277.
- Corlett, R. (2011) Impacts of warming on tropical lowland rainforests. *Trends in Ecology and Evolution*, **26**, 606-613.

- Crawford, A.J. (2003) Relative rates of nucleotide substitution in frogs. *Journal of Molecular Evolution*, **57**, 636-641.
- Crawford, A.J., Bermingham, E. & Polanía, C.S. (2007) The role of tropical dry forest as a long-term barrier to dispersal: a comparative phylogeographical analysis of dry forest tolerant and intolerant frogs. *Molecular Ecology*, **16**, 4789-4807.
- Daly, C., Helmer, E.H. & Quiñones, M. (2003) Mapping the climate of Puerto Rico, Vieques and Culebra. *International Journal of Climatology*, **23**, 1359-1381.
- de Queiroz, K. (2007) Species concepts and species delimitation. *Systematic Biology*, **56**, 879-886.
- Departamento de Estado (2004) Reglamento para regir las especies vulnerables y en peligro de extinción en el estado libre asociado de Puerto Rico (by G. Romero García). Reglamento 6766, Departamento de Recursos Naturales y Ambientales, San Juan, Puerto Rico.
- Donoghue, M. (1985) A critique of the biological species concept and recommendations for a phylogenetic alternative. *Bryologist*, **88**
- Drewry, G. (1970) Factors affecting activity of rain forest frog populations as measured by electrical recording of sound pressure levels. *A tropical rain forest* (ed. by H. Odum and R. Pigeon). Division of technical information, U.S. Atomic Energy Commission, Oak Ridge, Tennessee.
- Drewry, G.E. & Jones, K.L. (1976) A new ovoviviparous frog, *Eleutherodactylus jasperi* (Amphibia, Anura, Leptodactylidae). *Journal of Herpetology*, **10**, 161-165.
- Drewry, G.E. & Rand, A.S. (1983) Characteristics of an acoustic community: Puerto Rican frogs of the genus *Eleutherodactylus*. *Copeia*, 941-953.



- Drummond, A.J. & Rambaut, A. (2007) BEAST: Bayesian evolutionary analysis by sampling trees. *BMC Evolutionary Biology*, **7**, 214.
- Dutilleul, P. (1993) Modifying the *t*-test for assessing correlation between two spatial processes. *Biometrics*, **49**, 305-314.
- Edgar, R.C. (2004) MUSCLE: multiple sequence alignment method with high accuracy and high throughput. *Nucleic Acids Research*, **32**, 1792-1797.
- Elith, J. & Leathwick, J.R. (2009) Species distribution models: ecological explanation and prediction across space and time. *Annual Review of Ecology, Evolution, and Systematics*, **40**, 677-697.
- Ewel, J.J. & Whitmore, J.L. (1973) The ecological life zones of Puerto Rico and the U.S. Virgin Islands. Forest Service Research Paper ITF-18. Río Piedras, PR: United States Department of Agriculture, Forest Service, International Institute of Tropical Forestry. 74 p.
- Excoffier, L., Laval, G. & Schneider, S. (2005) Arlequin (version 3.0): an integrated software package for population genetics data analysis. *Evolutionary Bioinformatics Online*, **1**, 47-50.
- Falush, D., Stephens, M. & Pritchard, J. (2003) Inference of population structure using multilocus genotype data: linked loci and correlated frequencies. *Genetics*, **164**, 1567-1587.
- Feeley, K.J., Silman, M.R., Bush, M.B., Farfan, W., Garcia Cabrera, K., Malhi, Y., Meir, P., Salinas Revilla, N., Quisíyupanqui, M. & Saatchi, S. (2011) Upslope migration of Andean trees. *Journal of Biogeography*, **38**, 783-791.

- Felsenstein, J. (1988) Phylogenies from molecular sequences: inference and reliability. *Annual Review of Genetics*, **22**, 521-565.
- Figueroa Colón, J.C. (1996) Phytogeographical trends, centers of high species richness and endemism, and the question of extinctions in the native flora of Puerto Rico. *The scientific survey of Puerto Rico and the Virgin Islands: an eighty-year reassessment of the islands' natural history* (ed. by J.C. Figueroa Colón), pp. 89-102. Annals of the New York Academy of Sciences, New York, New York.
- Frankham, R. (1998) Inbreeding and extinctions: island populations. *Conservation Biology*, **12**, 665-675.
- Fu, Y.-X. (1997) Statistical tests of neutrality of mutations against population growth, hitchhiking and background selection. *Genetics*, **147**, 915-925.
- Galbreath, K.E., Cook, J.A., Eddingsaas, A.A. & Dechaine, E.G. (2011) Diversity and demography in Beringia: multilocus tests of paleodistribution models reveal the complex history of arctic ground squirrels. *Evolution*, **65**, 1879-1896.
- Garrick, R.C., Sunnucks, P. & Dyer, R.J. (2010) Nuclear gene phylogeography using PHASE: dealing with unresolved genotypes, lost alleles, and systematic bias in parameter estimation. *BMC Evolutionary Biology*, **10**, 118.
- Gibbard, P., Head, M. & Walkers, M., And the Subcommision on Quaternary Stratigraphy (2010) Formal ratification of the Quaternary System/Period and the Pleistocene Series/Epoch with a base at 2.58 Ma. *Journal of Quaternary Science*, **25**, 96-102.

- Gibbs, M.J., Armstrong, J.S. & Gibbs, A.J. (2000) Sister-scanning: a Monte Carlo procedure for assessing signals in recombinant sequences. *Bioinformatics*, **16**, 573-582.
- Gillespie, R.G., Caridge, E.M. & Roderick, G.K. (2008) Biodiversity dynamics in isolated island communities: interaction between natural and human-mediated processes. *Molecular Ecology*, **17**, 45-57.
- Giribet, G. & Wheeler, W. (1999) On gaps. *Molecular Phylogenetics and Evolution*, **13**, 132-143.
- González, C., Dupont, L.M., Behling, H. & Wefer, G. (2008) Neotropical vegetation response to rapid climate changes during the last glacial period: palynological evidence from the Cariaco Basin. *Quaternary Research*, **69**, 217-230.
- Goodfriend, G. & Mitterer, R. (1993) A 45,000-yr record of tropical lowland biota: the land snail fauna from cave sediments at Coco Ree, Jamaica. *Geological Society of America Bulletin*, **105**, 18-29.
- Goslee, S.C. & Urban, D.L. (2007) The ecodist package for dissimilarity-based analysis of ecological data. *Journal of Statistical Software*, **22**, 1-19.
- Gould, W.A., Alarcón, C., Fevold, B., Jiménez, M.E., Martinuzzi, S., Potts, G., Quiñones, M., Solórzano, M. & Ventosa, E. (2008) The Puerto Rico Gap Analysis Project. Volume 1: Land cover, vertebrate species distributions, and land stewardship. Gen. Tech. Rep. IITF-GTR-39. Río Piedras, PR: United States Department of Agriculture, Forest Service, International Institute of Tropical Forestry. 165 p.

- Graham, C., Moritz, C. & Williams, S.E. (2006) Habitat history improves prediction of biodiversity in rainforest fauna. *Proceedings of the National Academy of Sciences, USA*, **103**, 632-636.
- Guilderson, T.P., Fairbanks, R.G. & Rubenstone, J.L. (2001) Tropical Atlantic coral oxygen isotopes: glacial-interglacial sea surface temperatures and climate change. *Marine Geology*, **172**, 75-89.
- Hasegawa, M., Kishino, H. & Yano, T.-A. (1985) Dating of the human-ape splitting by a molecular clock of mitochondrial DNA. *Journal of Molecular Evolution*, **22**, 160-174.
- Hasumi, H. & Emori, S. (2004) K-1 coupled GCM (MIROC) description. K-1 Technical Report No. 1. Center for Climate System Research, University of Tokyo, Japan.
- Hedges, S. & Díaz, L. (2011) The conservation status of amphibians in the West Indies. *Conservation of Caribbean island herpetofaunas volume 1: conservation biology and the wider Caribbean* (ed. by A. Hailey, B. Wilson and J. Horrocks), pp. 281-292. Brill, Leiden, the Netherlands.
- Heinicke, M., Duellman, W., Trueb, L., Means, D., Macculloch, R. & Hedges, S. (2009) A new frog family (Anura: Terrarana) from South America and an expanded direct-developing clade revealed by molecular phylogeny. *Zootaxa*, **2211**, 1-35.
- Heinicke, M.P., Duellman, W.E. & Hedges, S.B. (2007) Major Caribbean and Central American frog faunas originated by ancient oceanic dispersal. *Proceedings of the National Academy of Sciences, USA*, **104**, 10092-10097.
- Heled, J. & Drummond, A.J. (2008) Bayesian inference of population size history from multiple loci. *BMC Evolutionary Biology*, **8**, 289.

- Henderson, R.W. & Powell, R. (1999) West Indian herpetoecology. *Caribbean amphibians and reptiles* (ed. by B.I. Crother), pp. 223-268. Academic Press, San Diego, CA.
- Herrera-Montes, A. & Brokaw, N. (2010) Conservation value of tropical secondary forest: a herpetofaunal perspective. *Biological Conservation*, **143**, 1414-1422.
- Hessler, I., Dupont, L., Bonnefille, R., Behling, H., González, C., Helmens, K.F., Hooghiemstra, H., Lebamba, J., Marie-Pierre, L., Lézine, A.-M., Maley, J., Marret, F. & Vincens, A. (2010) Millennial-scale changes in vegetation records from tropical Africa and South America during the last glacial. *Quaternary Science Reviews*, **29**, 2882-2899.
- Hey, J. (2006) Recent advances in assessing gene flow between diverging populations and species. *Current Opinion in Genetics and Development*, **16**, 592-596.
- Hey, J. (2010) Isolation with migration models for more than two populations. *Molecular Biology and Evolution*, **27**, 905-920.
- Hey, J. & Nielson, R. (2004) Multilocus methods for estimating population sizes, migration rates and divergence time, with applications to the divergence of *Drosophila pseudoobscura* and *D. persimilis*. *Genetics*, **167**, 747-760.
- Higuera-Gundy, A., Brenner, M., Hodell, D.A., Curtis, J.H., Leyden, B.W. & Binford, M.W. (1999) A 10,300 <sup>14</sup>C yr record of climate and vegetation change from Haiti. *Quaternary Research*, **52**, 159-170.
- Hodell, D.A., Anselmetti, F.S., Ariztegui, D., Brenner, M., Curtis, J.H., Gilli, A., Grzesik, D.A., Guilderson, T.P., Müller, A.D., Bush, M.B., Correa-Metrio, A.Y., Escobar,

- J. & Kutterolf, S. (2008) An 85-ka record of climate change in lowland Central America. *Quaternary Science Reviews*, **27**, 1152-1165.
- Hoffman, A.A. & Sgró, C.M. (2011) Climate change and evolutionary adaptation. *Nature* **470**, 479-485.
- Holsinger, K. & Weir, B.S. (2009) Genetics in geographically structured populations: defining, estimating and interpreting  $F_{ST}$ . *Nature Reviews Genetics*, **10**, 639-650.
- Hubisz, M., Falush, D., Stephens, M. & Pritchard, J. (2009) Inferring weak population structure with the assistance of sample group information. *Molecular Ecology Resources*, **9**, 1322-1332.
- Hudson, R.R., Kreitman, M. & Aguadé, M. (1987) A test of neutral molecular evolution based on nucleotide data. *Genetics*, **116**, 153-159.
- Hugall, A., Moritz, C., Moussall, A. & Stanistic, J. (2002) Reconciling paleodistribution models and comparative phylogeography in the wet tropics rainforest land snail *Gnarosiphia bellendenkerensis* (Brazier 1875). *Proceedings of the National Academy of Sciences, USA*, **99**, 6112-6117.
- IUCN (2011) *IUCN Red List of Threatened Species*. IUCN Species Survival Commission, Gland, Switzerland.
- Jensen, J.L., Bohonak, A.J. & Kelley, S.T. (2005) Isolation by distance, web service. *BMC Genetics*, **6**, 13.
- Joglar, R.L. (1998) *Los coquíes de Puerto Rico: su historia natural y conservación*. Editorial de la Universidad de Puerto Rico, San Juan.
- Joglar, R.L., Álvarez, A.O., Aide, T.M., Barber, D., Burrowes, P.A., García, M.A., León-Cardona, A., Longo, A.V., Pérez-Buitrago, N., Puente, A., Rios-López, N. &

- Tolson, P.J. (2007) Conserving the Puerto Rican herpetofauna. *Applied Herpetology*, **4**, 327-345.
- Katoh, K., Misawa, K., Kuma, K. & Miyata, T. (2002) MAFFT: a novel method for rapid multiple sequence alignment based on fast Fourier transform. *Nucleic Acids Research*, **30**, 3059-3066.
- Knowles, L.L. & Alvarado-Serrano, D.F. (2010) Exploring the population genetic responses of the colonization process with spatio-temporally explicit models: insights from coupled ecological, demographic, and genetic models in montane grasshoppers. *Molecular Ecology*, **19**, 3727-3745.
- Knowles, L.L. & Carstens, B.C. (2006) Estimating a geographically explicit model of population divergence. *Evolution*, **61**, 477-493.
- Kukla, G.J., Bender, M.L., de Beaulieu, J.-L., Bond, G., Broecker, W.S., Bond, G., Cleveringa, P., Gavin, J.E., Herbert, T.D., Imbrie, J., Jouzel, J., Keigwin, L.D., Knudsen, K.-L., Mcmanus, J.F., Merkt, J., Muhs, D.R., Müller, H., Poore, R.Z., Porter, S.C., Seret, G., Shackleton, N.J., Turner, C., Tzedakis, P.C. & Winograd, I.J. (2002) Last interglacial climates. *Quaternary Research*, **58**, 2-13.
- Longo, A.V. & Burrowes, P.A. (2010) Persistence with chytridiomycosis does not assure survival of direct-developing frogs. *EcoHealth*, **7**, 185-195.
- MacPhee, R. (2009) *Insulae infortunatae*: establishing a chronology for late Quaternary mammal extinctions in the West Indies. *American megafaunal extinctions at the end of the Pleistocene* (ed. by G. Haynes), pp. 169-193. Springer, New York, NY.
- Maddison, W.P. & Knowles, L.L. (2006) Inferring phylogeny despite incomplete lineage sorting. *Systematic Biology*, **55**, 21-30.

- Mantel, N. (1967) The detection of disease clustering and a generalized regression approach. *Cancer Research*, **27**, 209-220.
- Martin, D.P., Lemey, P., Lott, M., Moulton, V., Posada, D. & Lefevre, P. (2010) RDP3: a flexible and fast computer program for analyzing recombination. *Bioinformatics*, **26**, 2462-2463.
- Martin, D.P., Williamson, C. & Posada, D. (2005) RDP2: recombination detection and analysis from sequence alignments. *Bioinformatics*, **21**, 260-262.
- Maynard Smith, J. (1992) Analyzing the mosaic structure of genes. *Journal of Molecular Evolution*, **34**, 126-129.
- Mccormack, J., Heled, J., Delaney, K., Peterson, A.T. & Knowles, L.L. (2010) Calibrating divergence times on species trees versus gene trees: implications for speciation history of *Aphelocoma* jays. *Evolution*, **65**, 184-202.
- Meyerhoff, H.A. (1933) Geology of Puerto Rico. *Monographs of the University of Puerto Rico Series B*, **1**, 169-171.
- Moussalli, A., Moritz, C., Williams, S. & Carnaval, A. (2009) Variable responses of skinks to a common history of rainforest fluctuation: concordance between phylogeography and palaeo-distribution models. *Molecular Ecology*, **18**, 483-499.
- Muhs, D.R., Simmons, K.R. & Steinke, B. (2002) Timing and warmth of the Last Interglacial period: new U-series evidence from Hawaii and Bermuda and a new fossil compilation for North America. *Quaternary Science Reviews*, **21**, 1355-1383.
- Nei, M. (1972) Genetic distance between populations. *American Naturalist*, **106**, 283-392.



- Nielson, R. & Wakeley, J. (2001) Distinguishing migration from isolation: a Markov chain Monte Carlo approach. *Genetics*, **158**, 885-896.
- Nogués-Bravo, D. (2009) Predicting the past distribution of species climatic niches. *Global Ecology and Biogeography*, **18**, 521-531.
- Noonan, B. & Wray, K. (2006) Neotropical diversification: the effects of a complex history on diversity within the poison frog genus *Dendrobates*. *Journal of Biogeography*, **33**, 1007-1020.
- Orvis, K.H., Clark, G.M., Horn, S.P. & Kennedy, L.M. (1997) Geomorphic traces of Quaternary climates in the Cordillera Central, Dominican Republic. *Mountain Research and Development*, **17**, 323-331.
- Otto-Bliesner, B.L., Marshall, S.J., Overpeck, J.T., Miller, G.H. & Hu, A. (2006) Simulating arctic climate warmth and icefield retreat in the Last Interglaciation. *Science*, **311**, 1751-1753.
- Ovaska, K.E. (2005) The frog (*Eleutherodactylus antillensis*). *Island: fact and theory in nature* (ed. by J.D. Lazell, Jr.), pp. 175-180. University of California Press, Berkeley, CA.
- Ovaska, K.E. & Caldbeck, J. (1997) Vocal behaviour of the frog *Eleutherodactylus antillensis* on the British Virgin Islands. *Animal Behavior*, **54**, 181-188.
- Ovaska, K.E., Caldbeck, J. & Lazell, J.D., Jr. (2000) New records and distributional and ecological notes of Leptodactylid frogs, *Leptodactylus* and *Eleutherodactylus*, from the British Virgin Islands. *Breviora*, **508**, 1-25.
- Padidam, M., Sawyer, S. & Fauquet, C.M. (1999) Possible emergence of new geminiviruses by frequent recombination. *Virology*, **265**, 218-225.

- Parmesan, C. (2006) Ecological and evolutionary responses to recent climate change. *Annual Review of Ecology, Evolution, and Systematics*, **37**, 637-669.
- Pearson, R.G., Raxworthy, C.J., Nakamura, M. & Peterson, A.T. (2007) Predicting species' distributions from small numbers of occurrence records: a test case using cryptic geckos in Madagascar. *Journal of Biogeography*, **34**, 102-117.
- Phillips, S.J., Anderson, R.P. & Schapire, R.E. (2006) Maximum entropy modeling of species geographic distributions. *Ecological Modelling*, **190**, 231-259.
- Phillips, S.J. & Dudík, M. (2008) Modeling of species distributions with Maxent: new extensions and a comprehensive evaluation. *Ecography*, **31**, 161-175.
- Phillips, S.J., Dudík, M., Elith, J., Graham, C.H., Lehman, A., Leathwick, J.R. & Ferrier, S. (2009) Sample selection bias and presence-only distribution models: implications for background and pseudo-absence data. *Ecological Applications*, **19**, 181-197.
- Phillips, S.J., Dudík, M. & Schapire, R.E. (2004) A maximum entropy approach to species distribution modeling. In: *Proceedings of the 21st International Conference on Machine Learning*, pp. 655-662. ACM Press, New York
- Posada, D. & Crandall, K.A. (1998) Modeltest: testing the model of DNA substitution. *Bioinformatics*, **14**, 817-818.
- Posada, D. & Crandall, K.A. (2001) Intraspecific gene genealogies: trees grafting into networks *Trends in Ecology and Evolution*, **16**, 37-45.
- Pough, F., Taigen, T., Stewart, M. & Brussard, P. (1983) Behavioral modification of evaporative water loss by a Puerto Rican frog. *Ecology*, **64**, 244-252.

- Pritchard, J., Stephens, M. & Donnelly, P. (2000) Inference of population structure using multilocus genotype data. *Genetics*, **155**, 945-959.
- R Development Core Team (2010) *R: A language and environment for statistical computing*. R Foundation for Statistical Computing, Vienna, Austria.  
<http://www.r-project.org>.
- Rambaut, A. & Drummond, A.J. (2007) *Tracer*, version 1.5. Available at:  
<http://beast.bio.ed.ac.uk/Tracer>.
- Rangel, T., Diniz-Filho, J. & Bini, L. (2006) Towards an integrated computational tool for spatial analysis and macroecology and biogeography. *Global Ecology and Biogeography*, **15**, 321-327.
- Renken, R.A., Ward, W.C., Gill, I.P., Gómez-Gómez, F. & Rodríguez-Martínez, J. (2002) Geology and hydrogeology of the Caribbean islands aquifer system of the commonwealth of Puerto Rico and the U.S. Virgin Islands. *U.S. Geological Survey Professional Paper*, **1419**, 1-148.
- Ricklefs, R.E. & Bermingham, E. (2008) The West Indies as a laboratory of biogeography and evolution. *Philosophical Transactions of the Royal Society B-Biological Sciences*, **363**, 2393-2413.
- Rivero, J.A. & Mayorga, H. (1963) Notes on the distribution of some Puerto Rican frogs with a discussion on the possible origin of *Eleutherodactylus locustus*. *Caribbean Journal of Science*, **3**, 81-85.
- Rodríguez-Robles, J.A., Jezkova, T. & Leal, M. (2010) Climatic stability and genetic divergence in the tropical insular lizard *Anolis krugi*, the Puerto Rican 'Lagartijo Jardinero de la Montaña'. *Molecular Ecology*, **19**, 1860-1876.

- Rosenberg, N.A. (2004) DISTRUCT: a program for the graphical display of population structure. *Molecular Ecology Notes*, **4**, 137-138.
- Rousset, F. (1997) Genetic differentiation and estimation of gene flow from  $F$ -statistics under isolation by distance. *Genetics*, **145**, 1219-1228.
- Salminen, M.O., Carr, J.K., Burke, D.S. & Mccutchan, F.E. (1995) Identification of breakpoints in intergenotypic recombinants of HIV type 1 by bootscanning. *AIDS Research and Human Retroviruses*, **11**, 1423-1425.
- Scatena, F.N. (1998) An assessment of climate change in the Luquillo Mountains of Puerto Rico. In: *Third international symposium on tropical hydrology and fifth Caribbean Islands water resources congress* (ed. R.I. Segarra-García), pp. 193-198. American Water Resources Association, San Juan, Puerto Rico.
- Sheldon, F.H., Jones, C.E. & Mccracken, K.G. (2000) Relative patterns and rates of evolution in heron nuclear and mitochondrial DNA. *Molecular Biology and Evolution*, **17**, 437-450.
- Shirk, A., Wallin, D., Cushman, S., Rice, C. & Warheit, K. (2010) Inferring landscape effects on gene flow: a new model selection framework. *Molecular Ecology*, **19**, 3603-3619.
- Simmons, M. & Ochoterena, H. (2000) Gaps as characters in sequence-based phylogenetic analyses. *Systematic Biology*, **49**, 369-381.
- Stephens, M. & Donnelly, P. (2003) A comparison of Bayesian methods for haplotype reconstruction from population genotype data. *American Journal of Human Genetics*, **73**, 1162-1169.

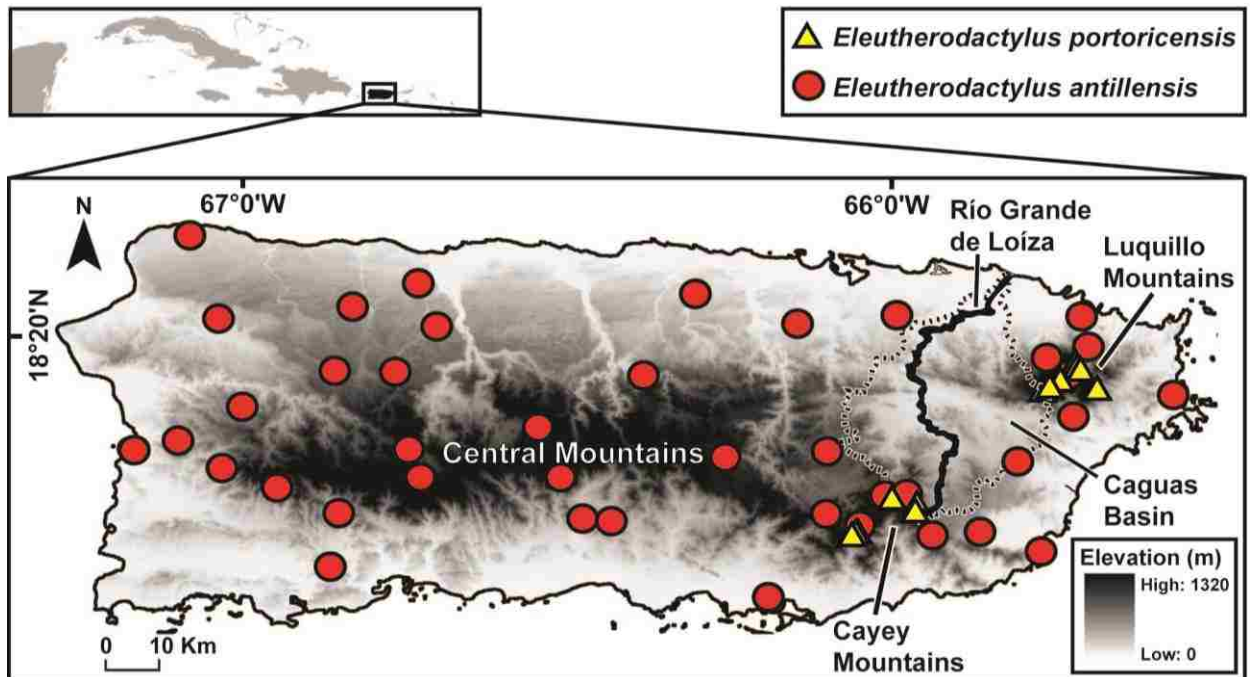
- Stephens, M., Smith, N.J. & Donnelly, P. (2001) A new statistical method for haplotype reconstruction from population data. *American Journal of Human Genetics*, **68**, 978-989.
- Stewart, M.M. (1985) Arboreal habitat use and parachuting in a subtropical forest frog. *Journal of Herpetology*, 391-401.
- Stewart, M.M. (1995) Climate driven population fluctuations in rain forest frogs. *Journal of Herpetology*, **29**, 437-446.
- Stewart, M.M. & Woolbright, L.L. (1996) Amphibians. *The food web of a tropical rainforest* (ed. by D.P. Reagan and R.B. Waide), pp. 273-320. The University of Chicago Press, Chicago, IL.
- Svenning, J.-C., Fløjgaard, C., Marske, K., Nógues-Bravo, D. & Normand, S. (2011) Applications of species distribution modeling to paleobiology. *Quaternary Science Reviews*, **30**, 2930-2947.
- Swofford, D.L. (2000) *PAUP\*: phylogenetics analysis using parsimony (\*and other methods)*. Version 4. Sinauer Associates, Sunderland, MA.
- Tajima, F. (1983) Evolutionary relationship of DNA sequences in finite populations. *Genetics*, **105**, 437-460.
- Tajima, F. (1989) Statistical method for testing the neutral mutation hypothesis by DNA polymorphisms. *Genetics*, **123**, 585-595.
- Thomas, R. (1966) New species of Antillean *Eleutherodactylus*. *Quarterly Journal of the Florida Academy of Science*, **28**, 375-391.
- Townsend, D.S. (1985) Ontogenetic shift in habitat use by *Eleutherodactylus coqui*. Thesis, State University of New York, Albany, USA.

- U.S. Federal Register (1996) Policy regarding the recognition of distinct vertebrate population segments under the Endangered Species Act. **61**, 4722.
- van Berkum, F., Pough, F.H., Stewart, M.M. & Brussard, P.F. (1982) Altitudinal and interspecific differences in the rehydration abilities of Puerto Rican frogs. *Physiological Zoology*, **55**, 130-136.
- Vandergast, A.G., Perry, W.M., Lugo, R.V. & Hathaway, S.A. (2011) Genetic landscapes GIS Toolbox: tools to map patterns of genetic divergence and diversity. *Molecular Ecology Resources*, **11**, 158-161.
- Velo-Antón, G., Burrowes, P.A., Joglar, R.L., Martínez-Solano, I., Beard, K.H. & Parra-Olea, G. (2007) Phylogenetic study of *Eleutherodactylus coqui* (Anura: Leptodactylidae) reveals deep genetic fragmentation in Puerto Rico and pinpoints origins of Hawaiian populations. *Molecular Phylogenetics and Evolution*, **45**, 716-728.
- Waltari, E., Hijmans, J., Peterson, A.T., Nyári, Á.S., Perkins, S.L. & Guralnick, R.P. (2007) Locating Pleistocene refugia: comparing phylogeographic and ecological niche model predictions. *PLoS ONE*, e563.
- Watterson, G. (1975) On the number of segregating sites in genetical models without recombination. *Theoretical Population Biology*, **7**, 256-276.
- Williams, S.E., Williams, Y.M., Vanderwal, J., Isaac, J.L., Shoo, L.P. & Johnson, C.N. (2009) Ecological specialization and population size in a biodiversity hotspot: how rare species avoid extinction. *Proceedings of the National Academy of Sciences, USA*, **106**, 19737-19741.

- Woolbright, L. & Stewart, M. (1987) Foraging success of the tropical frog, *Eleutherodactylus coqui*: the cost of calling. *Copeia*, **1987**, 69-75.
- Woolbright, L.L. (1985) Patterns of nocturnal movement and calling by the tropical frog *Eleutherodactylus coqui*. *Herpetologica*, **41**, 1-9.
- Woolbright, L.L. (1997) Local extinctions of anuran amphibians in the Luquillo Experimental Forest of northeastern Puerto Rico. *Journal of Herpetology*, **31**, 572-576.
- Wright, S. (1943) Isolation by distance. *Genetics*, **28**, 114-138.
- Zimmerman, N., Edwards Jr., T.C., Graham, C.H., Pearman, P.B. & Svenning, J.-C. (2010) New trends in species distribution modeling. *Ecography*, **33**, 985-989.

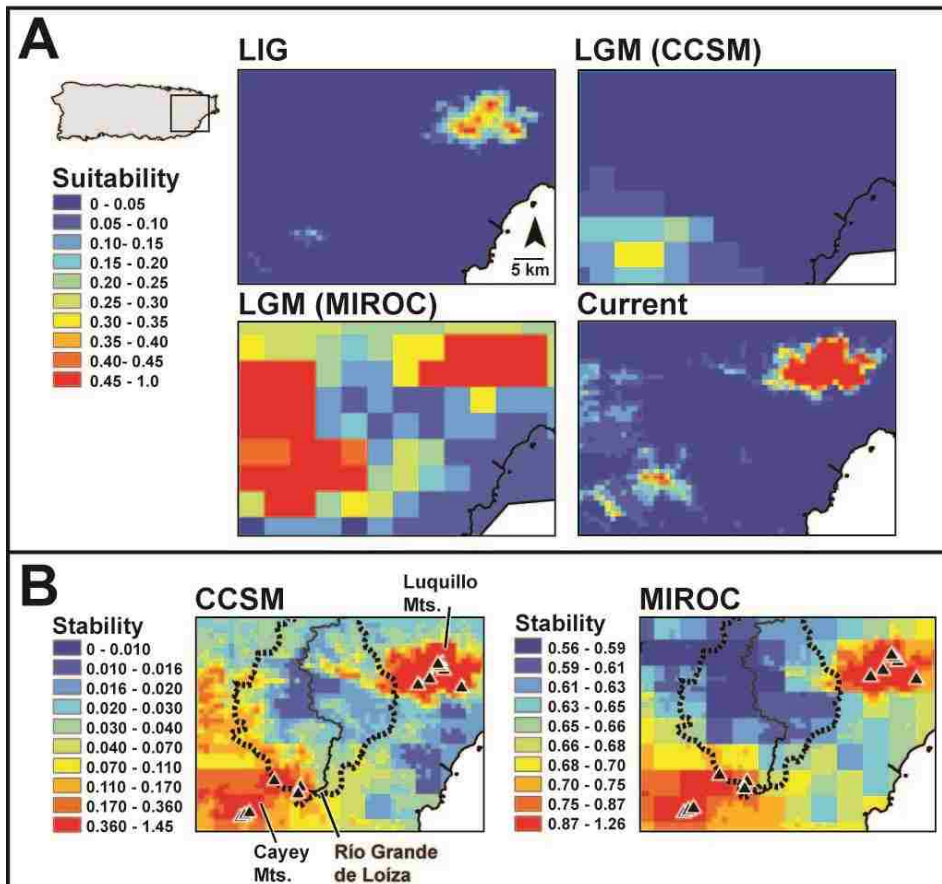
## Figures and Tables

**Fig. 1** Map of Puerto Rico showing the topography of the island and the approximate geographic locations of the *Eleutherodactylus portoricensis* and *E. antillensis* samples included in this study. The location of the Central Mountains (=Cordillera Central), the Cayey Mountains (=Sierra de Cayey), the Luquillo Mountains (=Sierra de Luquillo) and the Río Grande de Loíza are indicated. The dotted line depicts the approximate distribution of the Río Grande de Loíza Basin. The Caguas Basin is nested within the Río Grande de Loíza Basin.

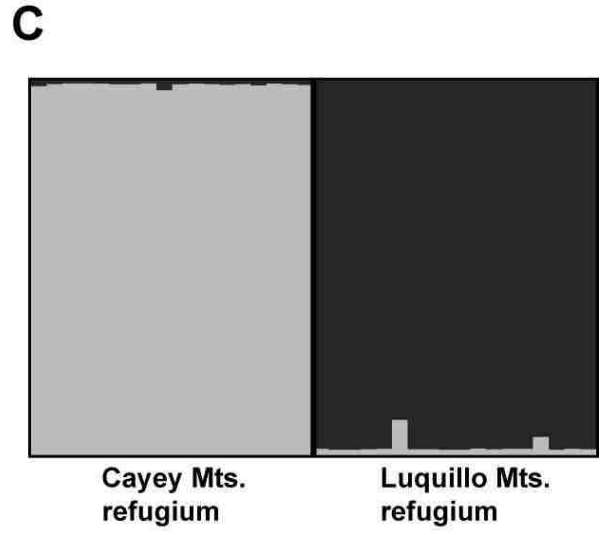
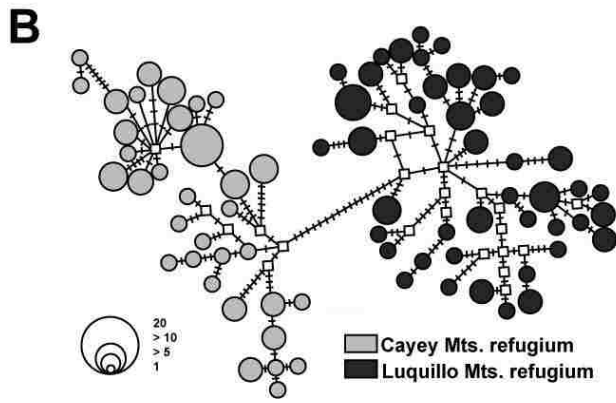
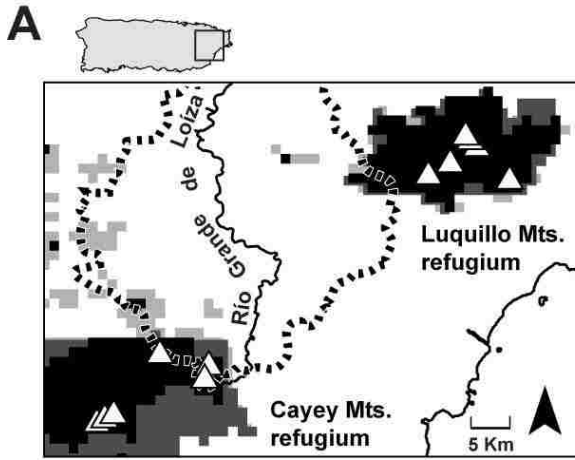




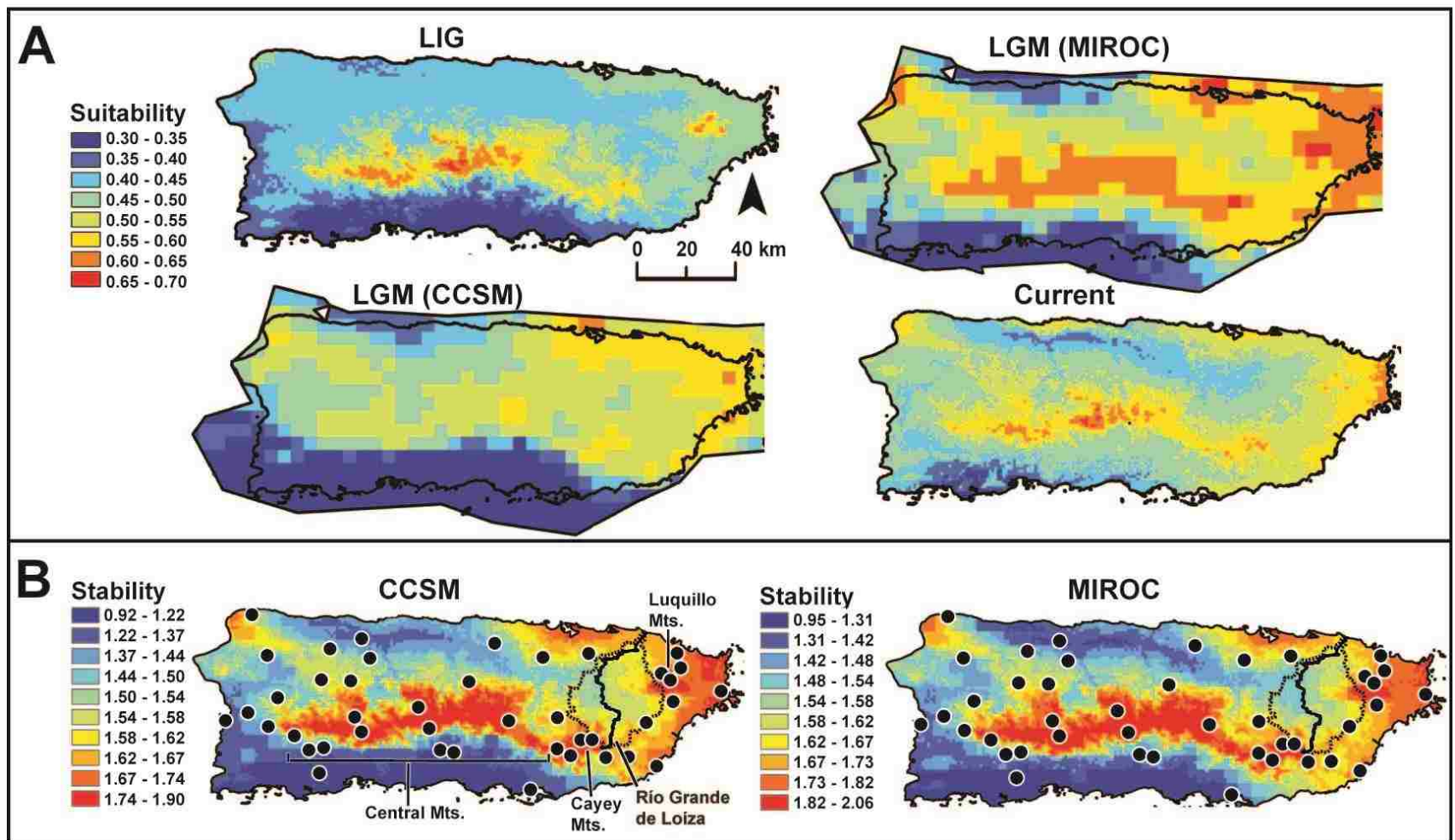
**Fig. 2** Logistic output of ecological niche models (ENMs) for *Eleutherodactylus portoricensis* in Puerto Rico under last interglacial (LIG), last glacial maximum [under CCSM [LGM (CCSM)] and MIROC [LGM (MIROC) scenarios], and current climates. (B) Habitat stability surfaces estimated for *E. portoricensis* by taking the sum of the suitability pixels through the three time periods; one stability surface was estimated using the ENM under the CCSM, and the other was estimated using the ENM under the MIROC scenario of LGM climate. Stability surfaces are presented in 10 classes with an equal number of values in each. Triangles indicate sampling localities for *E. portoricensis*, the dotted line depicts the approximate distribution of the Río Grande de Loíza Basin, the Cayey Mountains, Luquillo Mountains, and Río Grande de Loíza are indicated.



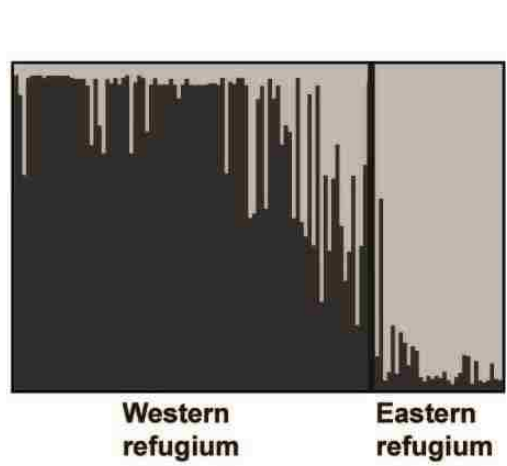
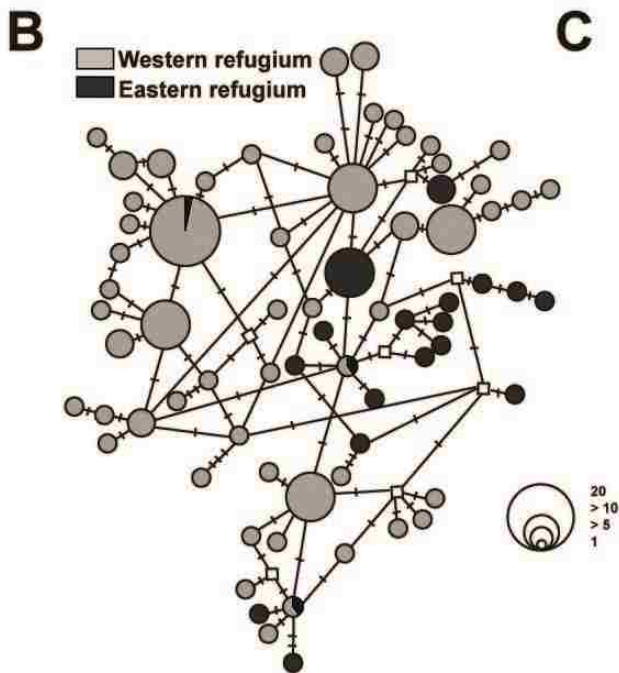
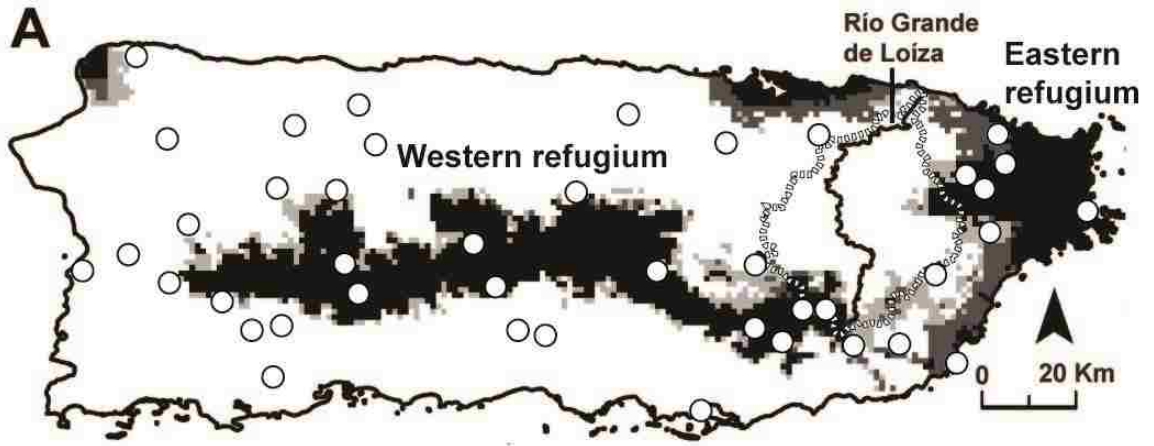
**Fig. 3** (A) Map showing the top 20% (black), 25% (dark gray), and 30% (light gray) values of the stability surface for *Eleutherodactylus portoricensis* (Fig. 2B), with areas containing at least one sampling locality representing the Luquillo Mountains and Cayey Mountains refugia. The Río Grande de Loíza is indicated, and the dotted line depicts the approximate distribution of the Río Grande de Loíza Basin. (B) Maximum parsimony network for *E. portoricensis* inferred from mtDNA control region sequences (redrawn from Barker et al. 2011). Circles represent unique haplotypes; hatch marks depict single mutations; empty squares indicate missing (i.e. extant unsampled or extinct ancestral) haplotypes. Circle size is proportional to haplotype frequency, and the shade of gray for each circle indicates the predicted habitat refugium from which it was sampled, as shown in A. (C) Results of assignment of individual *E. portoricensis* to population clusters, based on four nuclear DNA loci (CRYBA, MYH, RH1, RPL9int4). Bar plots are shown for the best estimate of  $K$  ( $K = 2$ ), where  $K$  is number of population clusters. Each vertical bar shows the proportional representation of the estimated cluster membership for a single individual.



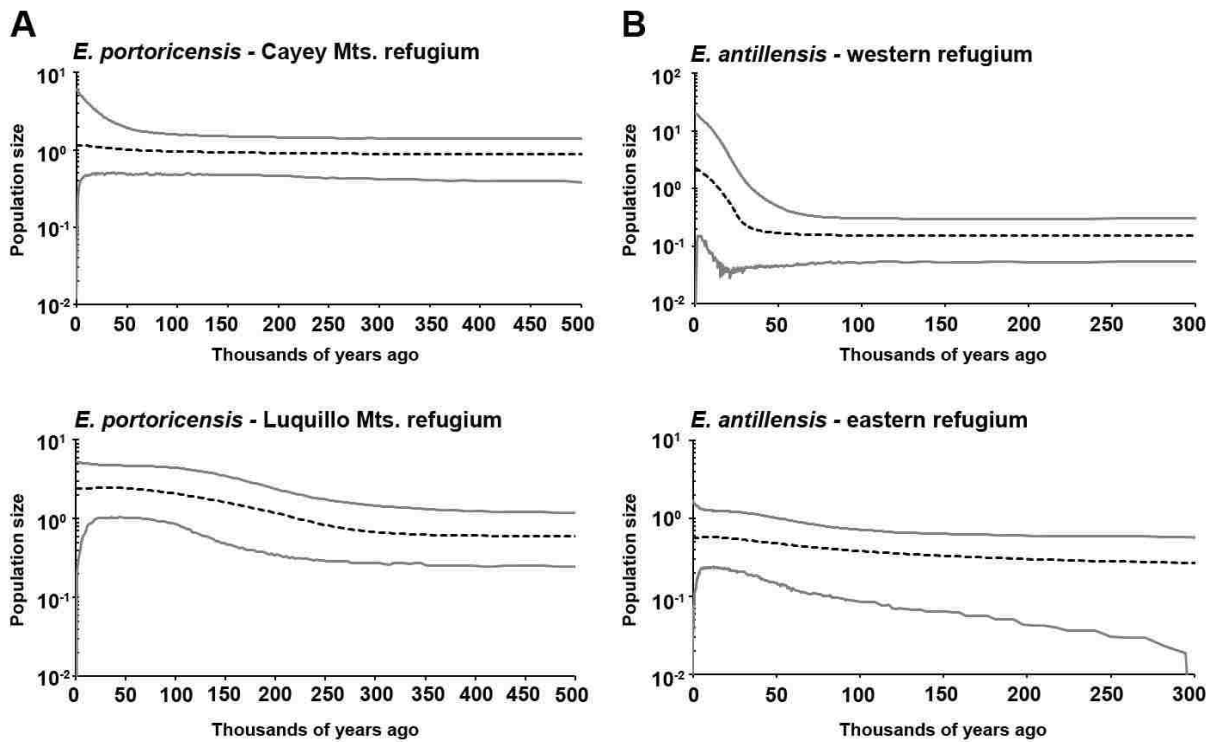
**Fig. 4** Logistic output of ecological niche models (ENMs) for *Eleutherodactylus antillensis* in Puerto Rico under last interglacial (LIG), last glacial maximum [under CCSM [LGM (CCSM)] and MIROC [LGM (MIROC) scenarios], and current climates. (B) Habitat stability surfaces estimated for *E. antillensis* by taking the sum of the suitability pixels through the three time periods; one stability surface was estimated using the ENM under the CCSM, and the other was estimated using the ENM under the MIROC scenario of LGM climate. Stability surfaces are presented in 10 classes with an equal number of values in each. Circles indicate sampling localities for *E. antillensis*, the dotted line depicts the approximate distribution of the Río Grande de Loíza Basin, and the Central Mountains, Cayey Mountains, Luquillo Mountains, and Río Grande de Loíza are indicated.



**Fig. 5** (A) Map showing the top 20% (black), 25% (dark gray), and 30% (light gray) values of the stability surface for *Eleutherodactylus antillensis* (Fig. 4B), with areas containing at least one sampling locality representing the western and eastern refugia. The Río Grande de Loíza is indicated, and the dotted line depicts the approximate distribution of the Río Grande de Loíza Basin. (B) Maximum parsimony network for *E. antillensis* inferred from mtDNA control region sequences. Circles represent unique haplotypes; hatch marks depict single mutations; empty squares indicate missing (i.e. extant unsampled or extinct ancestral) haplotypes. Circle size is proportional to haplotype frequency, and the shade of gray for each circle indicates the predicted habitat refugium from which it was sampled, as shown in A. (C) Results of assignment of individual *E. antillensis* to population clusters, based on four nuclear DNA loci (CRYBA, MYH, RH1, RPL9int4). Bar plots are shown for the best estimate of  $K$  ( $K = 2$ ), where  $K$  is the number of population clusters. Each vertical bar shows the proportional representation of the estimated cluster membership for a single individual, and is sorted by the longitude (e.g. west to east) of its sampling site of origin for display purposes.

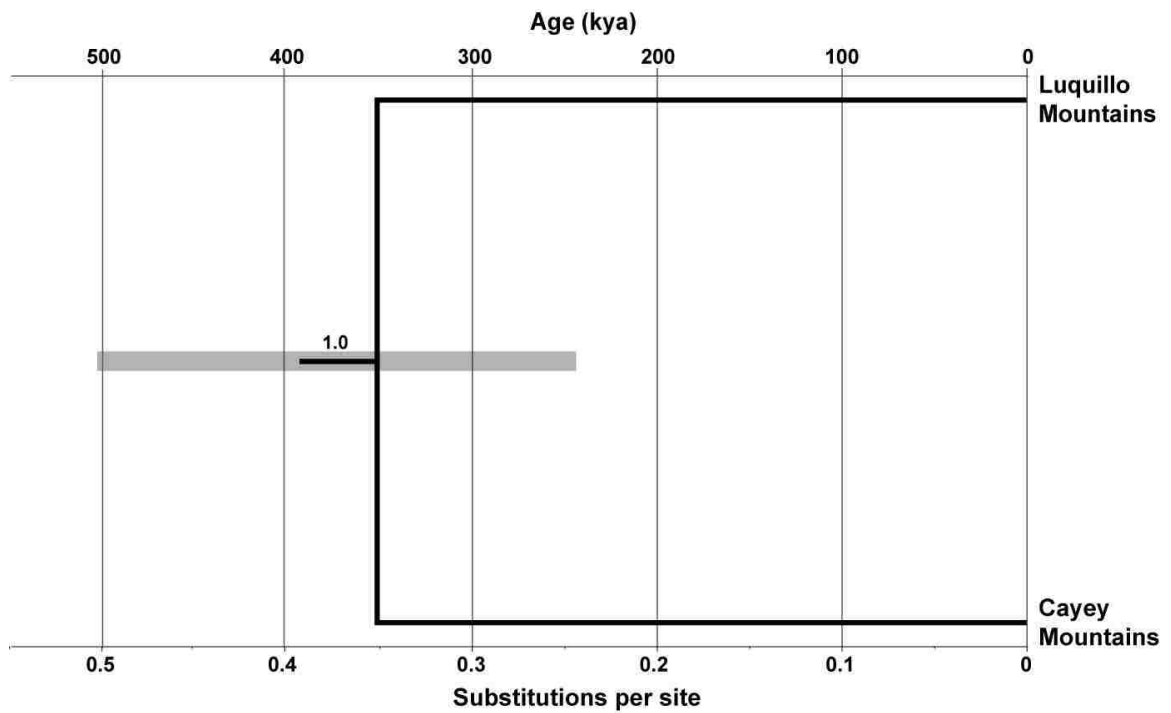


**Fig. 6** Extended Bayesian skyline plots for populations of *Eleutherodactylus portoricensis* in the Cayey Mountains and Luquillo Mountains refugia (A), and for *E. antillensis* populations in western and eastern refugia (B), based on the mtDNA control region (CR) and four nuDNA intron loci (CRYBA, MYH, RH1, RPL9int4). The plots show effective population size plotted as a function of time (units =  $4N_e\mu$ , the product of effective population size and mutation rate [log-transformed]). The time-scale (x-axis, in thousands of years ago) begins with the present on the left. The y-axis indicates estimated population size. The middle line represents the median value upper and lower lines indicate the 95% confidence interval.





**Fig. 7** Results of coalescent analysis of phylogeny and divergence time for *Eleutherodactylus portoricensis* using \*BEAST. The number at the node is the posterior probability. The node is positioned along the axis to reflect the mean divergence estimate and the gray bar on the node is the 95% credible interval around this estimate. The scale on the top and bottom axis indicates divergence time (top), in thousands of years, as a function of substitutions per site (bottom).



**Table 1** Descriptive statistics for the five loci used in this study. The following statistics are reported for Cayey Mountains and Luquillo Mountains populations of *Eleutherodactylus portoricensis* and for western and eastern populations of *E. antillensis*: number of individuals (N), length of sequence (L), number of haplotypes (*h*); haplotype diversity ( $H_d$ ); nucleotide diversity ( $\pi$ ); Tajima's  $D$  ( $D$ ), and Fu's  $F_S$  ( $F_S$ ). Significant  $D$  values at  $P < 0.05$  and  $F_S$  values at  $P < 0.02$  are indicated with an asterisk.

Locus	Population	N	L	$H_d$	$\pi$	$D$	$F_S$	Model
<i>E. portoricensis</i>								
CR	Cayey Mtns.	71	565	0.959	0.0120	-0.555	-12.260*	HKY + I + $\Gamma$
	Luquillo Mtns.	73	564	0.978	0.0130	-1.387	-24.230*	GTR + I + $\Gamma$
Cyt <i>b</i>	Cayey Mtns.	18	646	0.804	0.0040	-1.414	-3.032	HKY
	Luquillo Mtns.	18	646	0.948	0.0060	-1.107	-5.616*	HKY
CRYBA	Cayey Mtns.	18	191	0.790	0.0023	1.138	1.358	HKY + I + $\Gamma$
	Luquillo Mtns.	18	191	0.879	0.0238	1.401	-1.729	GTR
MYH	Cayey Mtns.	18	338	0.425	0.0014	-1.268	-3.470*	HKY
	Luquillo Mtns.	18	338	0.706	0.0028	-1.461	-2.516	HKY
RH1	Cayey Mtns.	18	596	0.798	0.0030	-0.846	-2.833	HKY + I
	Luquillo Mtns.	18	596	0.500	0.0010	1.580	1.749	HKY
RPL9int4	Cayey Mtns.	18	268	0.676	0.0046	0.702	0.839	GTR + I
	Luquillo Mtns.	18	268	0.875	0.0138	-0.060	1.107	HKY + I
<i>E. antillensis</i>								
CR	Western	153	552	0.934	0.0062	-1.246	-26.239*	GTR + I
	Eastern	50	552	0.926	0.0063	-0.678	-5.649*	HKY + I + $\Gamma$
CRYBA	Western	93	192	0.181	0.0022	-0.727	-1.575	HKY
	Eastern	30	192	0.352	0.0029	-0.998	-0.465	HKY
MYH	Western	93	463	0.154	0.0005	-1.394	-4.693*	HKY
	Eastern	30	463	0.624	0.0018	-0.859	-1.391	HKY

**Table 1 cont.**

RH1	Western	93	596	0.621	0.0021	0.827	1.708	HKY
	Eastern	30	596	0.445	0.0009	-1.223	-1.788	HKY
RPL9int4	Western	93	382	0.570	0.0049	-0.978	-5.247	HKY + I
	Eastern	30	382	0.942	0.0102	0.320	-13.544*	HKY + I + $\Gamma$

---

**Table 2** The five variables that contributed most strongly to the MAXENT ecological niche models for *Eleutherodactylus portoricensis* and *E. antillensis*. The description of each variable is followed by its abbreviation in the WorldClim dataset.

Climate variable	Percent contribution	
	<i>E. portoricensis</i>	<i>E. antillensis</i>
Precipitation seasonality (coefficient of variation) - Bio 15	41.0%	30.3%
Mean temperature of coldest quarter - Bio 11	15.7%	–
Annual precipitation - Bio 12	9.6%	–
Max temperature of warmest month - Bio 5	8.0%	15.8%
Isothermality (Bio2 / Bio7) (*100)	–	15.9%
Min temperature of coldest month - Bio 6	–	14.1%
Precipitation of coldest quarter - Bio 19	5.7%	–
Precipitation of wettest month - Bio 13	–	5.4%
Total	80.0%	81.5%

**Table 3** Models of genetic isolation tested for *Eleutherodactylus portoricensis*. Pearson’s correlation coefficients ( $r$ ) (with 95% bootstrap confidence intervals) and the associated  $P$  value are presented for Mantel tests correlating genetic distance and one geographic factor (either geographic distance or the presence of unstable habitat barriers), and for partial Mantel tests correlating genetic distance and one geographic factor after removing the effect of the other. Results of analyses based on Nei’s genetic distance and Rousset’s genetic distance of mtDNA CR and a multi-locus mean for nuDNA are presented.

Model	Nei’s genetic distance				Rousset’s genetic distance			
	CR $r$	$P$ value	nuDNA $r$	$P$ value	CR $r$	$P$ value	nuDNA $r$	$P$ value
Simple mantel								
Geographic distance	0.900 (0.880-0.921)	0.0001	0.830 (0.805-0.863)	0.0001	0.848 (0.829-0.880)	0.0001	0.758 (0.721-0.30)	0.0009
Barrier	0.989 (0.988-0.992)	0.0026	0.883 (0.858-0.922)	0.0022	0.903 (0.889-0.934)	0.0024	0.836 (0.800-0.908)	0.0026
Partial mantel								
Geographic distance and barrier	0.324 (0.259-0.437)	0.0146	0.211 (0.106-0.321)	0.0950	0.230 (0.206-0.286)	0.0708	0.063 (0.038-0.154)	0.6029
Barrier and geographic distance	0.949 (0.936-0.961)	0.0017	0.568 (0.489-0.658)	0.0023	0.617 (0.522-0.686)	0.0026	0.542 (0.474-0.670)	0.0025

**Table 4** Models of genetic isolation tested for *Eleutherodactylus antillensis*. Pearson's correlation coefficients ( $r$ ) (with 95% bootstrap confidence intervals) and the associated  $P$  value are presented for Mantel tests correlating genetic distance and one geographic factor (either geographic distance or the presence of unstable habitat barriers), and for partial Mantel tests correlating genetic distance and one geographic factor after removing the effect of the other. Results of analyses based on Nei's genetic distance and Rousset's genetic distance of mtDNA CR and a multi-locus mean for nuDNA are presented.

Model	Nei's genetic distance				Rousset's genetic distance			
	CR $r$	$P$ value	nuDNA $r$	$P$ value	CR $r$	$P$ value	nuDNA $r$	$P$ value
Simple mantel								
Geographic distance	0.497 (0.452-0.562)	0.0001	0.093 (0.041-0.148)	0.0167	-0.008 (-0.133-0.279)	0.6666	-0.025 (-0.032-0.292)	0.7795
Barrier	0.269 (0.188-0.353)	0.0016	0.200 (0.140-0.259)	0.0026	0.034 (-0.033-0.109)	0.0002	-0.040 (-0.051-0.145)	0.6089
Partial mantel								
Geographic distance and barrier	0.446 (0.393-0.563)	0.0001	0.025 (-0.039-0.080)	0.2471	-0.021 (-0.131-0.050)	0.7611	-0.012 (-0.032-0.013)	0.660
Barrier and geographic distance	0.115 (0.020-0.207)	0.0764	0.179 (0.121-0.251)	0.0050	0.039 (0.014-0.051)	0.1337	-0.034 (-0.043-0.015)	0.7297

**Table 5** Estimated divergence time ( $t$ ), ancestral population sizes ( $N_A$ ), current population sizes ( $N_{e1}$  and  $N_{e2}$ ) and population migration rates ( $2NM$ ) for isolation with migration (IM) models of *Eleutherodactylus portoricensis* and *E. antillensis*. The peak value and 95% highest posterior density (HPD) are indicated for each demographic parameter. For *E. portoricensis*, analyses were carried out with a lower  $t$  upper prior that excluded the older divergence time (see text for details). Asterisks identify curves that are statistically significant by the test of Nielson and Wakeley (2001): \* $P < 0.05$  and \*\* $P < 0.01$ .

Population 1 × population 2	$t$ (years)	$N_A$	$N_{e1}$	$N_{e2}$	$2N_1m_{1→2}$	$2N_2m_{2→1}$
<i>E. portoricensis</i>						
Cayey Mts. × Luquillo Mts.						
Lower $t$ prior						
Peak value	172,944	268,045	207,913	478,323	1.277	1.407
Lower 95% HPD	106,633	106,172	128,524	297,655		
Upper 95% HPD	256,786	459,335	293,930	685,091		
Higher $t$ prior						
Peak value	1,459,978	313,901	330,567	659,116	3.911*	6.956**
Lower 95% HPD	195,763	0	207,031	432,765		
Upper 95% HPD	2,714,883	854,566	463,723	906,162		
<i>E. antillensis</i>						
western × eastern						
Peak value	4,720	5,781	9,242	14,838	3.747*	1.453
Lower 95% HPD	492	833	3,966	3,865		
Upper 95% HPD	15,452	10,484	15,537	31,856		

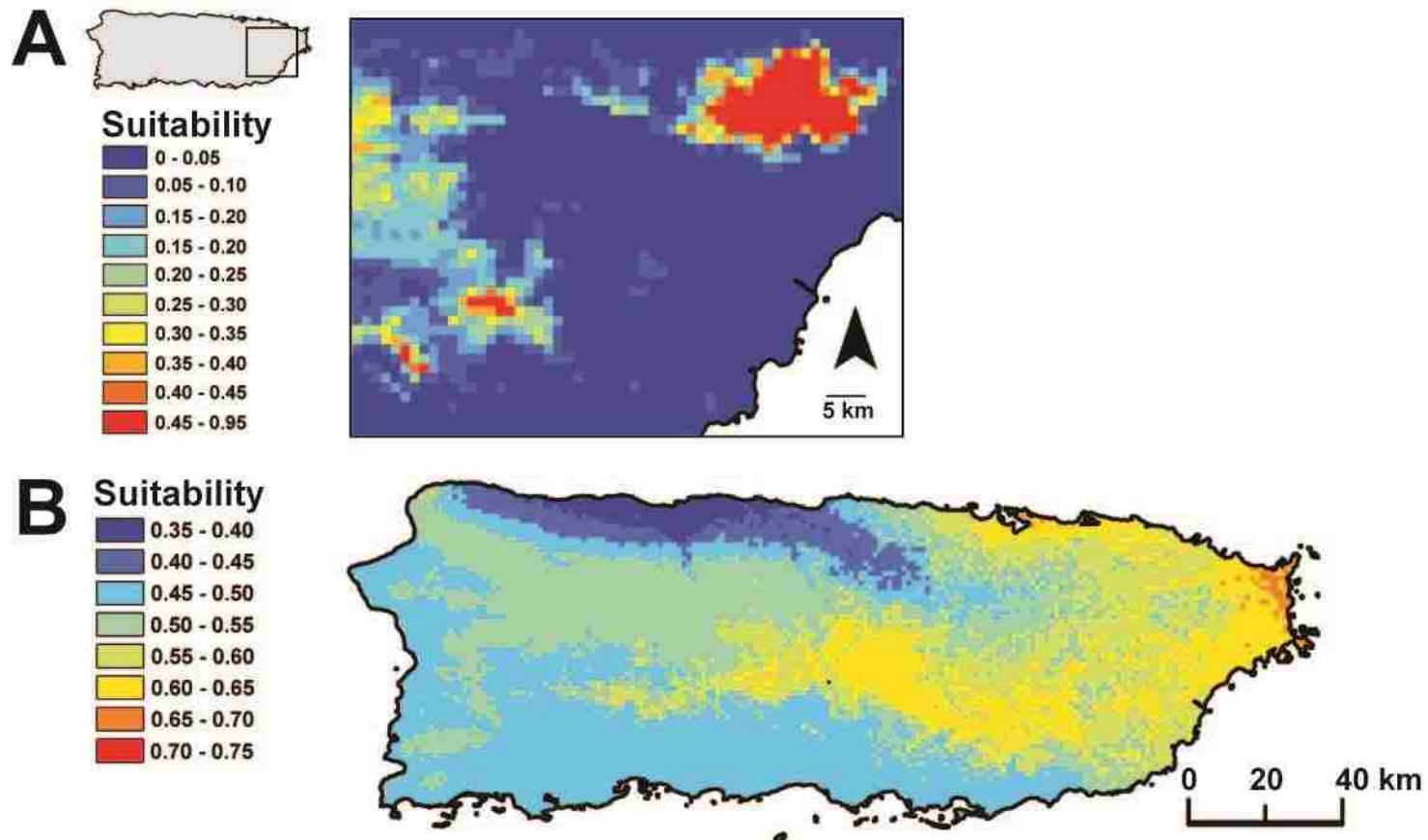
**Table 6** Correlations between habitat stability surfaces and mtDNA CR and nuDNA genetic diversity surfaces [Watterson's  $\theta$  ( $\hat{\theta}_w$ ) and average number of pairwise differences ( $\hat{\pi}_n$ )] for *Eleutherodactylus antillensis*. Two stability surfaces were generated to account for different estimates of LGM climate (CCSM and MIROC). The corrected  $P$  value accounts for the effects of spatial autocorrelation using Dutilleul's method.

	Pearson's correlation coefficient ( $r$ )	Uncorrected $P$ -value	Corrected $P$ -value
Habitat stability surface (LGM – CCSM)			
CR $\hat{\theta}_w$	-0.121	< 0.001	0.322
nuDNA $\hat{\theta}_w$	0.208	0.000	0.089
CR $\hat{\pi}_n$	0.022	0.296	0.847
nuDNA $\hat{\pi}_n$	-0.014	0.519	0.915
Habitat stability surface (LGM – MIROC)			
CR $\hat{\theta}_w$	-0.154	< 0.001	0.244
nuDNA $\hat{\theta}_w$	0.178	< 0.001	0.072
CR $\hat{\pi}_n$	-0.055	0.815	0.968
nuDNA $\hat{\pi}_n$	0.015	0.482	0.898

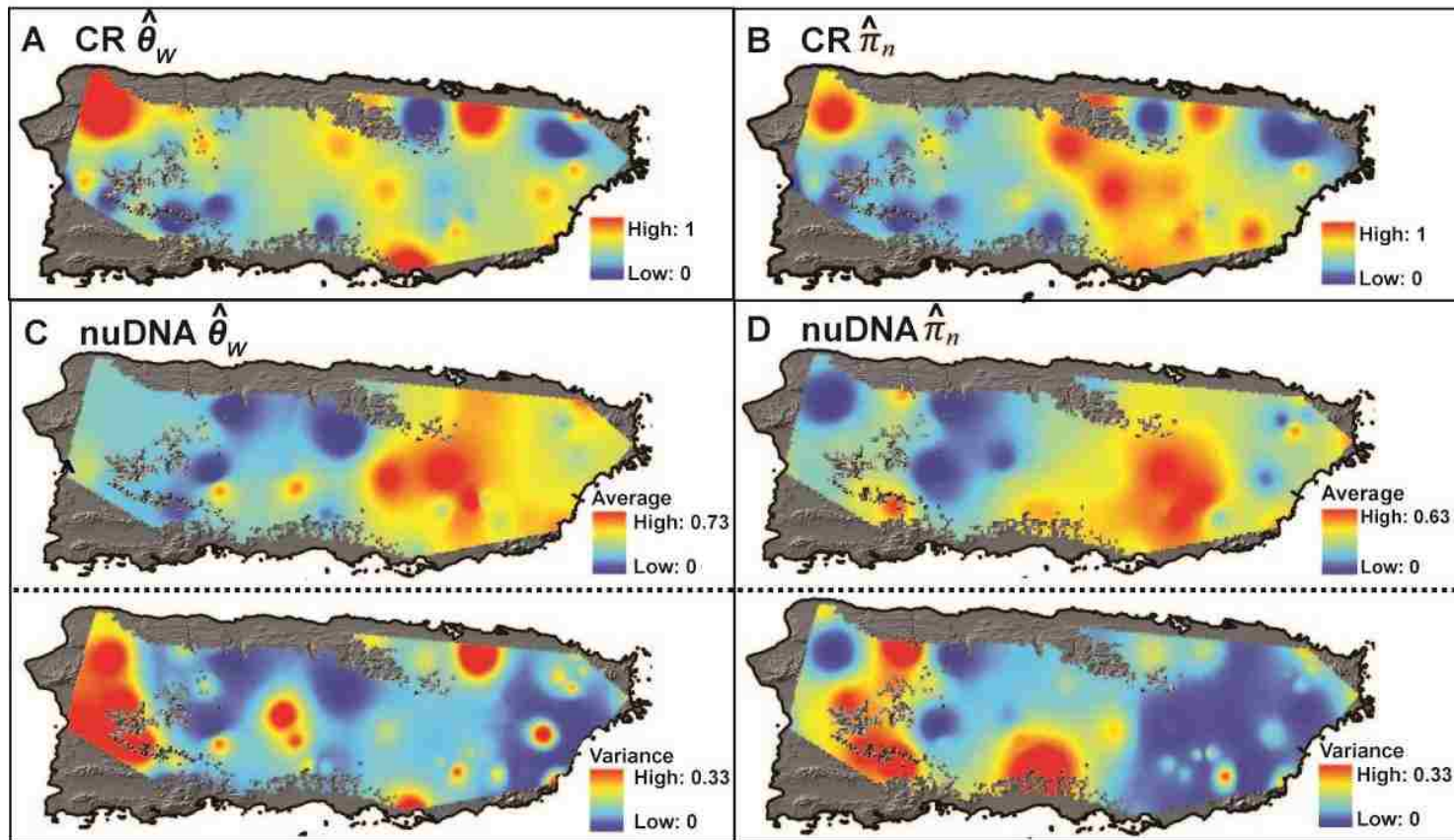


## Supporting Information

**Fig. S1** Ecological niche models for *Eleutherodactylus portoricensis* (A) and *E. antillensis* (B) under current conditions using only the two highest-contributing parameters.



**Fig. S2** Genetic landscapes for genetic diversity of *Eleutherodactylus antillensis* across Puerto Rico, based on mitochondrial DNA (mtDNA) control region (CR; A and B) and on averages for four individual nuclear DNA (nuDNA) loci (C and D). Metrics of genetic diversity include Watterson's estimate of the population mutation rate ( $\hat{\theta}_w$ ) and the average number of pairwise differences among individuals ( $\hat{\pi}_n$ ). The corresponding variance surface of the genetic landscape for average nuDNA  $\hat{\theta}_w$  and  $\hat{\pi}_n$  is depicted below the dotted lines of C and D.



**Table S1** GenBank accession numbers of DNA sequences for *Eleutherodactylus portoricensis* that were newly generated for this study. Museum catalogue numbers for photographic voucher specimens deposited in the Museum of Southwestern Biology (MSB) at the University of New Mexico, Albuquerque, are indicated. CRYBA,  $\beta$ -crystallin; MYH, myosin heavy chain; RPL9int4, ribosomal protein 9 intron 4.

Museum catalogue number	Latitude, Longitude	Elev. (m)	GenBank accession numbers		
			CRYBA	MYH	RPL9int4
Puerto Rico: Municipality of Guayama, Cerro de la Tabla, Km 4.4 on Road 7741	18.049, -66.129	829			
MSB 77434			#####	#####	#####
MSB 77454			#####	#####	#####
MSB 77456			#####	#####	#####
Puerto Rico: Municipality of Guayama, Cerro de la Tabla, Km 3.1 on Road 7741	18.052, -66.122	811			
MSB 77140			#####	#####	#####
MSB 77143			#####	#####	#####
MSB 77352			#####	#####	#####
Puerto Rico: Municipality of Guayama, Cerro de la Tabla, Km 2.1 on Road 7741	18.057, -66.116	756			
MSB 77414			#####	#####	#####
MSB 77415			#####	#####	#####
MSB 77443			#####	#####	#####

Puerto Rico: Municipality of San Lorenzo, Carite State Forest, Km 6.1 on Road 7740	18.101, -66.028	725			
MSB 77369			#####	#####	#####
MSB 77375			#####	#####	#####
MSB 77376			#####	#####	#####
Puerto Rico: Municipality of San Lorenzo, Carite State Forest, Charco Azul	18.091, -66.032	607			
MSB 77100			#####	#####	#####
MSB 77101			#####	#####	#####
MSB 77110			#####	#####	#####
Puerto Rico: Municipality of Patillas, Carite State Forest, near Cerro la Santa, Km 20 on Road 179	18.113, -66.070	762			
MSB 77425			#####	#####	#####
MSB 77448			#####	#####	#####
MSB 77449			#####	#####	#####
Puerto Rico: Municipality of Río Grande, El Yunque National Forest, near Baño de Oro, Km 12.6 on Road 191	18.296, -65.791	752			
MSB 77501			#####	#####	#####
Puerto Rico: Municipality of Río Grande, El Yunque National Forest, near Baño de Oro, Km 12.3 on Road 191	18.298, -65.788	700			
MSB 77507			#####	#####	#####
MSB 77508			#####	#####	#####

Puerto Rico: Municipality of Río Grande, El Yunque National Forest, El Yunque Rock	18.311, -65.792	1,028			
MSB 76694			#####	#####	#####
MSB 76963			#####	#####	#####
MSB 76969			#####	#####	#####
Puerto Rico: Municipality of Río Grande, El Yunque National Forest, before Mt. Britton Spur on Forest Service Road 10	18.303, -65.795	896			
MSB 76945			#####	#####	#####
MSB 76951			#####	#####	#####
MSB 76954			#####	#####	#####
Puerto Rico: Municipality of Río Grande, El Yunque National Forest, Pico del Este	18.269, -65.758	1,021			
MSB 76985			#####	#####	#####
MSB 76986			#####	#####	#####
MSB 76993			#####	#####	#####
Puerto Rico: Municipality of Río Grande, El Yunque National Forest, Tradewinds Trail	18.283, -65.811	849			
MSB 77035			#####	#####	#####
MSB 77038			#####	#####	#####
MSB 77040			#####	#####	#####
Puerto Rico: Municipality of Río Grande, El Yunque National Forest, Pico el Toro, 6.92 Km from El Toro trailhead on Km 10.8 on Road 186	18.272, -65.829	1,051			

MSB 77527

#####

#####

#####

MSB 77528

#####

#####

#####

Puerto Rico: Municipality of Río Grande, 18.272, -65.833 991  
El Yunque National Forest, El Toro  
Trail, 6.5 Km from El Toro trailhead on  
Km 10.8 on Road 186

MSB 77538

#####

#####

#####

## CHAPTER 5

### Conclusion

Climatic oscillations of the Quaternary (Pleistocene – Holocene; ~2.5 million years ago to the present) may have influenced population dynamics of insular species by affecting the amount of suitable habitat and severity of vicariant barriers within and among islands, yet how these events influenced evolution of tropical insular biota is not well understood. My dissertation elucidated the evolutionary consequences of past climate change in a tropical insular system by exploring the role of topographic complexity and climate-driven range shifts in shaping genetic structure and past population demographics of two *Eleutherodactylus* frogs (Anura: Eleutherodactylidae) in the Puerto Rican Bank, an archipelago in the eastern Caribbean Sea. The Mountain Coquí, *Eleutherodactylus portoricensis*, occurs on the highest mountains of eastern Puerto Rico (Schwartz & Henderson, 1991), whereas the Red-eyed Coquí, *E. antillensis*, has one of the broadest elevational (sea level to 1,219 m) and geographic ranges of any species in the Puerto Rican Bank (Henderson & Powell, 1999). Collectively, the results of this dissertation revealed that topography, habitat stability, and species-specific habitat requirements have shaped population genetic structure and the depth of genetic isolation in these species.

Vicariance resulting from the gradual erosion of mountains which once connected the Luquillo and Cayey Mountains at the eastern edge of the Río Grande de Loíza Basin (Meyerhoff, 1933) probably initiated allopatric divergence in *E. portoricensis*, and populations became increasingly isolated as the basin lowered and became warmer and dryer. Divergence occurred before the last interglacial, and migration probably did not

occur between these mountain ranges following this splitting event, which suggests that climate-driven elevational range shifts were not extensive enough to bring isolated populations into secondary contact (Chapter 4). The reciprocal monophyly and deep divergence of *E. portoricensis* populations in the Luquillo and Cayey Mountains suggest the presence of two species (Chapter 2, Chapter 4), and I suggest that these lineages should be managed as distinct population segments.

A multilocus phylogeographic analysis of *E. antillensis* revealed that land-bridge connections across the Puerto Rican Bank during the last glacial period facilitated colonization of the Eastern Islands from sources in eastern Puerto Rico (Chapter 3). Genetic signatures supporting this hypothesis (Eastern Dispersal Hypothesis) include: i) Eastern Islands populations sharing most nuDNA haplotypes with Puerto Rican populations; ii) highest support for a model where gene flow occurs between eastern Puerto Rico and the Eastern Islands; and iii) highest support for a model with eastern Puerto Rican and Eastern Islands populations diverging between the last glacial period and the Holocene interglacial. I inferred relatively low support for the Sea Vicariance Hypothesis, suggesting that populations of *E. antillensis* did not persist in a refugium in the Eastern Islands prior to the last glacial period. Larger patches of suitable habitat, greater topographic and ecological diversity, and less pronounced inundations in Puerto Rico (Ewel & Whitmore, 1973) may have promoted populations persistence of *E. antillensis*, producing higher group structure in this island. Collectively, the results of Chapter 3 illustrate how varying degrees of connectivity and isolation interact to produce phylogeographic patterns in tropical island systems.



In Chapter 4, I demonstrated that the continuous presence of suitable habitats plays an important role in shaping the distribution of genetic endemism in *E. portoricensis* and *E. antillensis*. Hypotheses formulated from ecological niche models of these species under last interglacial *sensu stricto* (LIG; ~130 – 116 thousand years ago [kya]), last glacial maximum (LGM; ~21 kya), and current climates were supported. For *E. portoricensis*, the Cayey-Luquillo Refugia Hypothesis predicts deep differentiation between populations in the Cayey and Luquillo Mountains, with divergence dating to the LIG or earlier, due to complete geographic isolation resulting from unstable habitat in the Río Grande de Loíza Basin and surrounding coastal lowlands. This hypothesis was strongly supported, as shown by (i) individuals from the Cayey and Luquillo refugia all have a strong ( $\geq 0.90$ ) probability of belonging to separate clusters, (ii) a high correlation between mtDNA CR and nuDNA genetic distances and the presence of a wide band (i.e.  $\geq 30$  km) of unstable habitat around the two refugia after removing the effects of geographic distance, (iii) and the inference that divergence of the Cayey Mountains and Luquillo Mountains populations began prior to the LIG. For *E. antillensis*, the West-East Refugia Hypothesis predicts shallow differentiation between populations in western and eastern Puerto Rico due to partial geographic isolation resulting from unstable habitat in the Río Grande de Loíza Basin and surrounding coastal lowlands. This hypothesis was also supported, as shown by (i) 64% and 76% of individuals from western and eastern refugia, respectively, have a strong probability ( $\geq 0.90$ ) of belonging to separate clusters, and (ii) eastern and western populations diverged after the LGM, with significant levels of migration occurring from eastern to western populations after the splitting event. The wider physiological tolerances of *E. antillensis* compared to *E. portoricensis* (Beuchat *et*

*al.*, 1984), combined with the close proximity and even partial connectivity of refugia, may in part explain the much shallower levels of divergence between populations on opposite sides of the Río Grande de Loíza Basin.

The distinctive past population demographics of *E. portoricensis* and *E. antillensis* are probably a reflection of the total amount of habitat that each species occupies. Populations of *E. portoricensis* in the Cayey and Luquillo Mountains did not appear to experience climate-driven changes in size during the late Quaternary (Chapter 4). Elevational shifts of *E. portoricensis* may simply not have been large enough to detectably influence population sizes, and/or population sizes remain sufficiently high and uniform in core suitable areas so that extirpation of peripheral population at lower elevation does not demonstrably affect overall trends. Indeed, montane specialist herpetofauna in the Australian Wet Tropics maintain high and uniform local abundances within their narrow ranges (Williams *et al.*, 2009). In addition to occupying mountainous regions of Puerto Rico, the habitat generalist *E. antillensis* is distributed across the relatively flat and wide lowlands of this island. Unsuitable climatic regimes may displace more populations in the wide lowlands of Puerto Rico compared to those along mountain slopes, which may only need to slightly shift in elevational distribution. Indeed, western Puerto Rican populations began a large and rapid increase in size *ca.* 20 ka, which coincides with the onset of increasing mesic climate in Puerto Rico (Renken *et al.*, 2002) and the expansion of lowland mesic forests throughout the Greater Antilles (Higuera-Gundy *et al.*, 1999; Hodell *et al.*, 2008). After accounting for differences in area, eastern Puerto Rico has a higher percentage of stable habitats than western Puerto Rico (Chapter 4), which may explain why eastern populations did not experience a similar increase in

size. Source populations in eastern Puerto Rico supplied migrants to those in western Puerto Rico, potentially facilitating demographic expansion in this region (Chapter 4). A comparative phylogeographic study of multiple, codistributed lowland and highland species in the Puerto Rican Bank may provide further insight into the relationship between habitat associations and organismal response to past climate change.

Support for hypotheses tested in this dissertation may be improved by adding independent DNA loci, and by using finer scale paleoclimatic data. The ability to distinguish between complex population genetic models (e.g., incorporating admixture or changes in population size) may improve with additional independent loci (Beerli & Palczewski, 2010; Cornuet *et al.*, 2010; Robert *et al.*, 2011), especially if they have higher mutation rates than the loci used in my dissertation. Indeed, the addition of independent loci to the *E. portoricensis* Bayesian Skyline Plot analysis in Chapter 4 provided different results than those from an earlier analysis based on a single mtDNA locus, an analysis that depicted a lack of demographic growth (Chapter 2). Using paleoclimate data with a smaller spatial resolution would probably improve ecological niche models under past climatic conditions, potentially providing greater insight into the role of late Quaternary habitat stability in shaping genetic diversity.

High levels of biotic perturbation and extinction risk are predicted to occur under future climate change (Parmesan, 2006), yet data regarding dispersal and adaptive capabilities are lacking for many species (La Sorte & Jetz, 2010). Tropical species are expected to undergo elevational shifts in distribution in response to changing climate, potentially leading to local declines in biodiversity due to reductions in suitable habitat and population size (e.g. Chen *et al.*, 2009; Corlett, 2011; Feeley *et al.*, 2011). Narrowly

restricted montane endemics may be especially prone to population contractions and local extinction with further warming. Still, *E. portoricensis* populations have evidently persisted through past warming events. However, because of several additional present-day threats (e.g., deforestation, invasive species, and disease), the apparent resilience of this narrow-ranged endemic to past climate change does not assure their continued survival.

Similar to those in other Caribbean islands, endemic species in the Puerto Rican Bank are subject to strong anthropogenic influences, mostly in the form of deforestation (Hedges & Díaz, 2011). Rapid and diverse land-cover changes in the Puerto Rican Bank over the past century have eliminated most of its original vegetation, and pressure from urbanization is ongoing (Helmer *et al.*, 2002; Kennaway *et al.*, 2008). Puerto Rico is unique from most Caribbean islands in that considerable areas of remaining primary forest are currently protected (Helmer, 2004; Hedges & Díaz, 2011). However, recent extirpations and population declines of *E. portoricensis* and other codistributed anurans are attributed to the interacting effects of extended drought periods and the infectious disease chytridiomycosis (Burrowes *et al.*, 2008; Longo & Burrowes, 2010). Despite extensive search effort at nine historical localities across the Cordillera Central, I did not find any populations of *E. portoricensis*, suggesting that populations in this region are either extremely reduced or have undergone recent extirpation (unpublished data). Because *E. portoricensis* is already of conservation concern, the recognition of two species (Chapter 4) would mean that these species have a much more restricted distribution comprised of fewer populations, and, consequently, fewer individuals. In contrast, *E. antillensis*'s ecological flexibility and tendency to discover unoccupied

habitats-allows it to thrive in many edge habitats created by anthropogenic land-use, such as roadsides and pastures (Joglar, 1998; Henderson & Powell, 1999).

Ironically, anthropogenic influences have apparently facilitated the expansion of *E. antillensis* (Chapter 3). Failure to identify a single unique *E. antillensis* haplotype on St. Croix, an island that has never had a direct land connection with the Puerto Rican Bank (Gill *et al.*, 1989), supports anecdotal evidence of a human-mediated introduction to this island in 1937 (Grant & Beatty, 1944). St. Croix populations most likely originated from Eastern Islands sources (Chapter 3). A study of the colonization dynamics and spread of this population may reveal the frequency of single versus multiple sources of introductions, and provide a framework to explore evolutionary dynamics of an invasive population of *E. antillensis* in Panamá City, Panamá (de Sousa *et al.*, 1989). An evaluation of the role of human transport in shaping gene flow among populations of this frog would be best approached using a suite of rapidly evolving DNA markers, such as microsatellites or single nucleotide polymorphisms (SNPs) (Anderson *et al.*, 2010).

With only 11.3% its original primary vegetation, and 2.3 and 2.9% of the world's endemic plants and vertebrates, respectively, the Caribbean region is one of the earth's "hottest hotspots" (Myers *et al.*, 2000). Exploring the historical processes of colonization and persistence in highly endemic and threatened island ecosystems in this region is important for understanding observed patterns of endemic biodiversity, and their potential sensitivity to future climate change and anthropogenic influences.

Phylogeographic studies of insular organisms can contribute fundamental information for decisions related to the management of tropical insular systems.

## References

- Anderson, C., Epperson, B., Fortin, M.-J., Holdregger, R., James, P.M.A., Rosenberg, M., Scribner, K. & Spear, S. (2010) Considering spatial and temporal scale in landscape-genetic studies of gene flow. *Molecular Ecology*, **19**, 3565-3575.
- Beerli, P. & Palczewski, M. (2010) Unified framework to evaluate panmixia and migration direction among multiple sampling locations. *Genetics*, **185**, 313-326.
- Beuchat, C.A., Pough, F.H. & Stewart, M.M. (1984) Response to simultaneous dehydration and thermal stress in three species of Puerto Rican frogs. *Journal of Comparative Physiology B*, **154**, 579-585.
- Burrowes, P.A., Longo, A.V., Joglar, R.L. & Cunningham, A.A. (2008) Geographic distribution of *Batrachochytrium dendrobatidis* in Puerto Rico. *Herpetological Review*, **39**, 321-324.
- Chen, I.-C., Shiu, H.-J., Benedick, S., Holloway, J.D., Khen Chey, V., Barlow, H.S., Hill, J.K. & Thomas, C.D. (2009) Elevation increases in moth assemblages over 42 years on a tropical mountain. *Proceedings of the National Academy of Sciences, USA*, **106**, 1479-1483.
- Corlett, R. (2011) Impacts of warming on tropical lowland rainforests. *Trends in Ecology and Evolution*, **26**, 606-613.
- Cornuet, J.-M., Ravigné, V. & Estoup, A. (2010) Inference on population history and model checking using DNA sequence and microsatellite data with the software DIYABC (v. 1.0). *BMC Bioinformatics*, **11**, 401.
- de Sousa, F., Arosemena, F., Castillo, J.A. & Mallorga, H.M. (1989) Una nueva distribución geográfica de *Eleutherodactylus antillensis* (Reinhardt y Lutken,

- 1863) (Amphibia: Anura: Leptodactylidae), identificación y hábitos ecológicos en la ciudad de Panamá. *Scientia (Panamá)*, **4**, 87-102.
- Ewel, J.J. & Whitmore, J.L. (1973) The ecological life zones of Puerto Rico and the U.S. Virgin Islands. Forest Service Research Paper ITF-18. Río Piedras, PR: United States Department of Agriculture, Forest Service, International Institute of Tropical Forestry. 74 p.
- Feeley, K.J., Silman, M.R., Bush, M.B., Farfan, W., Garcia Cabrera, K., Malhi, Y., Meir, P., Salinas Revilla, N., Quisiyupanqui, M. & Saatchi, S. (2011) Upslope migration of Andean trees. *Journal of Biogeography*, **38**, 783-791.
- Gill, I.P., Hubbard, D.K., Mclaughlin, P. & Moore, C. (1989) Sedimentological and tectonic evolution of Tertiary St. Croix. In: *12th Caribbean Geological Conference* (ed. D.K. Hubbard), pp. 49-71, Teague Bay, St. Croix, West Indies Laboratory.
- Grant, C. & Beatty, H.A. (1944) Herpetological notes on St. Croix, Virgin Islands. *Herpetologica*, **2**, 110-113.
- Hedges, S. & Díaz, L. (2011) The conservation status of amphibians in the West Indies. *Conservation of Caribbean island herpetofaunas volume 1: conservation biology and the wider Caribbean* (ed. by A. Hailey, B. Wilson and J. Horrocks), pp. 281-292. Brill, Leiden, the Netherlands.
- Helmer, E.H. (2004) Forest conservation and land development in Puerto Rico. *Landscape Ecology*, **19**, 29-40.

- Helmer, E.H., Ramos, O., Lopez, T.D., Quinones, M. & Diaz, W. (2002) Mapping the forest type and land cover of Puerto Rico, a component of the Caribbean biodiversity hotspot. *Caribbean Journal of Science*, **38**, 165-183.
- Henderson, R.W. & Powell, R. (1999) West Indian herpetoecology. *Caribbean amphibians and reptiles* (ed. by B.I. Crother), pp. 223-268. Academic Press, San Diego, CA.
- Higuera-Gundy, A., Brenner, M., Hodell, D.A., Curtis, J.H., Leyden, B.W. & Binford, M.W. (1999) A 10,300 <sup>14</sup>C yr record of climate and vegetation change from Haiti. *Quaternary Research*, **52**, 159-170.
- Hodell, D.A., Anselmetti, F.S., Ariztegui, D., Brenner, M., Curtis, J.H., Gilli, A., Grzesik, D.A., Guilderson, T.P., Müeller, A.D., Bush, M.B., Correa-Metrio, A.Y., Escobar, J. & Kutterolf, S. (2008) An 85-ka record of climate change in lowland Central America. *Quaternary Science Reviews*, **27**, 1152-1165.
- Joglar, R.L. (1998) *Los coquíes de Puerto Rico: su historia natural y conservación*. Editorial de la Universidad de Puerto Rico, San Juan.
- Kennaway, T.A., Helmer, E.H., Lefsky, M.A., Brandeis, T.A. & Sherrill, K.R. (2008) Mapping land cover and estimating forest structure using satellite imagery and coarse resolution lidar in the Virgin Islands. *Journal of Applied Remote Sensing*, **2**
- La Sorte, F.A. & Jetz, W. (2010) Projected range contractions of montane biodiversity under global warming. *Proceedings of the Royal Society B: Biological Sciences*, **277**, 3401-3410.
- Longo, A.V. & Burrowes, P.A. (2010) Persistence with chytridiomycosis does not assure survival of direct-developing frogs. *EcoHealth*, **7**, 185-195.



- Meyerhoff, H.A. (1933) Geology of Puerto Rico. *Monographs of the University of Puerto Rico Series B*, **1**, 169-171.
- Myers, N., Mittermeier, R.A., Mittermeier, C.G., Da Fonseca, G.a.B. & Kent, J. (2000) Biodiversity hotspots for conservation priorities. *Nature*, **403**, 853-858.
- Parmesan, C. (2006) Ecological and evolutionary responses to recent climate change. *Annual Review of Ecology, Evolution, and Systematics*, **37**, 637-669.
- Renken, R.A., Ward, W.C., Gill, I.P., Gómez-Gómez, F. & Rodríguez-Martínez, J. (2002) Geology and hydrogeology of the Caribbean islands aquifer system of the commonwealth of Puerto Rico and the U.S. Virgin Islands. *U.S. Geological Survey Professional Paper*, **1419**, 1-148.
- Robert, C.P., Cornuet, J.-M., Marin, J.-M. & Pillai, N.S. (2011) Lack of confidence in approximate Bayesian computation model choice. *Proceedings of the National Academy of Sciences*, **108**, 15112-15117.
- Schwartz, A. & Henderson, R.W. (1991) *Amphibians and reptiles of the West Indies*. University of Florida Press, Gainesville, FL.
- Williams, S.E., Williams, Y.M., Vanderwal, J., Isaac, J.L., Shoo, L.P. & Johnson, C.N. (2009) Ecological specialization and population size in a biodiversity hotspot: how rare species avoid extinction. *Proceedings of the National Academy of Sciences, USA*, **106**, 19737-19741.